

**UNIVERSITA' DEGLI STUDI DI MILANO**  
**Doctorate School of Chemical Sciences and Technologies**  
**Dipartimento di Chimica**  
**Industrial Chemistry – XXV Cycle**



**DESIGN, SYNTHESIS, CHARACTERISATION AND BIOLOGICAL TESTING OF  
NEW DERIVATIVES OF HYALURONAN FOR THE PRECONDITIONING OF  
STEM CELLS FOR THE THERAPY OF MUSCULAR DYSTROPHIES AND THE  
DEVELOPMENT AND REGENERATION OF SKELETAL MUSCLE**

**CHIM/06**

**Tutor: Prof. Francesco SANNICOLLO'**

**Co-Tutor: Prof. Giulio COSSU**

**Co-Ordinator: Prof. Dominique ROBERTO**

**PhD student: Arianna GENNARI**

**2011-2012**



***Table of Contents***

|          |  |           |
|----------|--|-----------|
| <b>1</b> | <b>INTRODUCTION</b>  | <b>1</b>  |
| 1.1      | NEW THERAPIES FOR MUSCULAR DYSTROPHY                                       | 1         |
| 1.1.1    | <i>The pharmacological approach</i>  | 3         |
| 1.1.2    | <i>Gene therapy</i>  | 5         |
| 1.1.3    | <i>Cell therapy</i>  | 6         |
| 1.2      | MESOANGIOBLASTS: VASCULAR PROGENITORS FOR EXTRAVASCULAR MESODERMAL TISSUES | 8         |
| 1.3      | BIOMATERIALS APPROACH TO EXPAND AND DIRECT DIFFERENTIATION OF STEM CELLS   | 15        |
| 1.4      | HYALURONAN   | 18        |
| 1.5      | AIMS AND OBJECTIVES  | 21        |
| 1.6      | REFERENCES   | 22        |
| <b>2</b> | <b>CHEMICAL MODIFICATION OF THE HYALURONIC ACID</b>                        | <b>25</b> |
| 2.1      | INTRODUCTION   | 25        |
| 2.1.1    | <i>Modification of the carboxylic acid group</i>                           | 27        |
| 2.1.2    | <i>Modification of the hydroxy group</i>                                   | 35        |
| 2.2      | AMIDATION  | 39        |
| 2.2.1    | INTRODUCTION   | 39        |
| 2.2.2    | EXPERIMENTAL PROCEDURES  | 42        |
| 2.2.3    | RESULTS AND DISCUSSION   | 45        |
| 2.2.4    | CONCLUSION   | 53        |
| 2.3      | DIISIOCYANATES AS CROSS-LINKER AGENTS FOR HA                               | 55        |

---

## Contents

---

|       |   |     |
|-------|---|-----|
| 2.3.1 | <i>INTRODUCTION</i>   | 55  |
| 2.3.2 | <i>EXPERIMENTAL PROCEDURES</i>  | 57  |
| 2.3.3 | <i>RESULTS AND DISCUSSION</i>   | 62  |
| 2.3.4 | <i>CONCLUSION</i>   | 72  |
| 2.4   | <i>HA MODIFICATION VIA Cu<sup>I</sup> CATALYSED 1,3-CYCLOADDITION</i>   | 74  |
| 2.4.1 | <i>INTRODUCTION</i>   | 74  |
| 2.4.2 | <i>EXPERIMENTAL PROCEDURES</i>  | 82  |
| 2.4.3 | <i>RESULTS AND DISCUSSION</i>   | 98  |
| 2.4.4 | <i>CONCLUSION</i>   | 116 |
| 2.5   | <i>PROLIFERATION AND DIFFERENTIATION OF MESOANGIOBLASTS ON HYALURONAN DERIVATIVES</i>   | 118 |
| 2.5.1 | <i>INTRODUCTION</i>   | 118 |
| 2.5.2 | <i>EXPERIMENTAL PROCEDURES</i>  | 121 |
| 2.5.3 | <i>RESULTS AND DISCUSSION</i>   | 124 |
| 2.5.4 | <i>CONCLUSION</i>   | 133 |
| 2.6   | <i>ACKNOWLEDGEMENTS</i>   | 134 |
| 2.7   | <i>REFERENCES</i>   | 135 |
| 2.8   | <i>SUPPORTING INFORMATION</i>   | 141 |
| 3     | <i>EFFECTS OF ENVIRONMENTAL FACTORS AND REACTANT ARCHITECTURE ON THE OUTCOME OF THE MICHAEL-TYPE ADDITION USED FOR BIOCONJUGATION</i> | 145 |
| 3.1   | <i>INTRODUCTION</i>   | 145 |
| 3.1.1 | <i>The Michael reaction</i>   | 145 |
| 3.1.2 | <i>Reaction mechanism and kinetics</i>  | 147 |
| 3.1.3 | <i>Reversibility of Michael-type reaction</i>   | 156 |

---

## Contents

---

|       |  |     |
|-------|--|-----|
| 3.1.4 | <i>Bioconjugates via Michael addition</i>  | 161 |
| 3.2   | <i>EXPERIMENTAL PROCEDURES</i>   | 167 |
| 3.2.1 | <i>Materials</i>   | 167 |
| 3.2.2 | <i>General methods</i>   | 167 |
| 3.2.3 | <i>Synthetic procedures</i>  | 168 |
| 3.2.4 | <i>Determination of thiol <math>pK_a</math></i>  | 173 |
| 3.2.5 | <i>Thiol oxidation study</i>   | 174 |
| 3.2.6 | <i>Validation of Ellman's assay</i>  | 174 |
| 3.2.7 | <i>Determination of the observed Michael-type addition rate constants</i>  | 175 |
| 3.2.8 | <i>Stability of Michael-type acceptors</i>   | 176 |
| 3.2.9 | <i>Stability of Michael-type adducts</i>   | 176 |
| 3.3   | <i>RESULTS AND DISCUSSION</i>  | 178 |
| 3.3.1 | <i>Thiol titration</i>   | 178 |
| 3.3.2 | <i>Kinetic studies</i>   | 180 |
| 3.3.3 | <i>Stability of Michael-type acceptors</i>   | 191 |
| 3.3.4 | <i>Stability of Michael-type adducts</i>   | 195 |
| 3.4   | <i>CONCLUSION</i>  | 201 |
| 3.5   | <i>ACKNOWLEDGEMENTS</i>  | 203 |
| 3.6   | <i>REFERENCES</i>  | 204 |
| 3.7   | <i>SUPPORTING INFORMATION</i>  | 208 |
| 3.7.1 | <i>SCREENING DIFFERENT CONDITIONS FOR MICHAEL-TYPE REACTION BETWEEN 3-MERCAPTOPROPIONIC (3-MPA) ACID AND 2-HYDROXYETHYL ACRYLATE (1)</i> | 208 |
| 3.7.2 | <i>HPLC ANALYSIS OF THE SYNTHESISED COMPOUNDS</i>  | 210 |

---

## Contents

---

|       |   |     |
|-------|---|-----|
| 3.7.3 | <i>Calibration curves of 3-MPA and NAC via Ellman's assay</i> | 222 |
| 3.7.4 | <i>Calibration curve of maleimide 7</i>                       | 224 |

---

## ***List of Figures***

|   |    |
|---|----|
| <i>Figure 1: Dystrophin in normal and dystrophic muscle</i>   | 1  |
| <i>Figure 2: Different delivery strategies of the therapeutic agents</i>  | 2  |
| <i>Figure 3: Expression of <math>\alpha</math>-SG and other dystrophin-associated proteins in <math>\alpha</math>-SG null mice after intra-arterial delivery of wild-type mesoangioblasts</i> | 10 |
| <i>Figure 4: In vitro myogenic differentiation of human pericyte derived cells</i>  | 13 |
| <i>Figure 5: Structure of hyaluronan</i>  | 18 |
| <i>Figure 6: Chemical conjugation and chemical cross-linking of a polymer</i>   | 26 |
| <i>Figure 7: Repetitive unit of hyaluronan showing the primary sites for chemical modification</i>  | 27 |
| <i>Figure 8: HA esterification using alkyl halides</i>  | 28 |
| <i>Figure 9: HA esterification with tetraethylene glycol ditosylate</i>   | 28 |
| <i>Figure 10: HA esterification using trimethylsilyl diazomethane</i>   | 29 |
| <i>Figure 11: EDCI-mediated HA amidation</i>  | 31 |
| <i>Figure 12: CDMT-mediated HA amidation</i>  | 32 |
| <i>Figure 13: Structure of DMTMM</i>  | 33 |
| <i>Figure 14: Proposed structure of the network formed by HA via Ugi's condensation with aqueous formaldehyde, cyclohexylisocyanide and lysine ethyl ester</i>                                | 35 |
| <i>Figure 15: HA cross-linking with butanediol-diglycidyl ether in alkaline conditions</i>  | 36 |
| <i>Figure 16: HA cross-linking with divinyl sulfone</i>   | 37 |
| <i>Figure 17: HA esterification with methacrylic anhydride</i>  | 37 |
| <i>Figure 18: HA oxidation with sodium periodate</i>  | 38 |
| <i>Figure 19: Reaction scheme of the synthesis of the organo-silane HA derivative</i>   | 40 |

---

## Contents

---

|  |     |
|--|-----|
| <i>Figure 20: Evaluation of the amine remained in the HA samples</i>   | 47  |
| <i>Figure 21: DOSY spectrum of <b>HA-Acr</b></i>   | 50  |
| <i>Figure 22: Reaction of primary amine with fluorescamine</i>   | 51  |
| <i>Figure 23: Obtained degree of functionalisation measured by fluorescamine assay</i>                               | 52  |
| <i>Figure 24: <sup>1</sup>H NMR spectra of <b>HA-CL<sub>1</sub></b> (cross-linking degree 10%)</i>                   | 65  |
| <i>Figure 25: UV spectra of <b>HA-CL<sub>3</sub></b></i>   | 66  |
| <i>Figure 26: Swelling measurement (<math>S_w</math>) for cross-linked HA</i>  | 67  |
| <i>Figure 27: Schematic illustration of the sinusoidally varying stress and strain in dynamic oscillatory test</i>   | 69  |
| <i>Figure 28: Rheological measurement on <b>HA-CL<sub>1</sub></b></i>  | 70  |
| <i>Figure 29: Huisgen thermal 1,3-cycloaddition</i>  | 75  |
| <i>Figure 30: Proposed catalytic cycle for 1,3-cycloaddition catalysed by Cu<sup>I</sup></i>                         | 77  |
| <i>Figure 31: Representation of the Formation of HA-based click-gels</i>   | 79  |
| <i>Figure 32: Formation of hydrogels from modified-HA by the use of click chemistry with different cross-linkers</i> | 80  |
| <i>Figure 33: <sup>1</sup>H NMR spectra of HA, HABA, HAAA and FT-IR spectrum of HAAA</i>                             | 101 |
| <i>Figure 34: <sup>1</sup>H NMR spectrum of <b>HA-TR1</b></i>  | 103 |
| <i>Figure 35: <sup>1</sup>H NMR spectrum of <b>HA-TR3</b></i>  | 110 |
| <i>Figure 36: <sup>1</sup>H NMR of <b>HA-TR4</b></i>   | 114 |
| <i>Figure 37: HA-derivatives tested as substrates for stem cell cultures</i>   | 125 |
| <i>Figure 38: Population doubling of human pericyte derived cells on HA coated petri dishes</i>                      | 126 |
| <i>Figure 39: Segmentation of phase contrast images</i>  | 127 |
| <i>Figure 40: Morphological analysis of human pericyte derived cells planted on HA-derivatives</i>                   | 128 |

---



## Contents

---

|   |     |
|---|-----|
| <i>Figure 41: Comparison of hydrophobicity between HA-Na and HA-TR1</i>   | 129 |
| <i>Figure 42: Analysis of images recorded by immunofluorescence microscopy</i>  | 131 |
| <i>Figure 43: Analysis on the differentiation of human pericyte derived cells planted on HA-derivatives</i>   | 132 |
| <i>Figure 44: Schematic depiction of the Michael addition reaction.</i>   | 145 |
| <i>Figure 45: Classical examples of Michael addition</i>  | 146 |
| <i>Figure 46: Mechanism of Michael addition</i>   | 148 |
| <i>Figure 47 : Reactivity towards GSH of selected Michael-type acceptors</i>  | 151 |
| <i>Figure 48 : The first example of a stereoselective aza-Michael addition</i>  | 153 |
| <i>Figure 49: Solvent effect on the reaction rate of the Michael addition of malonodinitrile to chalcone catalyzed by 5% mol of N-methylimidazole</i>   | 156 |
| <i>Figure 50: Reversible Michael-type addition reaction between ethacrynic acid and glutathione</i>   | 158 |
| <i>Figure 51: Degradation of maleimide-thiol adducts in reducing environment</i>  | 159 |
| <i>Figure 52: Proposed mechanism for the influence of the conjugation site on linker stability and therapeutic activity of antibody conjugates.</i>     | 161 |
| <i>Figure 53: Strategies for the Use of Michael-type for surfaces modification</i>  | 163 |
| <i>Figure 54: Bioconjugation on HA with a RGD-containing peptide via Michael-type addition</i>  | 166 |
| <i>Figure 55: Thiol/thiolate equilibrium</i>  | 178 |
| <i>Figure 56: Recorded UV absorbance spectra of thiol (at low pH) and thiolate (at high pH) for 3-MPA in TRIS buffer 100 mM/EtOH 80:20 v/v, at 30°C</i> | 179 |
| <i>Figure 57: Titration curve for 3-MPA in TRIS 100 mM/EtOH 80:20 v/v, at 30°C</i>  | 179 |
| <i>Figure 58: Oxidation of 3-MPA at different pH values</i>   | 183 |
| <i>Figure 59: Evaluation of the stability of Michael-type acceptors towards NTB<sup>-</sup></i>   | 184 |
| <i>Figure 60 : Reaction between 3-MPA acid and 2-hydroxyethyl acrylate (1)</i>  | 185 |

---

## Contents

---

|  |     |
|--|-----|
| <i>Figure 61 : <math>k_{obs}</math> as a function of pH for Michael-type addition reaction between compounds 1-6 and 3-MPA</i>                                 | 187 |
| <i>Figure 62: <math>k_{obs}</math> vs <math>\alpha</math> obtained from the results of the Michael-type addition of 3-MPA and 2-hydroxyethyl acrylate 1</i>    | 190 |
| <i>Figure 63: Hydrolysis of maleimide based compounds</i>  | 192 |
| <i>Figure 64: Spectra of maleimide 7 and hydrolysed form</i>   | 193 |
| <i>Figure 65: Spectrophotometrical study of the hydrolysis of compound 7</i>   | 194 |
| <i>Figure 66: <math>^1H</math> NMR study of the hydrolysis of compound 7</i>   | 195 |
| <i>Figure 67: Measured rate constants for the disappearance of Michael-type adducts in 50 mM phosphate buffer at pH 37°C with 10 times molar excess of GSH</i> | 199 |
| <br>   |     |
| <i>Figure S 1: HPLC analysis of 2-(acetylamino)ethyl acrylate (3)</i>  | 210 |
| <i>Figure S 3: HPLC analysis of 2-(acetylamino)ethyl 2-methylacrylate (4)</i>  | 211 |
| <i>Figure S 4: HPLC analysis of N-[2-(acetylamino)ethyl]acrylamide (5)</i>   | 212 |
| <i>Figure S 5: HPLC analysis of N-[2-(acetylamino)ethyl]-2-methylacrylamide (6)</i>  | 213 |
| <i>Figure S 6: HPLC analysis of N-[2-(2,5-dioxo-2,5-dihydro-1H-pyrrol-1-yl)ethyl]acetamide (7)</i>   | 214 |
| <i>Figure S 7: HPLC analysis of N-acetyl-S-[3-(2-hydroxyethoxy)-3-oxopropyl]cysteine (MA1-NAC)</i>   | 215 |
| <i>Figure S 8: HPLC analysis of N-acetyl-S-[3-(2-hydroxyethoxy)-2-methyl-3-oxopropyl]cysteine (MA2-NAC)</i>  | 216 |
| <i>Figure S 9: HPLC analysis of N-acetyl-S-{3-[2-(acetylamino)ethoxy]-3-oxopropyl}cysteine (MA3-NAC)</i>   | 217 |
| <i>Figure S 10: HPLC analysis of N-acetyl-S-{3-[2-(acetylamino)ethoxy]-2-methyl-3-oxopropyl}cysteine (MA4-NAC)</i>   | 218 |
| <i>Figure S 11: HPLC analysis of N-acetyl-S-(3-{[2-(acetylamino)ethyl]amino}-3-oxopropyl)cysteine (MA5-NAC)</i>  | 219 |

---

## Contents

---

|   |     |
|---|-----|
| <i>Figure S 12: : HPLC analysis of N-acetyl-S-{1-[2-(acetylamino)ethyl]-2,5-dioxopyrrolidin-3-yl}cysteine (MA6-NAC)</i> | 220 |
| <i>Figure S 13: HPLC analysis of N-acetyl-S-{1-[2-(acetylamino)ethyl]-2,5-dioxopyrrolidin-3-yl}cysteine (MA7-NAC)</i>   | 221 |
| <i>Figure S 14: Calibration curve of 3-MPA</i>  | 222 |
| <i>Figure S 15: Calibration curve of NAC</i>  | 223 |
| <i>Figure S 16: Calibration curve of 7</i>  | 224 |

---

## Contents

---

---

***List of Tables***

|   |            |
|---|------------|
| <i>Table 1: Measured <math>pK_a</math> of the different sulphur containing nucleophiles</i>   | <i>178</i> |
| <i>Table 2: Calculated thiol oxidation rate constants</i>   | <i>183</i> |
| <i>Table 3: Experimental rate constants (<math>k_{obs}</math>) for Michael-type addition reaction between compounds <b>1-6</b> and 3-MPA or NAC</i>     | <i>188</i> |
| <i>Table 4: Individual rate constants of thiol and thiolate of the Michael-type addition between 3-MPA or NAC and Michael-type acceptors <b>1-6</b></i> | <i>191</i> |
| <i>Table 5: Pseudo-first order rate constants measured for the disappearance of Michael-type adducts with NAC incubated in reducing environment</i>     | <i>200</i> |
| <i>Table S 1: Different experimental condition tested for the Michael-type reaction between 3-MPA and compound <b>1</b></i>                             | <i>209</i> |

---

## Contents

---

---

## *List of Schemes*

|   |     |
|---|-----|
| <i>Scheme 1: Modification of the HA carbodiimide mediated</i>   | 46  |
| <i>Scheme 2: Synthesis of amidated HA featuring an acrylamide</i>   | 49  |
| <i>Scheme 3: Synthesis of diisocyanate <b>TEG-2IB</b> via Curtius rearrangement</i>   | 63  |
| <i>Scheme 4: Synthesis of cross-linked HA-derivative</i>  | 64  |
| <i>Scheme 5: Synthesis of HA-bromoacetate (HABA)</i>  | 99  |
| <i>Scheme 6: Synthesis of HA-azidoacetate (HAAA)</i>  | 100 |
| <i>Scheme 7: Sharpless cycloaddition with HAAA and propargyl alcohol</i>  | 102 |
| <i>Scheme 8: Synthesis of propargyl benzoate and its use in the Sharpless cycloaddition with HAAA</i>   | 104 |
| <i>Scheme 9: Synthesis of a protected precursor of the RGD sequence featuring a terminal alkyne</i>   | 106 |
| <i>Scheme 10: Synthesis of <b>HA-TR3</b></i>  | 109 |
| <i>Scheme 11: Synthesis of the water soluble linker featuring a terminal alkyne</i>   | 111 |
| <i>Scheme 12: Synthesis of protected arginine functionalised with the water-soluble linker and a terminal alkyne and of the HA conjugates <b>HA-TR4</b> and <b>HA-TR5</b></i> | 113 |
| <i>Scheme 13: Synthesis of the protected RGD sequence bearing a water soluble linker with a terminal alkyne functionality</i>   | 115 |
| <i>Scheme 14: General scheme of Michael-type addition and reactants employed for this study</i>   | 181 |
| <i>Scheme 15 : Synthesis of Michael-type adducts with NAC</i>   | 197 |
| <br>  |     |
| <i>Scheme S 1: Pathway followed for the synthesis of Boc-Arg(Z)<sub>2</sub>-Gly-Asp(OBn)-OMe</i>  | 141 |
| <i>Scheme S 3: Michael-type reaction between 3-MPA and compound <b>1</b></i>  | 208 |

---

## Contents

---

---



## Contents

---

### *Abbreviations*

|                          |   |
|--------------------------|---|
| [bmim]PF <sub>6</sub>    | 1-butyl-3-methylimidazolium hexafluorophosphate           |
| [bmmim]PF <sub>6</sub>   | 1-butyl-2,3-dimethylimidazolium hexafluorophosphate       |
| [emim]SO <sub>4</sub> Et | 1-ethyl-3-methylimidazolium ethylsulfate                  |
| 3-MPA                    | 3-Mercaptopropionic acid                                  |
| Ac                       | Acetyl  |
| Arg                      | Arginine  |
| Asp                      | Aspartic acid   |
| ATR                      | Attenuated total reflectance                              |
| BHT                      | Butylated hydroxytoluene                                  |
| BINOL                    | 1,1'-Bi-2-naphthol  |
| Bn                       | Benzyl  |
| Boc                      | tert-Butyloxycarbonyl                                     |
| CBZ                      | Carboxybenzyl   |
| CDMT                     | Chloro-4,6-dimethoxy-1,3,5-triazine                       |
| DAPI                     | 4',6'-diamidino-2-phenylindole                            |
| DCC                      | N,N'-Dicyclohexylcarbodiimide                             |
| DCM                      | Dichloromethane   |
| DIC                      | 1,3-Diisopropylcarbodiimide                               |
| DIPEA                    | N,N-Diisopropylethylamine                                 |
| DMAP                     | 4-Dimethylaminopyridine                                   |
| DMD                      | Duchenne muscular dystrophy                               |
| DMEM                     | Dulbecco's modified Eagle's medium                        |
| DMF                      | Dimethylformamide   |
| DMSO                     | Dimethyl sulfoxide  |
| DMTMM                    | 4-(4,6-Dimethoxy-1,3,5-triazin-2-yl)-4-methylmorpholinium |
| DOSY                     | Diffusion-ordered spectroscopy                            |
| DTNB                     | 5,5'-Dithiobis-(2-nitrobenzoic acid); Ellman's reagent    |
| ECM                      | Extracellular matrix                                      |
| EDCI                     | N-(3-dimethylpropyl)-N'-ethylcarbodiimide hydrochloride   |
| EDTA                     | Ethylenediaminetetraacetic acid                           |
| GAG                      | Glycosaminoglycan   |
| GAG                      | Glucosaminoglycan   |
| Gly                      | Glycine   |
| GRMD                     | Golden retriever muscular dystrophy                       |
| GSH                      | L-Reduced glutathione                                     |
| h                        | Hour  |

---

## Contents

---

|                  |  |
|------------------|--|
| HA               | Hyaluronic acid  |
| Has              | Hyaluronan synthases   |
| HBTU             | O-Benzotriazole-N,N,N',N'-tetramethyl uronium hexafluoro phosphate |
| HEPES            | 4-(2-Hydroxyethyl)-1-piperazineethanesulfonic acid                 |
| HOBt             | Hydroxybenzotriazole   |
| IL               | Ionic liquid   |
| MES              | 2-Morpholinoethanesulfonic acid                                    |
| mp               | Melting point  |
| MWCO             | Molecular weight cut off   |
| NAC              | N-acetyl-L-cysteine  |
| NHS              | N-Hydroxysuccinimide   |
| NMM              | N-methylmorpholine   |
| NTB <sup>-</sup> | 2-nitro-5-thiobenzoate   |
| PEG              | Polyethylene glycol  |
| Prop             | Propargyl  |
| RGD              | Arginine-Glycine-Aspartic acid                                     |
| RP               | Reverse phase  |
| SG               | Sarcoglycan  |
| S <sub>w</sub>   | Swelling capacity  |
| t                | Time   |
| TBA              | Tetrabutylammonium   |
| TEG              | Triethylene glycol   |
| TFA              | Trifluoroacetic acid   |
| Tris             | Tris(hydroxymethyl)aminoethane                                     |
| Ts               | Tosyl  |
| W <sub>d</sub>   | Weight of the dry polymeric network                                |
| W <sub>s</sub>   | Weight of the swollen gel  |
| Z                | Carboxybenzyl  |

---

***Abstract***

Università degli Studi di Milano  
Arianna Gennari

**DESIGN, SYNTHESIS, CHARACTERISATION AND BIOLOGICAL TESTING OF NEW DERIVATIVES OF HYALURONAN FOR THE PRECONDITIONING OF STEM CELLS FOR THE THERAPY OF MUSCULAR DYSTROPHIES AND THE DEVELOPMENT AND REGENERATION OF SKELETAL MUSCLE**

Regenerative medicine is the process of creating living, functional tissues to repair or replace tissue or organ functions lost due to age, disease, damage, or congenital defects. Related to regenerative medicine is field of tissue engineering. Numerous strategies currently used to engineer tissues depend on employing a specific material. These scaffolds serve as a synthetic extra cellular matrix thus to direct the growth and the formation of a desired tissue.

Recent work has suggested application of mesoangioblasts for stem cell therapies for muscular dystrophy. Experiments in dystrophic mice and dogs have shown that mesoangioblasts transplantation can restore muscle function. Anyway, the possibility of using this novel strategy for the cell therapy in genetic diseases is strictly related to the capacity to expand mesoangioblasts in culture in a reproducible and efficient way. Hence, the aim of this project is to investigate the ability of the hyaluronic acid (HA) to act as a basement for cells culture; cells are in fact very sensitive to their environment and the contact with something mimicking the extra cellular matrix could, in theory, assure a better proliferation and differentiation.

Hyaluronan can be chemically modified to introduce drugs, ligands or other bioactive molecules, or to cross-link the linear chains affording reticulated networks. Several different methods to provide modified HA have been performed in order to develop robust protocols; specifically we focused on Sharpless cycloaddition, on the use of diisocyanates as cross-linker agents and on the activation of the carboxylic acid moiety towards amines.

Mesoangioblasts were cultured using HA and its derivatives as substrates to evaluate their biological influence on *in vitro* proliferation and differentiation.

Furthermore a deep investigation concerning the kinetics of the Michael-type addition was performed. Due to its versatility, Michael addition is a precious tool for the bioconjugation often used also for HA-derivatisation. Thus we deeply studied the effect of the reagents architecture (influence of the Michael donor and acceptor), their stability and that of the Michael adducts.

---

## Contents

---

---

*To my mummy, daddy, sister and all the rest of my family.*



# 1 INTRODUCTION

## 1.1 NEW THERAPIES FOR MUSCULAR DYSTROPHY

Muscular dystrophies are a clinically and molecularly heterogeneous class of genetic disorders that are characterized by the primary wasting of skeletal muscle, and hence seriously compromise patient mobility and quality of life. In the most severe case, Duchenne muscular dystrophy (DMD), respiratory and cardiac functions are affected, leading to wheelchair dependency, respiratory failure and premature death. DMD is a severe X-linked recessive, progressive muscle-wasting disease affecting 1 in 3500 boys. The average life expectancy for patients afflicted with DMD is around 25.

The mutation affects the proteins that form a link between the cytoskeleton and the basal lamina, e.g. the dystrophin (Figure 1). A mutation in one of these proteins often causes the disassembly of the whole complex, leading to increased fragility of the sarcolemma, especially during intense contractile activity and focal or diffuse damage to the fibers. With time, the muscle tissue is progressively replaced by connective and adipose tissue.<sup>1</sup>

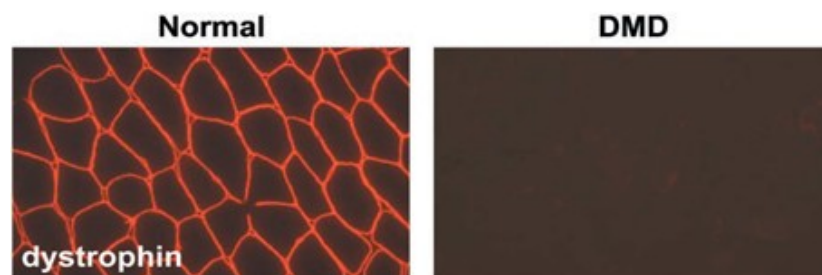


**Figure 1: Dystrophin in normal and dystrophic muscle**

Immunohistochemistry images visualize dystrophin in human muscle taken from healthy controls (first column) and from patients with Duchenne muscular dystrophy (second column).<sup>1</sup>

Muscular dystrophies are among the most difficult diseases to treat: this is due to the fact that

skeletal muscle is very abundant in the body and is composed of large multinucleated fibers, the nuclei of which have permanently lost the ability to divide. Consequently, any cell or gene replacement must restore proper gene expression in hundreds of millions of postmitotic nuclei, which are embedded in a highly structured cytoplasm and surrounded by a thick basal lamina.

Similarly, most pharmacological trials must overcome the complex biochemical mechanism of fiber degeneration. Nevertheless, the results that have been accumulated during the last few years have opened new perspectives.

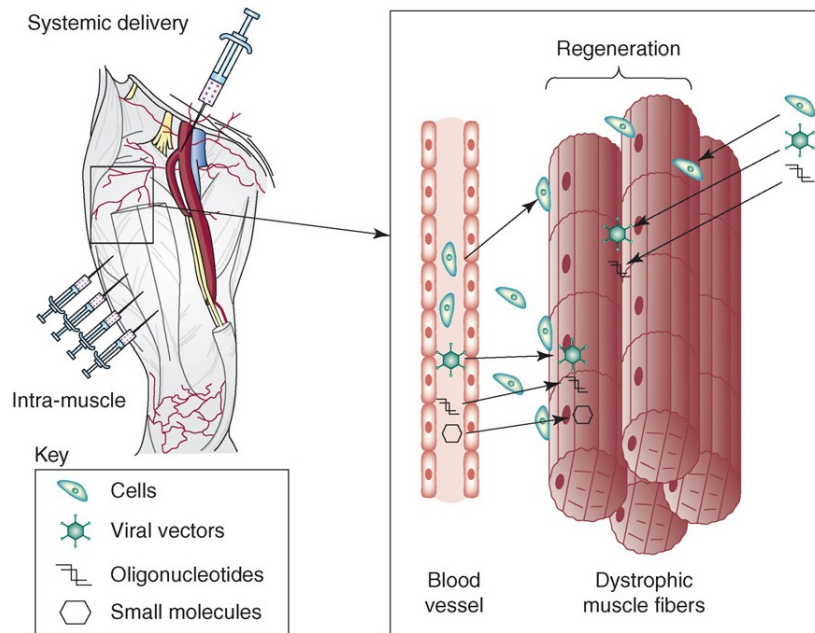


**Figure 2: Different delivery strategies of the therapeutic agents**

Different delivery strategies for cells, viral vectors and small molecules. Intramuscular injection will require multiple injections for delivery to only a small volume of a given muscle. Systemic delivery would overcome this limitation, but crossing the vessel wall and the muscle basal lamina could be a problem. Small molecules will usually be administered orally and reach the muscle through the circulation.<sup>3</sup>

Although muscular dystrophies still lack in an effective therapy, several novel strategies are

---



entering or are ready to enter clinical trials. The different approaches are based on drug, gene and cell therapies and clinical experimentation has already begun.<sup>2,3</sup>

It is important to underline that each strategy has advantages and limitations: for example, strategies that repair the dystrophin gene might be suitable only for a subset of mutations, whereas cell and gene therapies are limited by costs related to cell or vector production and can be available only for a limited number of patients. A second consideration is that local delivery of the therapeutic agent is necessary as proof of principle but real clinical benefit can only follow systemic delivery. Similarly, possible adverse events will be apparent following systemic delivery only (Figure 2).

Nevertheless, the results that have been accumulated during the last few years have opened new perspectives for all these different approaches.

### **1.1.1 The pharmacological approach**

Several pharmacological strategies have been attempted to counteract the consequences of the dystrophic process. Among them the most common envisage the use of protease inhibitors, calcium blockers and drugs that act on protein and lipid metabolism.<sup>4</sup> Only few of these have produced promising results in mice and even fewer have entered clinical trials, with modest final success.

These are based on the knowledge about chronic inflammation that accompanies fiber degeneration and that leads to sclerosis and reduction of the vascular supply. This starts a vicious circle that reduces oxygen supply and increases the degeneration for surviving and regenerates fibers.<sup>1</sup> Therefore, anti-inflammatory molecules appeared to be the logical therapeutic strategy and, for more than a decade, corticosteroids have represented the only pharmacological therapy with relatively modest but consistent beneficial consequences.

Recent data indicate that corticosteroid treatment in DMD can delay the loss of independent

---

ambulation by 2 to 4 years, significantly reduces the risk of developing skeletal defects and delays the respiratory and cardiac failure. However, their use is associated with significant side effects, such as weight gain and osteoporosis with the risk of bone fractures.<sup>5</sup>

Recently, insulin growth factor 1, which is a well known muscle growth factor, and myostatin, a negative regulator of muscle growth, have been identified as important factors regulating the functionality in muscle tissue. In fact, when mice overexpressing growth factor 1 were crossed to mdx mice (a model for DMD), dystrophy was attenuated.<sup>6</sup> Similarly, when neutralizing antibodies against myostatin were systemically delivered to mdx mice, dystrophic mice showed a dramatic delay of muscle wasting.<sup>7</sup>

Other proteins have been identified that stimulate muscle regeneration and ameliorate dystrophy, such as integrin  $\alpha 7$ , acetyl-*N*-galactosamine transferase, and A disintegrin and metalloprotease 12.<sup>8</sup>

As an alternative approach, a high-throughput screen for small molecules was carried out but, so far, no new candidate drugs have been identified.

Finally, the expression of nitric oxide synthase increased angiogenesis and also resulted in the amelioration of the mdx phenotype by counteracting the reduced vascular supply that accompanies fiber degeneration, inflammation and sclerosis.<sup>9</sup>

In conclusion, considering that muscular dystrophy defects result from the premature degradation of proteins that are important for muscle function and maintenance, these pharmacological agents might be invaluable for slowing down the progression of the disease, ameliorating the quality of life of the patient and, at the same time, increasing the chance of success for gene or cell therapy. Anyway, it remains to be seen whether these strategies can be applied as a treatment, since the toxicity of these molecules must be assessed.

### 1.1.2 Gene therapy

As gene therapy are named the strategies act to replace the mutated gene. Common problems with this strategy are the immune response to the vectors, and specific to muscular dystrophy is the gene delivery to the majority of postmitotic muscle fibers. In fact the task of replacing a missing gene in all, or at least in a good proportion, of the post-mitotic nuclei of skeletal muscle is clearly daunting.

Adenoviral are vectors with the property not to be integrated into the genome and not to replicated during cell division; they raised much hopes in the past but, because of their great immunogenicity and large size (limiting diffusion in the muscle tissue), they are no longer used.<sup>10</sup>

Adeno-associated vectors instead, are characterized by reduced size and lower immunogenicity and are currently the vectors of choice.<sup>11</sup>

In France the intramuscular injection in the radial muscle of  $\gamma$ -sarcoglycan-expressing adeno-associated viral vectors is already at phase I and II in clinical trials for limb girdle muscular dystrophy 2C.

In the case of dystrophin, two strategies are currently being tested in the dystrophic dog and have already entered, or are ready to enter, clinical experimentation: exon skipping and expression of dystrophin variants of reduced size.

Exon skipping is based on the use of small pieces of DNA, called antisense oligonucleotides, which act as “molecular patches”; this molecular strategy prevents the transcription of the exon containing the mutation. DMD, for example, is characterised by the lack of exon 53 in the gene encoding the production of dystrophin, hence the use of a “molecular patch” designed to mask exon 53 may be able to reduce the symptoms of DMD by the production of dystrophin protein shorter but functional.<sup>12</sup>

In an alternative strategy, minigenes were constructed with reduced number of centrally located spectrin-like domains and preserved amino- and carboxy-terminal domains. The minigenes have been shown to substitute for the wild-type gene when expressed as transgenes in mdx mice, a model for DMD.<sup>13</sup> However, the resulting microdystrophins were found to be less effective in protecting muscle fiber integrity in larger animals, as indicated by dog studies.<sup>14</sup>

### 1.1.3 Cell therapy

Satellite cells are small mononuclear progenitor cells found in mature muscle. They are precursors to skeletal muscle cells, able to give rise to satellite cells or differentiated skeletal muscle cells.<sup>15</sup> These cells represent the oldest known adult stem cell niche, and are involved in the normal growth of muscle, as well as in regeneration following injury or disease. In undamaged muscle, the majority of satellite cells are *quiescent*; they neither differentiate nor undergo cell division. In response to mechanical strain, satellite cells become *activated*. Activated satellite cells initially proliferate as skeletal myoblasts before undergoing myogenic differentiation.

Since the identification of satellite cells, two alternatives appeared: the first one contemplated the use of cells obtained from a healthy donor, which express the normal copy of the mutated gene but induce an immune rejection, unless the patient is permanently immune suppressed; the second one involved the use of cells obtained from the patient, which do not require immune suppression but must be genetically corrected *in vitro* (to restore the expression of the mutated protein).

Satellite cells and cell lines have been used since the late 1970s, mainly through intra-muscular injection.<sup>3</sup> In a first study, the injection of wild-type myoblasts into mdx mice resulted in the conversion of muscles from dystrophin-negative to dystrophin-positive.<sup>16</sup> Unluckily, several of the subsequent clinical trials failed, mainly because of the poor survival and the very limited migratory capacity of injected donor cells.

---

Myogenic cell transplantation was continued and optimized in few laboratories in preclinical studies. However, the major problem still faced by this approach, is the lack of dispersion of donor cells, which remain in the area of injection, making it difficult to reach an even distribution within the whole muscle.

Anyway, the use of blood-born stem or progenitor cells might overcome the aforementioned limitation: in fact circulating cells make possible a systemic delivery, while satellite cells cannot cross the endothelial layer. This perspective became theoretically possible in the late 1990s, with the demonstration of cells in the bone marrow that could contribute to muscle regeneration following bone marrow transplantation;<sup>17</sup> even in this case, the extent of colonization by donor cells was very small, far from any hope of clinical benefit. However, during the last years, several reports have convincingly demonstrated that bone marrow stem-progenitor cells can be really promising to regenerate muscle.

## **1.2 MESOANGIOBLASTS: VASCULAR PROGENITORS FOR EXTRAVASCULAR MESODERMAL TISSUES**

Mesoangioblasts are multipotent progenitors of mesodermal tissues that express the key marker of angiopoietic progenitors. These cells are physically associated with the embryonic dorsal aorta in avian and mammalian species.<sup>18</sup>

Mesoangioblasts have been recently isolated and characterized from mouse, dog and human tissues;<sup>19</sup> interestingly, when transplanted *in vivo*, they give rise to multiple differentiated mesodermal phenotypes. Moreover, their ability to extensively self-renew *in vitro*, while retaining multipotency, and differentiate into most mesoderm types when exposed to certain cytokines or to differentiating cells of a mesodermal tissue, qualifies mesoangioblasts as a novel class of stem cells.

The demonstration that postnatal murine bone marrow contains a transplantable, circulating progenitor that can differentiate into skeletal muscle had important basic and applicative implications. Previously, skeletal muscle was thought to be capable of limited regeneration potential, conveyed by a local population of proliferation-restricted, committed progenitors, the satellite cells.<sup>20</sup>

Currently, the developmental origin of mesoangioblasts, their phenotypic heterogeneity, and the relationship with other mesoderm stem cells are not understood in detail and are the subject of active research. However, from a practical point of view, these cells have been successfully used in cell transplantation protocols that have yielded a significant rescue of structure and function in skeletal muscle of dystrophic mice and dogs. Since the corresponding human cells have been recently isolated and characterized, a clinical trial with these cells is planned in the near future.

The intra-arterial delivery of mesoangioblasts is possible because, when injected into the blood

---

circulation, they accumulate in the first capillary filter encountered and then these cells are able to migrate outside the vessel, but only in the presence of inflammation, as in the case of dystrophic muscle. Indeed, mesoangioblasts express many receptors for inflammatory cytokines and are able to migrate *in vitro* and *in vivo* in response to nuclear proteins released by necrotic cells and acting as potent inflammatory cytokine.<sup>21</sup> This property of mesoangioblasts was considered particularly interesting because if, in theory, these cells were injected into an artery, they would accumulate into the capillary filter and from there into the interstitial tissue of downstream muscles.

To test this possibility, in 2003, Cossu et al. injected wild-type mesoangioblasts into the right femoral artery of  $\alpha$ -sarcoglycan ( $\alpha$ -SG) null mice.<sup>22</sup>

The sarcoglycans (SG) are a family of transmembrane proteins involved in the protein complex responsible for connecting the muscle fibre cytoskeleton to the extracellular matrix, preventing damage to the muscle fibre sarcolemma. Duclos et al. attempted to generate a murine model by disrupting the  $\alpha$ -SG gene.  $\alpha$ -SG null mice developed progressive muscular dystrophy and ongoing muscle necrosis with age, a hallmark of the human disease.<sup>23</sup>

Following the injection through the femoral artery, tissue distribution of donor cells was analyzed after 24 hours; mesoangioblasts were detected outside the vessel wall and within the extracellular matrix of all downstream skeletal muscles, especially in areas where degeneration and regeneration were occurring.

The same research group also investigated whether injection of wild-type mesoangioblasts in the muscles of  $\alpha$ -SG null mice might restore expression of  $\alpha$ -SG and of the whole dystrophin complex. Very promising results were obtained: in fact, two months after a single injection of wild-type mesoangioblasts into  $\alpha$ -SG null mice, many areas of the quadriceps, tibialis anterior, soleus and gastrocnemius expressed  $\alpha$ -SG, whereas the protein was completely absent from the muscles of the untreated null mouse (Figure 3). Importantly no immune reaction occurred

---

against reconstituted fibers.

Furthermore the long-term effect of donor wild-type mesoangioblasts was studied injecting wild-type mesoangioblasts three times (at 40-day intervals) into the femoral artery of 2-month-old  $\alpha$ -SG null mice. Animals were then analyzed 4 months after the first injection. Also in this case, histological analysis of skeletal muscle tissue of mice treated by three injections showed an increased number of apparently normal fibers and reduction of the necrotic areas and of cellular infiltrates. Consistent with histology, immunofluorescence analysis revealed the widespread presence of  $\alpha$ -SG throughout the whole soleus muscle (more than 50% of the fibers), in contrast with the total absence of signal in untreated  $\alpha$ -SG null mice.

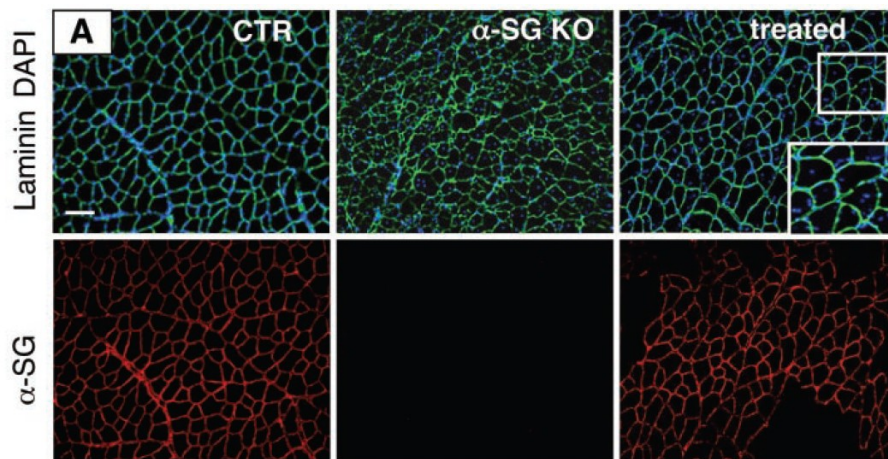


**Figure 3: Expression of  $\alpha$ -SG and other dystrophin-associated proteins in  $\alpha$ -SG null mice after intra-arterial delivery of wild-type mesoangioblasts**

(A) Low magnification of quadriceps from control (CTR) mice (left),  $\alpha$ -SG null ( $\alpha$ -SG KO) mice (centre), and treated  $\alpha$ -SG null mice (injected with wild-type mesoangioblasts 2 months before killing) (right). Large areas of the treated muscle expressed  $\alpha$ -SG after staining with a specific antibody (red). Sections were also stained with antibodies to laminin (green) and with DAPI (blue). Inset: Higher magnification of treated muscle with centrally located nuclei.<sup>22</sup>



The same paper<sup>22</sup> tested whether autologous, genetically corrected stem cells might represent a possible model for the therapy of muscular dystrophy: mesoangioblasts were isolated from vessels of juvenile dystrophic mice and genetically transduced to express  $\alpha$ -SG.

Four months after three intra-arterial injections of  $\alpha$ -SG dystrophic mesoangioblasts, many fibers expressed  $\alpha$ -SG on the membrane. In contrast, very few  $\alpha$ -SG-positive fibers were detected in the contralateral muscles of the noninjected leg. After long-term treatment with genetically corrected mesoangioblasts,  $\alpha$ -SG null mice had restored specific force and also showed an ameliorated motility.

As already mentioned, intra-arterial transplantation of donor mesoangioblasts was performed to ameliorate defective muscle structure and function not only in dystrophic mice, but also in dogs.<sup>14</sup>

The only animal model specifically reproducing the alterations in the dystrophin gene and the full spectrum of human pathology is the golden retriever dog model. Golden retriever muscular dystrophy (GRMD) affected animals present a single mutation in intron 6, resulting in the complete absence of the dystrophin protein, and early and severe muscle degeneration with nearly complete loss of motility and walking ability.<sup>24</sup> Death usually occurs at about 1 year of age as a result of failure of respiratory muscles.

To test the efficacy of cell or gene therapy, GRMD dogs were transplanted with either autologous genetically corrected or donor wild-type mesoangioblasts, under different regimes of immune suppression.<sup>14</sup>

Overall, the results showed that donor wild-type mesoangioblasts significantly ameliorate many symptoms of canine muscular dystrophy, whereas autologous genetically corrected cells are much less effective.

Specifically, they showed that it is possible to transplant mesoangioblasts into dystrophic dogs

---

and obtain an extensive reconstitution of fibres expressing dystrophin, an improvement in the contraction force and, in many cases, a preservation of walking ability. Even if, extensive variability exists between dystrophic dogs, this is the situation that will be faced with patients. Donor wild-type mesoangioblasts seemed to be more efficient than autologous, genetically corrected cells. Four of six dogs treated with donor cells showed clear clinical amelioration; of the remaining two, one died early and could not be analysed in detail and the other one probably received too few cells. At the end of immune suppression, two of the four dogs showing amelioration continued to walk well until the end of the experiment, whereas the other two, rapidly lost walking ability. This difference may reflect the different survival of transplanted organs after the end of immune suppression. Thus, the work reported really sets the logical premise for the start of clinical experimentation that may lead to an efficacious therapy for Duchenne muscular dystrophy.

As said above, isolation and characterization of the human counterparts of mouse mesoangioblasts from adult skeletal muscle was accomplished and they have been more precisely indicated as “pericyte-derived cells”.<sup>25</sup>

Cells derived from blood vessels of human skeletal muscle can regenerate skeletal muscle, similarly to embryonic mesoangioblasts. However, adult cells do not express endothelial markers, but instead express markers of pericytes, which are cells found in the central nervous system. Pericytes are more specifically located surrounding the endothelial cell layers of the capillary network in the brain.

Pericyte-derived cells differentiate into smooth muscle, osteoblasts or adipocytes after appropriate stimuli. When skeletal-muscle differentiation was induced by coculturing human adult pericyte-derived cells with mouse myogenic cells, a very high percentage (more than 50%) of nuclei fused into hybrid myotubes. Moreover, when exposed to muscle-differentiation medium, a large proportion (ranging between 20 and 40% in different experiments) of human

adult pericyte-derived cells spontaneously differentiated into myosin-positive multinucleated myotubes. No significant differences were observed between cells from normal or DMD muscle. Under similar conditions, approximately 60% of the myogenic cells derived from normal satellite cells differentiated into multinucleated myotubes. (Figure 4)

This result indicates the high skeletal myogenic potential for human pericyte derived cells.

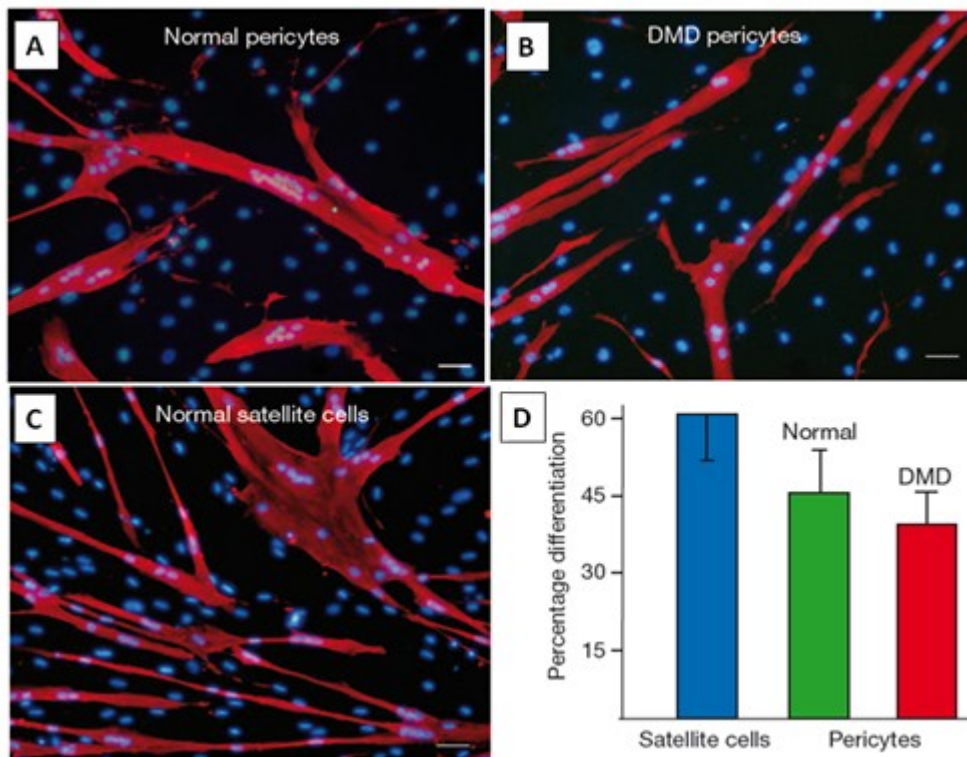


**Figure 4: *In vitro* myogenic differentiation of human pericyte derived cells**

Spontaneous differentiation of normal (A) and dystrophic (B) human pericyte-derived cells, cultured in differentiation medium on matrigel coated dishes. Normal human satellite cell-derived myotubes are shown in C for comparison. A quantitative analysis of the percentage of differentiation is shown in D.<sup>25</sup>

---

Pericyte-derived cells, when transplanted into severe combined immune deficient–X-linked, mouse muscular dystrophy mice, colonize host muscle and generate numerous fibres expressing human dystrophin.

Similar cells isolated from Duchenne patients, and engineered to express human mini-dystrophin, also give rise to many dystrophin-positive fibres *in vivo*. These data show that myogenic precursors, distinct from satellite cells, are associated with microvascular walls in the human skeletal muscle. They may represent a correlate of embryonic ‘mesoangioblasts’ present after birth and may be a promising candidate for future cell-therapy protocols in patients. For this purpose, from a strictly applicative point of view, the ideal cell population should be: present in easily accessible postnatal tissues; expandable *in vitro* to the large number of cells presumably required for systemic treatment; easily transducible with viral vectors; able to reach skeletal muscle through a systemic route; able to differentiate into skeletal muscle cells *in vivo* with high efficiency. Parietal cells, isolated from the microvasculature of human skeletal-muscle cells, were characterised and fulfil all these criteria.

Anyway, the possibility of using this novel strategy for the cell therapy in genetic diseases is strictly related to the capacity of expanding cells in culture in a reproducible and efficient way. Furthermore, a major limitation in the translation of stem cell technologies to clinical applications is the supply of cells. Advances in biomaterials engineering and scaffold fabrication enable the development of *ex vivo* cell expansion systems to address this limitation.<sup>26</sup> Progress in biomaterial design has also allowed directed differentiation of stem cells into specific lineages.<sup>27</sup>

## **1.3 BIOMATERIALS APPROACH TO EXPAND AND DIRECT DIFFERENTIATION OF STEM CELLS**

Whether cell-based therapies can achieve regeneration through direct tissue replacement or regenerative induction in resident tissue, a requirement common to all approaches is the organized delivery of cells to the area of interest. The rapidly expanding field of tissue engineering may supply the solutions.

Conventional definitions of tissue engineering focus on the development of biological substitutes to restore or replace damaged tissues. Impressive advances have been made in the fabrication of biocompatible and biodegradable scaffolds, cell seeding techniques, and implantation protocols.<sup>28</sup>

The final aim for clinical application is to provide a non-cytotoxic scaffold that acts as a template for three-dimensional tissue growth and as support for a variety of tissue types including fibrous, vascular, and organ-specific cells.

It is presumed that, as the seeded cells proliferate and integrate into the recipient tissue bed, the scaffold would be degraded, eventually dissolving completely and leaving behind a mature construct indistinguishable from the surrounding tissue. Current scaffold designs employ a variety of natural (collagen, hydroxyapatite, alginate) and synthetic (polyglycolide, polylactide, polylactide-coglycolide) materials as a basis for cell adhesion and differentiation.<sup>29</sup>

Incorporation of adhesion peptides such as RGD (Arg-Gly-Asp) into biomaterials and nanoscale surface manipulation have enhanced cell adhesion and migration.<sup>30-32</sup> The association of stimulatory growth factors has enhanced the proliferation of specific cell types.<sup>33</sup> It is expected that the scaffold would be incorporated into the host and eventually provide support for seeded and native cells equally. However, seeding and expanding the scaffold prior to implantation requires *ex vivo* nutrient exchange for the developing construct.

---

As biomaterial design and integration advance, it is important to consider the role of implanted materials in manipulating the recipient environment to promote regeneration in adult tissues. Growth factor and targeted gene delivery systems have already been used in biomaterial design to improve the native wound healing response around the implant.<sup>34</sup>

A logical next step in biomaterial design is to further manipulate the native environment to expose both seeded and endogenous stem cell populations to stimuli favouring regeneration.

A fundamental bottleneck that must be overcome to exploit stem cells for tissue engineering is the adequate supply of cells. This problem will become more critical when the engineering of bulk tissue or complex organs is contemplated, particularly when autologous tissue production is desired. Such goals would necessitate the maintenance of large quantities of undifferentiated cells to provide sufficient starting material. The long doubling time of most types of stem cell weighs directly on this problem. The doubling time of stem cells ranges from 36 h for human embryonic stem cells to an estimated 45 days for human hematopoietic stem cells.<sup>26</sup> Although a number of commercially available cell culture matrices such as Matrigel and Cartrigel have produced encouraging results, the animal origin of these products renders them undefined and precludes their widespread use in human clinical applications. A recent trend favours the use of animal-free products, with recombinant human substitutes for such animal products emerging as an attractive alternative. Concerns about exposure of human tissues to xenogenic products have been substantiated experimentally. Besides the risk of contamination by adventitious infectious agents, there are good evidences to suggest that human cells could incorporate and express immunogenic molecules present in animal products. Synthetic biomaterials could play a significant role in meeting the demands for well-defined systems for derivation and maintenance of stem cells.

Another important potential clinical application of stem cells is their use in cell replacement therapy for inherited genetic disorders. Indeed, using viral vector transduction, stem cells can

---

be manipulated *in vitro* to correct genetic aberrations or deficiencies. Hence they could be transplanted into patients to restore normal tissue function.<sup>26</sup>

A problem that must be faced when stem cells are used is the risk of tumorigenicity, due to their huge differentiation repertoire. Undifferentiated cells that retain pluripotency give rise to tumours known as teratomas. Hence, it is critical for any therapeutic strategy employing a stem cell-based approach to ensure complete and irreversible differentiation of stem cells into the desired progenitors or terminal target cell type. This may be accomplished by supplementing the appropriate trophic factors in the culture medium, or delivering them from a scaffold in a controlled manner.<sup>35</sup>

The mechanical properties of a scaffold or culture surface can also exert significant influence on the differentiation of the seeded stem cells. By exerting traction forces on a substrate, many mature cell types such as epithelial cells, fibroblasts, muscle cells, and neurons sense the stiffness of the substrate and show dissimilar morphology and adhesive characteristics.<sup>36</sup>

Another important role of the scaffolds is to prevent their cellular cargos to be destroyed from the host immune system, obviating the need for a harsh immunosuppressive regime to promote the survival of grafts. The incorporation of immuno-modulatory molecules into biomaterial designs may represent a strategy to tackle the issue of immune-rejection.

In conclusion, the convergence of two important disciplines, i.e. biomaterials engineering and stem cell research, promises to revolutionize regenerative medicine. New applications and improvement upon current designs will depend heavily on innovations in biomaterials engineering.

---

## 1.4 HYALURONAN

A tissue engineered implant has to be designed specifically for a given tissue; it has to match the mechanical properties of the receiving body, with limited immuno- or antigenicity, and tunable biodegradability. Therefore, in order to optimize the physical and biological characteristics of the engineered tissue, the choice of the biomaterial is crucial. This study is focused on different methodologies that can be used for the chemical modification of the hyaluronic acid (HA), key building block for producing advanced biomaterials.

Hyaluronic acid (also known as hyaluronan or hyaluronate) (HA) is structurally the simplest glucosaminoglycan (GAG). It is composed of alternating units of a repeating disaccharide, (1→4)-β linked D-Glucuronic and (1→3)-β linked *N*-acetyl-D-Glucosamine, alternate in a linear chain; in their repetition, they offer alternating hydrophobic and hydrophilic disaccharidic faces, which provide an amphiphilic “ribbon” structure to HA (Figure 5).<sup>37</sup>

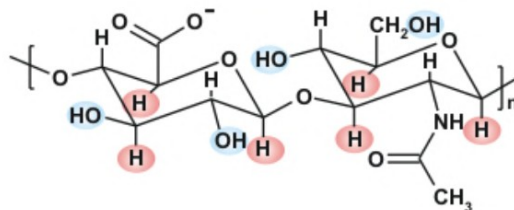


**Figure 5: Structure of hyaluronan**

The mere unit of the polysaccharide is composed by glucuronic acid (with a charged carboxylic acid at physiological pH) and *N*-acetyl glucosamine. As highlighted in red in this figure, a cluster of hydrogen atoms is on one face of the disaccharide, which may confer a more hydrophobic tendency to one face of the polymer as it is bearing on the other face hydrophilic groups highlighted in blue.

HA is a major component of the ECM of soft tissue (vitreous humor of the eye, synovial fluid, skin, brain, liver), and, in contrast to other GAGs, it is not covalently linked to a core protein.



It is synthesized by the hyaluronan synthases, Has1, Has2 or Has3, which are generally localized in the inner space of the plasmic membrane. HA is extruded in the ECM as it is synthesized and its molecular weights can range from  $10^3$  (serum) to  $10^7$  Da (eye vitreous humor).

In dilute solution, HA chains occupy a large volume because of the electrostatic repulsion between carboxyl groups, with a considerable amount of water trapped inside the coiled structure and the hydrophilic face of the polymer.

In more concentrated solutions, HA chains entangle, generating a sort of porous non-crosslinked dynamic network, with intrinsic swelling pressure due to an increasing intra- and intermolecular electrostatic repulsion, which allows to rapidly re-swell the material after a mechanical action has squeezed the water away. Consequently, HA is capable of profound effects on the distribution and movements of water and plays a major role in water homoeostasis. This hydrodynamic characteristic provides flexibility to the tissue and hyaluronan-rich matrices can generate enough internal pressure to mechanically break structures in order to create open spaces for cells to move into.

Literature evidence points out that HA can have an inhibitory or stimulatory effect on cellular proliferation depending on its size and concentration within the tissue.<sup>38</sup>

HA has been often regarded as excellent space filler, which can be advantageous for mediating deformations during cell proliferation or tissue remodelling. Its viscous properties indeed confirm this interpretation.<sup>39</sup>

The viscosity of HA homogeneous solutions at very low or null shear rate depends on its concentration and molecular weight in a non-linear fashion. This depends on the extent of interactions/overlap between polymer coils. Additionally, no clear evidence of HA inter-chain association has been discovered to date, confirming, therefore, that HA macromolecular can be seen as largely non-entangled water-rich coils, i.e. efficacious space fillers and shock

---

absorbers.<sup>40</sup>

Due to its peculiar physico-chemical properties and rather easy chemical derivatization, HA has been used in a number of clinical applications, that can be categorized as follows:<sup>41</sup>

1. visco-surgery – to protect delicate tissues and provide space during surgical manipulations, as in ophtalmological surgeries;
2. visco-augmentation – to fill and augment tissue spaces, as in skin, sphincter muscles, vocal and pharyngeal tissues;
3. visco-separation – to separate connective tissue surfaces traumatized by surgical procedures or injury, in order to prevent adhesions and excessive scar formation;
4. visco-supplementation – to replace or supplement tissue fluids, such as replacement of synovial fluid in painful arthritis, and to relive pain;
5. visco-protection – to protect healthy, wounded, or injured tissue surfaces from dryness or noxious environmental agents, and to promote the healing of such surfaces.

Generally, successful clinical biomaterial products should be simple and should have defined chemical composition that can be easily used by physicians.<sup>42</sup> Moreover the use of biopolymers ensures intrinsic biodegradation pathways and recognition by biological systems while many commonly used synthetic materials cause some degree of inflammatory response, lack an intrinsic biological interaction with delivered cells and host tissues, and are cleared by non-biological degradation mechanisms.

## **1.5 AIMS AND OBJECTIVES**

A wide range of materials based on HA that have been developed in recent years. The versatility in HA macromer synthesis and processing of the materials has transitioned into materials with a range of properties useful in applications such as tissue engineering and drug delivery.

Additionally, HA-based derivatives may impart biological activity to cells, as evident by changes in cellular behavior, including stem cell differentiation, when interaction occurs with biomaterials based on HA compared to other polymers. One area that deserves investigation is the potential utility of HA-based materials in translational applications, related in particular to the processing capabilities, biocompatibility, and efficacy of these materials.

The present study is focused on different methodologies that can be used for the chemical modification of the HA, key building block for producing advanced biomaterials.

Our interest merges with that about the biology of skeletal muscle stem cells and seeking to harness the information for clinical applications. By learning more about stem cells and other mesodermal skeletal muscle progenitors, we can learn how to better use them to repair muscle. Considering, however, that the main limitations of stem cells are the loss of “stemness” upon culture and an inability to cross the vessel wall for the systemic delivery, a biomaterial that could help to overcome these issues would be a key tool for the development of an effective cell-based therapy for DMD.

---

## 1.6 REFERENCES

- 1 Blake, D. J., Weir, A., Newey, S. E. & Davies, K. E. Function and Genetics of Dystrophin and Dystrophin-Related Proteins in Muscle. *Physiological Reviews* **82**, 291-329, doi:10.1152/physrev.00028.2001 (2002).
- 2 Cossu, G. & Sampaolesi, M. New therapies for muscular dystrophy: cautious optimism. *Trends in Molecular Medicine* **10**, 516-520, doi:10.1016/j.molmed.2004.08.007 (2004).
- 3 Cossu, G. & Sampaolesi, M. New therapies for Duchenne muscular dystrophy: challenges, prospects and clinical trials. *Trends in Molecular Medicine* **13**, 520-526, doi:10.1016/j.molmed.2007.10.003 (2007).
- 4 Urtizbera, J. A. Therapies in Muscular Dystrophy: Current Concepts and Future Prospects. *European Neurology* **43**, 127-132 (2000).
- 5 Manzur, A. Y., Kuntzer, T., Pike, M. & Swan, A. Glucocorticoid corticosteroids for Duchenne muscular dystrophy. *Cochrane Database Syst Rev*, CD003725, doi:10.1002/14651858.CD003725.pub2 (2004).
- 6 Barton, E. R., Morris, L., Musaro, A., Rosenthal, N. & Sweeney, H. L. Muscle-specific expression of insulin-like growth factor I counters muscle decline in mdx mice. *J Cell Biol* **157**, 137-148, doi:10.1083/jcb.200108071 (2002).
- 7 Bogdanovich, S. *et al.* Functional improvement of dystrophic muscle by myostatin blockade. *Nature* **420**, 418-421, doi:10.1038/nature01154 (2002).
- 8 Engvall, E. & Wewer, U. M. The new frontier in muscular dystrophy research: booster genes. *FASEB J* **17**, 1579-1584, doi:10.1096/fj.02-1215rev (2003).
- 9 Wehling, M., Spencer, M. J. & Tidball, J. G. A nitric oxide synthase transgene ameliorates muscular dystrophy in mdx mice. *J Cell Biol* **155**, 123-131, doi:10.1083/jcb.200105110 (2001).
- 10 Douglas, J. T. Adenoviral vectors for gene therapy. *Mol Biotechnol* **36**, 71-80, doi:MB:36:1:71 (2007).
- 11 Wang, Z. *et al.* Sustained AAV-mediated dystrophin expression in a canine model of Duchenne muscular dystrophy with a brief course of immunosuppression. *Mol Ther* **15**, 1160-1166, doi:6300161/10.1038/sj.mt.6300161 (2007).
- 12 Goyenvalle, A. *et al.* Rescue of dystrophic muscle through U7 snRNA-mediated exon skipping. *Science* **306**, 1796-1799, doi:1104297/10.1126/science.1104297 (2004).
- 13 Deconinck, N. *et al.* Expression of truncated utrophin leads to major functional improvements in dystrophin-deficient muscles of mice. *Nat Med* **3**, 1216-1221 (1997).
- 14 Sampaolesi, M. *et al.* Mesoangioblast stem cells ameliorate muscle function in dystrophic dogs. *Nature* **444**, 574-579, doi:nature05282/10.1038/nature05282 (2006).
- 15 Mauro, A. Satellite cell of skeletal muscle fibers. *J Biophys Biochem Cytol* **9**, 493-495 (1961).

- 16 Partridge, T. A., Morgan, J. E., Coulton, G. R., Hoffman, E. P. & Kunkel, L. M. Conversion of mdx myofibres from dystrophin-negative to -positive by injection of normal myoblasts. *Nature* **337**, 176-179, doi:10.1038/337176a0 (1989).
  - 17 Ferrari, J. D. & Bach, B. R., Jr. Bone graft procurement for patellar defect grafting in anterior cruciate ligament reconstruction. *Arthroscopy* **14**, 543-545 (1998).
  - 18 Cossu, G. & Bianco, P. Mesoangioblasts — vascular progenitors for extravascular mesodermal tissues. *Current Opinion in Genetics & Development* **13**, 537-542, doi:10.1016/j.gde.2003.08.001 (2003).
  - 19 Tonlorenzi, R., Dellavalle, A., Schnapp, E., Cossu, G. & Sampaolesi, M. Isolation and characterization of mesoangioblasts from mouse, dog, and human tissues. *Curr Protoc Stem Cell Biol* **Chapter 2**, Unit 2B.1 (2007).
  - 20 Ferrari, G. *et al.* Muscle regeneration by bone marrow-derived myogenic progenitors. *Science* **279**, 1528-1530 (1998).
  - 21 Scaffidi, P., Misteli, T. & Bianchi, M. E. Release of chromatin protein HMGB1 by necrotic cells triggers inflammation. *Nature* **418**, 191-195, doi:10.1038/nature00858 (2002).
  - 22 Sampaolesi, M. *et al.* Cell Therapy of  $\alpha$ -Sarcoglycan Null Dystrophic Mice Through Intra-Arterial Delivery of Mesoangioblasts. *Science* **301**, 487-492, doi:10.1126/science.1082254 (2003).
  - 23 Duclos, F. *et al.* Progressive muscular dystrophy in alpha-sarcoglycan-deficient mice. *J Cell Biol* **142**, 1461-1471 (1998).
  - 24 Sharp, N. J. *et al.* An error in dystrophin mRNA processing in golden retriever muscular dystrophy, an animal homologue of Duchenne muscular dystrophy. *Genomics* **13**, 115-121 (1992).
  - 25 Dellavalle, A. *et al.* Pericytes of human skeletal muscle are myogenic precursors distinct from satellite cells. *Nat Cell Biol* **9**, 255-267, doi:ncb1542/10.1038/ncb1542 (2007).
  - 26 Chai, C. & Leong, K. W. Biomaterials approach to expand and direct differentiation of stem cells. *Mol Ther* **15**, 467-480, doi:6300084/10.1038/sj.mt.6300084 (2007).
  - 27 Engler, A. J., Sen, S., Sweeney, H. L. & Discher, D. E. Matrix elasticity directs stem cell lineage specification. *Cell* **126**, 677-689, doi:S0092-8674(06)00961-5/10.1016/j.cell.2006.06.044 (2006).
  - 28 Martina, M. & Hutmacher, D. W. Biodegradable polymers applied in tissue engineering research: a review. *Polymer International* **56**, 145-157, doi:10.1002/pi.2108 (2007).
  - 29 Jagur-Grodzinski, J. Polymers for tissue engineering, medical devices, and regenerative medicine. Concise general review of recent studies. *Polymers for Advanced Technologies* **17**, 395-418, doi:10.1002/pat.729 (2006).
  - 30 Shu, X. Z. *et al.* Attachment and spreading of fibroblasts on an RGD peptide–modified injectable hyaluronan hydrogel. *Journal of Biomedical Materials Research Part A* **68A**, 365-375, doi:10.1002/jbm.a.20002 (2004).
  - 31 Ouasti, S., Kingham, P. J., Terenghi, G. & Tirelli, N. The CD44/integrins interplay and the significance of receptor binding and re-presentation in the uptake of RGD-functionalized
-

- hyaluronic acid. *Biomaterials* **33**, 1120-1134, doi:10.1016/j.biomaterials.2011.10.009 (2012).
- 32 Park, H. & Lee, K. Y. Facile control of RGD-alginate/hyaluronate hydrogel formation for cartilage regeneration. *Carbohydrate Polymers* **86**, 1107-1112, doi:10.1016/j.carbpol.2011.05.032 (2011).
- 33 Odorico, J. S., Kaufman, D. S. & Thomson, J. A. Multilineage differentiation from human embryonic stem cell lines. *Stem Cells* **19**, 193-204, doi:10.1634/stemcells.19-3-193 (2001).
- 34 Gurtner, G. C., Callaghan, M. J. & Longaker, M. T. Progress and potential for regenerative medicine. *Annu Rev Med* **58**, 299-312, doi:10.1146/annurev.med.58.082405.095329 (2007).
- 35 Zhang, Y., Lim, C. T., Ramakrishna, S. & Huang, Z. M. Recent development of polymer nanofibers for biomedical and biotechnological applications. *J Mater Sci Mater Med* **16**, 933-946, doi:10.1007/s10856-005-4428-x (2005).
- 36 Discher, D. E., Janmey, P. & Wang, Y. L. Tissue cells feel and respond to the stiffness of their substrate. *Science* **310**, 1139-1143, doi:10.1126/science.1116995 (2005).
- 37 Weissmann, B. & Meyer, K. The Structure of Hyalobiuronic Acid and of Hyaluronic Acid from Umbilical Cord<sup>1,2</sup>. *Journal of the American Chemical Society* **76**, 1753-1757, doi:10.1021/ja01636a010 (1954).
- 38 Huber, L. C. *et al.* Synovial fibroblasts: key players in rheumatoid arthritis. *Rheumatology (Oxford)* **45**, 669-675, doi:10.1093/rheumatology/kei065 (2006).
- 39 Fouissac, E., Milas, M. & Rinaudo, M. Shear-rate, concentration, molecular weight, and temperature viscosity dependences of hyaluronate, a wormlike polyelectrolyte. *Macromolecules* **26**, 6945-6951, doi:10.1021/ma00077a036 (1993).
- 40 Cowman, M. K. & Matsuoka, S. Experimental approaches to hyaluronan structure. *Carbohydrate Research* **340**, 791-809, doi:http://dx.doi.org/10.1016/j.carres.2005.01.022 (2005).
- 41 Goa, K. L. & Benfield, P. Hyaluronic acid. A review of its pharmacology and use as a surgical aid in ophthalmology, and its therapeutic potential in joint disease and wound healing. *Drugs* **47**, 536-566 (1994).
- 42 Prestwich, G. D. Engineering a clinically-useful matrix for cell therapy. *Organogenesis* **4**, 42-47 (2008).
-

## **2 CHEMICAL MODIFICATION OF THE HYALURONIC ACID**

### **2.1 INTRODUCTION**

Hyaluronic acid (HA) is a glycosaminoglycan ubiquitous in extracellular tissues of mammals. It is a material of increasing importance to biomaterials science and it is finding applications in diverse areas ranging from tissue culture scaffolds to cosmetic materials. Its properties, both physical and biochemical, in solution or in hydrogel form, are extremely attractive for various technologies concerned with body repair. The fabrication of new HA based scaffolding materials has been achieved by a variety of chemical modifications to provide mechanically and chemically robust materials. Even if the resulting derivatives might have physicochemical properties significantly different from the native polymer, they usually retain the biocompatibility and the biodegradability of native HA.

HA can be chemically modified in two different ways: cross-linking or conjugation. Basically the same chemical reactions are used in both cases but, while, in the first case, a compound is grafted onto one HA chain by a single bond, in the second case, different HA chains are linked together by two or more bonds, as depicted in Figure 6. In addition, there are different types of cross-linking procedures: direct crosslinking, crosslinking of HA derivatives and cross-linking of different HA derivatives.

## Chemical Modification of the Hyaluronic Acid

---

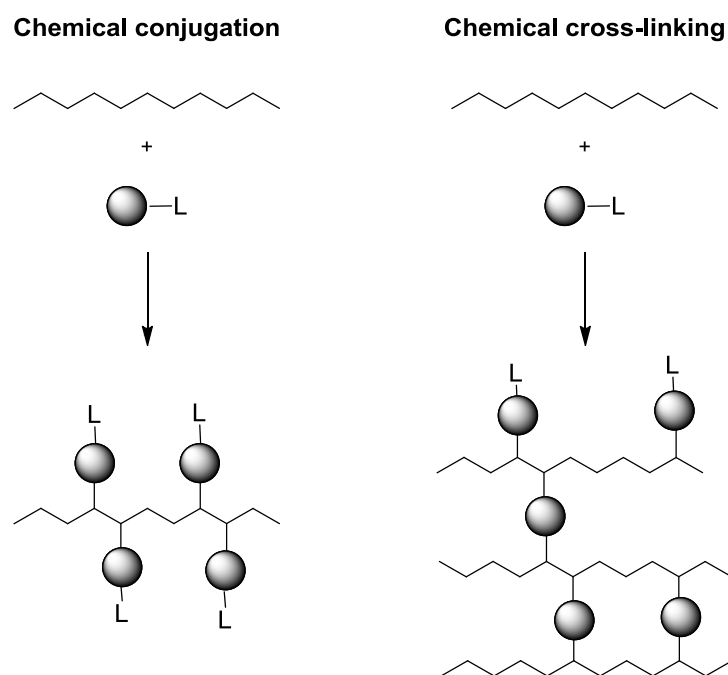


**Figure 6: Chemical conjugation and chemical cross-linking of a polymer**

The two available sites to chemically modify the HA are the carboxylic acid group and the hydroxyl group (Figure 7). Actually an amino group can also be made available by deacetylation of the *N*-acetyl group<sup>1</sup> the conditions required might cause the hydrolysis of the polymer. It is not possible to exactly know which of the hydroxy groups reacts, though it is reasonable to assume that the reaction occurs mainly at the hydroxyl of the C6 of the *N*-acetylglucosamine moiety of HA because of the better accessibility of primary alcohols for the reagents.

Although many of the modification techniques employed today have individual advantages, there is room for further improvement.



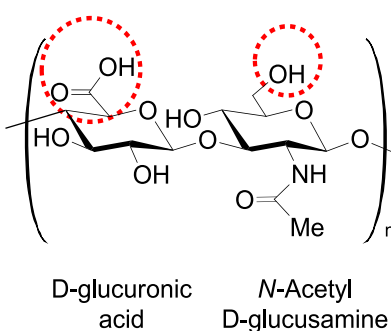


Figure 7: Repetitive unit of hyaluronan showing the primary sites for chemical modification

## 2.1.1 Modification of the carboxylic acid group

### 2.1.1.1 Esterification

Among the different techniques available for the formation of a new ester bond, a considerable number of them received particular attention for the derivatisation of HA, in order to provide materials suitable for tissue engineering.<sup>2</sup> Some examples are reported below.

#### 2.1.1.1.1 Ester formation by alkylation using alkyl halides

The esterification of HA carboxylic groups using alkyl halides, such as alkyl iodides or bromides, was patented in 1986 by Della Valle and Romeo.<sup>3</sup> The reaction was performed after the transformation of the hyaluronan in its TBA salt (soluble in DMSO and DMF), which was then reacted with an alkyl halide in an organic solvent, over a 12 h reaction time at 30 °C (Figure 8).

A similar approach has been used for the conjugation of ceramide, a cellular component, to HA. Chloromethyl-benzoyl chloride was chosen as linker; it was firstly reacted with ceramide and then with HA leading to the formation of a new ester bond.<sup>4</sup>

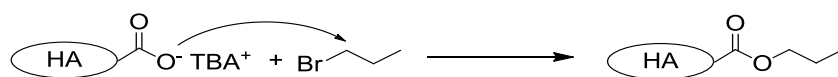


**Figure 8: HA esterification using alkyl halides**

### 2.1.1.1.2 Ester formation by alkylation using tosylates

In 2006 the cross-linking of HA by esterification using tetraethylene glycol was performed.<sup>5</sup> Briefly, tetraethylene glycol was converted into its di-tosylate, then the reaction of the latter with HA was performed in DMSO solution (Figure 9).

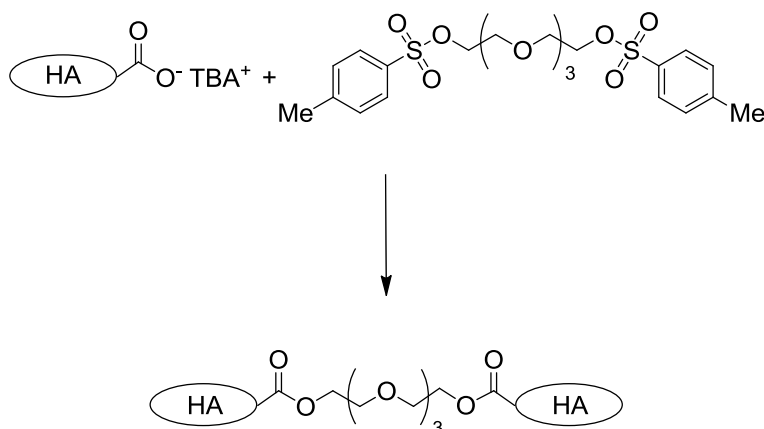


**Figure 9: HA esterification with tetraethylene glycol ditosylate**

### 2.1.1.1.3 Ester formation using diazomethane

The esterification of HA using diazomethane was reported for the first time by Jeanloz and Forchielli in 1950. Also in this case the reaction was performed on the HA-TBA salt in an organic

---

solvent, i.e. DMSO.<sup>6</sup>

Further development described the preparation of the methyl ester of HA using trimethylsilyl diazomethane (TMSD) as the carboxylic acid group activator (Figure 10).<sup>7</sup>

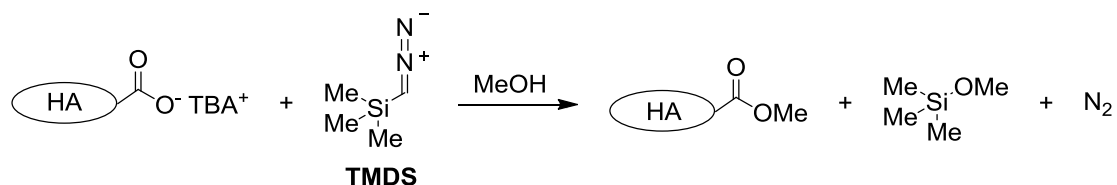


**Figure 10: HA esterification using trimethylsilyl diazomethane**

### 2.1.1.2 Amidation

The activation of the carboxylic acid function of the glucuronic unit has been accomplished by using several different methodologies well known in peptide synthesis, employing, in particular different activating agents (e.g. carbodiimides and triazolols) have been used in water on the sodium salt,<sup>8</sup> in organic solvents on the TBA salt,<sup>9</sup> or even under heterogeneous conditions.<sup>10</sup> This section reports only some of the most widely used techniques employed to activate the carboxylic acid function of the HA promoting the formation of a new amide. For a more exhaustive description, refer to recent reviews.<sup>11,12</sup>

#### 2.1.1.2.1 Carbodiimide-mediated HA amidation

Amidation with carbodiimides in water is one of the most widely used methods for HA modification.<sup>11</sup> The carbodiimide used is predominantly the 1-ethyl-3-[3-(dimethylamino)-propyl]-carbodiimide (EDCI) because of its remarkable solubility in water.<sup>13</sup> EDCI reacts with carboxylic acid, in water, at pH 4.75 to form activated intermediates, which then can react with

---

an amines. Amidation using EDCI offers the advantage related to the possibility of carrying out the reaction in water using native HA sodium salt, without preliminary handling. In addition, this method does not lead to the hydrolytic cleavage of the HA, maintaining its high molecular weight, which is responsible for its valuable viscoelastic properties.

The reaction mechanism for the formation of amide-based conjugates using carbodiimides involves two main steps: the first one is the activation of the carboxylic acid group of HA, where the carboxylate anion attacks the central carbon on the carbodiimide to form a reactive *O*-acyl-isourea intermediate; the second step involves the attack of a nucleophile onto the reactive *O*-acyl-isourea intermediate, resulting in the formation of an amide bond and an urea derivative as byproduct. As known, the *O*-acyl-isourea intermediate is susceptible to hydrolysis and can also rearrange to form a stable *N*-acyl urea by-product, which does not undergo any further reactions with amines. (Figure 11)

The reaction is very delicate as it is strongly pH-dependent and the optimal pH for the two steps is different. Indeed, carboxylic acid activation by EDCI is best performed in an acidic environment (pH 3.5–4.5), whereas the amide formation is best developed at high pH values, when the amine is deprotonated. But at such a high pH, EDCI is more rapidly hydrolyzed into the *N*-acyl urea byproduct and amidation might not occur. The compromise is therefore not easy and amines with high  $pK_a$  values are not smoothly conjugated to HA using this method even though contradictory experimental data have been reported: most authors have shown evidence of amidation under these conditions, while others reported that no amide linkage was formed between the carboxylic acid groups of HA and amino groups. Only the *N*-acylurea byproduct was obtained using the same pH of 4.75 as previously described by some authors.<sup>11</sup>

## Chemical Modification of the Hyaluronic Acid

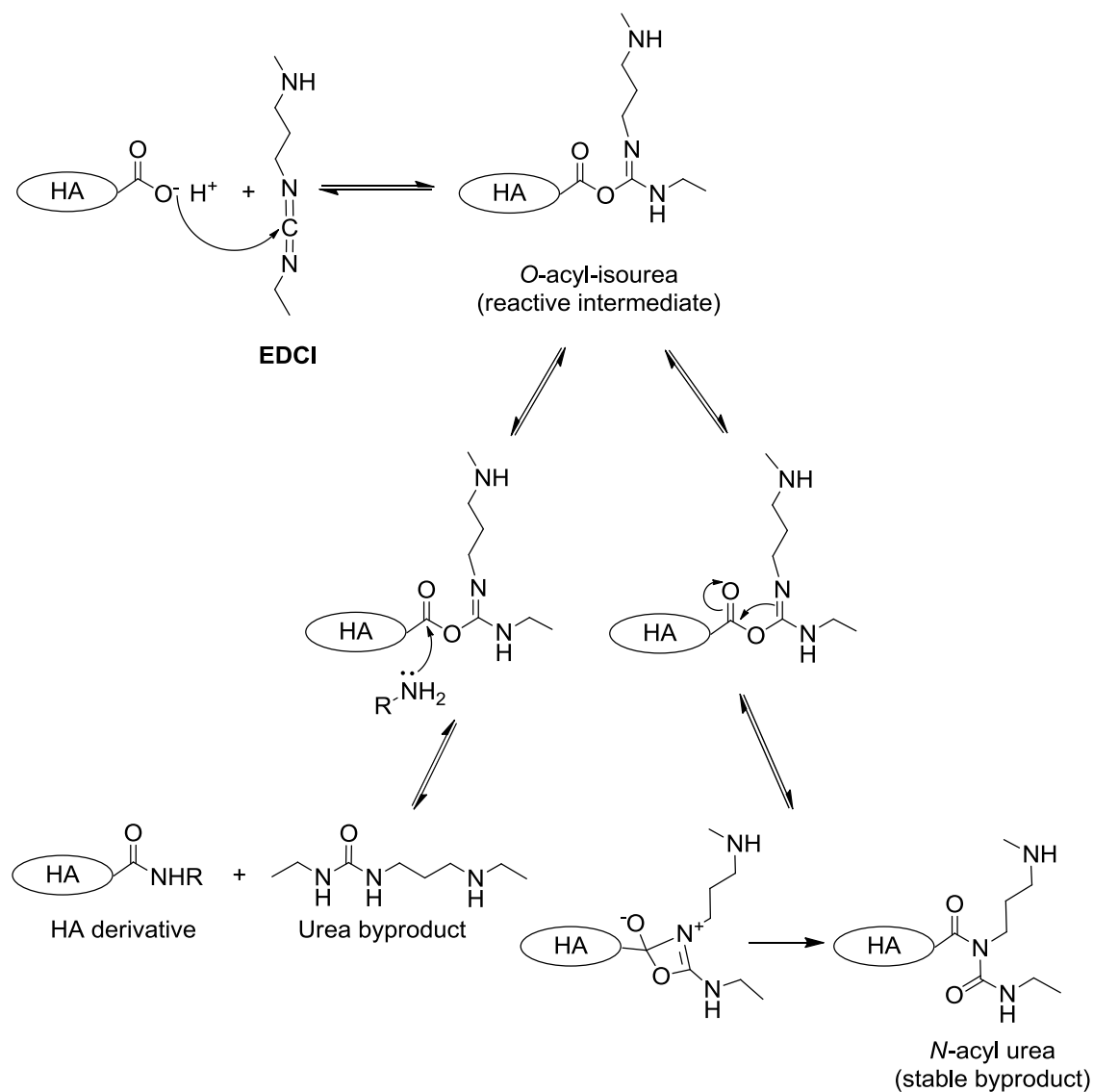


**Figure 11: EDCI-mediated HA amidation**

An important milestone in hyaluronan modification chemistry was the recognition that hydrazides, which display  $pK_a$  values between 2 and 4 for the corresponding conjugate acids, would retain their nucleophilicity at pH 4.75 and would couple efficiently to carbodiimide-activated glucuronic acid residues of hyaluronan.<sup>14</sup>

Other strategies reported in order to prevent the formation of the irreversible *N*-acylurea byproduct, contemplated the use of *N*-hydroxysuccinimide (NHS) or 1-hydroxybenzotriazole (HOBt) with EDCI to form more hydrolysis-resistant and non-rearrangeable intermediates.<sup>15</sup>

### 2.1.1.2.2 Chloro-4,6-dimethoxy-1,3,5-triazine (CDMT)-mediated amidation

More recently, Bergman reported a novel method for HA functionalisation using the carboxylic acid activator CDMT in the presence of *N*-methylmorpholine (NMM) as base.<sup>16</sup> The proposed reaction mechanism involves the formation of an activated HA-ester intermediate that can react with amines to generate the new amide bonds. (Figure 12)

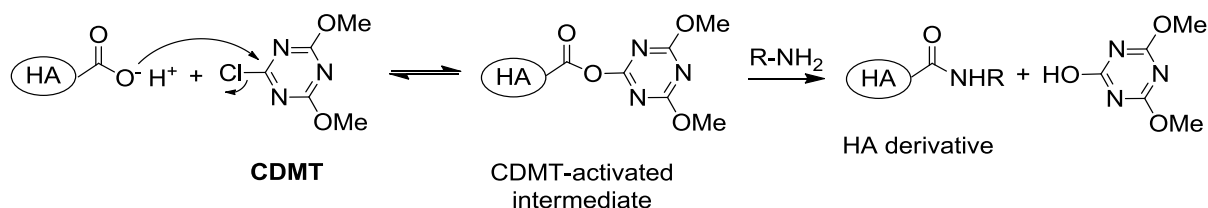


**Figure 12: CDMT-mediated HA amidation**

Using this amidation method (in a 3:2 water/acetonitrile mixture), a series of different amines have been grafted onto HA, resulting in substitution degrees up to 20%. This was achieved by employing a HA:CDMT molar ratio of only 1:0.5, and the authors suggested that an even higher degree of substitution could be achieved by decreasing this ratio.

The advantage of this amidation strategy is that the amine coupling efficiency mediated by CDMT is significantly higher compared to that typically achieved with carbodiimides and the reaction conditions are milder (i.e. pH 7). However, a mixture of both water and organic solvent is required for an acceptable solubilisation of CDMT.

---

### 2.1.1.2.3 4-(4,6-Dimethoxy-1,3,5-triazin-2-yl)-4-methylmorpholinium (DMTMM) mediated amidation

In the same year in which Bergman published his work on CDMT-mediated amidation of HA,<sup>16</sup> the group of Farkaš and Bystrický described the use of a more convenient one-step amidation reaction using the novel carboxylic acid activating agent DMTMM chloride, the quaternary ammonium chloride salt derived from CDMT and NMM (Figure 13).<sup>17</sup>

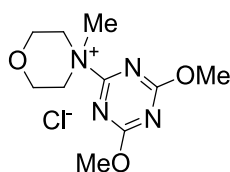


**Figure 13: Structure of DMTMM**

DMTMM allowed the amidation reaction to be carried out in aqueous-media without the need of an organic co-solvent and under mild conditions. The reaction mechanism is very similar to that of the CDMT-mediated amidation in the presence of NMM. Briefly, DMTMM chloride reacts with the carboxylic acid group of HA via an addition-elimination mechanism to form a DMTMM-activated HA ester intermediate, with NMM as the leaving group. Amines present in solution can then attack the activated ester to form the new amide bond.

By using this strategy, a number of amines have been linked to HA, reaching degrees of substitution up to 74 % using only a slight excess of DMTMM (1.5 equivalents with respect to the carboxylic acid groups of HA).

From these results, it can be concluded that DMTMM is an effective carboxylic acid activating mediators, superior to other activating agents such as the carbodiimides or CDMT, since it promotes the highest degrees of substitution in a convenient and simple one-step procedure, without the need of a large excess of reagents. Furthermore, the DMTMM-mediated amidation

---

of HA, carried out in aqueous media under mild conditions, does not involve the formation of concurred undesirable side-products.

### ***2.1.1.3 Multicomponents reactions***

The carboxylic acid function of HA showed to be active in some multicomponent reactions, like Ugi's and Passerini's reactions.<sup>18</sup> Several authors have described the Ugi condensation for HA crosslinking<sup>19,20</sup> using a diamine as a cross-linker to form diamide linkages between different polysaccharide chains.

The reaction with formaldehyde, cyclohexyl isocyanide and the diamine is performed in water at pH 3. The mechanism involves the initial condensation of the diamine with formaldehyde to form a protonated diimine species which then reacts with the cyclohexyl isocyanide. The carboxyl group of HA then eliminates the activated cyanide intermediate to form an (acylamino) amide bond (Figure 14).

As a drawback, the use of formaldehyde, which is known to be carcinogenic, requires specific handling. However, this method leads to the formation of a secondary amide, adding a second pending group, in this case, a cyclohexyl.



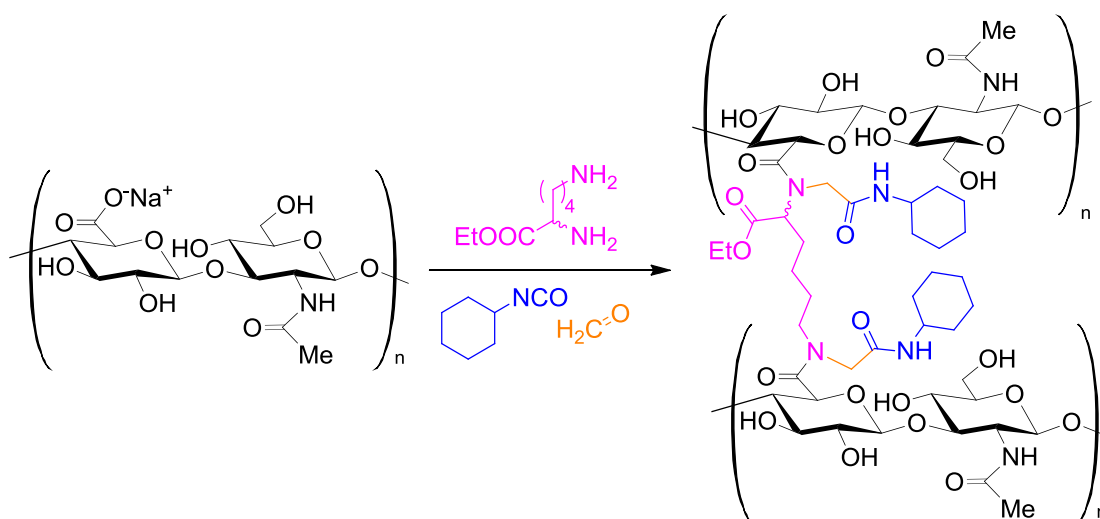


Figure 14: Proposed structure of the network formed by HA via Ugi's condensation with aqueous formaldehyde, cyclohexylisocyanide and lysine ethyl ester

### 2.1.2 Modification of the hydroxy group

The alcoholic moiety present on the hyaluronan scaffold exhibits reactivity towards electrophiles and several HA-derivatives have already been synthesised taking advantage of this property. It is not very well known which one of the hydroxy groups is the most reactive; anyway, it is reasonable to assume, that the reaction occurs mainly at the primary hydroxy group, since it is better accessible for reagents. Furthermore its  $pK_a$  value is sensibly lower than that of the other ones (i.e. about 9 for the primary alcohol group and about 13 for the others).

Some interesting modifications occurring at the alcoholic function are reported.

### 2.1.2.1 Ether formation

#### 2.1.2.1.1 Ether formation using epoxides

Epoxide ring opening, to form ether bonds with the HA hydroxy groups, has been reported by several authors.<sup>11</sup> Bisepoxides have been used to prepare crosslinked HA gels, such as ethylene glycol diglycidyl ether and polyglycerol polyglycidyl ether. The reaction is usually performed in aqueous solution at high pH values to promote the deprotonation of the hydroxy groups, thus increasing its nucleophilicity which should be higher than that of the deprotonated carboxy groups (Figure 15). The epoxides, therefore, react preferentially with the hydroxy groups to form ether bonds. However, if the pH is lower than the  $pK_a$  value of the hydroxy group, only a small quantity of hydroxy groups is deprotonated and the reactivity of the carboxylate anion is predominant, thus promoting the ester bond formation.<sup>21</sup>

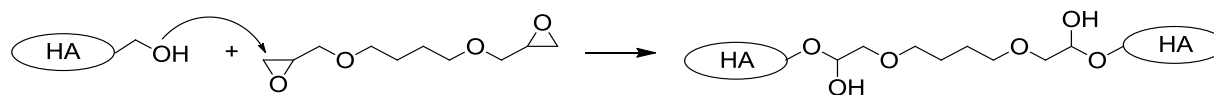
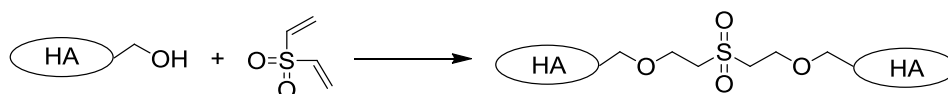


Figure 15: HA cross-linking with butanediol-diglycidyl ether in alkaline conditions

#### 2.1.2.1.2 Ether formation using divinyl sulfone

The cross-linking of HA with divinyl sulfone was patented in 1968.<sup>22</sup> The reaction is performed at high pH values (0.2M NaOH at pH > 13) at room temperature and creates sulfonyl bis-ethylene linkages between the hydroxy groups of HA (Figure 16). Interestingly they also found that the presence of salts such as NaCl in the reaction medium increases the cross-linking degree.



**Figure 16: HA cross-linking with divinyl sulfone**

### 2.1.2.2 Ester formation

The reactivity of the HA-alcohol with acyl-chlorides in organic solvents to create new ester bonds has been published.

In 2004 Ventura et al. described a novel method to form mixed butyric and retinoic acid esters of hyaluronan.<sup>23</sup> Specifically the TBA alcohol of HA-TBA was reacted in dry DMF, at room temperature, with the freshly prepared acyl-chlorides of butyric and retinoic acids. The synthesized compound afforded a high throughput for cardiogenesis in embryonic stem cells.

A parallel study presented a similar method to graft poly(lactic acid) oligomers activated by chloroacylation with thionyl chloride. In this case HA was previously converted into a cetyl-trimethylammonium salt, which is soluble in DMSO.<sup>24</sup>

HA esterification with anhydrides has been also successfully accomplished. In this case, due to the higher stability of anhydrides respect to acyl-chlorides, the reaction can be performed in water solution, even at rather high pH value. Methacrylated-HA was prepared by reacting HA with methacrylic acid anhydride, in ice cold water solution, for 12 h, at pH 8-10 (Figure 17).<sup>25</sup>

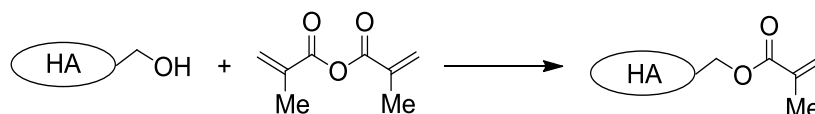


**Figure 17: HA esterification with methacrylic anhydride**

Moreover, HA was converted into two haloacetate derivatives, HA-bromoacetate (HABA) and HA-iodoacetate (HAIA). HABA was obtained by treating HA with bromoacetic acid anhydride under basic reaction conditions to favor the deprotonation of the primary alcohol. A high molar excess of reactant is required because of the formation of the mixed anhydride between bromoacetic acid anhydride and HA, which rapidly hydrolyses to restore the carboxylic acid groups. The final product (HABA) was converted into the iodo-derivative by nucleophilic substitution reaction with NaI.<sup>26</sup>

### 2.1.2.3 Periodate oxidations

The oxidation with sodium periodate of vicinal alcohol functions is a standard method for the chemical activation of glycoproteins. Reactive bis-aldehyde functionalities have been generated from hyaluronan following this strategy.<sup>11</sup> The resulting product can undergo reductive coupling with primary amines, cross-linking, insertion of peptides containing cell attachment domains or immobilized materials. Unfortunately the harsh conditions employed in the oxidative treatment also introduces chain fragmentation and potentially immunogenic linkages into the hyaluronan biomaterial.

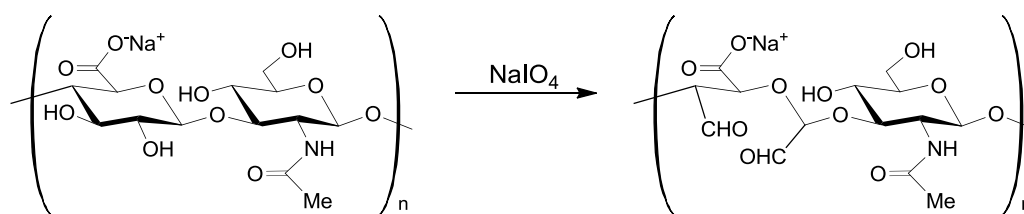


Figure 18: HA oxidation with sodium periodate

## 2.2 AMIDATION

### 2.2.1 INTRODUCTION

Polysaccharides are of great interest as immunogenic effectors and biocompatible carriers of small bioactive molecules and hyaluronan is attracting today great interest as a biomaterial for many medical applications.<sup>12</sup>

Obstacles to the development of new treatments taking advantage from its biocompatibility and biological effects, are its fast enzymatic degradation and the poor mechanical properties. Many chemical modifications and other physical techniques have been extensively described to prolong HA's residence in the body after administration in the body, to graft important bioactive molecules or drugs, and also to introduce new reactive groups on the HA scaffold.<sup>11</sup>

Carboxylated polysaccharides are suitable for many kinds of chemical modifications. The effective activation of the carboxy groups is the critical step. One of the commonly used methods rely on the activation with water-soluble carbodiimides (e.g. EDCI) which form intermediates that are able to link the nucleophilic groups of ligands (See 2.1.1.2.1 for a detailed description of the mechanism).

For example, Pasqui reported in 2007 the synthesis of an organo-silane HA derivative obtained by EDCI-mediated amidation with (3-aminopropyl)-trimethoxysilane. The reaction satisfactorily occurred in a 2-morpholino-ethanesulfonic acid (MES) buffer at pH 4.75, using a large excess of amine (Figure 19).<sup>8</sup>

The use of hydroxybenzotriazole (HOBt), *N*-hydroxysuccinimide (NHS) or other nucleophiles that react with the *O*-acyl-isourea intermediate to afford more stable activated species is also reported.<sup>11</sup>

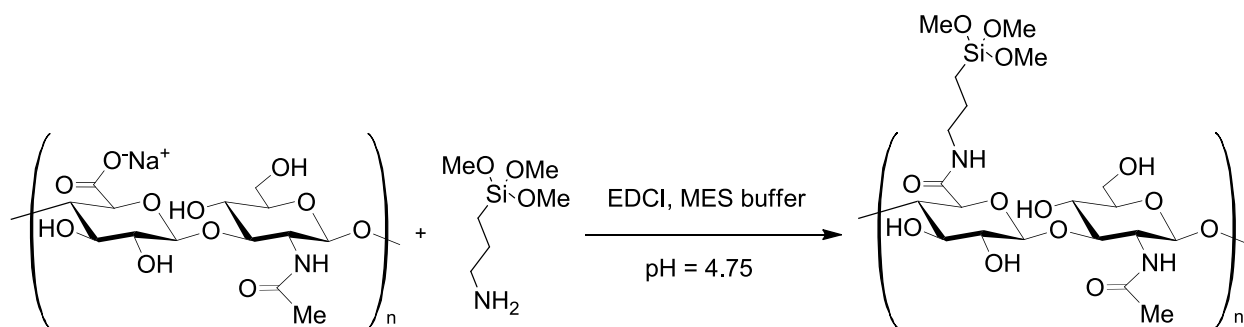


**Figure 19: Reaction scheme of the synthesis of the organo-silane HA derivative**

An alternative synthetic method contemplates the use of alkoxychloro-1,3,5-triazine as the carboxy group activator. It was originally used in peptide syntheses in anhydrous solvents.<sup>27</sup>

In 2007, the application of these types of activators on HA was reported.

In particular, Bergman presented a method for the preparation of HA derivatives obtained through triazine-activated amidation. A number of amines were successfully employed in HA amidation mediated by 2-chloro-4,6-dimethoxy-1,3,5-triazine (CDMT) as an activating species in a mixture of water and acetonitrile as solvent, under neutral conditions (See 2.1.1.2.2 for a detailed description of the mechanism).<sup>16</sup>

Farkaš envisaged the possibility of using the 4-(4,6-dimethoxy-1,3,5-triazin-2-yl)-4-methylmorpholinium chloride (DMTMM) as a more effective, as well as water soluble, condensing agent for the activation of the polysaccharide carboxyl groups.<sup>17</sup> It was observed that EDCI, under the same conditions, was much less efficient than DMTMM. Additionally, in situ preparation of the reagent primarily prevents the irritant properties of the CDMT component. Furthermore DMTMM became recently commercially available. The mechanism of the activation mediated by DMTMM involves the reaction of the ammonium salt through a  $S_NAr$  pathway to form a reactive triazinyl ester capable of undergoing the attack of a nucleophilic

species (e.g. the amine group). Thus, the two main advantages of using DMTMM over the conventional carbodiimides are certainly the structural purity of the products as well as the higher reaction yields. Moreover, DMTMM is more stable in water solution, whereas EDCI is prone to decompose at lower pH values.

In conclusion the amidation of HA is a very useful tool to modify the HA scaffold inserting bioactive molecules, forming reticulated network or adding new functional groups for further use in bioconjugation. Anyway a precise control of the degree of functionalisation remains an important issue. Moreover the development of techniques assuring an easy purification of the products and granting the chemoselectivity of the whole process is a key point in the study of new scaffolds for tissue engineering.

## **2.2.2 EXPERIMENTAL PROCEDURES**

### **2.2.2.1 Materials**

Sodium Hyaluronate (HA) RESILEN-200 (average molecular weight 235 kDa) was gently supplied by Kyowa Italiana Farmaceutici s.r.l. (Milan, Italy); HA sodium salt with Mw 35 or 305 kDa was purchased from Medipol (SA, Lausanne).

Spectrum Spectra/Por 6 RC Dialysis Membrane Tubing (10, 50, 100 kDa MWCO) was used to dialyse the samples.

*N*-(2-aminoethyl)acrylamide hydrochloride was gently synthesised by Dr Enrique Lallana Ozores (University of Manchester).

All reagents and solvents, if not otherwise specified, were purchased from Sigma-Aldrich (Milan, Italy or Gilligham, Dorset, UK) used as received.

### **2.2.2.2 General methods**

#### **2.2.2.2.1 Molecular characterization**

<sup>1</sup>H NMR spectra were recorded on a BRUKER AC300 or a BRUKER AC400 spectrometers.

Infrared spectra were recorded on a Jasco FT/IR 4100 or, in ATR mode (Golden gate), on a Tensor 27 Bruker spectrometer.

Absorbance readings were recorded on a BIOTek® Synergy 2 multi-mode microplate reader (NorthStar Scientific Ltd., Leeds, UK).

#### **2.2.2.2.2 Fluorescamine assay**

The degree of functionalisation of HA derivatives amidated with DMTMM was monitored by



measuring the remnant amine (i.e. *N*-(2-aminoethyl)acrylamide hydrochloride) content in final reaction samples. Briefly, an aliquot of 75  $\mu$ L of each reaction mixture was pipetted into a 96-wells black plate and diluted 1:2 with 4-(2-hydroxyethyl)-1-piperazinyl-ethanesulfonic acid (HEPES) buffer (100 mM, pH 7.4), followed by addition of 50  $\mu$ L of a freshly-prepared fluorescamine solution (3mg/ml) in acetonitrile. After the addition of fluorescamine the plate was shaken for 10 minutes, at medium speed, at 30 °C. The fluorescence was then determined using a plate reader with a 400 nm, 30 nm bandwidth, excitation filter and a 460 nm, 40 nm bandwidth emission filter.

### **2.2.2.2.3 Statistics**

Spectrophotometric experiments were carried out in triplicate, and the mean and standard deviations calculated for each reaction condition.

### **2.2.2.3 Synthetic procedures**

#### **2.2.2.3.1 General procedure for the synthesis of amidated-HA using EDCI**

100 mg of sodium HA (0.25 mmol of carboxy group, Mw: 235 kDa) was dissolved in 10 mL of phosphate buffer (100 mM, pH 4.5), to which EDCI (40 mg, 0.25 mmol, 1 eq.) was added, followed by addition of 10 eq. of the desired amine. The pH value was adjusted to 4.75 and the reaction mixture was stirred at room temperature for 24 h. The product was then transferred to a dialysis membrane (MWCO 50 kDa) and dialysed against distilled water for 7 days. The product was then freeze-dried to yield 70-78 mg (70-78% wt) of a white solid.

#### **2.2.2.3.2 General procedure for the synthesis of acrylamidated-HA using DMTMM (HA-Acr)**

100 mg of sodium HA (0.25 mmol of carboxy group, Mw: 35, 305 kDa) was dissolved in 10 mL of 4-(2-hydroxyethyl)-1-piperazinyl-ethanesulfonic acid (HEPES) buffer (100 mM, pH 7.4), to

---

which DMTMM (4 eq. respect to the desired degree of functionalisation: 0.40, 0.20 and 0.04 mmol respectively) was added and the mixture was stirred for 10 minutes. Thereafter *N*-(2-aminoethyl)acrylamide hydrochloride was added (1.2 eq. respect to the desired degree of functionalisation: 0.12, 0.06 and 0.01 mmol respectively). The reaction was stirred at room temperature for 24 hours. Then, the product was precipitated by dropwise addition of cold ethanol (approximately 20 times the reaction volume) under constant stirring. After centrifugation the supernatant was removed and the product transferred to a dialysis membrane (MWCO 10 or 100 kDa) and dialysed. Two different methods to dialyse were investigated:

*Method A:* the sample was dialysed against distilled water (4 °C) until constant conductivity of the outer water (about 3 days).

*Method B:* the sample was dialysed against a 1 mM solution of NaCl (4°C) for 24 hours and then against distilled water (4 °C) until constant conductivity of the outer water (about 3 days).

The product was then freeze-dried to yield 80-85 mg (80-85% wt) of a white solid. <sup>1</sup>H NMR (400 MHz, D<sub>2</sub>O) ( $\delta$  = ppm): 6.22 (m, 2H on unsaturated carbon), 5.79 (d,  $J$  = 8.6 Hz, 1H on unsaturated carbon), 4.54 (bs, 2H), 3.91-3.28 (m, 10H), 2.01 (s, 3H).

## 2.2.3 RESULTS AND DISCUSSION

### 2.2.3.1 *Carbodiimide activation*

It is well known that, to perform a reaction between a carboxy group and a nucleophile, an activating agent is required; 1-ethyl-3-[3-(dimethylamino)propyl]carbodiimide (EDCI), in particular has been widely used in organic synthesis because it shows a good activity also in aqueous media. In particular, the formation of amides from carboxylic acids and amines in aqueous media using EDCI is generally performed at pH 4.75; at this pH, the carboxylic acid is not deprotonated, and a small percentage of the amine may remain as a base in its nucleophilic form to produce a covalent adduct.<sup>13</sup> We initially tried this kind of reaction by using a set of different amines (Scheme 1).

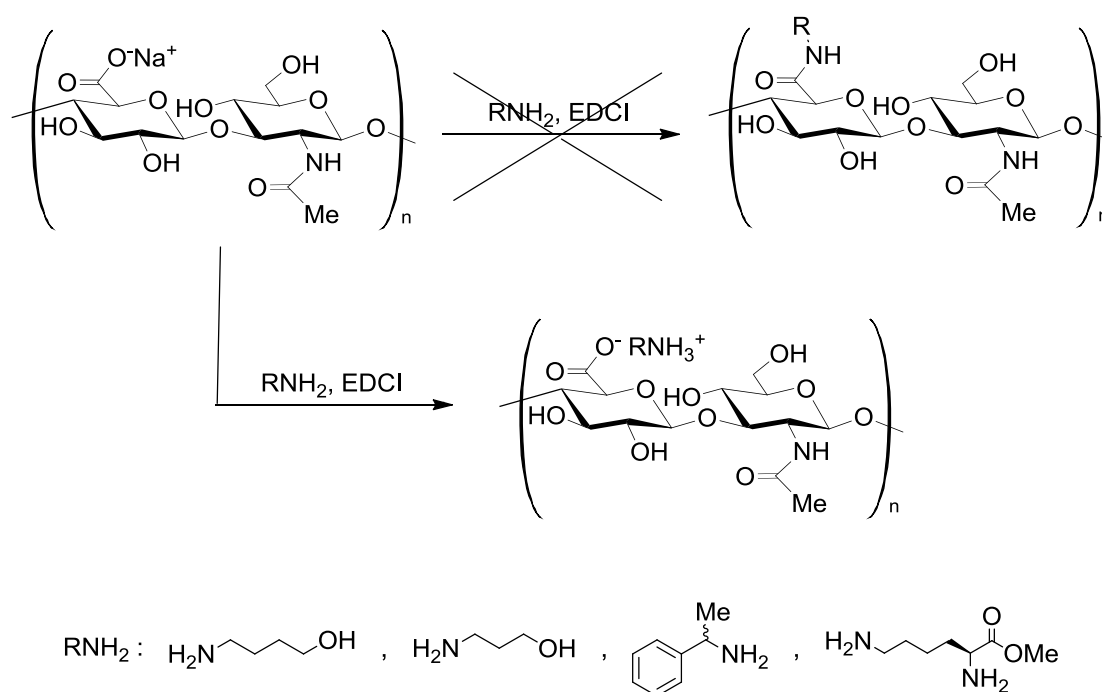
Different primary amines have been chosen meeting different purposes. In detail, 3-aminopropanol and 4-aminobutanol have been chosen to take advantage of the higher nucleophilicity of a primary amines respect to primary alcohols and, at the same time, to insert another nucleophile less sterically hindered respect to the others present on the HA backbone.  $\alpha$ -Methylbenzylamine was attractive in order to have a well defined <sup>1</sup>H NMR signal useful to evaluate the degree of functionalisation; furthermore, an interesting possibility was the development of a methodology allowing the cleavage of benzyl bonds through hydrogenolysis directly on HA-conjugates. A conjugate with lysine methyl ester should have combined both biological and chemical new aspects; it would have been a new amine decorating the polymer chain and, moreover, HA derivatives obtained by grafting amino-acids pendants, showed improved enzymatic stability.<sup>28</sup>

Specifically, EDCI and different amines were added to a solution of HA at controlled pH. The aim was to modify the hyaluronan with the maximum degree of functionalisation (defined as the ratio between modified and unmodified units) of 10%; higher levels of modification of the HA, in fact, affect its biological properties. The reagents were used in large excess respect to the

---

desired degree of functionalisation. However, no amide product was produced, the major product being the rearranged *N*-acylurea adducts which was hydrolysed to give back the free acid.

The purification process showed to be particularly challenging. During these experiments we found that, after the dialysis of the reaction mixture, part of the amine remains in the sample probably as counter ion (Scheme 1). This phenomenon could be observed and quantified by  $^1\text{H}$  NMR analysis. In order to check the importance of the cation in a biological environment, different hyaluronate salts have been tested in cultures of human pericyte-derived cells (See 2.5).



**Scheme 1: Modification of the HA carbodiimide mediated**

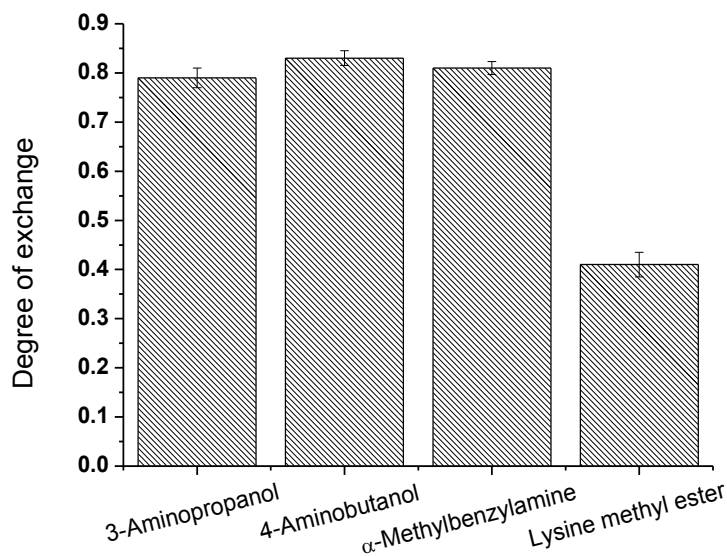


**Figure 20: Evaluation of the amine remained in the HA samples**

After extensive dialysis of the reaction mixture containing HA, EDCI and different amines, part of the amine remains in the sample. This phenomenon was quantified by  $^1\text{H}$  NMR analysis. The degree of exchange indicates the ratio between the number of moles of amine and the number of moles of repeating disaccharide units of HA.

We clearly demonstrated that no amide formation occurred by repeating the dialysis; in this case, the sample was dialysed against against a 1 mM solution of NaCl for 24 hours to promote the cation exchange and then against distilled water. Pure HA was recovered after this treatment.

Almost the same degree of exchange was observed for every sample (Figure 20) considering the ratio between the number of moles of amine and the number of moles of repeating disaccharide units of HA; in fact it was calculated to be 0.79 for 3-aminopropanol, 0.83 for 4-aminobutanol, 0.81 for  $\alpha$ -methylbenzylamine and 42% for lysine methyl ester but, in this case, the molecule featured two primary amines and hence two cations.

### **2.2.3.2 Triazolol activation**

Considering the very modest reactivity of amines as nucleophiles at pH 4.75, a different strategy has been investigated in order to provide amidation carboxylic acid of HA.

DMTMM is known to be an effective as well as water stable condensing agent for the activation of the polysaccharide carboxy groups and its efficiency in reaction involving HA had already been demonstrated.<sup>17</sup>

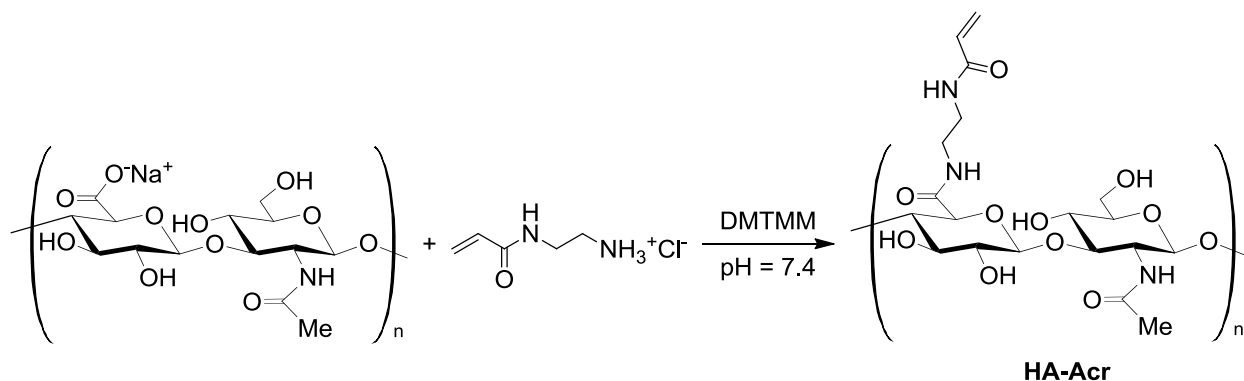
Our aim was to provide a derivative of HA featuring an acrylamide available as acceptor in Michael-type addition reaction. In fact, due to its versatility, Michael addition is a precious tool for bioconjugating specific bioactive molecules on different polymers. Several strategies for modifying and functionalising HA, taking advantage from this reaction, have already been reported.<sup>29,30</sup> A deep investigation on the factors influencing the outcome of the Michael-type addition between different  $\alpha,\beta$ -unsaturated compounds and thiol-containing nucleophiles highlighted that acrylamides provide adducts stable in front of the hydrolysis or of the retro-Michael reaction for a long time interval. Moreover the kinetics of the addition of *N*-acetyl cysteine on the double bond is reasonable for pH values higher than 8. These properties identify acrylamides as suitable functions for grafting bioactive molecules (e.g. peptides) to the HA scaffold. (See Chapter 3)

A very important target is the control of the loading of the bioactive molecule on the HA; hence a method allowing the modification of the HA with different degrees of functionalisation is required; moreover an analytical technique able to give a precise indication about the yield of the reaction is necessary. Activation of HA with DMTMM and evaluation of the degree of functionalisation with fluorescamine assay permitted to attain the desired target.

The synthesis of six different derivatives of the HA has been accomplished, specifically we used HA characterised by two different average molecular weights (i.e. 35 and 305 kDa), trying to

obtain three different degrees of functionalisation (i.e. 1, 5, 10%). As already mentioned, the 10% is the maximum degree of functionalisation which allows to preserve the biological properties of native hyaluronan.

The carboxylic acid groups of the HA were activated with DMTMM (4 eq. respect to the desired degree of functionalisation), at pH 7.4 and then reacted with *N*-(2-aminoethyl)acrylamide hydrochloride (1.2 eq. respect to the desired degree of functionalisation) at room temperature for 24 hours (Scheme 2).



**Scheme 2: Synthesis of amidated HA featuring an acrylamide**

The product was recovered after precipitation, effected by adding ethanol, dialysis and lyophilisation. The precipitation of the product as the first purification process, sensibly reduces the dialysis time.

Pure products have been obtained both dialysing the samples against distilled water or against a 1 mM solution of NaCl first, and then against distilled water. Furthermore, the conductivity of the dialysis water compartment was monitored in order to gain a clear indication of the time required for the completion of the process.

<sup>1</sup>H NMR confirmed the reaction between HA and *N*-(2-aminoethyl)acrylamide and the peaks of

---

the protons on the double bond were clearly recognised at 6.20 and 5.80 ppm (Figure 21). Thanks to a Diffusion-ordered spectroscopy (DOSY) experiment, we could confirm that the signals were really belonging to a molecule having the same HA's diffusion coefficient, thus amidation product (Figure 21).

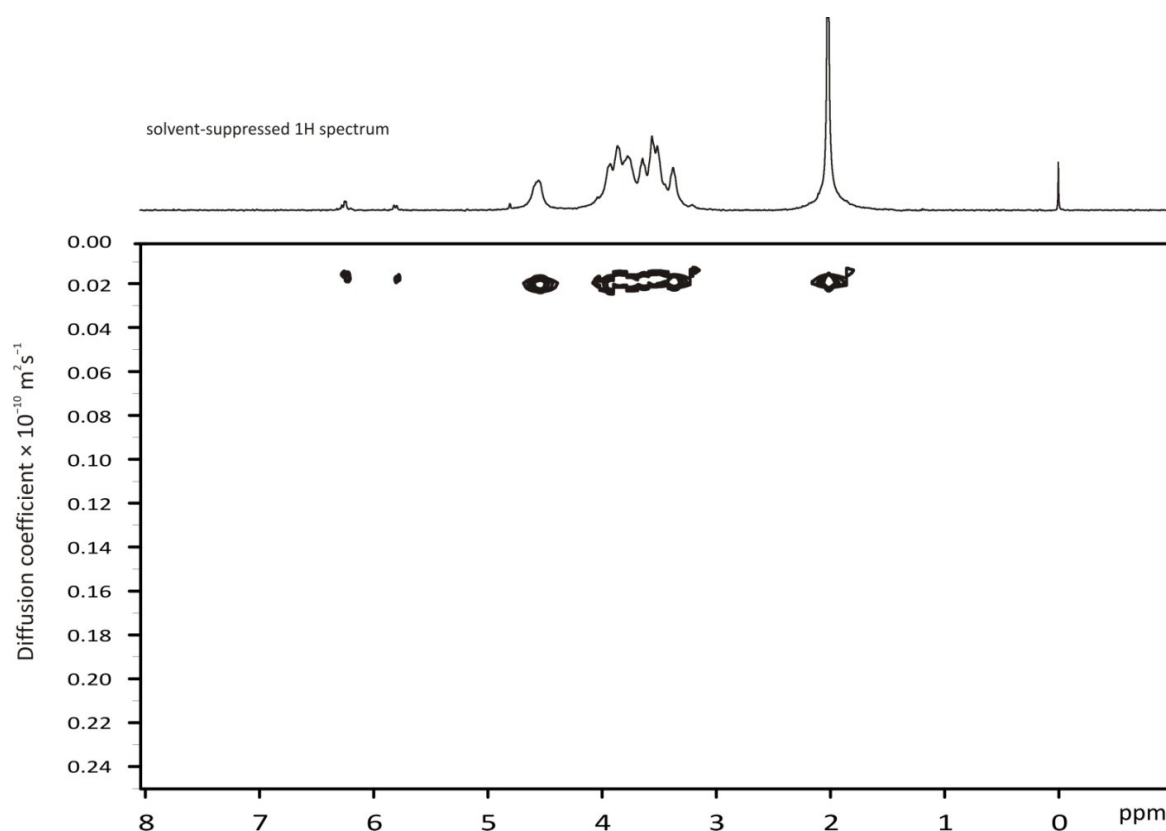


**Figure 21: DOSY spectrum of HA-Acr**

DOSY spectrum of the **HA-Acr** (the one relative to the derivative with  $M_w$ : 305 kDa and degree of functionalisation: 10% is depicted) was recorded in  $D_2O$  using a 400 MHz spectrometer. NMR diffusion experiments provide a way to separate the different compounds in a mixture based on the differing translation diffusion coefficients (and therefore differences in the size and shape of the molecule, as well as physical properties of the surrounding environment such as viscosity, temperature, etc) of each chemical species in solution.



By the way,  $^1\text{H}$  NMR was not found a method sensitive enough to establish the loading of double bonds on the HA scaffold. Hence we performed in parallel a fluorescent assay which could ensure high sensitivity and extremely low detection limits: the fluorescamine assay.

So, first of all, a calibration curve relating emission (at 460 nm) and concentration was plotted. Hence, subsequent dilution of small aliquots of the reaction mixtures at time zero (at known concentration of *N*-(2-aminoethyl)acrylamide) provided solutions at different known concentrations (ranging from  $10^{-8}$  to  $10^{-4}$  M); these samples were then reacted with an excess of fluorescamine (See 2.2.2.2.2). Six calibration curves were calculated, one for each batch, to ensure the highest possible accuracy; in fact we found that the molecular weight and the concentration of HA greatly influence the fluorescence; moreover, the linear range showed to be quite narrow.

The fluorescence of the final reaction solutions was measured again to give a precise indication of the degree of functionalisation (Figure 23).

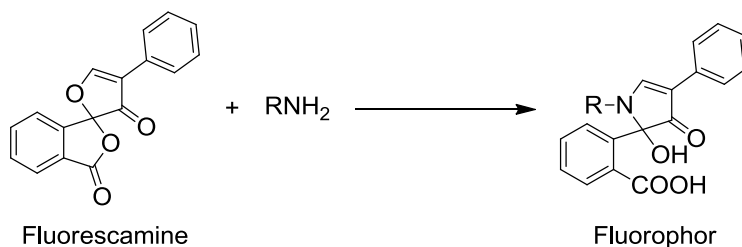


**Figure 22: Reaction of primary amine with fluorescamine**

Fluorescamine assay is well known for protein quantitation and has been developed in an attempt to alleviate the difficulties presented when using absorbance based assays.<sup>31</sup> It is based on the rapid reaction of fluorescamine, a non-fluorescent compound, with primary amines to form highly fluorescent moieties emitting at 460 nm after excitation at 400 nm.

Functionalisation of low molecular weight HA (35 kDa) showed to be more efficient than the one of high molecular weight HA (305 kDa). In addition, as expected, the yield of the reaction decreased on decreasing the concentration of the reactants; hence, the yields were excellent when the desired degree of modification was of the 10%, good for the 5% and moderate for the 1%.

These results suggested that a very good control on degree of functionalisation could be obtained by tuning the excess of reagents. A screening is in course of study to determine the best experimental conditions.

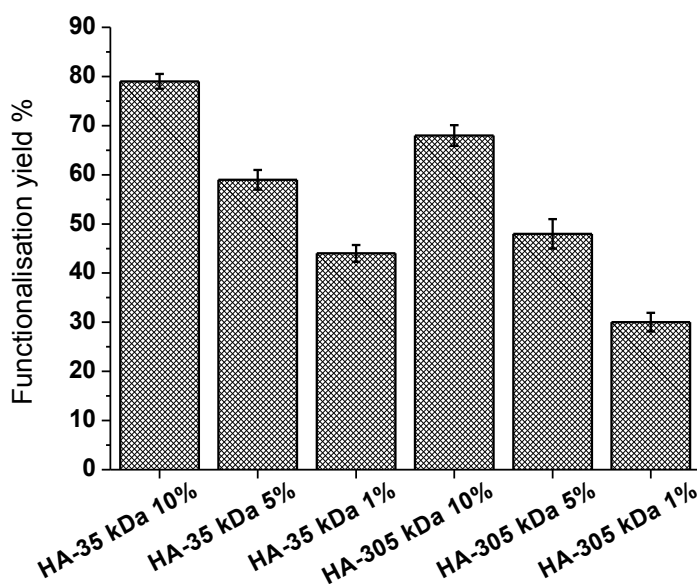


**Figure 23: Obtained degree of functionalisation measured by fluorescamine assay**

The functionalisation yield indicates the ratio between the obtained and the desired degree of functionalisation. Error bars represent standard deviation over three spectrophotometric measurements.

## 2.2.4 CONCLUSION

Two different strategies have been investigated to promote the activation of the carboxylic acid function of the hyaluronan and its reaction with amines via acyclic nucleophilic substitution.

Specifically, a carbodiimide-based reagent (EDCI) was used with different primary amines. This reagent is known to be active, in water, in acidic environment (around pH 4.75); the only drawback is related to the fact that only a small percentage of amine remains not protonated, and thus nucleophilic, at this pH value. In fact, we found EDCI totally ineffective in promoting HA amidation even in the presence of a large excess of reagents. Moreover the purification of the reaction mixtures resulted particularly complex and challenging.

Recent literature suggested that triazolol-based compounds could be suitable candidates for the activation of carboxylic acid functionalised polysaccharides for the preparation of conjugates.<sup>16,17</sup> Hence, we envisaged the DMTMM as good candidate to promote HA amidation.

By using this reagent in an aqueous environment, at pH 7.4, six different HA conjugates have been synthesised: in detail, two different molecular weight polymers have been used (i.e. 35 and 305 kDa) and three degrees of functionalisation (nominally 1, 5 and 10%). In particular the use of *N*-(2-aminoethyl)acrylamide as nucleophile allowed the decoration of the HA scaffold with an  $\alpha,\beta$ -unsaturated compound suitable for further reaction via Michael-type addition reaction (See Chapter 3).

The formation of the desired products and their purity have been confirmed by DOSY NMR experiment. Moreover a protocol for the application of fluorescamine assay to measure the yields of the reaction was successfully set up.

In conclusion experimental conditions to perform the reaction of HA with primary amines to form amides using DMTMM as activating agent have been realised. Moreover the purification process to obtain a pure adduct has been optimised. Particular attention was also given as well

to the analytical techniques required for the identification of the conjugate and the evaluation of its purity and of the functionalisation degree.

Future development will concern the identification of the best excess of reagents to ensure the desired degree of functionalisation. Moreover, HA functionalised with acryloyl moieties will be used for the bioconjugation of cysteine containing peptides, like RGD containing peptides, which are important ligands to promote specific biological processes.

## 2.3 DIISIOCYANATES AS CROSS-LINKER AGENTS FOR HA

### 2.3.1 INTRODUCTION

Biomaterials deserve a central role in the field of tissue engineering by directing cellular processes based on the structural and biochemical properties of the scaffold. Hydrogels, based both on synthetic and biopolymers, find numerous applications in biomedical devices, due to their high water content and tissue like physical, biochemical and mechanical properties.<sup>32</sup> The advantages of hydrogels based on synthetic polymers rely on the ability to determine their properties through tailored polymer synthesis and choice of cross-linking mechanism. This allows to have a fine control over the degree of swelling, stability and biodegradability, mechanical strength and enables the generation of responsiveness to external stimuli. Biopolymers on the other hand offer the advantage of inherent functionalities for example for the reversible binding of growth factors, the creation of a microenvironment close to the natural situation and the degradation through specific enzymatic processes.

Hyaluronan has a combination of unique physicochemical properties and biological functions that enable it to serve as an important starting material for the preparation of new biocompatible and biodegradable polymers. Soluble HA has been used in clinical applications including ocular surgery, visco-supplementation for arthritis and wound healing; however, due to the poor mechanical properties, rapid degradation and clearance *in vivo* of uncross-linked soluble HA limit many direct clinical applications. To improve the mechanical properties, degradation rate, and clearance, HA can be chemically modified or cross-linked to form hydrogel materials.<sup>12</sup>

HA can be modified in many ways to tune the properties of the resulting materials. Chemical modifications of HA target three functional groups: the glucuronic acid carboxylic acid, the hydroxyl groups, and the *N*-acetyl group (following deamidation). Similar reaction have been

applied both for bioconjugation and cross-linking (See 2.1); nonetheless cautions are required to ensure biological compatibility of the cross-linking chemistry, as well as to establish whether that the reagents and by-products are benign in both short- and long-term applications. There are different types of cross-linking procedures: direct cross-linking, cross-linking of HA derivatives or cross-linking of different HA derivatives. Among them the use of diisocyanates as cross-linkers has never been reported in literature, and we envisaged as an attracting strategy to use these cheap and highly reactive bifunctional molecules to introduce chemical bonds between non terminal units of different macromolecules creating reticulated networks. This approach could represent a simple and modular methodology to prepare a series of hyaluronan derivatives, assuring an efficient control of the properties of the hydrogel by varying both the type of diisocyanate and its relative amount.

The reactivity of isocyanates has been studied with HA only in multi-component reactions.<sup>18</sup> Specifically HA derivatives have been prepared *via* three- and four-component reactions known as the Passerini reaction and Ugi reactions.<sup>11</sup> In the Passerini reaction, an aqueous solution of hyaluronan is mixed with aqueous glutaraldehyde (or another water-soluble dialdehyde) and added to a known amount of a highly reactive isocyanide, usually cyclohexylisocyanide. In the Ugi four-component reaction, a diamine is added to this three-component mixture. This methodology has been used both for conjugation<sup>29</sup> or to cross-link native hyaluronan;<sup>19</sup> in this case the degree of cross-linking is controlled by the amount of aldehyde and diamine.

We decided to test the reactivity of HA as nucleophile with diisocyanates: our plan was to introduce new non conventional urethane bridges between different chains.

## **2.3.2 EXPERIMENTAL PROCEDURES**

### **2.3.2.1 Materials**

Sodium Hyaluronate (HA) RESILEN-200 (average molecular weight 235 kDa) was kindly supplied by Kyowa Italiana Farmaceutici s.r.l. (Milan, Italy).

Spectrum Spectra/Por 6 RC Dialysis Membrane Tubing (50 KDa MWCO) was used to dialyse the samples.

All reagents and solvents, if not otherwise specified, were purchased from Sigma-Aldrich (Milan, Italy) used as received. Dry solvents were used as received and stored under inert gas.

For thin-layer chromatography (TLC) analysis, Macherey-Nagel Alugram® sil G/UV 254 pre-coated plates were used.

### **2.3.2.2 General methods**

#### **2.3.2.2.1 Molecular characterization**

$^1\text{H}$  NMR and  $^{13}\text{C}$  NMR were measured on a BRUKER AC300, BRUKER AC200 or BRUKER AV400 spectrometers.

Infrared spectra were recorded on a Jasco FT/IR 4100.

UV spectra were recorded on a Jasco FT V-630 spectrophotometer.

#### **2.3.2.2.2 Swelling measurement**

The swelling capacity,  $S_w$ , is defined as the ratio between the weight of swollen gels ( $W_s$ ) after extensive dialysis against distilled water and the weight of the dry networks ( $W_d$ ):

$$S_w = W_s/W_d$$

Equation 1

10 mg ( $W_d$ ) of cross-linked samples in 0.5 mL of water were dialysed, in a 5 cm of dialysis tube, against distilled water at 40 °C for four hours. The outside of the tube was then carefully dried with paper, and the material recovered from the tube weighted ( $W_s$ ) to calculate  $S_w$ .

### 2.3.2.2.3 Rheological measurement

The rheological characterisation of hydrogels was performed with a Rheometrics Scientifics SR200 controlled stress rheometer with parallel plates (25 mm) geometry, 1 mm gap and 30 °C temperature. Dynamic experiments were carried out, under isothermal frequency sweep ( $10^{-1}$ - $10^1$  Hz) in an autostress-adjustment mode. Solutions 12 mg/mL of samples were used. The experiment allowed the monitoring of  $G'$ ,  $G''$  versus  $\omega$  trends. In order to make reliable measurements, the test was carried out within the linear viscoelastic region, that is, generally at small strain levels. In the present frequency sweep experiment the applied stress was progressively tuned in order to keep deformations below the 5%.

### 2.3.2.3 Synthetic procedures

#### 2.3.2.3.1 Synthesis of cross-linked HA

##### *Synthesis of HA-TBA*

12,5 g of Dowex® 50WX-8-400 (hydrogen form) were washed with pure water (3 x 250 mL). Then 24.5 mL of 1.5 M TBA-OH were added and the mixture was shaken for 30 minutes. The resin was then filtered and added to 1 g of sodium hyaluronate (HA-Na). After 3 h, the supernatant layer was filtered and the solution obtained freeze-dried for 3 days to afford the product. Yield: 90% wt.  $^1\text{H}$  NMR (300 MHz,  $\text{D}_2\text{O}$ ): 4.60 (bs, 2H), 3.90-3.30 (m, 10H), 3.26 (t,  $J = 8.4$  Hz, 8H), 2.09 (s, 3H), 1.69 (m, 8H), 1.42 (m, 8H), 1.02 (t,  $J = 7.3$  Hz, 12H).



### *Synthesis of cross-linked HA*

540 mg of HA-TBA were dissolved in 75 mL of dry DMSO under nitrogen atmosphere. After complete dissolution the cross-linker was added: 0.10 and 0.05 eq. for examethylene- and octamethylene-diisocyanate, respectively (15 and 8 mg of examethylene-diisocyanate for **HA-CL<sub>1</sub>**; 17 and 9 mg of octamethylene-diisocyanate for **HA-CL<sub>1</sub>**) or 0.30, 0.20 and 0.10 eq. of **TEG-2IB** (105, 70, 35 mg respectively for **HA-CL<sub>3</sub>**), while the reaction was vigorously stirred. The mixture was left under stirring overnight at room temperature and then poured into 400 mL of cold AcOEt to precipitate the HA-derivative. The product was filtered on a microfilter (pore size: 0.45  $\mu\text{m}$ ) and washed with 200 mL of AcOEt to completely remove the unreacted cross-linker. The resulting white precipitate was then dissolved in 70 mL of distilled water and dialysed against 0.1 M NaCl for 1 day, then against pure water for 5 days and finally freeze-dried affording the pure product as a white solid.

*HA-CL<sub>1</sub> 10%:* Yield: 80% wt. White solid.  $^1\text{H}$  NMR (400 MHz, D<sub>2</sub>O): 4.46 (bs, 1H), 4.37 (bs, 1H), 3.74-2.89 (m, 10H), 1.96 (s, 3H), 1.56-1.26 (m, 0.80H), 0.85 (m, 0.15H).

*HA-CL<sub>1</sub> 5%:* Yield: 84% wt. White solid.  $^1\text{H}$  NMR (400 MHz, D<sub>2</sub>O): 4.47 (bs, 1H), 4.37 (bs, 1H), 3.76-2.90 (m, 10H), 1.98 (s, 3H), 1.56-1.20 (m, 0.35H), 0.85 (m, 0.10H).

*HA-CL<sub>2</sub> 10%:* Yield: 78% wt. White solid.  $^1\text{H}$  NMR (400 MHz, D<sub>2</sub>O): 4.48 (bs, 1H), 4.37 (bs, 1H), 3.77-2.89 (m, 10H), 1.96 (s, 3H), 1.60-1.33 (m, 0.95H), 0.85 (m, 0.20H).

*HA-CL<sub>2</sub> 5%:* Yield: 84% wt. White solid.  $^1\text{H}$  NMR (400 MHz, D<sub>2</sub>O): 4.45 (bs, 1H), 4.36 (bs, 1H), 3.77-2.88 (m, 10H), 1.96 (s, 3H), 1.61-1.29 (m, 0.45H), 0.85 (m, 0.10H).

*HA-CL<sub>3</sub> 10%:* Yield: 81% wt. White solid.  $^1\text{H}$  NMR (400 MHz, D<sub>2</sub>O): 4.40 (bs, 2H), 3.79-2.88 (m, 10H), 2.00 (s, 3H).

*HA-CL<sub>3</sub> 5%:* Yield: 85% wt. White solid.  $^1\text{H}$  NMR (400 MHz, D<sub>2</sub>O): 4.39 (bs, 2H), 3.69-2.87 (m,

10H), 1.98 (s, 3H).

### 2.3.2.3.2 Synthesis of [ethane-1,2-diylbis(oxy)]bis(ethane-2,1-diyl) bis(2-isocyanato benzoate) (TEG-2IB):

*Synthesis of 2,2'-(2,5,8,11-tetraoxadodecane-1,12-dioyl)dibenzoic acid (TEG-2BA).<sup>33</sup>*

2.96 g (20 mmol, 1 eq.) of phthalic anhydride were dissolved in 100 mL of dry DCM under nitrogen atmosphere. The solution was cooled to 0 °C, then triethylene glycol (1.50 g, 10 mmol, 1 eq.) and TEA (3.0 g, 30 mmol, 1.5 eq.) were added, under stirring. The reaction mixture was maintained at 0 °C for 4 h and then at room temperature for 5h (the progress of the reaction was monitored by TLC, and the reaction stopped when the anhydride was completely reacted). The solvent was evaporated, the residue cooled to 0 °C and 200 mL of a saturated NaHCO<sub>3</sub> added. The mixture was extracted with diethyl ether (3 x 50 mL); the aqueous layer was cooled to 0 °C and acidified with 1 M hydrochloric acid followed by extraction with DCM (4x 100 mL). The combined organic layers, dried over MgSO<sub>4</sub> and the solvent removed under reduced pressure to afford the pure product. Yield: 96% wt. Yellow oil. <sup>1</sup>H NMR (300 MHz, CDCl<sub>3</sub>): 9.80 (bs, 2H), 7.76 (m, 4H), 7.55 (m, 4H), 4.48 (t, *J* = 4.3 Hz, 4H), 3.85 (t, *J* = 4.3 Hz, 4H), 3.77 (m, 4H).

*Synthesis of [ethane-1,2-diylbis(oxy)]bis(ethane-2,1-diyl) bis(2-isocyanatobenzoate) (TEG-2IB):*

The diacylchloride was prepared by refluxing 3.90 g (9.5 mmol, 1 eq.) of **TEG-2BA** in neat thionyl chloride (6.5 mL, 62 mmol, 6.5 eq.) for 3 h. The thionyl chloride excess was removed under reduced pressure to afford the diacylchloride which was used for the next step without further purification as a residue.

The residue was dissolved in 100 mL of dry THF and the solution added dropwise to solution of NaN<sub>3</sub> (4.5 g, 66 mmol, 6.9 eq. dissolved in 60 mL of water), under cooling in an ice bath. The reaction mixture was allowed to warm up at room temperature and stirred overnight, then 150

mL of toluene and 150 mL of a saturated solution of NaHCO<sub>3</sub> were added. The aqueous layer was extracted with toluene (2 x 150 mL). The collected organic phases were dried over MgSO<sub>4</sub>, filtered and the solvent removed under reduced pressure at 40 °C promoting the Curtius rearrangement and affording the corresponding diisocyanate. Yield: 72% wt. Orange oil. <sup>1</sup>H NMR (200 MHz, CDCl<sub>3</sub>): 8.03 (m, 2H), 7.51 (m, 2H), 7.20 (m, 4H), 4.50 (t, *J* = 4.7 Hz, 4H), 3.85 (t, *J* = 4.7 Hz, 4H), 3.71 (m, 4H); FT-IR (cm<sup>-1</sup>): 3257, 2874, 2257, 2143, 1714, 1592, 1528, 1452, 1299, 1261, 1213, 1143, 1075, 955, 756, 697.

### *<sup>1</sup>H NMR study on the reactivity of the diisocyanate **TEG-2IB**:*

To check the reactivity of the diisocyanate **TEG-2IB**, 10 μL of MeOH were added to 1 mL of a 10 mM solution of **TEG-2IB** in CDCl<sub>3</sub>. The <sup>1</sup>H NMR of the solution, recorded after 1 day at room temperature, showed only the signal relative to the MeOH (3.49 ppm) and the ones corresponding to the methylurethane of compound **TEG-2IB** [<sup>1</sup>H NMR (200 MHz, CDCl<sub>3</sub>): 8.42 (m, 2H), 8.02 (m, 2H), 7.55 (m, 2H), 7.00 (m, 2H), 4.45 (t, *J* = 4.9 Hz, 4H), 3.83 (t, *J* = 4.9 Hz, 4H), 3.77 (m, 4H)].

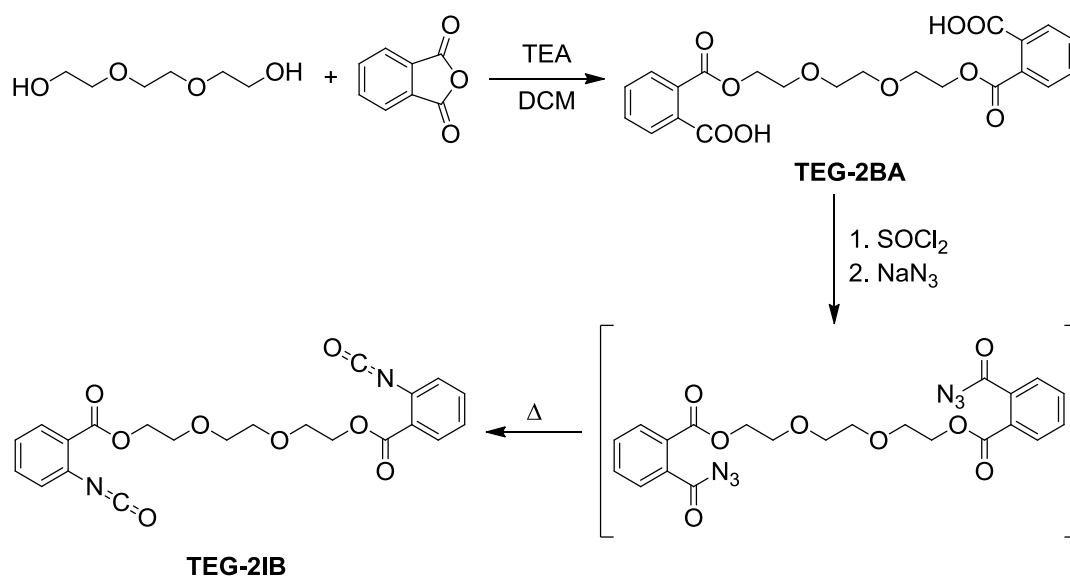
## 2.3.3 RESULTS AND DISCUSSION

### 2.3.3.1 *Synthesis of new cross-linked derivatives of the hyaluronic acid*

On account of the observation that HA is endowed with rather poor mechanical properties, chemical modifications of the hyaluronan are essential to reach stiffer hydrogels, with an increased stability in front of in vitro degradation. The use of diisocyanates as cross-linkers has never been reported, and we focused our attention on the use these cheap and highly reactive homo-bifunctional molecules to reticulate the different HA chains in a simple and modular way; a series of hyaluronan derivatives has been prepared by varying both the type of diisocyanate and its relative amount.

By using an ion exchange resin, commercial HA (purchased as sodium salt) was first converted into its tetrabutylammonium salt, which is soluble in polar aprotic solvents like DMF and DMSO. The aim was to avoid water for the cross-linking reaction to ensure the absence of others nucleophiles which could compete with the primary hydroxy group of HA, which is supposed to be the most reactive function with electrophiles (Scheme 4).

## Chemical Modification of the Hyaluronic Acid



**Scheme 3: Synthesis of diisocyanate TEG-2IB via Curtius rearrangement**

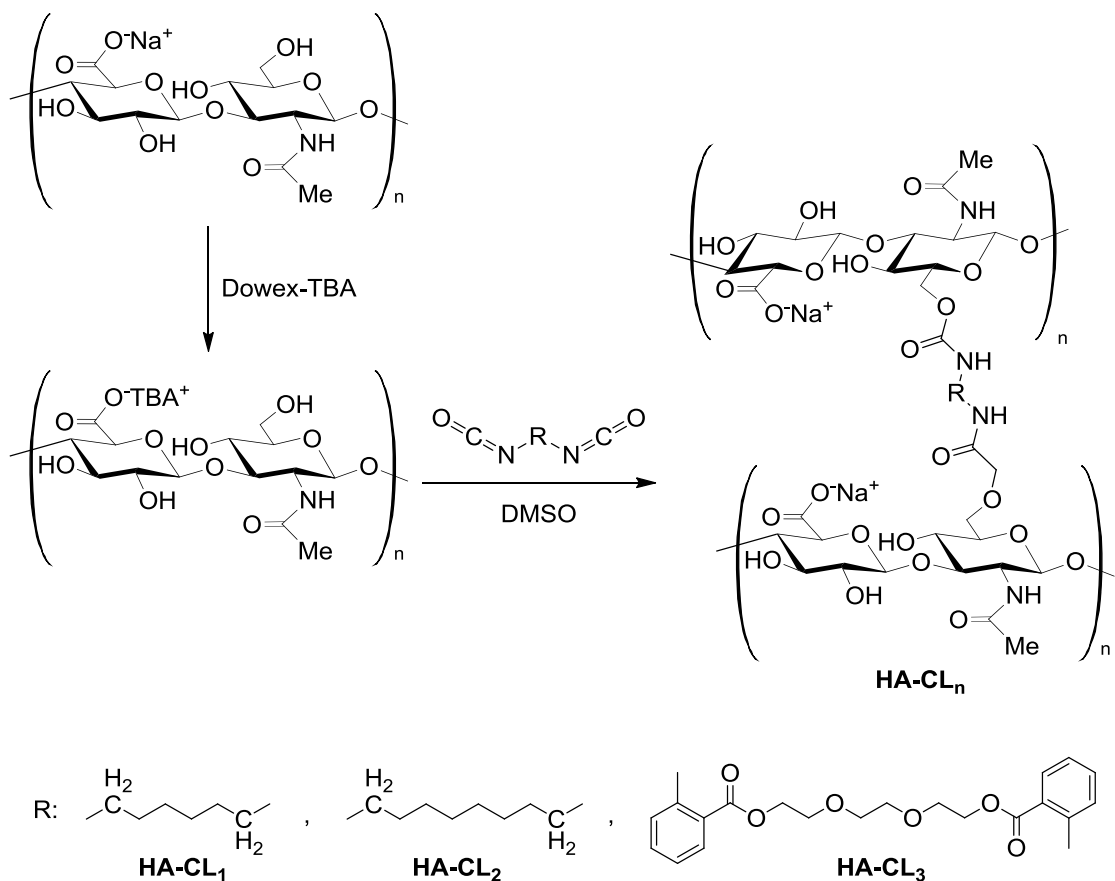
Diisocyanate **TEG-2IB** featuring two terminal aromatic isocyanate groups was synthesised by reacting triethylene glycol with phthalic anhydride. The resulting dicarboxylic acid was then converted into its dichloride which was treated *in situ* with sodium azide to provide the diacylazide. The latter undergoes Curtius rearrangement to **TEG-2IB** even at 40 °C.

The cross-linking reaction was then carried out in dry DMSO solution with commercially available hexamethylene- and octamethylene-diisocyanate, and with the diisocyanate **TEG-2IB**, synthesized by Curtius rearrangement (Scheme 3) affording products characterized by urethane bridges between different chains (Scheme 4).

Two different cross-linking ratios (defined as the ratio between the number of moles of cross-linker employed and the total number of repeating units of HA) were used with hexamethylene- and octamethylene-diisocyanate, i.e. 5% and 10%, while with diisocyanate **TEG-2IB**, three kinds of adducts were synthesised characterised by adding 10%, 20% and 30% equivalents of cross-linker.

## Chemical Modification of the Hyaluronic Acid

---



**Scheme 4: Synthesis of cross-linked HA-derivative**

Precipitation of the product with ethyl acetate facilitated the removal of the unreacted cross-linker. Purification was performed by dialysis, first against a 0.1M NaCl solution to restore the sodium as counterion, and then against distilled water to remove impurities.

<sup>1</sup>H NMR analysis of the cross-linked HA confirmed the presence of the aliphatic chains and the total restoration of the sodium as counterion for the materials resulting from the reaction

---

derivative with the two commercially available diisocyanates **HA-CL<sub>1</sub>** and **HA-CL<sub>2</sub>** at both the cross-linking degrees (5% and 10%) (Figure 24).

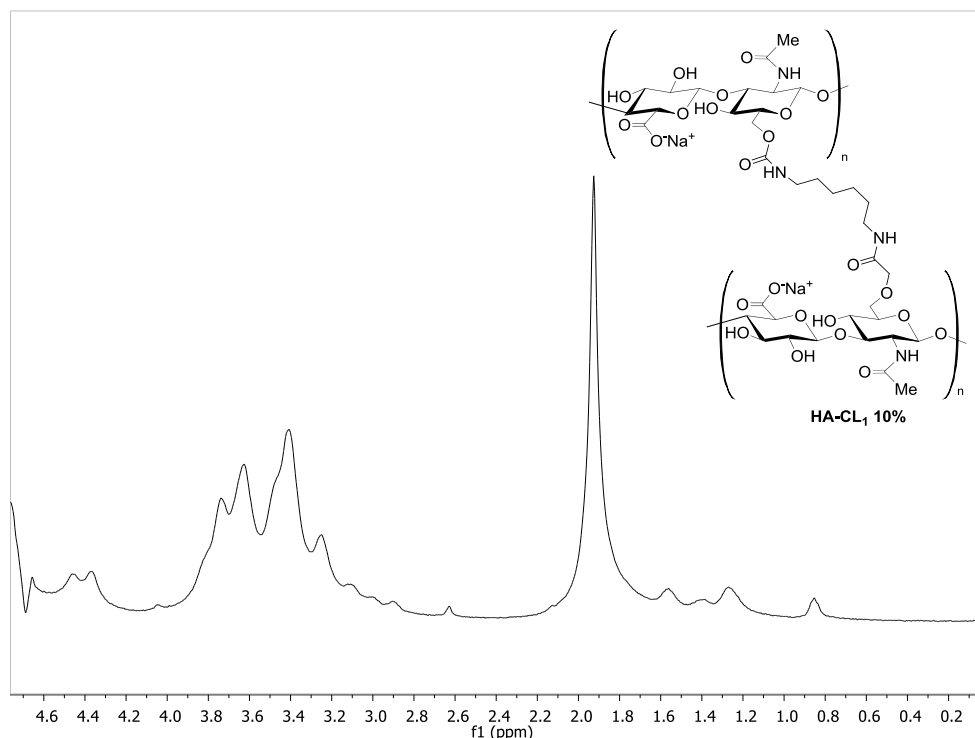


**Figure 24: <sup>1</sup>H NMR spectra of HA-CL<sub>1</sub> (cross-linking degree 10%)**

<sup>1</sup>H NMR spectrum of **HA-CL<sub>1</sub>** (D<sub>2</sub>O, 400 MHz) showing the signals relative to the hyaluronan (two signals at 4.45 and 4.35 ppm due to the methylene groups adjacent to the primary alcohol, broad signals from 3.89 to 3.10 attributable to the protons on the glucosaminic and glucuronic rings and a singlet at 1.90 ppm, related to the acetamide moiety) and new small peaks (1.60-0.80 ppm) confirming the presence of the aliphatic chains.

**HA-CL<sub>3</sub>** <sup>1</sup>H NMR analysis could not be performed, since the HA-derivatives were not completely soluble in water and only the signals of the native hyaluronan were observed. The samples have been then analysed by UV spectroscopy and the increasing of a peak of absorbance at 220 nm was observed for increasing degrees of cross-linkage. For the sake of comparison, we recorded

also the spectrum of the methyl urethane resulting from **TEG-2IB** and we observed a peak at 220 nm.

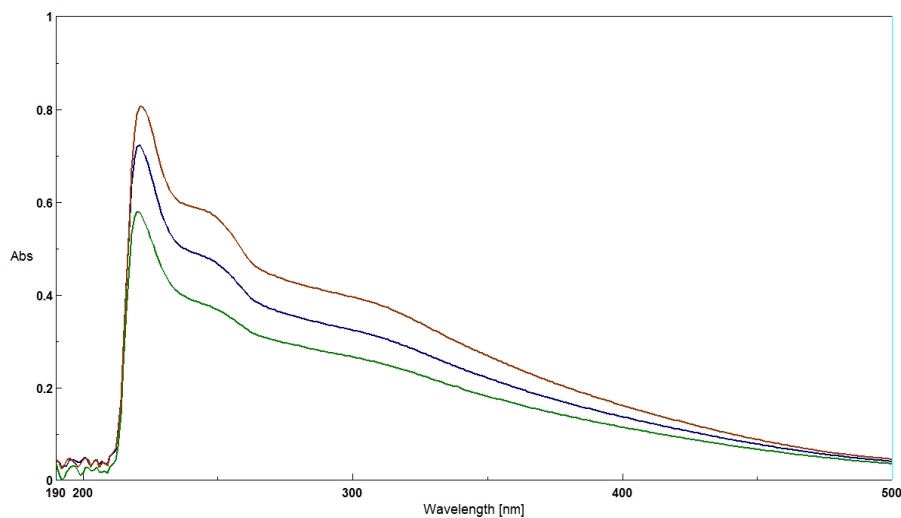


**Figure 25: UV spectra of HA-CL<sub>3</sub>**

UV spectra of **HA-CL<sub>3</sub>** were recorded on 1 mM aqueous solution of samples. The red line corresponds to the nominal degree of cross-linking of the 30%, the blue of 20% and the green of 10%.

### ***2.3.3.2 Swelling measurement***

The swelling is defined as the ratio between the weight of the swollen gel ( $W_s$ ) and the weight of the corresponding dry polymer ( $W_d$ ). The value is usually an indication to compare the cross-linking densities of HA with different cross-linking agents. As a general rule, the higher is the cross-linking degree, the lower is the swelling.<sup>11</sup>

As already mentioned, **HA-CL<sub>3</sub>** was not analysed by <sup>1</sup>H NMR because of its poor solubility in water; hence we did not perform any swelling measurement on these samples.

We measured  $S_w$  for the HA-derivative with examethylene- and octamethylene-diisocyanates and we found results in accordance with the theoretical cross-linking degree. Specifically, it was



found that the  $S_w$  showed an inverse proportionality to the cross-linking degree; moreover, the samples obtained by reaction with 5% equivalents of diisocyanate do not differ significantly from native HA, while remarkable differences were found in the materials resulting from the reaction with the 10% of cross-linker. However, the data obtained for the materials obtained by using examethylene- and octamethylene-diisocyanate are quite similar.

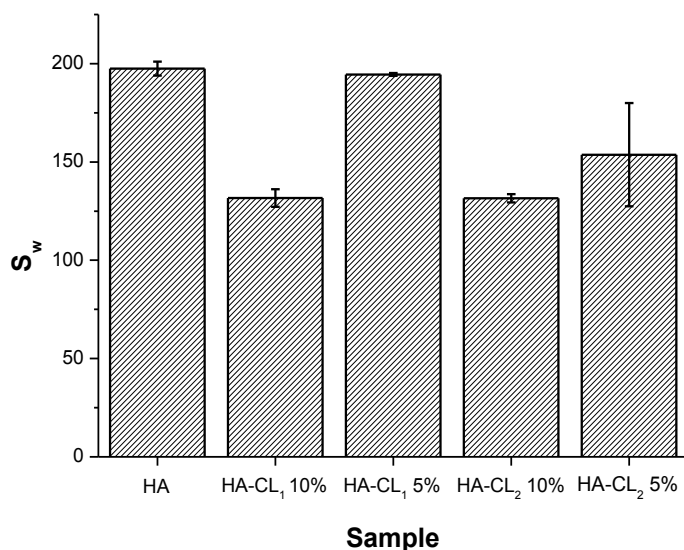


**Figure 26: Swelling measurement ( $S_w$ ) for cross-linked HA**

$S_w$  is the ratio between the weight of swollen gel ( $W_s$ ) and the weight of the dry network ( $W_0$ ).  $W_s$  was measured after extensive dialysis against distilled water at 40 °C. Error bars represent standard deviation ( $n = 3$ ).

### 2.3.3.3 Rheological measurement

Dynamic shear experiments were carried out in order to investigate the viscoelastic mechanical behaviour of gels. *Viscoelasticity* is a concept that draws from theories describing ideal materials and their behaviour in front of applied forces; Hook's law defines the behaviour of

---

ideal solids, whereas Newton's theory defines the behaviour of ideal liquids:

Hook's law:  $\sigma = G\gamma$  **Equation 2**

Newton's law  $\sigma = \eta\dot{\gamma}$  **Equation 3**

Where  $\sigma$  = shear stress ( $\text{N/m}^2 = \text{Pa}$ ),  $\gamma$  = shear strain (unitless),  $G$  = shear modulus (Pa),  $\dot{\gamma}$  = shear rate or strain rate ( $\text{s}^{-1}$ ) and  $\eta$  = coefficient of viscosity (Pa·s).

Equation 2 and Equation 3 fully describe the linear stress-strain and the stress-strain rate relationship. However, real materials exhibit a combination of elastic and viscous properties (i.e. they are viscoelastic) and therefore, other, more complex equations are necessary to quantitatively describe those material properties.

Rheological tests for the characterisation of the viscoelastic properties of a material are usually dynamic shear oscillatory tests. Specifically, an oscillatory (sinusoidal) deformation (stress or strain) is applied to a sample and the response of the material as well as the phase angle, or phase shift, between the deformation and response, are measured. The sinusoidally varying shear stress and the resulting shear strain are illustrated in Figure 27 and can be described mathematically as:

$\sigma(t) = \sigma_0 \sin(\omega t) = \sigma_0 e^{i\omega t}$  **Equation 4**

$\gamma(t) = \gamma_0 \sin(\omega t + \delta) = \gamma_0 e^{i(\omega t + \delta)}$  **Equation 5**

Where  $\sigma_0$  = stress amplitude (Pa),  $\gamma_0$  = strain amplitude,  $\omega$  = oscillatory frequency ( $\text{rad}\cdot\text{s}^{-1}$ ),  $t$  = time (s),  $\delta$  = phase angle ( $^\circ$ ).

---

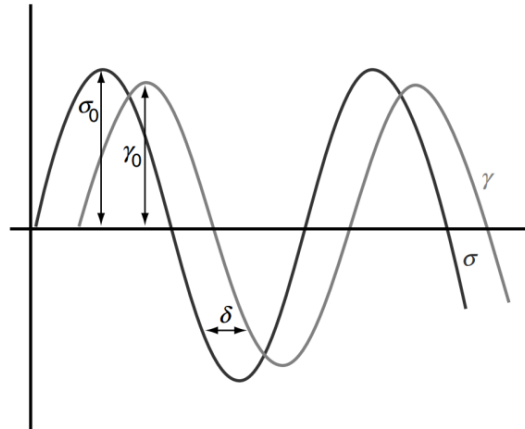


**Figure 27: Illustration of the sinusoidally varying stress and strain in dynamic oscillatory test**

Specifically:  $\sigma_0$  = stress amplitude (Pa),  $\gamma_0$  = strain amplitude and  $\delta$  = phase angle ( $^\circ$ ).

The phase angle ( $\delta$ ) is the phase difference between stress and strain in the oscillatory test and has a value between  $0^\circ$  and  $90^\circ$ . It can be used as a measure of the viscous and elastic ratio of a material; it will be  $0^\circ$  for an ideal solid and  $90^\circ$  for an ideal fluid. In the case of viscoelastic materials, such as a polymer or a polymer-based hydrogel, the mechanical response is somehow intermediate between an ideal elastic solid and an ideal viscous liquid and the phase difference has a value between  $0^\circ$  and  $90^\circ$ .

The ratio between stress and strain is called complex modulus ( $G^*$ ) and can be described as:

$$G^* = \left(\frac{\sigma_0}{\gamma_0}\right) \cos \delta + i \left(\frac{\sigma_0}{\gamma_0}\right) \sin \delta = G' + iG''$$

**Equation 6**

Where  $G'$  = shear storage or elastic modulus (Pa) and  $G''$  = shear loss or viscous modulus (Pa).  $G'$  provides information about the energy elastically stored in the material during deformation, whereas  $G''$  describes the viscous character or the energy dissipated as heat. It is important to note that the terminology “hydrogel” is often applied to materials where the storage shear

---

modulus is higher than the loss one ( $G' > G''$ ), although strictly speaking one should consider the independence of  $G'$  on frequency as a criterion.

We used dynamic frequency sweep experiments in which the material response to increasing frequency (rate of deformation) to a material that is placed between a defined geometry (most commonly parallel plate or cone and plate geometry) is monitored at a constant amplitude (stress or strain) and temperature. The experiment allowed the monitoring of  $G'$ ,  $G''$  versus  $\omega$  trends.

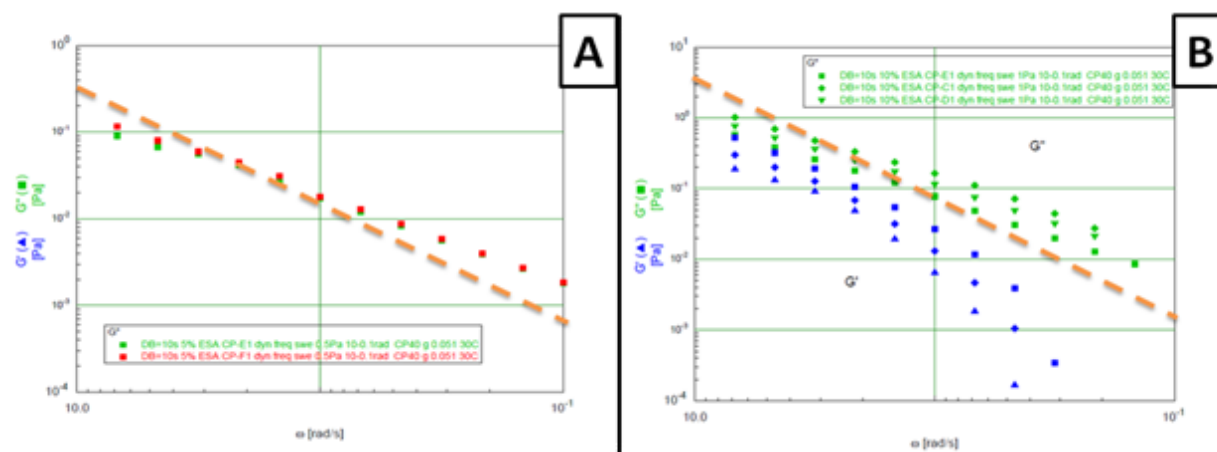


**Figure 28: Rheological measurement on HA-CL<sub>1</sub>**

Dynamic experiments were carried out on solutions (12 mg/mL) of the sample at 30 °C, with a frequency sweep range from  $10^{-1}$  to  $10^1$  Hz in the autostress-adjustment mode. The tests were carried out within the linear viscoelastic region. **A**: two measurements were performed for **HA-CL<sub>1</sub>** 5% (red and green), only  $G''$  was recorded (■). **B**: three measurements were performed for **HA-CL<sub>1</sub>** 10% (▲, ■, ◆),  $G'$  values are in blue while  $G''$  ones are in green. As a reference, the linear range relative to the  $G''$  of HA 235 kDa is reported (orange dash line).

Basically the studies on the rheological behavior of the products let us ascertain that there were no significant differences between the cross-linked polymer and the linear one. In fact  $G''$  is the predominant component influencing the viscoelastic properties of the samples (Figure 28) while hydrogels feature for definition  $G' > G''$ . A possible explanation is that local precipitation occurred in the areas where the cross-linker is present; the reason could be

related either to the hydrophobicity of the aliphatic *core* of the reticulating agent or to the impossibility of the polymer to change conformation, passing from DMSO to water, because of the presence of new covalent bonds.

### 2.3.4 CONCLUSION

The development of new strategies to improve the mechanical properties of HA and reducing its clearance maintaining its biocompatibility is a very important task in tissue engineering. Usually, the cross-linking of the linear chains of HA creating a reticulated network helps for the creation of new materials suitable for cells culture and implantation.

An unconventional methodology to cross-link HA has been developed. Specifically the reactivity of the primary hydroxyl group as a nucleophile with isocyanates has been demonstrated.

Diisocyanates are cheap molecules never used as cross-linker agents with HA; in order to control their high reactivity, reactions were carried out in DMSO instead of in water. The complete solubility of hyaluronan in this solvent was ensured by changing its counterion and using, hence, its TBA salt.

In particular two commercially available diisocyanates have been used (hexamethylene- and octamethylene-diisocyanate) providing water soluble products in which the presence of aliphatic bridges was confirmed by  $^1\text{H}$  NMR analysis and swelling measurements.

Another aryl diisocyanate, characterised by a triethylene glycol chain, was prepared by Curtius rearrangement; in this case, the cross-linked products were found was slightly soluble and we could prove the formation of the adducts by UV analysis only.

Subsequent studies on the rheological behavior of the products let us ascertain that there were no significant differences between the cross-linked polymer and the linear one. A possible explanation is that hydrophobic and short-chain reticulating agents were responsible for local precipitation of the substrat in the areas where the cross-linker is present.

Anyway this strategy opens applicative perspectives to be applied for the formation of mixed hydrogels, e.g. HA and PEG or collagen, or with different diisocyanates.

Furthermore, the use of the substrates to coat petri dishes on which mesoangioblasts were cultured showed the complete atoxicity of the materials and a cellular proliferation very similar to that observed for the standard conditions (See 2.5).

## **2.4 HA MODIFICATION VIA Cu<sup>I</sup> CATALYSED 1,3-CYCLOADDITION**

### **2.4.1 INTRODUCTION**

The demand for new chemical materials and biologically active molecules is continuously growing today; an emerging class of reactions is the one named as “click chemistry,” identifying a set of powerful, simple and selective reactions that generate links based on heteroatoms, offering a unique approach to this problem.<sup>34</sup> All the reactions that require only benign conditions, simple workup and purification procedures and can rapidly create molecular diversity through the use of reactive modular building blocks can be defined as “click”. Sharpless and co-workers have identified a number of reactions meeting these criteria;<sup>35</sup> according to their definition, a “click reaction” is characterized by a gain in thermodynamic enthalpy of at least 20 kcal·mol<sup>-1</sup>. Common features of these transformations are related to their orthogonality, regioselectivity and highly efficiency; moreover, click reactions can be performed in aqueous solutions at room or physiological temperature and generally display outstanding functional group tolerance; not surprisingly, these characteristics make them compelling reactions within the bioengineering toolkit for polymer synthesis and bioconjugation.<sup>36</sup>

In particular, tissue engineering has the aim of delivering biomolecules, cells, and supporting structures to the body promoting self-healing. To accomplish this task, biocompatible materials are required to serve either as structural supports for tissue regeneration or as delivery vehicles for cells and drugs transplantation. To make relevant progresses in this field, the development of synthetic organic techniques aiming to facilitate the chemoselective cross-linking and the functionalisation with bioactive molecules of synthetic and natural polymer, is a key point.

---



Recently, the click chemistry has been widely used within regenerative medicine both for forming new cross-linked hydrogels and for implementing bioconjugation techniques involving the decoration of 2D cell substrates or even the immobilisation of bioactive factors within 3D scaffolds. Common reactions for this purpose are the Diels–Alder reactions and other highly efficient reactions, such as nucleophilic substitutions, radical additions, Michael additions (in particular when thiol-nucleophiles are involved), but one of the most powerful transformations discovered to date is the Cu<sup>I</sup> catalyzed variant of the Huisgen 1,3-dipolar cycloaddition of azides to alkynes to afford 1,2,3-triazoles. This reaction is very similar to the classic Huisgen cycloaddition where an organic azide reacts with an alkyne to form a triazole ring (Figure 29).<sup>37</sup>

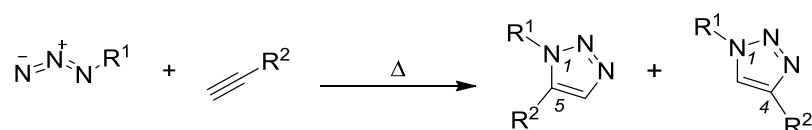


**Figure 29: Huisgen thermal 1,3-cycloaddition**

The final product of thermal 1,3-cycloaddition, proposed by Huisgen in 1968, is an almost 1:1 mixture of the two regioisomers depicted in the Figure.

In 2002, Sharpless demonstrated that the Huisgen cycloaddition reaction can proceed at low temperatures with high rates, high efficiency and regioselectivity (only the 1,4-adduct is formed) by using a Cu<sup>I</sup> catalyst; the *in situ*-generated catalyst, deriving by the use of copper(II) sulfate and ascorbic acid as the reducing agent, showed to be efficient as well.<sup>38</sup> Moreover, a nearly perfect conversion is obtainable both in aqueous and organic solvents.

The advantages of this reaction in biomedical applications are related to the fact that the starting materials, azides and terminal alkynes, are remarkably stable within biological systems, enabling a facile introduction of these reactive groups into a wide range of biomolecules.

---

Furthermore these reactive groups are basically absent in nature and this fact greatly limits the formation of by-products.

The mechanism proposed for this reaction explains the experimental evidences that make this transformation so unique: it tolerates very many organic functional groups and shows a wide scope with respect to both alkyne and azide reactants; in addition it proceeds in a great variety of solvents, tolerates a wide range of pH values and performs efficiently over a broad temperature range.

Researchers proposed that the stepwise catalytic cycle begins with the formation of a  $\text{Cu}^I$  acetylide species formed via a  $\pi$  complex (Figure 30). Even if alkyne  $\pi$  complexation requires ligand dissociation, hence a slightly endothermic reaction, in aqueous solution, however, the next step involving the formation of the copper species is remarkably exothermic. Copper coordination reduces the  $\text{pK}_a$  of the alkyne C-H by up to 9.8 pH units, thus promoting deprotonation. Probably, a dynamically changing family of different  $\text{Cu}^I$  acetylide species may exist in solution, depending on the reaction conditions; in fact, kinetic studies indicate that the rate of the catalytic process is second order in copper, but that, by increasing copper concentrations, less reactive species, such as metal aggregates, are formed. The role of the second copper atom seems to be the activation of the azide functionality, but the  $\pi$  complexation of a terminal acetylide function bound to a neighboring copper atom may also occur. This complexation increases acetylide activity toward cyclization by reducing the alkyne electron density. The formation of the active copper acetylide species is followed by azide displacement of one ligand generating a copper acetylide-azide complex. At this point cyclization occurs: complexation of the azide activates it toward the nucleophilic attack of acetylide carbon C(4) at N(3) of the azide (numbers based on the traditional triazole nomenclature), generating a metallacycle. Subsequent ring contraction, protonation of the triazole-copper derivative and dissociation of the resulting product close the reaction and regenerates the catalyst.

---

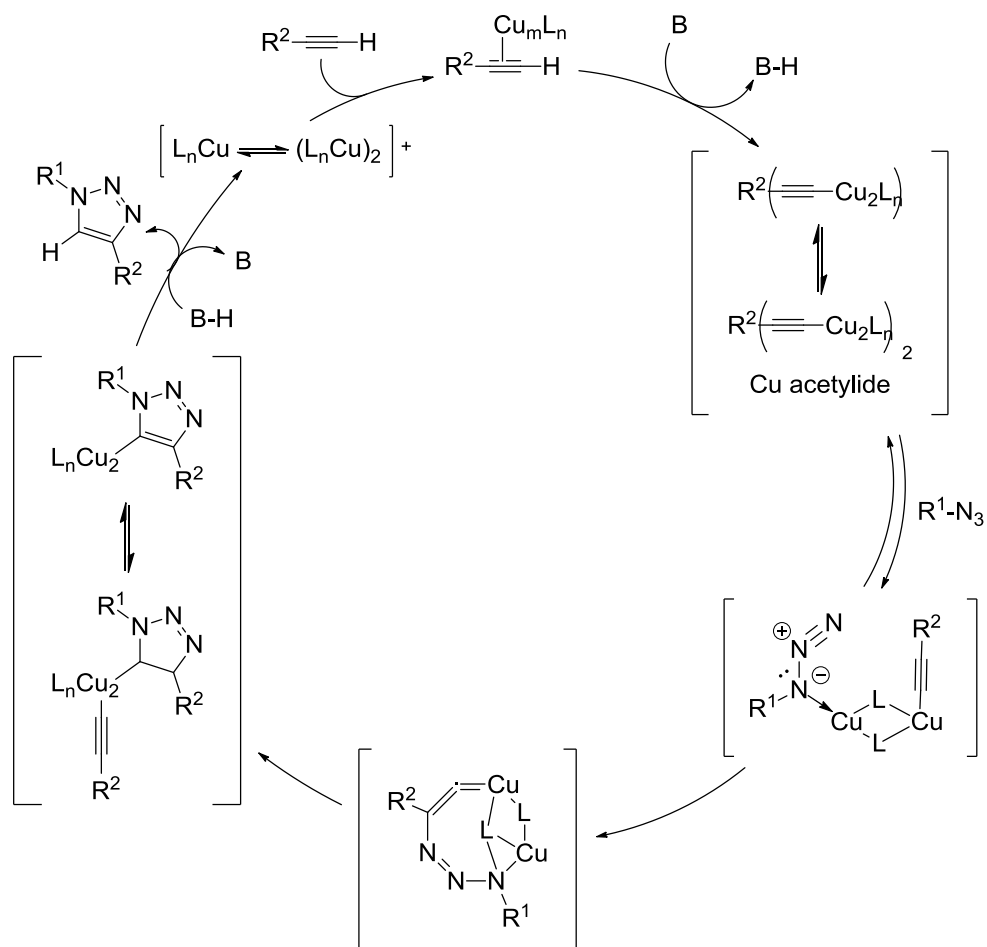


Figure 30: Proposed catalytic cycle for 1,3-cycloaddition catalysed by Cu<sup>I</sup>

#### 2.4.1.1 HA-based hydrogels crosslinked by Cu<sup>I</sup>-catalysed azide-alkyne cycloaddition

The dipolar cycloaddition between an azido group and a terminal alkyne group presents numerous advantages that make it very appealing for application in the case of HA. In particular, it occurs at physiological pH and temperature, ensuring a complete biocompatibility

during cell encapsulation or incorporation of biologically active molecules. Furthermore, the use of Cu<sup>I</sup> catalyst accelerates the process, preserving the inertness of both azides and alkynes toward the vast majority of functional groups that are typical of the biological environment.

Only few examples regarding the chemical modification of HA by Sharpless cycloaddition are present in the literature, all focused on the *in situ* gel formation of systems that might act as vehicles for sustained drug delivery and tissue engineering applications.

The first person who exploited this route was Crescenzi who synthesized hydrogels of HA using a novel procedure for the rapid chemical gelation of aqueous solutions of previously modified hyaluronan.<sup>39</sup> Specifically, new derivatives bearing azido and alkyne groups linked by short arms to the polysaccharide main chains were prepared by amidation mediated by EDCI. Once the two types of derivatives are mixed in aqueous medium, they give rise to the dipolar 1,3-cycloaddition, after the addition of CuCl in a catalytic amount (Figure 31). The formed gel has been characterized (rheology, IR spectroscopy, swelling properties and, in particular, NMR spectral features) and employed in drug delivery studies. In fact, carrying out the gelation process in aqueous solutions containing benzidamine and doxorubicin, respectively, the polysaccharide networks acted as drug reservoirs and the drug release resulted well controllable by acting on the degree of cross-linking. Furthermore, encouraging results were obtained when the click-gels were formed using aqueous suspensions of *Saccharomyces cerevisiae* yeast cells; in this case, a scaffold inside which the cells were homogeneously distributed and smoothly adhered to the inner pores surfaces was observed. Moreover, after 24 h about 60% of the entrapped cells were still exhibiting some proliferating activity.

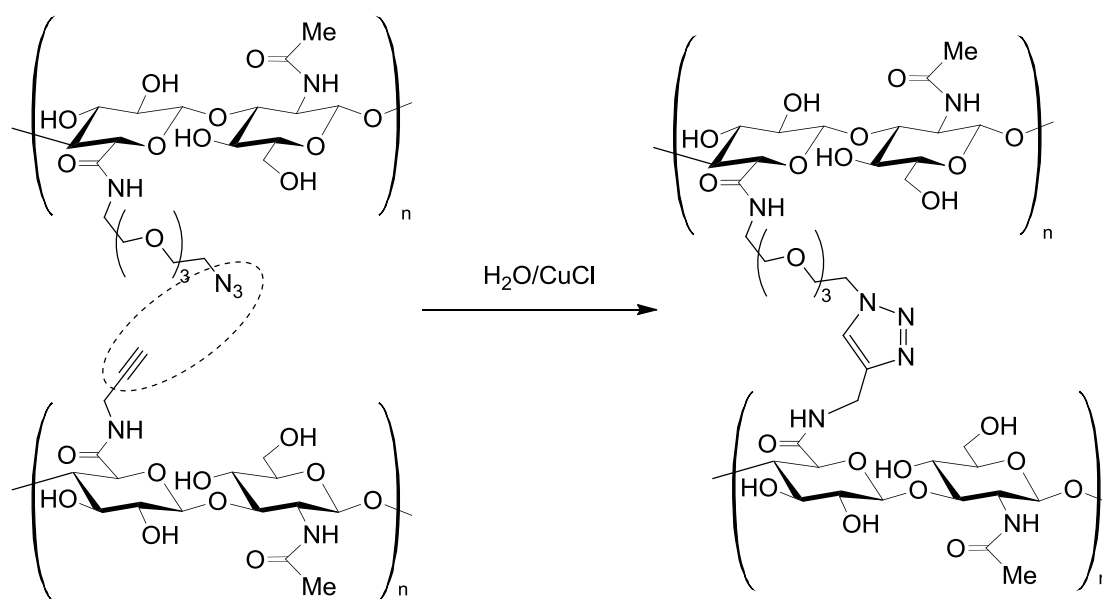


**Figure 31: Representation of the Formation of HA-based click-gels**

Two years later, the same research group published the use of the same azido derivative (Figure 31) in combination with a series of dialkyne reagents differing in the length of the bridge. In this case the catalyst was generated *in situ* combining copper sulfate and ascorbic acid.<sup>40</sup> The aim of the investigation was to evaluate the influence of the typology of the cross-linker; they found that the degree of cross-linking was in an inverse relationship with the flexibility of the bridging unit: longer spacer arm gave rise to higher cross-linking densities. Both the kinetic of gelation and the the elastic moduli value determined of by rheology, as well as the swelling ratios were in good agreement with the experimental findings.

In similar a study published in 2011,<sup>41</sup> hyaluronic acid-based hydrogels with tunable mechanical properties were prepared by exploiting the copper-catalysed azide-alkyne cycloaddition of alkyne-functionalized hyaluronic acid crosslinked with linkers carrying two terminal azide functionalities. The cross-linker density as well as the length and the rigidity of the linker

molecules were varied (Figure 32).

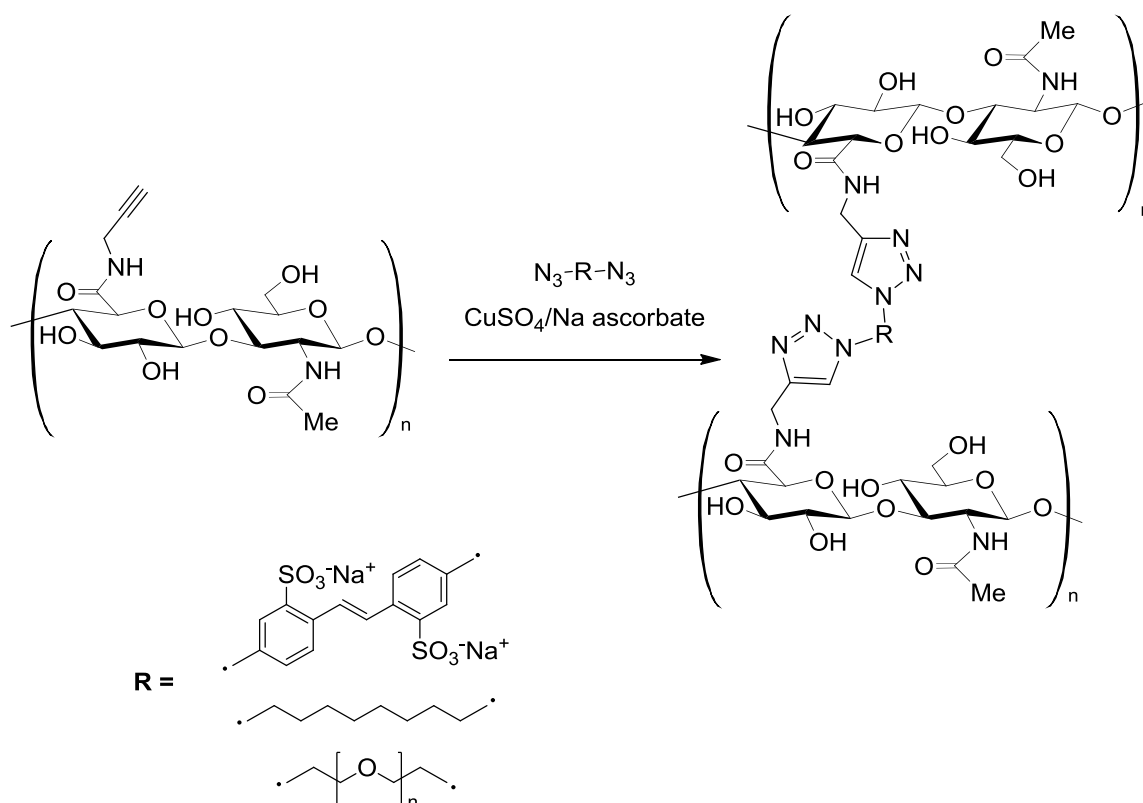


**Figure 32: Formation of hydrogels from modified-HA by the use of click chemistry with different cross-linkers**

The target of the last example present in literature regarding the use of an HA-derivative in the Sharpless cycloaddition reaction specifically was to mimic the natural cartilage extracellular matrix: a biological hydrogel was synthesized from the HA biopolymers, chondroitin sulfate and gelatin.<sup>42</sup> HA and chondroitin sulfate were modified with 11-azido-3,6,9-trioxaundecan-1-amine to insert an azide function, and gelatin was modified with propiolic acid in order to have a terminal alkyne. The azide groups of HA and chondroitin sulfate were reacted with the

acetylene groups of gelatin, catalyzed by  $\text{Cu}^I$ , to form triazole rings, thereby forming a cross-linked hydrogel. As expected, the gelation time decreased with increasing the catalyst concentration. The hydrogel obtained in this way was used as a substrate for *in vitro* cell culture and the results confirmed that chondrocytes could adhere and proliferate on it.

In conclusion, the use of the copper catalysed cycloaddition seems to be a promising strategy to provide biocompatible hydrogels with tailored and tunable mechanical properties, but the examples found in literature on its application on HA were directed to cross-link the polymer. On these bases, we decided to try to fill the gap on the knowledge about the applicability of 1,3-dipolar cycloaddition in bioconjugation reactions. Specifically we tried to develop a strategy to covalently link bioactive molecules, or poorly soluble precursors, to the HA scaffold and then to proceed with further modifications to provide a versatile tool for the design of a multifunctionalised HA bearing different molecules capable of developing synergic biological effects.

## 2.4.2 EXPERIMENTAL PROCEDURES

### 2.4.2.1 *Materials*

Sodium Hyaluronate (HA) RESILEN-200 (average molecular weight 235 kDa) was gently supplied by Kyowa Italiana Farmaceutici s.r.l. (Milan, Italy).

Spectrum Spectra/Por 6 RC Dialysis Membrane Tubing (50 KDa MWCO) was used to dialyse the samples.

All reagents and solvents, if not otherwise specified, were purchased from Sigma-Aldrich (Milan, Italy) and used as received. Dry solvents were used as received and stored under inert gas. All the amino acids derivatives employed displayed the natural stereochemical configuration.

For thin-layer chromatography (TLC) analysis, Macherey-Nagel Alugram® sil G/UV 254 pre-coated plates were used. Column chromatography was performed on Macherey-Nagel MN Kieselgel silica gel.

### 2.4.2.2 *General methods*

#### 2.4.2.2.1 **Molecular characterization**

Melting point (mp) determinations were performed by using a Buchi B-540 instrument.

$^1\text{H}$  NMR and  $^{13}\text{C}$  NMR were measured on a BRUKER AC300, BRUKER AC200 or BRUKER AV400 spectrometers.

Optical rotations ( $[\alpha]_D^{25}$ ) were measured on a JASCO P-1030 polarimeter with a 1 dm cell at the sodium D line ( $\lambda = 589$  nm).

Mass analyses were performed using a VG 7070 EQ-HF instrument.

---



Infrared spectra were recorded on a Jasco FT/IR 4100.

### 2.4.2.3 *Synthetic procedures*

#### 2.4.2.3.1 **Synthesis of HA derivatives**

##### *Synthesis of bromoacetate derivatised Hyaluronan (HABA):<sup>26</sup>*

2.0 g of HA (5 mmol) were dissolved in 200 mL of distilled water. The pH of the solution was adjusted to 9.0 by adding 1 M NaOH. Bromoacetic anhydride (13 g, 50 mmol, 10 eq.) was then added dropwise to the solution at 0 °C. The reaction was stirred for 24 h at 4 °C, then the reaction mixture was dialyzed (MWCO 50000) for 7 days against distilled water. The sample was then freeze-dried and analysed. Yield: 65% wt. White solid. <sup>1</sup>H NMR (400 MHz, D<sub>2</sub>O) (δ = ppm): 4.88 (bs, 2H, CH<sub>2</sub>OC=O), 3.97 (s, 0.1 H, COCH<sub>2</sub>Br), 3.86-3.40 (m, 10H), 2.03 (s, 3H, NHCOCH<sub>3</sub>).

##### *Synthesis of azidoacetate derivatised Hyaluronan (HAAA):*

1.0 g of **HABA** (2.5 mmol of monomeric unit of HA) was dissolved in 100 mL of distilled water to which 200 mg of NaN<sub>3</sub> (2.5 mmol, 1 eq.) were added. The reaction was stirred for 24 h at room temperature. The reaction mixture was then dialyzed (MWCO 50000) for 7 days against distilled water. The sample was then freeze-dried and analysed. Yield: 75% wt. White solid. <sup>1</sup>H NMR (400 MHz, D<sub>2</sub>O) (δ = ppm): 4.59 (bs, 1H), 4.51 (bs, 1H), 3.87-3.38 (m, 10H), 2.05 (s, 3H, NHCOCH<sub>3</sub>); FT-IR (cm<sup>-1</sup>): 3382, 2921, 2153 (N<sub>3</sub>), 1651, 1417, 1206, 1155, 947, 894, 447.

##### *Synthesis of click-HA conjugates:*

If not specified, this general procedure was followed for the synthesis of HA-based conjugates via copper catalysed Huisgen cycloaddition; the triple bond-containing compound (2 eq. respect to the monomeric unit of HA) was added to a 1% w/v solution of **HAAA** in distilled water. Then, an aqueous solution 5% w/v of sodium ascorbate (0.5 eq. respect to the monomeric unit of HA)

---

was added, followed by the addition of a 5% w/v solution of  $\text{CuSO}_4 \cdot 5\text{H}_2\text{O}$  in distilled water (0.1 eq. respect to the monomeric unit of HA). The mixture was stirred for 24 h at room temperature. The reaction mixture was then dialyzed (MWCO 50000) against EDTA solution (10 mM) for 24 h and finally against distilled water for 7 days. The sample was then freeze-dried and analysed.

### *Synthesis of the propargyl alcohol-HA conjugate (HA-TR1):*

For this synthesis the general procedure was followed using, respectively, 100 mg of **HAAA** (0.25 mmol of monomeric unit of HA), 30 mg of propargyl alcohol (0.5 mmol, 2eq.), 20 mg of sodium ascorbate (0.125 mmol, 0.5 eq.) and 6 mg of  $\text{CuSO}_4 \cdot 5\text{H}_2\text{O}$  (0.025 mmol, 0.1 eq.). Yield: 60% wt. White solid.  $^1\text{H}$  NMR (400 MHz,  $\text{D}_2\text{O}$ ) ( $\delta$  = ppm): 7.36 (s, 0.04 H, aromatic H on the triazole ring), 4.51 (bs, 2H,  $\text{CH}_2\text{OC}=\text{O}$ ), 3.94-3.37 (m, 10H), 2.06 (s, 3H,  $\text{NHCOCH}_3$ ); FT-IR ( $\text{cm}^{-1}$ ): 3417, 2920, 1633, 1416, 1379, 1205, 1152, 1076, 947, 895.

### *Synthesis of the propargyl benzoate-HA conjugate (HA-TR2):*

For this synthesis the general procedure was followed using, respectively, 200 mg of **HAAA** (0.5 mmol of monomeric unit of HA), 160 mg of propargyl benzoate (1.0 mmol, 2 eq.), 45 mg of sodium ascorbate (0.25 mmol, 0.5 eq.) and 13 mg of  $\text{CuSO}_4 \cdot 5\text{H}_2\text{O}$  (0.05 mmol, 0.1 eq.). Yield: 70% wt. White solid.  $^1\text{H}$  NMR (300 MHz,  $\text{D}_2\text{O}$ ) ( $\delta$  = ppm): 7.29 (s, 0.02H aromatic H), 4.49 (d,  $J$  = 7 Hz, 1H), 4.42 (d,  $J$  = 7 Hz, 1H), 3.98-3.40 (m, 10H), 1.93 (s, 3H); FT-IR ( $\text{cm}^{-1}$ ): 3397, 2926, 1728, 1628, 1413, 1377, 1312, 1241, 1154, 1047, 945, 893.

### *Synthesis of [3Z-Arg-Gly-Asp(OBn)-NHProp]-HA conjugate:*

3Z-Arg-Gly-Asp(OBn)-NHProp (44 mg, 0.05 mmol, 0.2 eq.) was added to 1% w/v a solution of **HAAA** (100 mg, 0.25 mmol of monomeric unit of HA) in distilled water. Then, a 5% w/v aqueous solution of sodium ascorbate (45 mg, 0.25 mmol, 1 eq.) was added followed by  $\text{CuSO}_4 \cdot 5\text{H}_2\text{O}$  5% w/v in distilled water (13 mg, 0.05 mmol, 0.2 eq.). The mixture was stirred for

---

48 h at room temperature. The reaction mixture was then dialyzed (MWCO 50000) against an EDTA solution (10 mM) for 24 h and finally against distilled water for 7 days. The sample was then freeze-dried and analysed. No traces of the product were detected.

### *Synthesis of (H<sub>2</sub>N-Arg-Gly-OProp)-HA conjugate (HA-TR3):*

To a solution of 250 mg of **HAAA** (0.6 mmol of monomeric unit of HA) in 50 mL of distilled water, 2 g of Dowex-TBA resin (See 0) were added and the mixture was gently shaken for 3 hours. The supernatant liquid was removed by filtration and the solution concentrated to a final volume of 10 mL. Additional 15 mL of DMSO were added to the flask, and the addition followed by a further addition of 20 mg (0.03 mmol, 0.2 eq.) of 3Z-Arg-Gly-OProp; as soon as the mixture resulted homogeneous, 1 mL of distilled water containing 50 mg (0.3 mmol, 0.5 eq.) of sodium ascorbate was added dropwise, followed by the further addition of 1 mL of an aqueous solution containing 15 mg (0.06 mmol, 0.1 eq.) of CuSO<sub>4</sub>·5H<sub>2</sub>O. The reaction was stirred at room temperature for 2 days; then 50 mg (0.9 mmol, 1.5 eq.) of propargyl alcohol were added to completely ensure the quenching of all the azido groups on the **HAAA**; the reaction was stirred for further 12 h and then dialysed against a solution containing EDTA (10 mM) and tetrabutylammonium hydroxide (10 mM) for 24 h and then against pure water for 24 h.

The aqueous solution of the product was submitted to heterogeneous hydrogenation without further characterization. Specifically, the solution was concentrated at reduced pressure to a final volume of 10 mL, then an equal volume of MeOH was added. 25 mg of Palladium (5% on activated charcoal catalyst) were added and the reaction was vigorously stirred under hydrogen pressure (6 bar) in a closed autoclave, overnight. The crude mixture was then filtered over a plug of celite, the solvent removed under reduced pressure, and the film obtained dissolved again in 20 mL of distilled water, then dialysed for 24 h against EDTA (10 mM), against NaCl (10 mM) for 48 h and finally against pure water for 72 h. The product was analysed after freeze-drying. Yield: 40% wt. White solid. <sup>1</sup>H NMR (400 MHz, D<sub>2</sub>O) (δ = ppm): 8.59-7.48 (m, 0.02H),

6.10-5.10 (m, 0.10H), 4.58 (d,  $J = 8$  Hz, 1H), 4.49 (d,  $J = 8$  Hz, 1H), 3.94 (d,  $J = 8$  Hz), 3.87-3.35 (m, 10H), 1.95 (s, 3H); FT-IR (cm<sup>-1</sup>): 3287, 2909, 1615, 1406, 1373, 1315, 1151, 1024, 891.

*Synthesis of [Boc-Arg(Z)<sub>2</sub>-OTEG-OProp]-HA conjugate (HA-TR4):*

A slightly modified version of the general procedure was used in this case; specifically: to a 1% w/v solution of 280 mg of **HAAA** (0.7 mmol of monomeric unit of HA) in distilled water, a solution of 90 mg (0.13 mmol, 0.19 eq.) of (3Z)-Arg-OProp in 2 mL of MeOH was added dropwise. Then, sodium ascorbate and CuSO<sub>4</sub>·5H<sub>2</sub>O were added to the reaction mixture, as already described, using the following quantities, respectively: 60 mg (0.35 mmol, 0.5 eq.) of sodium ascorbate and 20 mg (0.07 mmol, 0.1 eq.) of CuSO<sub>4</sub>·5H<sub>2</sub>O. After 48 h stirring, the product was purified and recovered as mentioned above. Yield: 75% wt. White solid. <sup>1</sup>H NMR (300 MHz, D<sub>2</sub>O) ( $\delta =$  ppm): 8.39 (s, 0.04H, aromatic H on the triazole heterocycle), 7.39 (s, 0.20H, aromatic H on phenyl rings), 4.58 (d,  $J = 6$  Hz, 1H), 4.49 (d,  $J = 6$  Hz, 1H), 3.95-3.37 (m, 10H), 2.04 (s, 3H, NHCOCH<sub>3</sub>); FT-IR (cm<sup>-1</sup>): 3407, 2918, 1633, 1416, 1379, 1153, 1048.

*Synthesis of the (Boc-Arg(Z)<sub>2</sub>-OTEG-OProp)-HA conjugate (HA-TR5):*

A suspension of 200 mg (0.5 mmol) of **HA-TR4** in 50 mL of distilled water was stirred overnight under hydrogen pressure (6 bar), at room temperature, with 20 mg of Palladium catalyst (5% on activated charcoal). The mixture was then filtered over a plug of celite and then over a regenerate cellulose microfilter (pore size 0.2  $\mu$ m) and freeze-dried. Yield: 85% wt. White solid. <sup>1</sup>H NMR (300 MHz, D<sub>2</sub>O) ( $\delta =$  ppm): 8.50 (s, 0.04H, aromatic H on the triazole heterocycle), 4.59 (d,  $J = 6$  Hz, 1H), 4.49 (d,  $J = 6$  Hz, 1H), 3.96-3.35 (m, 10.2H), 2.05 (s, 3H, NHCOCH<sub>3</sub>); FT-IR (cm<sup>-1</sup>): 3375, 2918, 1613, 1416, 1377, 1321, 1149, 1079, 1046, 950, 899.

#### 2.4.2.3.2 Synthesis of bromoacetic anhydride:<sup>43</sup>

6.4 g of 1,3-diisopropylcarbodiimide (DIC, 50 mmol, 0.5 eq.) dissolved in 20 mL of dry DCM were added dropwise to a solution of 13.9 g (100 mmol, 1 eq.) of bromoacetic acid in 50 mL of

---

dry DCM, under nitrogen atmosphere, at -15 °C. After stirring the mixture at room temperature for 1 h, the solution was cooled and left at -20 °C for 5 hours, then filtered to remove the solid urea formed from DIC. Evaporation of the solvent under reduced pressure gave the product that was used without further purification. Yield: 99% wt. Yellow oil.  $^1\text{H}$  NMR (200 MHz,  $\text{CDCl}_3$ ) ( $\delta$  = ppm): 3.99 (s, 4H).

#### 2.4.2.3.3 Synthesis prop-2-yn-1-yl benzoate:<sup>44</sup>

To a stirred solution of benzoic acid (2.0 g, 16 mmol, 1 eq.), propargyl alcohol (1.0 g, 18 mmol, 1.1 eq.) and 4-dimethylaminopyridine (DMAP, 250 mg, 2 mmol, 0.1 eq.) in 30 mL of dry DCM, under nitrogen atmosphere, *N,N'*-dicyclohexylcarbodiimide (DCC, 3.7 g, 18 mmol) was added in small portions at room temperature. The mixture was stirred and monitored by TLC analysis until complete disappearance of benzoic acid (2 h). The crude mixture was then filtered and the product purified by column chromatography on silica gel (70-230 mesh) using a mixture 7:3 v/v of hexane and AcOEt as eluant. Yield: 79% wt. Yellow oil.  $^1\text{H}$  NMR (200 MHz,  $\text{CDCl}_3$ ) ( $\delta$  = ppm): 8.07 (m, 2H), 7.58 (m, 1H), 7.45 (m, 2H), 4.93 (d,  $J$  = 2.5 Hz, 2H), 2.52 (t,  $J$  = 2.5 Hz, 1H).

#### 2.4.2.3.4 Synthesis of 3Z-Arg-Gly-Asp(OBn)-NHProp:

*Synthesis of  $\text{H}_2\text{N-Gly-OtBu}$ :*

*Method A:*

Synthesis of Z-Gly-OH:

3.00 g (75 mmol, 1.1 eq.) of NaOH were dissolved in 50 mL of distilled water, then 50 mL of acetone were added and 5.00 g (67 mmol, 1 eq.) of glycine were added to the mixture. The solution was cooled down to 0 °C and a 1:1 v/v mixture of water and benzyl chloroformate (12.6 g, 74 mmol, 1.1 eq.) was added dropwise. After stirring at room temperature overnight, the acetone was removed under reduced pressure. The mixture was acidified with a 1M

---

hydrochloric acid solution and the resulting bilayered system was separated; to the lower layer 5 mL of DCM were added and the white precipitate formed filtered affording the pure product, which was dried under reduced pressure. Yield: 71% wt. White solid.  $^1\text{H}$  NMR (300 MHz,  $\text{CDCl}_3$ ) ( $\delta = \text{ppm}$ ): 7.36 (m, 5H), 5.23 (bs, 1H), 5.14 (s, 2H), 4.04 (d,  $J = 5.4$  Hz, 2H).

Synthesis of Z-Gly-OtBu:

To a stirred solution of Z-Gly-OH (2.5 g, 12 mmol, 1 eq.), *t*-butyl alcohol (1.3 g, 18 mmol, 1.5 eq.) and DMAP (25 mg, 0.2 mmol, 0.02 eq.) in 30 mL of dry DCM under nitrogen atmosphere, DIC (1.6 g, 13 mmol, 1.1 eq.) was added in small portions, at 0 °C. The reaction was stirred for 3 h and left under stirring overnight at -12 °C in order to promote the complete precipitation of the solid urea formed from the DIC. The crude mixture was then filtered and the product purified by flash chromatography over a silica gel column (230-400 mesh) using a 4:6 v/v mixture of hexane and AcOEt as eluant. Yield: 27% wt. Yellow oil.  $^1\text{H}$  NMR (200 MHz,  $\text{CDCl}_3$ ) ( $\delta = \text{ppm}$ ): 7.37 (m, 5H), 5.23 (bs, 1H), 5.13 (s, 2H), 3.88 (d,  $J = 5.3$  Hz, 2H), 1.47 (s, 9H).

Synthesis of  $\text{H}_2\text{N}$ -Gly-OtBu:

0.65 g (2.5 mmol) of Z-Gly-OtBu were dissolved in 5 mL of MeOH, then 10 mg of Palladium catalyst (5% on activated charcoal) were added and the reaction vigorously stirred overnight at room temperature, under hydrogen atmosphere. The crude mixture was then filtered on a plug of celite, then the evaporation of the solvent afforded the pure product. Yield: 88% wt. Yellow oil.  $^1\text{H}$  NMR (200 MHz,  $\text{CDCl}_3$ ) ( $\delta = \text{ppm}$ ): 3.48 (s, 2H), 1.47 (s, 9H).

*Method B:*<sup>45</sup>

Synthesis of *t*-butyl bromoacetate:

To a stirred solution of dimethyl aniline (5.0 g, 40 mmol, 1 eq.), *t*-butyl alcohol (3.0 g, 40 mmol, 1 eq.) in 10 mL of dry  $\text{Et}_2\text{O}$ , under nitrogen atmosphere, 8.0 g (40 mmol, 1 eq.) of bromoacetyl bromide were slowly added at 0 °C. The reaction was then stirred at room temperature for 4 h.

---

The separated dimethylaniline hydrobromide was dissolved by adding 10 mL of water and the organic layer was washed with 1M HCl solution(10 mL), with a saturated solution of NaHCO<sub>3</sub> (10 mL) and finally with water (10 mL). The organic extracts were dried over Na<sub>2</sub>SO<sub>4</sub> and the solvent removed to afford the product. Yield: 73% wt. Yellow oil. <sup>1</sup>H NMR (200 MHz, CDCl<sub>3</sub>) (δ = ppm): 3.75 (s, 2H), 1.48 (s, 9H).

Synthesis of *t*-butyl azidoacetate:

2.85 g (44 mmol, 1.5 eq.) sodium azide and 5.70 g (29 mmol, 1 eq.) of *t*-butyl bromoacetate were dissolved in a 60:40 v/v mixture of acetone and water. The mixture was refluxed on a steam bath for 14 h. The acetone was then removed under reduced pressure and the aqueous phase exhaustively extracted with Et<sub>2</sub>O (15 mL x 3); the combined organic layers were dried over Na<sub>2</sub>SO<sub>4</sub> and filtered. Removal of the solvent afforded the product. Yield: 95% wt. Orange oil. <sup>1</sup>H NMR (300 MHz, CDCl<sub>3</sub>) (δ = ppm): 3.74 (s, 2H), 1.50 (s, 9H).

Synthesis of H<sub>2</sub>N-Gly-OtBu:

To a solution of 2.60 g (26 mmol) of *t*-butyl azidoacetate in 15 mL of MeOH 50 mg of Palladium catalyst (5% on activated charcoal) were added and the mixture was vigorously stirred overnight, at room temperature, under hydrogen atmosphere (5 bar). The crude mixture was filtered on a plug of celite and the evaporation of the solvent afforded the pure product. Yield: 95% wt. Yellow oil. <sup>1</sup>H NMR (200 MHz, CDCl<sub>3</sub>) (δ = ppm): 3.48 (s, 2H), 1.47 (s, 9H).

*Synthesis of 3Z-Arg-OH:*<sup>46</sup>

Boc-Arg(Z)<sub>2</sub>-OH (1.80 g, 2.3 mmol, 1 eq.) was treated at 0°C with 60 mL of a 1:1 v/v solution of DCM and trifluoroacetic acid. After 1 h, the solvent was removed under reduced pressure. The residue was dissolved in DCM (50mL) and the solution concentrated under reduced pressure repeating this treatment for three times (3 x 50 mL). The residue was the trifluoroacetic acid salt. This material was dissolved in dioxane (60 mL) at 0 °C and a 1 M solution of Na<sub>2</sub>CO<sub>3</sub> (40 mL)

---

was added. After stirring the mixture for 10 minutes, a white precipitate was formed. Benzyl chloroformate (432 mg, 2.5 mmol, 1.1 eq.) was added and the solution stirred and allowed to warm up at room temperature over 12 h. Water (150 mL) was added and the aqueous layer acidified with citric acid and then extracted with DCM (3 x 100 mL) to afford the crude product, which was purified by crystallisation (1:1 v/v hexane and AcOEt, 15 mL as eluant). Yield: 75% wt. White solid.  $^1\text{H}$  NMR (200 MHz,  $\text{CDCl}_3$ ) ( $\delta$  = ppm): 7.30 (m, 15H), 5.21 (s, 2H), 5.10 (s, 2H), 5.02 (s, 2H), 4.35 (m, 1H), 3.96 (m, 2H), 1.69 (m, 4H).

### *Synthesis of 3Z-Arg-Gly-OtBu:*

To a stirred solution of 3Z-Arg-OH (1.27 g, 1.7 mmol, 1 eq.), HBTU (1.04 g, 2.75 mmol, 1.6 eq.), TEA (870 mg, 6.8 mmol, 4 eq.), DMAP (24 mg, 0.2 mmol, 0.1 eq.) in 10 mL of a 9:1 v/v mixture of DCM and DMF,  $\text{H}_2\text{N-Gly-OtBu}$  (287 mg, 1.2 mmol, 1 eq.) was added in 20 min. The mixture was stirred overnight at room temperature and then treated with water (10 mL), with a saturated solution of citric acid (10 mL), with an aqueous 0.1 M solution of NaOH (10 mL) and finally with water (10mL). The product was obtained in a pure state after column chromatography on silica gel (mesh 70-230), eluting with a 9/1 v/v mixture of DCM/AcOEt. Yield: 72% wt. White solid.  $^1\text{H}$  NMR (300 MHz,  $\text{CDCl}_3$ ) ( $\delta$  = ppm): 9.45 (bs, 1H), 9.31 (bs, 1H), 7.30 (m, 15H), 6.90 (bs, 1H), 6.10 (bd,  $J$  = 8.1 Hz, 1H), 5.22 (s, 2H), 5.09 (m, 4H), 4.34 (bt,  $J$  = 7.8 Hz, 1H), 4.10 (m, 2H), 3.73 (dd,  $J$  = 4.9, 18.6 Hz, 1H), 3.40 (dd,  $J$  = 4.9, 17.8 Hz, 1H), 1.71 (m, 4H), 1.41 (s, 9H).

### *Synthesis of 3Z-Arg-Gly-OH:*

550 mg (0.8 mmol, 1 eq.) of 3Z-Arg-Gly-OtBu were dissolved in 10 ml of DCM and 550  $\mu\text{L}$  (8 mmol, 10 eq.) of  $\text{H}_3\text{PO}_4$  85% were added dropwise at room temperature. The mixture was stirred for 4 h, monitoring the complete disappearance of the reagent in the organic phase, then, 10 mL of water were added. A white solid precipitated which was filtered, collected and dried at reduce pressure affording 230 mg (0.4 mmol) of the title product. The organic phase

---



was washed again with water (10 mL), dried over  $\text{MgSO}_4$  and filtered. Evaporation of the solvent gave further 200 mg (0.3 mmol) of product. Yield: 85% wt. White solid.  $^1\text{H}$  NMR (300 MHz, DMSO) ( $\delta$  = ppm): 9.13 (bs, 2H), 8.16 (t,  $J$  = 5.6 Hz, 1H), 7.35 (m, 15H), 5.21 (s, 2H), 5.04 (s, 2H), 4.99 (s, 2H), 4.02 (bt,  $J$  = 6.5 Hz, 1H), 3.83 (m, 2H), 3.68 (dd,  $J$  = 5.6, 17.5 Hz, 2H), 1.55 (m, 4H).

### *Synthesis of Boc-Asp(OBn)-NHProp:*

To a stirred solution of Boc-Asp(OBn)-OH (2.00 g, 6.2 mmol, 1 eq.), propargylamine (510 mg, 6.8 mmol, 1.1 eq.), TEA (2.50 g, 25.0 mmol, 4 eq.) and DMAP (76 mg, 0.62 mmol, 0.1 eq.) in 100 mL of a 95:5 v/v mixture of DCM and DMF, under a nitrogen atmosphere, 2.82 g (7.4 mmol, 1.2 eq.) of HBTU were added and the mixture stirred at room temperature overnight. The mixture was treated with a saturated solution of citric acid (100 mL), with a 0.1 M aqueous solution of NaOH (100 mL) and finally with water (100 mL). The product was obtained in a pure state after flash column chromatography on silica gel (mesh 230-400), eluting with a 97:3 v/v mixture of DCM and EtOH. Yield: 62% wt. Yellow oil.  $^1\text{H}$  NMR (200 MHz,  $\text{CDCl}_3$ ) ( $\delta$  = ppm): 7.35 (m, 5H), 6.72 (bs, 1H), 5.66 (bs, 1H), 5.14 (s, 2H), 4.53 (m, 1H), 4.02 (dd,  $J$  = 2.5, 5.3 Hz, 2H), 3.07 (dd,  $J$  = 4.5, 17.2 Hz, 1H), 2.73 (dd,  $J$  = 6.2, 17.1 Hz, 1H), 2.22 (t,  $J$  = 2.5, 1H), 1.46 (s, 9H); FAB-MS 361 ( $\text{M}+\text{H}$ )<sup>+</sup>.

### *Synthesis of $\text{H}_2\text{N}$ -Asp(OBn)-NHProp:*

1.30 g (3.6 mmol, 1eq.) of Boc-Asp(OBn)-NHProp were dissolved in 50 mL of DCM and 7 mL (36 mmol, 10 eq.) of  $\text{H}_3\text{PO}_4$  85% were slowly added. After stirring the mixture for 4 h, it was diluted with 50 mL of water and the aqueous phase neutralized first with a saturated  $\text{NaHCO}_3$  solution. then the pH was brought to 8.5 by addition of 1M NaOH. The aqueous layer was then extracted with DCM (3 x 50 mL) and the combined organic layers were dried over  $\text{MgSO}_4$  and filtered. Removal of the solvent afforded the pure product. Yield: 99% wt. Yellow oil.  $^1\text{H}$  NMR (300 MHz,  $\text{CDCl}_3$ ) ( $\delta$  = ppm): 7.60 (bs, 1H), 7.34 (m, 5H), 5.14 (d,  $J$  = 2.3 Hz, 2H), 4.03 (m, 2H), 3.72 (dd,  $J$  = 3.0, 8.1 Hz, 2H), 3.00 (dd,  $J$  = 3.9, 16.9 Hz, 1H), 2.71 (dd,  $J$  = 8.1, 16.9 Hz, 1H), 2.21 (t,  $J$  = 2.6, 1H).

---

*Synthesis of 3Z-Arg-Gly-Asp(OBn)-NHProp:*

3Z-Arg-Gly-OH (200 mg, 0.32 mmol, 1 eq.) was dissolved in 10 mL of DMF under nitrogen atmosphere, then in a sequence TEA (130 mg, 1.28 mmol, 4 eq.), DMAP (4 mg, 0.03 mmol, 0.1 eq.) and HBTU (133 mg, 0.35 mmol, 1.1 eq.) were added; after 15 minutes stirring, H<sub>2</sub>N-Asp-NH-Prop (97 mg, 0.35 mmol, 1.1 eq.) was added and the reaction was stirred overnight at room temperature. The crude mixture was concentrated to a final volume of 1 mL, then 25 mL of DCM were added and the organic phase washed with a saturated solution of citric acid (10 mL), with a saturated solution of NaHCO<sub>3</sub> (10 mL) and with water (10 mL). The organic layer was dried over MgSO<sub>4</sub>, filtered and the solvent removed under reduce pressure. The product was purified by flash cromatography on silica gel (mesh 230-400), eluting with a 97/3 v/v mixture of DCM/EtOH. Crystallisation from DCM afforded the pure title compound. Yield: 18% wt. White solid. <sup>1</sup>H NMR (300 MHz, DMSO) (δ = ppm): 9.13 (bs, 1H), 7.35 (m, 20H), 5.21 (s, 2H), 5.06 (s, 2H), 5.03 (s,2H), 4.99 (s, 2H), 4.68 (m, 1H), 4.01 (m, 1H), 3.83 (m, 2H), 3.82 (d, J = 2.3 Hz, 2H), 3.70 (m, 2H), 3.07 (t, J = 2.3 Hz, 1H), 2.81 (dd, J = 7.7, 16.1 Hz, 1H), 2.58 (dd, J = 7.8, 16.1 Hz, 1H), 1.56 (m, 4H); FAB-MS 877 (M+H)<sup>+</sup>.

**2.4.2.3.5 Synthesis of 3Z-Arg-Gly-OProp:**

To a stirred solution of 3Z-Arg-Gly-OH (200 mg, 0.25 mmol, 1 eq.) and propargyl alcohol (30 mg, 0.50 mmol, 2 eq.) in 8 mL of dry DMF, under nitrogen atmosphere, HBTU (105 mg, 0.28 mmol, 1.1 eq.), DMAP (3 mg, 0.025 mmol, 0.1 eq.) and TEA (100 mg, 1.0 mmol, 4 eq.) were added. The reaction was stirred overnight at room temperature, then the solvent removed and the crude residue suspended in 20 mL of a saturated solution of citric acid and extracted with DCM (15 mL x 3). The combined organic layers were dried over MgSO<sub>4</sub> and filtered, the solvent removed and the resulting oil purified by cromatographyc on a silica gel column (70-230 mesh), eluting with a 97:3 v/v mixture of DCM and EtOH. Yield: 32% wt. White solid. <sup>1</sup>H NMR (400 MHz, CDCl<sub>3</sub>) (δ = ppm): 9.40 (bd, 1H), 7.31 (m, 15H), 5.23 (s, 2H), 5.10 (m, 4H), 4.70 (d, J = 2.3 Hz, 0.7H), 4.62

(d,  $J = 2.3$  Hz, 1.3H), 4.39 (m, 1H), 4.26 (t,  $J = 4.8$  Hz, 1H), 4.10 (m, 1H), 3.81 (m, 1H), 3.70 (t,  $J = 4.8$  Hz, 1H), 2.48 (t,  $J = 2.3$  Hz, 0.4H), 2.42 (t,  $J = 2.3$  Hz, 0.6H), 1.69 (m, 4H); ESI-MS 694 (M+Na)<sup>+</sup>.

#### 2.4.2.3.6 Synthesis of Boc-Arg(Z)<sub>2</sub>-OTEG-OProp:

##### *Synthesis of TEG-OTs:*<sup>47</sup>

To a stirred solution of 6.01 g (40 mmol, 4 eq.) of triethylene glycole (TEG) and 2.00 g of TEA (20 mmol, 2 eq.) in 50 ml of DCM, 1.91 g (10 mmol, 1 eq.) of tosyl chloride (TsCl) were added in a single portion and the mixture stirred at room temperature for 6 h. The mixture was treated with a 1M HCl solution (3 x 50mL), then with a saturated NaHCO<sub>3</sub> solution (1 x 50 mL). The organic layer was dried over Na<sub>2</sub>SO<sub>4</sub>, filtered and the solvent removed under reduced pressure. The product was purified by chromatography on a silica gel column using a 95:5 v/v mixture of DCM and MeOH as eluant. Yield: 50% wt. Yellow oil. <sup>1</sup>H NMR (300 MHz, CDCl<sub>3</sub>) ( $\delta =$  ppm): 7.80 (d,  $J = 8.2$  Hz, 2H), 7.30 (d,  $J = 8.2$  Hz, 2H), 4.17 (t,  $J = 4.6$  Hz, 2H), 3.70 (m, 4H), 3.62 (m, 4H), 3.59 (t,  $J = 4.9$  Hz, 2H), 2.44 (s, 3H), 2.00 (bs, 1H); <sup>13</sup>C NMR (300 MHz; CDCl<sub>3</sub>) ( $\delta =$  ppm): 144.78, 132.80, 129.73, 127.79, 72.39, 70.59, 69.07, 68.52, 61.51, 21.46; FT-IR (cm<sup>-1</sup>): 3423, 2921, 2874, 1598, 1453, 1355, 1189, 1176, 1122, 1097, 1068, 1017, 923, 818, 776, 664, 554; EI-MS 305 (M+H)<sup>+</sup>.

##### *Synthesis of TEG-OProp:*<sup>48</sup>

A solution of 90 mg (1.6 mmol, 1 eq.) of propargyl alcohol in 5 mL of dry THF was cooled to -78 °C under nitrogen atmosphere. Then, 1 mL (1.6 mmol, 1 eq.) of butyllithium (1.6 M in hexane) was slowly added, keeping the temperature below -70 °C. After 5 minutes, 500 mg (1.6 mmol, 1 eq.) of TEG-OTs dissolved in 1 mL of dry DMF were added. The mixture was left to warm up to room temperature and stirred overnight. The reaction was quenched with 1 ml of distilled water, then the mixture was dried over Na<sub>2</sub>SO<sub>4</sub>, filtered and the solvent removed under reduced pressure. The pure product was obtained after flash chromatography over a silica gel

---

column (230-400 mesh), using a 98:2 v/v mixture of DCM and MeOH as eluant. Yield: 37% wt. Yellow oil.  $^1\text{H}$  NMR (200 MHz,  $\text{CDCl}_3$ ) ( $\delta$  = ppm): 4.20 (d,  $J$  = 2.4 Hz, 2H), 3.67 (m, 10H), 3.62 (t,  $J$  = 5.2 Hz, 2H), 2.44 (t,  $J$  = 5.2 Hz, 1H);  $^{13}\text{C}$  NMR (300 MHz;  $\text{CDCl}_3$ ) ( $\delta$  = ppm): 79.58, 74.81, 72.66, 70.60, 70.30, 69.08, 61.64, 28.40; FT-IR ( $\delta$  =  $\text{cm}^{-1}$ ): 3282, 2873, 2114, 1941, 1642, 1459, 1351, 1290, 1249, 1176, 1095, 1033, 925, 886, 839, 665; FAB-MS 189 ( $\text{M}+\text{H}$ ) $^+$ .

*Synthesis of Boc-Arg(Z)<sub>2</sub>-TEG-OProp:*

To a stirred solution of TEG-OProp (50 mg, 0.27 mmol, 1 eq.), Boc-Arg(Z)<sub>2</sub>-OH (144 mg, 0.27 mmol, 1 eq.) and DMAP (3 mg, 0.03 mmol, 0.1 eq.) in 5 mL of AcOEt at 0 °C a solution of 61 mg (0.30 mmol, 1.1 eq.) of DCC in 3 mL of ethyl acetate was added dropwise. The reaction mixture was left to warm up to room temperature and stirred for 3 hours and kept overnight at -20 °C. The precipitated urea formed from the DCC was filtered and the solvent removed under reduced pressure. The residue afforded the title compound which was obtained in a pure state after column chromatography on silica gel (70-230 mesh) using a 6:4 v/v mixture of hexane and AcOEt as eluant. Yield: 57% wt. Yellow oil.  $[\alpha]_D$  ( $c$  = 0.1 w/v;  $\text{CHCl}_3$ ): + 7.165;  $^1\text{H}$  NMR (300 MHz,  $\text{CDCl}_3$ ) ( $\delta$  = ppm): 7.38 (m, 10H), 5.24 (s, 2H), 5.14 (s, 2H), 4.28 (m, 1H), 4.19 (m, 2H), 4.18 (d,  $J$  = 2.4 Hz, 2H), 3.99 (t,  $J$  = 6.7 Hz, 2H), 3.29 (m, 10H), 2.42 (t,  $J$  = 2.4 Hz, 1H), 1.54 (m, 4H), 1.41 (s, 9H);  $^{13}\text{C}$  NMR (300 MHz;  $\text{CDCl}_3$ ) ( $\delta$  = ppm): 172.44, 163.82, 160.46, 155.78, 155.36, 136.92, 134.65, 128.37, 128.31, 127.88, 127.77, 79.71, 79.62, 74.56, 70.53, 70.47, 70.36, 69.04, 68.88, 68.82, 66.93, 64.18, 58.33, 53.24, 44.15, 29.43, 28.28, 24.28; FT-IR ( $\text{cm}^{-1}$ ): 3390, 3285, 3034, 2930, 1717, 1644, 1610, 1510, 1455, 1404, 1379, 1367, 1350, 1254, 1167, 1098; FAB-MS 713 ( $\text{M}$ ) $^+$ .

**2.4.2.3.7 Synthesis of Ac-Arg(Z)<sub>2</sub>-Gly-Asp(OBn)-TEG-OProp:**

*Synthesis of N-acetyl-Arg(Z)<sub>2</sub>-OH:*<sup>49</sup>

A solution of Boc-Arg(Z)<sub>2</sub>-OH (900 mg, 1.65 mmol, 1 eq.) in 20 mL of DCM was treated at 0 °C

---

---

with 20 mL of trifluoroacetic acid (TFA) for 1 h, then the solvent was removed under reduced pressure. 5 mL of DCM were added, followed by a further addition of 425 mg (3.3 mmol, 2 eq.) of *N,N*-diisopropylethylamine (DIPEA). The mixture was then treated with acetic anhydride (173 mg, 1.65 mmol, 1 eq.). After evaporation of the solvent, the residue was purified by column chromatography on silica gel (70-230 mesh) using a mixture of DCM/methanol 9/1 v/v as eluant. Yield: 31% wt. Colorless oil.  $[\alpha]_D$  (c = 0.6 w/v;  $\text{CHCl}_3$ ): + 5.088;  $^1\text{H}$  NMR (300 MHz,  $\text{CDCl}_3$ ) ( $\delta$  = ppm): 7.32 (m, 10H), 5.23 (s, 2H), 5.11 (s, 2H), 4.55 (m, 1H), 4.05 (m, 1H), 3.80 (m, 1H), 1.80 (s, 3H), 1.70 (m, 4H);  $^{13}\text{C}$  NMR (300 MHz;  $\text{CDCl}_3$ ) ( $\delta$  = ppm): 175.17, 171.69, 163.19, 160.62, 155.71, 136.31, 134.52, 128.96, 128.88, 128.53, 128.37, 128.22, 69.19, 67.38, 52.88, 44.35, 26.99, 25.00, 22.56; FT-IR ( $\text{cm}^{-1}$ ): 3387, 2605, 2498, 1714, 1652, 1255, 1097, 1009, 807, 777, 735, 696; FAB-MS 485 (M)<sup>+</sup>.

#### *Synthesis of N-acetyl-Arg(Z)<sub>2</sub>-Gly-OtBu:*

To a 10 mL solution of *N*-acetyl-Arg(Z)<sub>2</sub>-OH (170 mg, 0.36 mmol, 1 eq.) in DCM, TEA (144 mg, 1.20 mmol, 3.3 eq.) and hydroxybenzotriazole (HOBt, 73 mg, 0.54 mmol, 1.5 eq.) were added followed by the addition of 83 mg (0.43 mmol, 1.2 eq.) of EDCI. After 15 minutes stirring, the mixture was treated with 57 mg (0.43 mmol, 1.2 eq.) of H<sub>2</sub>N-Gly-OtBu. After stirring overnight at room temperature, the mixture was washed first with a saturated solution of NaHCO<sub>3</sub> (10 mL), then with a saturated solution of citric acid (10 mL) and finally with brine (10 mL). The organic layer was dried over MgSO<sub>4</sub>, filtered and the solvent evaporated to dryness; the residue was purified by chromatography on a silica gel column (70-230 mesh) using AcOEt as eluent. Yield: 48% wt. White solid (mp 125-128 °C).  $[\alpha]_D$  (c = 1.4 w/v;  $\text{CHCl}_3$ ): + 16.040;  $^1\text{H}$  NMR (300 MHz,  $\text{CDCl}_3$ ) ( $\delta$  = ppm): 9.51 (bs, 1H), 9.41 (bs, 1H), 7.36 (m, 10H), 7.07 (d, *J* = 7.8 Hz, 1H), 6.97 (t, *J* = 5.3 Hz, 1H), 5.23 (s, 2H), 5.13 (d, *J* = 1.9 Hz, 2H), 4.56 (m, 1H), 4.08 (m, 1H), 3.90 (m, 1H), 3.79 (dd, *J* = 17.9, 6.1 Hz, 1H), 3.49 (dd, *J* = 17.9, 5.0 Hz, 1H), 1.88 (s, 3H), 1.74 (m, 4H), 1.42 (s, 9H);  $^{13}\text{C}$  NMR (300 MHz;  $\text{CDCl}_3$ ) ( $\delta$  = ppm): 171.70, 170.21, 168.47, 163.26, 160.98, 155.78, 136.34, 135.54, 128.85, 128.62, 128.31, 81.83, 69.11, 67.23, 52.49, 44.24, 41.84, 28.22, 28.03,

---

24.64, 23.03; FT-IR ( $\text{cm}^{-1}$ ): 3371, 3287, 1758, 1725, 1647, 1598, 1548, 1403, 1265, 1251, 1192, 1152, 1100, 1035, 1010, 981, 938, 910, 848, 822, 811, 776, 697, 666, 639; FAB-MS 598 (M)<sup>+</sup>.

*Synthesis of N-acetyl-Arg(Z)<sub>2</sub>-Gly-OH:*

50 mg (0.08 mmol, 1 eq.) of N-acetyl-Arg(Z)<sub>2</sub>-Gly-OtBu were dissolved in 10 mL of DCM, then 85  $\mu\text{L}$  of H<sub>3</sub>PO<sub>4</sub> 85% (0.8 mmol, 10 eq.) were added and the reaction was stirred at room temperature for 6 h. The mixture was then washed with 15 mL of water. The layers were separated and the aqueous one was washed with DCM (3 x 10 mL); the collected organic layers were dried over MgSO<sub>4</sub> and filtered. Removal of the solvent afforded the pure product. Yield: 88% wt. White solid.  $[\alpha]_{\text{D}}^{25}$  (c = 0.5 w/v; MeOH): - 2.228; <sup>1</sup>H NMR (300 MHz, MeOD) ( $\delta$  = ppm): 8.10 (t,  $J$  = 5.6 Hz, 1H), 7.36 (m, 10H), 5.28 (s, 2H), 5.13 (s, 2H), 4.34 (t,  $J$  = 7.8 Hz, 1H), 3.85 (m, 4H), 1.91 (s, 3H), 1.73 (m, 4H); <sup>13</sup>C NMR (300 MHz; MeOD) ( $\delta$  = ppm): 174.42, 173.28, 172.75, 164.89, 162.05, 157.00, 138.40, 136.62, 130.21, 129.76, 129.68, 129.49, 129.06, 128.99, 128.22, 69.81, 68.28, 54.33, 45.62, 41.85, 29.96, 26.11, 22.51; FT-IR ( $\text{cm}^{-1}$ ): 3400, 3281, 1747, 1723, 1628, 1549, 1507, 1459, 1405, 1555, 1216, 1191, 1177, 1147, 1106, 1092, 1030, 10003, 978, 931, 907, 807, 781, 6970; FAB-MS 542 (M)<sup>+</sup>.

*Synthesis of Boc-Asp(OBn)-OTEG-OProp:*

Boc-Asp(OBn)-OH (171 mg, 0.53 mmol, 1 eq.), TEA (162 mg, 1.59 mmol, 3 eq.) and HBTU (241 mg, 0.64 mmol, 1.2 eq.) were dissolved in 10 mL of a 9/1 v/v mixture of DCM/DMF, under nitrogen atmosphere. After 15 minutes, 100 mg (0.53 mmol, 1 eq.) of TEG-OProp were added and the reaction was stirred at room temperature overnight. The solvent was removed under reduced pressure and the product purified by flash chromatography on a silica gel column (230-400 mesh) using a 6:4 v/v mixture of hexane and AcOEt as eluant. Yield: 61% wt. Yellow oil.  $[\alpha]_{\text{D}}^{25}$  (c = 1.0 w/v; CHCl<sub>3</sub>): - 0.030; <sup>1</sup>H NMR (300 MHz, CDCl<sub>3</sub>): 7.32 (m, 5H), 5.48 (d,  $J$  = 7.9 Hz, 1H), 5.10 (d,  $J$  = 1.3 Hz, 2H), 4.58 (m, 1H), 4.24 (td,  $J$  = 4.5, 1.9 Hz, 2H), 4.16 (d,  $J$  = 2.4 Hz, 2H), 3.64 (m, 10H), 3.01 (dd,  $J$  = 4.8, 16.9 Hz, 1H), 2.87 (dd,  $J$  = 4.8, 16.8 Hz, 1H), 2.41 (t,  $J$  = 2.4 Hz,

---

1H), 1.42 (s, 9H);  $^{13}\text{C}$  NMR (300 MHz; MeOD) ( $\delta$  = ppm): 171.03, 170.83, 170.52, 135.38, 128.49, 128.28, 128.18, 79.97, 47.47, 70.47, 70.33, 69.00, 68.69, 66.65, 64.61, 58.27, 50.00, 36.84, 28.20; FT-IR ( $\text{cm}^{-1}$ ): 3369, 3286, 3065, 3033, 2975, 2873, 2115, 1714, 1499, 1456, 1390, 1366, 1286, 1249, 1165, 1102, 1048, 1031, 921, 861, 780, 753, 699; FAB-MS 394 (M+H-Boc) $^+$ .

*Synthesis of H<sub>2</sub>N-Asp(OBn)-OTEG-OProp:*

To a stirred solution of Boc-Asp(OBn)-OTEG-OProp (115 mg, 0.29 mmol, 1 eq.) in 2 mL of DCM, cooled at 0 °C, 2 mL of TFA were added dropwise. The reaction was allowed to warm up at room temperature and stirred for 1.5 h. The pure product was obtained as a trifluoroacetic acid salt after removal of the solvent at reduced pressure. Yield: 99% wt. Yellow oil.  $[\alpha]_D$  (c = 1.0 w/v;  $\text{CHCl}_3$ ): - 0.166;  $^1\text{H}$  NMR (300 MHz,  $\text{CDCl}_3$ ): 7.34 (m, 5H), 5.15 (s, 2H), 4.45 (m, 1H), 4.35 (m, 2H), 4.15 (d,  $J$  = 2.3 Hz, 2H), 3.63 (m, 10H), 3.19 (d,  $J$  = 4.5 Hz, 2H), 2.46 (t,  $J$  = 2.3 Hz, 1H);  $^{13}\text{C}$  NMR (300 MHz;  $\text{CDCl}_3$ ) ( $\delta$  = ppm): 170.46, 167.37, 160.74 (q,  $J$  = 156 Hz), 134.70, 128.69, 128.47, 115.46 (q,  $J$  = 1332 Hz), 78.90, 76.62, 75.30, 70.173, 70.06, 69.87, 68.93, 68.38, 67.85, 65.55, 58.32, 49.95, 33.40; FT-IR ( $\text{cm}^{-1}$ ): 3448, 3285, 2918, 1752, 1675, 1525, 1456, 1397, 1359, 1306, 1174, 1029, 949, 839, 798, 753, 723, 702; EI-MS 394 (M+H) $^+$ .

*Synthesis of Ac-Arg(Z)<sub>2</sub>-Gly-Asp(OBn)-OProp:*

To a stirred solution of Ac-Arg(Z)<sub>2</sub>-Gly-OH (40 mg, 0.074 mmol, 1 eq.) in 2 mL of DMF, under nitrogen atmosphere, 70  $\mu\text{g}$  of TEA (0.3 mmol, 4 eq.) and 34 mg of HBTU (0.09 mmol, 1.2 eq.) were added. After 20 minutes a solution of H<sub>2</sub>N-Asp(OBn)-OProp (70 mg, 0.18 mmol, 2.41 eq.) in 1 mL of a 1:1 v/v mixture of DCM and DMF was added dropwise. The reaction was stirred at room temperature overnight. Yield: 24% wt. Yellow oil.  $^1\text{H}$  NMR (300 MHz,  $\text{CDCl}_3$ ): 7.36 (s, 15H), 6.56 (d,  $J$  = 8.8 Hz, 1H), 5.26 (s, 2H), 5.14 (m, 4H), 4.95 (m, 1H), 4.88 (m, 1H), 4.20 (d,  $J$  = 2.4 Hz, 2H), 4.16 (m, 1H), 4.01 (m, 1H), 3.65 (m, 16H), 2.43 (t,  $J$  = 2.4 Hz, 1H), 1.88 (s, 3H), 1.75 (m, 4H); FAB-MS 920 (M+H) $^+$ .

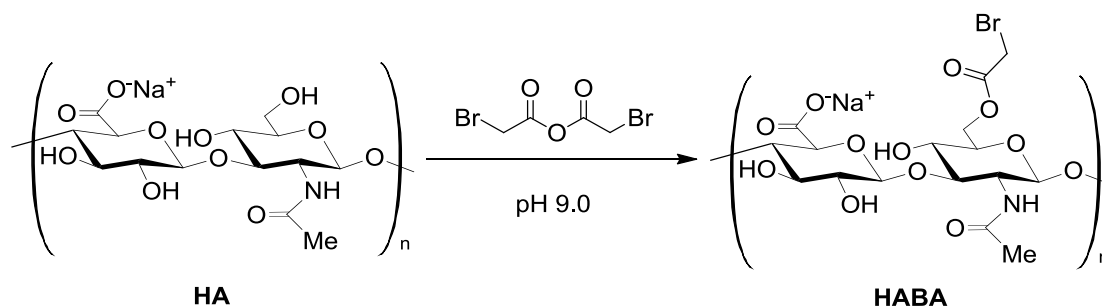
---

### 2.4.3 RESULTS AND DISCUSSION

As discussed before (See 2.1), chemical modification of HA can be performed at two different sites: the carboxylic acid group and the hydroxy group; in the second case it is reasonable to assume that reaction occurs on the primary hydroxy of the *N*-acetylglucosamine moiety, because of its better chemical accessibility. Few examples of modification of the HA with electrophiles reacting with the primary hydroxy group have been reported.<sup>11</sup> In particular, this nucleophilic centre is selected as the reacting centre with anhydrides; the synthesis and the characterization of two novel haloacetate derivatives of HA in aqueous media has been previously reported.<sup>26</sup> Specifically, a bromoacetate-derivatised HA was obtained by treating HA with bromoacetic anhydride under basic reaction conditions. The reaction procedure is characterised by a strict control of the pH, which must be maintained at the value of 9 to promote the deprotonation of the primary alcohol (which has a lower  $pK_a$  respect to the other ones), favoring the nucleophilic attack. Furthermore a high reactant (bromoacetic anhydride) molar excess is necessary because of the expected side reaction involving the formation of the mixed anhydride between bromoacetic anhydride and HA, followed by its hydrolysis to restore the HA glucuronic acid carboxy acid group. Hence, the consumption of the anhydride reagent reduces the overall possibility of modification of the primary hydroxyl groups.

We started our work by repeating the reaction described in literature to obtain the bromoacetate (HABA) derivative on the HA with the average molecular weight of 235 kDa (Scheme 5).

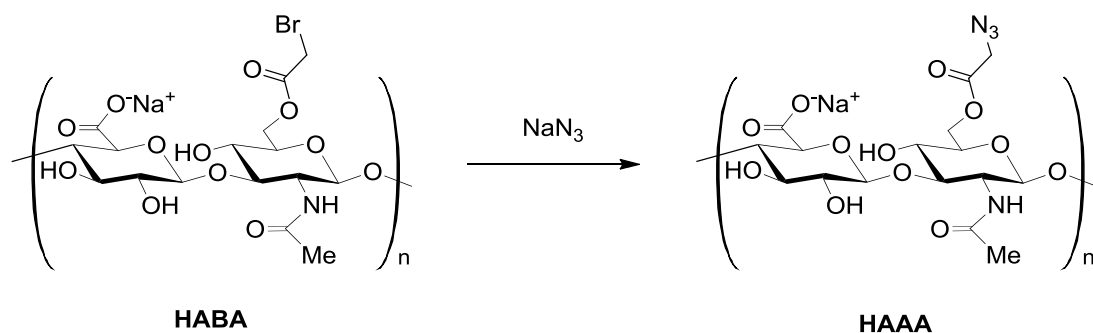




**Scheme 5: Synthesis of HA-bromoacetate (HABA)**

We slightly changed the experimental settings (mainly due to the technical equipment required); in fact, while Prestwich et al. maintained the reaction mixture at constant temperature of 4 °C all over the course of the reaction, we added freshly prepared bromoacetic anhydride at 0 °C and allowed the temperature slowly to rise up to 20 °C. The same changes in the <sup>1</sup>H NMR spectrum (D<sub>2</sub>O) as the ones reported in literature were observed. Compared to the spectrum of the starting material (Figure 33 A and B), a new broad resonance at 3.97 ppm appeared, corresponding to the methylene protons of the bromoacetate group; furthermore, the specific pattern of the signal related to the two protons of the methylene group on the *N*-acetylglucosamine moiety was modified.

The displacement of the bromine is reported in literature with sodium iodide, affording the corresponding iodoacetic derivative (HAIA). HABA and HAIA display different reactivities with thiols as nucleophiles and both polymers have already been investigated in biological assays. We decided to take advantage of the good reactivity of HABA towards nucleophiles, to insert an azido group by reaction with sodium azide via an S<sub>N</sub>2 nucleophilic substitution (Scheme 6).



**Scheme 6: Synthesis of HA-azidoacetate (HAAA)**

Thanks to the complete solubility of HABA in water, we could perform the substitution reaction without the addition of other salts, simplifying the purification process. We used a large molar excess of sodium azide to ensure the complete conversion in 24 hours. The final product could be recovered in a pure state after dialysis followed by freeze-drying. The progress of the reaction could be confirmed by IR analysis, by monitoring the appearance of the typical azide band at  $2150\text{ cm}^{-1}$  (Figure 33 D). Else more the  $^1\text{H}$  NMR of the sample, compared with the spectrum of the precursor, (Figure 33 B and C) showed that the peak corresponding to the methylene protons of the haloacetate group (at 3.97 ppm) completely disappeared. To the best of our knowledge this is the first example of insertion of an azide onto the HA backbone by a  $\text{S}_{\text{N}}2$  reaction; previous examples, in fact, reported the use of bifunctional molecules featuring both an azide and an amino group suitable for condensation with the HA through the usual coupling reagents, e.g. carbodiimides.<sup>39,50</sup> Thus, our strategy did not require the use of both sophisticated molecules, such as the namino-azides, and the excess of expensive reagents, such as the carboxy-activating agents, with remarkable advantage for atom economy.<sup>51</sup>

## Chemical Modification of the Hyaluronic Acid

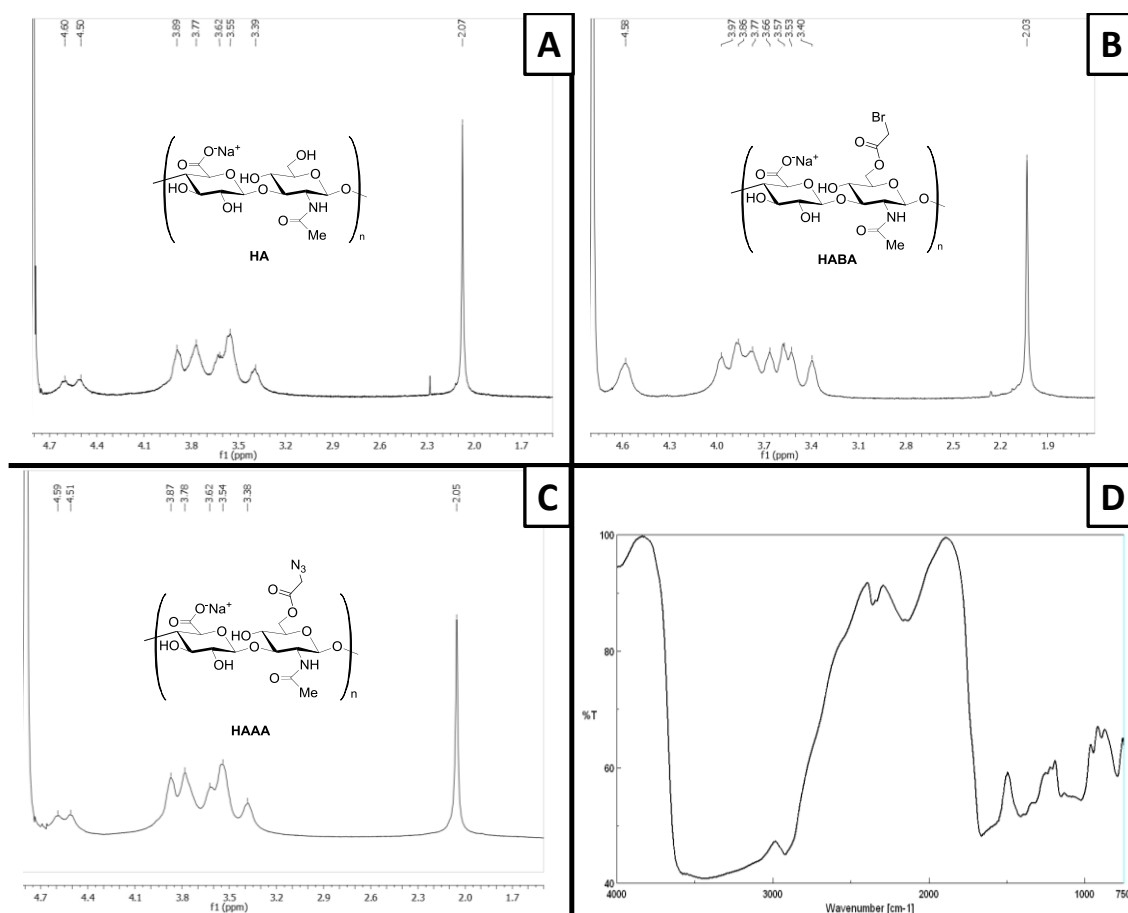


**Figure 33:**  $^1\text{H}$  NMR spectra of HA, HABA, HAAA and FT-IR spectrum of HAAA

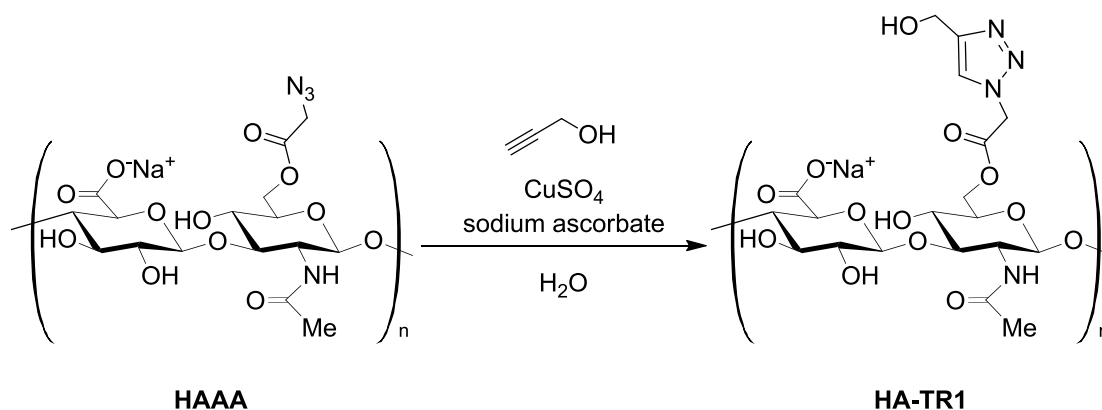
**A:**  $^1\text{H}$  NMR spectrum of HA (D<sub>2</sub>O, 400 MHz) showing two signals at 4.60 and 4.50 ppm due to the methylene close to the primary alcohol, broad signals from 3.89 to 3.39 of the protons on the glucosaminic and glucuronic rings and a singlet at 2.07 ppm relative to the acetamide moiety. **B:**  $^1\text{H}$  NMR spectrum of HABA (D<sub>2</sub>O, 400 MHz) where a new peak of the methylene protons of the bromoacetate group appeared at 3.97 ppm. **C:**  $^1\text{H}$  NMR spectrum of HAAA (D<sub>2</sub>O, 400 MHz) showing no more traces of the peak at 3.97 ppm. **D:** FT-IR spectrum of HAAA, the broad spectrum relative to the polymer features a new band at 2150 cm<sup>-1</sup> relative to the stretching vibrations of the azide.

The presence of the azide group on the HA skeleton allowed us to perform the Sharpless cycloaddition reaction, initially tested with propargyl alcohol, which is the model reagent for this transformation (Scheme 7).

FT-IR spectrum confirmed the absence of the azido group in the product, meaning that it had

completely reacted, affording the triazole heterocycle. In addition, thanks to the use of this small and hydrophilic alkyne, we ensured the water-solubility of the product, which was then analysed by  $^1\text{H}$  NMR in  $\text{D}_2\text{O}$  (Figure 34). In the NMR spectrum, the signal related to the aromatic proton of the triazole ring could be easily individuated and, from its integration, it was possible to calculate the degree of substitution, defined as modified groups per 100 disaccharide units. Specifically, both the ratio between the integral of the aromatic proton and the signal of the methyl group and the area of the peaks between 4.10 and 3.30 ppm were found in agreement with a substitution level of the 4%, which is an optimal value considering that the modification of more than the 10% of monomeric units of HA, invariably produces undesired effects on the biocompatibility of the substrate.

Furthermore we tested the biological effects promoted by the insertion of this new functional group on the HA *in vitro*, on human pericyte-derived cells (See 2.5).



**Scheme 7: Sharpless cycloaddition with HAAA and propargyl alcohol**

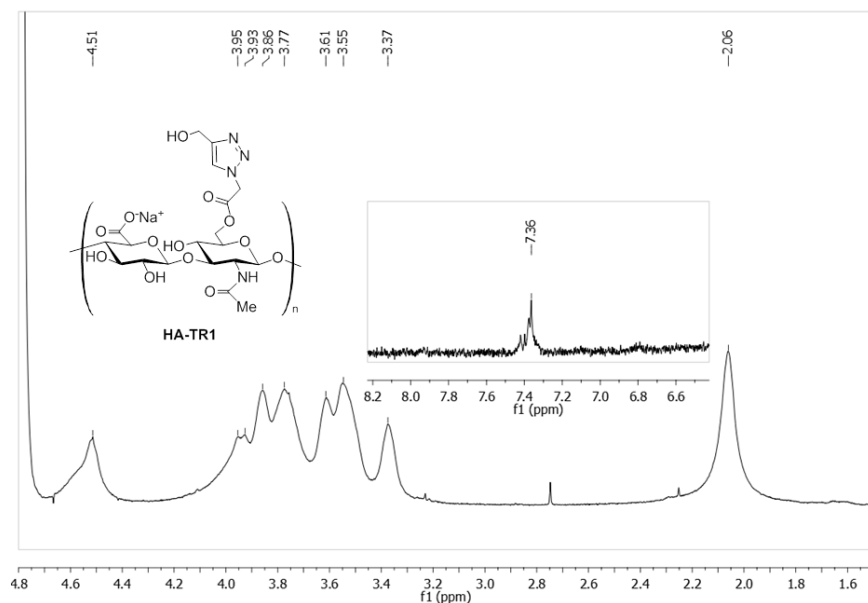


**Figure 34:  $^1\text{H}$  NMR spectrum of HA-TR1**

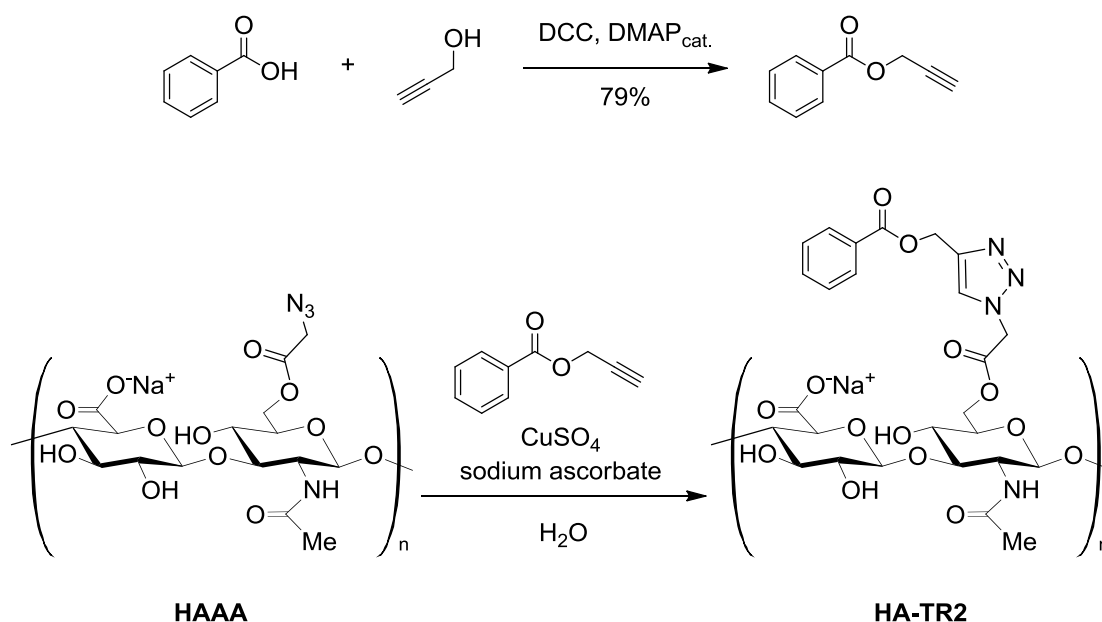
$^1\text{H}$  NMR spectrum of HA-TR1 ( $\text{D}_2\text{O}$ , 400 MHz) showing a new aromatic signal at 7.36 ppm relative to the proton on the triazole ring.

We repeated the copper catalysed cycloaddition with the benzoate of the propargyl alcohol described before (Scheme 8). The aim was, on the one hand, to have an even more precise indication of the degree of substitution and, on the other hand, to extend the scope of the reaction to more hydrophobic alkyne-containing compounds by using the same protocol.

Again, we have been able to confirm the reactivity of the azide group in click reactions following the disappearance of the peak at  $2150\text{ cm}^{-1}$  in the IR spectrum. After purification by dialysis, the product was found not completely soluble in water; hence, we did not observe two distinct  $^1\text{H}$  NMR signals for the different aromatic protons, as we were expecting for a better determination of the degree of substitution. The addition of 10% v/v deuterated DMSO did not help to complete solubilised the product.

## Chemical Modification of the Hyaluronic Acid

---



**Scheme 8: Synthesis of propargyl benzoate and its use in the Sharpless cycloaddition with HAAA**

We then directed our attention to the reactions of bioconjugation between HA and precursors of aminoacidic sequences, in order to investigate the versatility of this strategy and to extend its use to a plethora of compounds capable to be further modified directly on the HA scaffold. Our idea was to provide a versatile tool to be used with different bioactive compounds such as peptides, fatty acids, steroids, drugs. Furthermore the *in situ* modification could open the way to the design of a multifunctionalised HA, bearing different molecules as pendants in order to produce a synergic biological effect.

The synthesis of a fully protected tripeptide was accomplished as shown in Scheme 9.

We selected the tripeptide composed by Arginine-Glycine-Aspartate (RGD) because of its biological importance in mediating and regulating processes like cell adhesion, angiogenesis, apoptosis and cell migration.<sup>52-54</sup>

---

Furthermore, our aim was that to investigate whether it were possible to carry out some benzyl group deprotection reactions by heterogeneous hydrogenation directly on the HA derivative; hence, we designed a molecule featuring protecting groups labile in front of reductive cleavage.

For the synthesis of the RGD precursor, we first prepared three properly functionalised amino acids. Then, we formed the new amidic bonds using one of the most popular in situ activation reagents in solid and solution phase peptide synthesis, that is the HBTU. In addition to the high reactivity, HBTU has also been shown to limit epimerization during condensation and during DMAP catalyzed functionalisation.

We tried also to synthesise a RGD sequence that could be selectively deprotected at the *N*-terminus of the arginine to undergo further functionalisation with an alkyne. Unfortunately, the coupling reaction between the arginine unit and the fragment containing the glycine and the aspartate moiety failed (See Supporting Information 2.8.1.1).

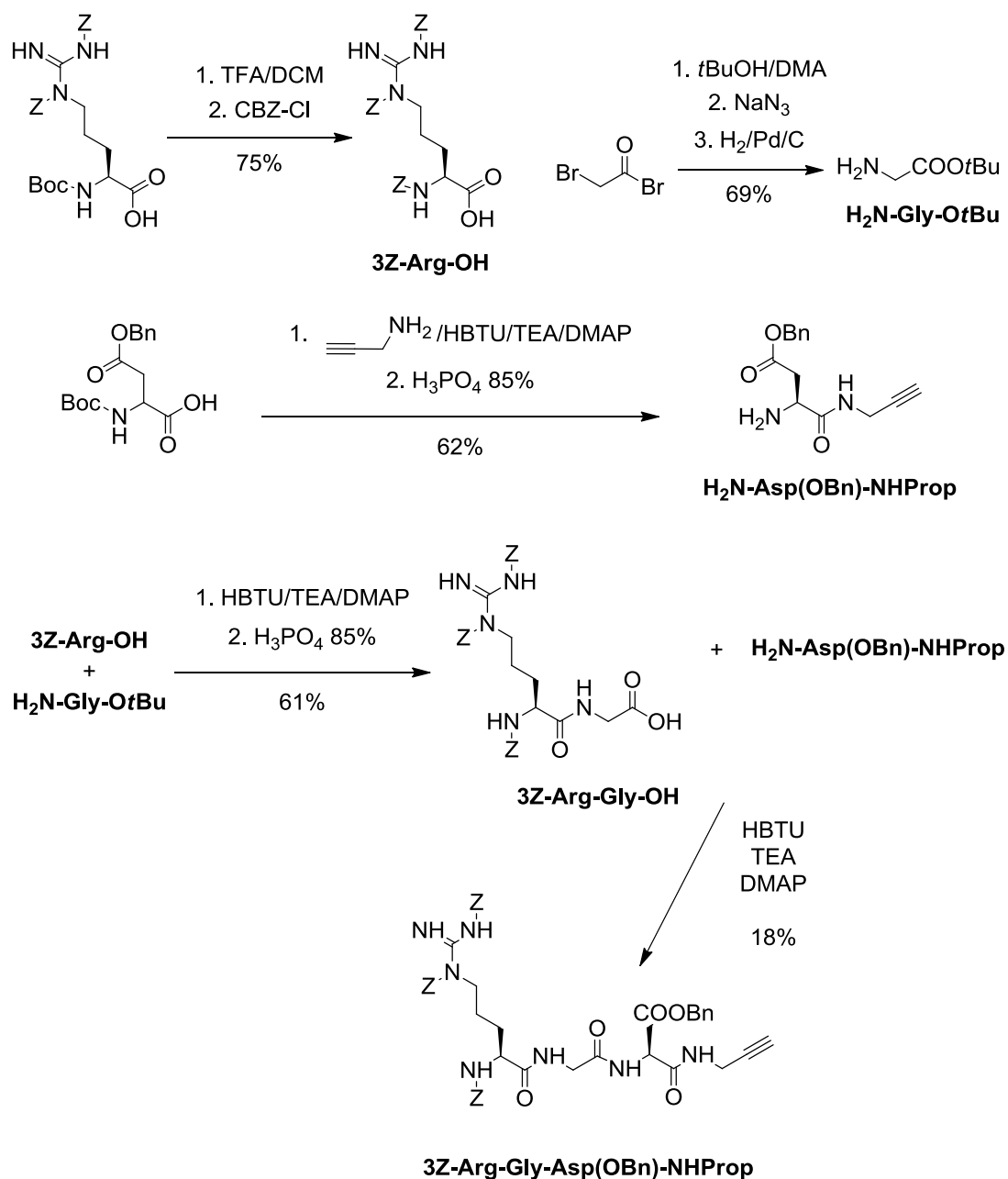
Trying to graft the RGD-alkyne containing sequence on the HAAA, we changed the commonly used protocols, to avoid the necessity of using a large excess of reagent; thus, in order to balance the kinetic of the reaction, we used twice the amount of catalyst present in the reaction medium, i.e. respectively 0.2 eq. of Cu<sup>II</sup> and 1.0 eq. of ascorbate respect to the monomeric unit of HA. We found, however, that even after two days the formation of the desired product did not occur: the click-reaction probably failed because of the poor solubility of the peptide in water.

To overcome this problem, we investigated two different strategies.

The first one contemplated the transformation of the HAAA into its tetrabutylammonium salt, replacing the sodium cation, in order to promote its solubility in organic solvents (e.g. dimethyl sulfoxide or dimethylformamide) in which the peptide exhibits a good solubility; at this point the cycloaddition could be performed in a mixture of water and organic solvent.

## Chemical Modification of the Hyaluronic Acid

The second strategy was based on the assumption that a water-soluble linker could promote the accessibility of the alkyne and then the development of the conjugation reaction.



**Scheme 9: Synthesis of a protected precursor of the RGD sequence featuring a terminal alkyne**



To examine the feasibility of the first pathway, we started with the synthesis of a fully protected dipeptide bearing a terminal propargyl ester (Scheme 10). Specifically derivatives of arginine and glycine were used to prepared a compound carrying protecting groups removable by heterogenous hydrogenation, and with solubility not very different from that of the tripeptide presented in Scheme 9, but synthesised through a reduced number of steps.

Conversion of the sodium salt of the HAAA into its tetrabutylammoniu salt was accomplished using a sulphonic ion-exchange polystyrenic resin (Dowex® 50WX-8-40). The procedure used for this purpose has already been reported for HA<sup>9</sup> and allows the synthesis of a polymer soluble in organic solvents (i.e. DMF and DMSO) in high yields, in short times and under mild conditions.

We were then able to perform the Sharpless cycloaddition reaction in a mixture of water and DMSO (1:1.5 v/v): we maintained the amount of catalyst and antioxidant used at the beginning (i.e. 0.5 eq. of Cu<sup>II</sup> and 1.0 eq. of sodium ascorbate respect to the monomeric unit of HA) and 0.2 eq. of the alkyne. After two days, we added a large excess of propargyl alcohol to ensure that all the azido groups on the polymer had been transformed. We checked the sample by IR, by drying a small sample under vacuum. As we were expecting, the peak relative to the azide progressively disappeared. Then, we removed the catalyst by dialysis; hence, we decided to directly submit the sample to heterogenous hydrogenation in order to avoid manipulations of the poorly soluble sample. Specifically, deprotection was accomplished with Palladium on activated charcoal as catalyst, with a 1:1 mixture of water and methanol as solvent and a positive pressure of hydrogen (6 bar) to ensure the complete deprotection. To the best of our knowledge, this is the first example of a successful heterogenous hydrogenation on HA derivatives. The product was purified by filtration to remove the solid catalyst and then by dialysis, which allowed also the reconversion of the product into the sodium salt (Scheme 10).

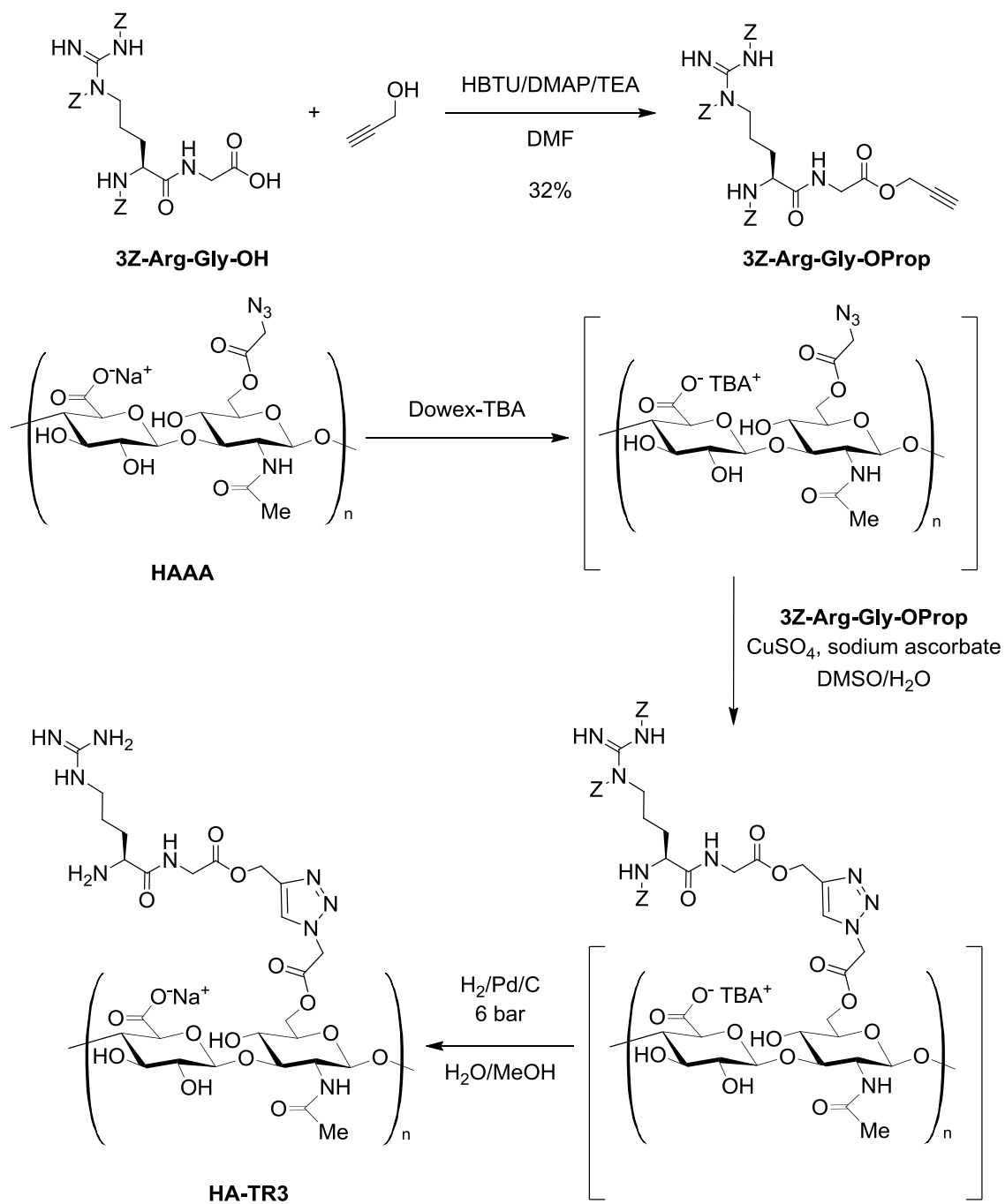
The aqueous solution of the final adduct resulted completely clear and could be analysed by <sup>1</sup>H NMR (Figure 35); the spectrum confirmed the presence of the arginine residue: in fact, a

multiplet related to the two methylene groups in  $\beta$  and  $\gamma$  position clearly appeared between 1.75 and 1.60 ppm. We could observe, however, also several peaks in the aromatic and benzylic region, indicating that the deprotection was probably not complete, or some impurities were still present in the sample. Furthermore, we could recover only the 40% of the initial weight; this was probably an indication that or the hydrolysis leading to smaller polymeric fragments (lost during dialysis) occurred, or part of the product was not soluble and was consequently lost during the filtration over celite, necessary to remove the Palladium catalyst.

We concluded that, even if this method could offer new hints, demonstrating that the Sharpless cycloaddition on HA can be performed in mixed (aqueous/organic) solvents in the presence of scarcely soluble reagents, the experimental set needs to be more deeply studied and improved, since deprotection and sample recovery was found lacking in efficiency.

Thus, we focused our attention on the second pathway presented before, in order to see if those conditions are more favourable for chemically modifying the HA.

## Chemical Modification of the Hyaluronic Acid



Scheme 10: Synthesis of HA-TR3

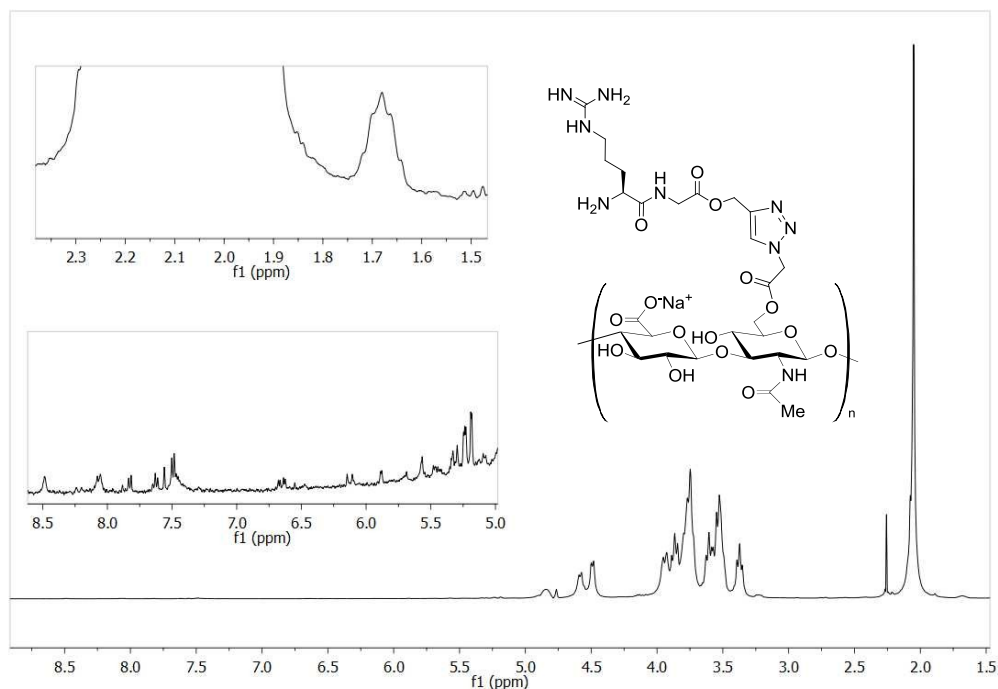


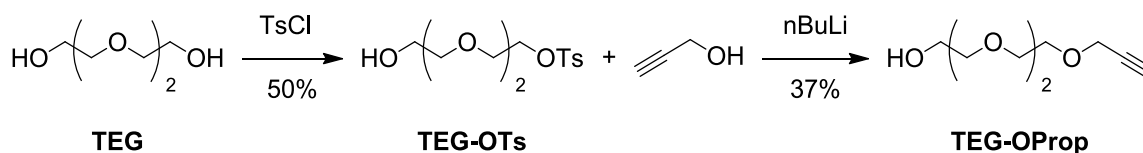
**Figure 35:  $^1\text{H}$ NMR spectrum of HA-TR3**

$^1\text{H}$  NMR ( $\text{D}_2\text{O}$ , 400 MHz, solvent peak suppression) showing a multiplet between 1.75 and 1.60 ppm, related to the two methylenes in  $\beta$  and  $\gamma$  position of the arginine, and several aromatic and benzylic signals.

The second strategy devised to overcome the problems caused by the poor solubility in water of the protected aminoacids and of their HA-conjugates, contemplated the use of a fragment of triethylene glycol as water-soluble linker between the triple bond and the peptide. Our aim was to promote the accessibility of the terminal alkyne in aqueous media. For this purpose, a bifunctional linker featuring a terminal alkyne and an alcoholic function suitable for further functionalisations, e.g. esterification with carboxylic acids, was synthesised as shown in Scheme 11.

The *core* constituted by the triethylene glycol was mono-activated as tosylate and the nucleophilic substitution effected with the anion of propargyl alcohol afforded the desired product. We tried both NaH and *n*BuLi to generate the alkoxyde and the use of the alchyllitium

as the base gave better yields, the 37%, while the 25% yield was obtained with NaH.



**Scheme 11: Synthesis of the water soluble linker featuring a terminal alkyne**

The linker was coupled with a protected arginine residue by esterification mediated by DCC as activating agent, in order to provide a simple compound characterised by two fragments with different solubility in water (Scheme 12).

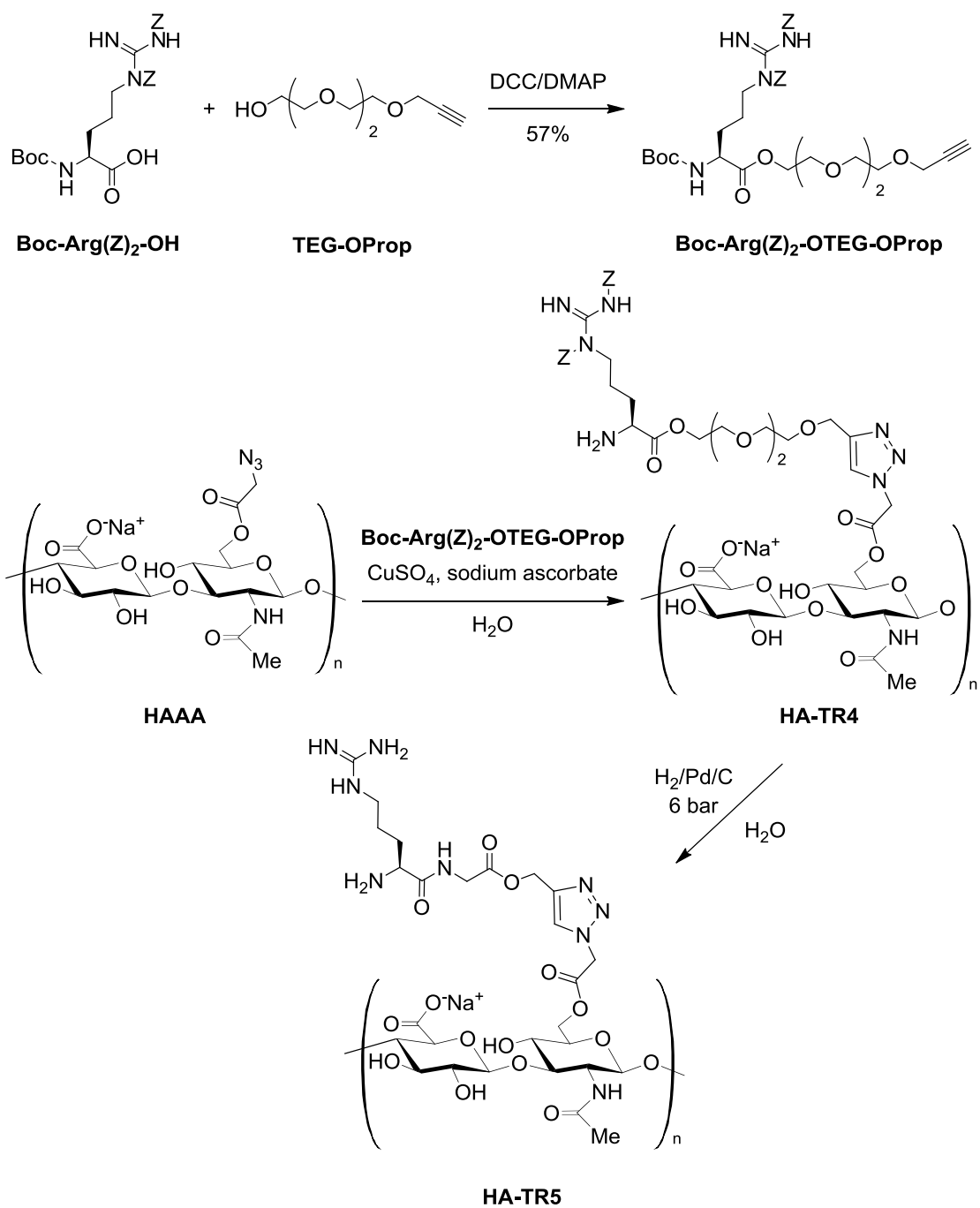
HA was successfully conjugated with a unit of the protected arginine through a copper(I) catalyzed reaction; in this case the reaction was carried out in water solution effected by maintaining the sodium as the counter ion of the biopolymer. After dialysis, carried out to remove the salts from the solution, it was possible to verify from the <sup>1</sup>H NMR spectrum the success of the reaction by recognizing and estimating two aromatic signals, one related to the Z protecting groups (7.39 ppm) and the other to the triazole unit (8.40 ppm) (Figure 36).

Deprotection from the Z protecting groups was effected by heterogeneous hydrogenation using water as solvent (Scheme 12). In this case the mass recovery of the product was excellent (85% wt) and the purity of the product, estimated by <sup>1</sup>H NMR, satisfactory as well; in fact, only one signal was still present at 8.50 ppm, indicating that the Z protecting groups had been completely cleaved and, moreover, that removal of the residues was successfully accomplished. Furthermore, the complete solubility in water of the final product allowed us to perform the purification of the product from the catalyst through a simple filtration.

---

Interestingly we did not observe any signal for the Boc protecting group neither in **HA-TR4** nor in **HA-TR5**; hence, we concluded that the reaction medium was acid enough, due to the presence of ascorbic acid and HA, to promote its hydrolysis.

## Chemical Modification of the Hyaluronic Acid



**Scheme 12: Synthesis of protected arginine functionalised with the water-soluble linker and a terminal alkyne and of the HA conjugates HA-TR4 and HA-TR5**

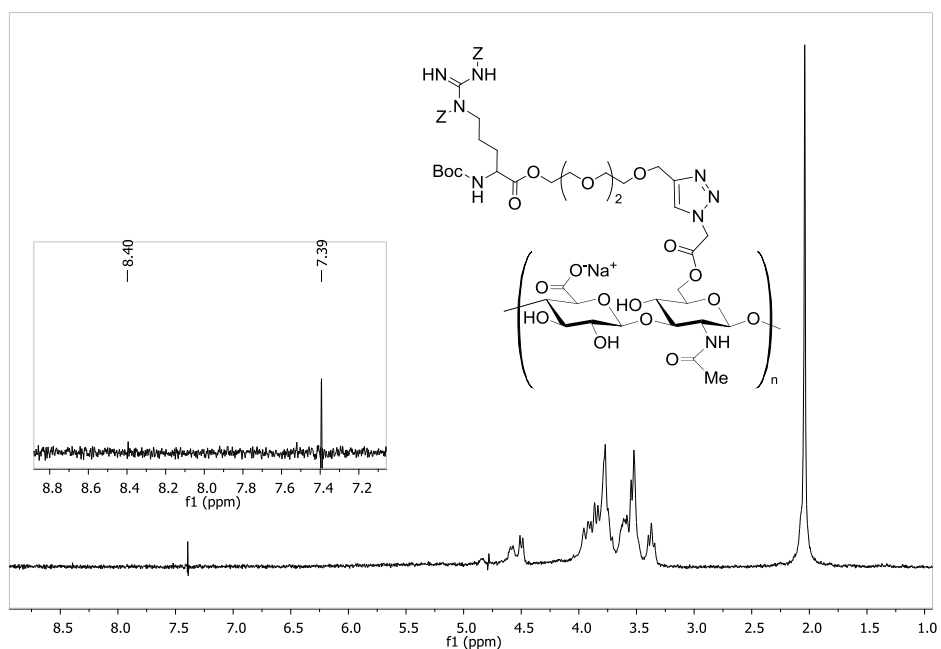


**Figure 36: <sup>1</sup>H NMR of HA-TR4**

<sup>1</sup>H NMR (D<sub>2</sub>O, 300 MHz, solvent peak suppression) showing two well different aromatic signals: one at 8.40 ppm (hydrogen atom on the triazole ring) and one at 7.39 ppm (protons on the phenyl groups of the Z protecting groups).

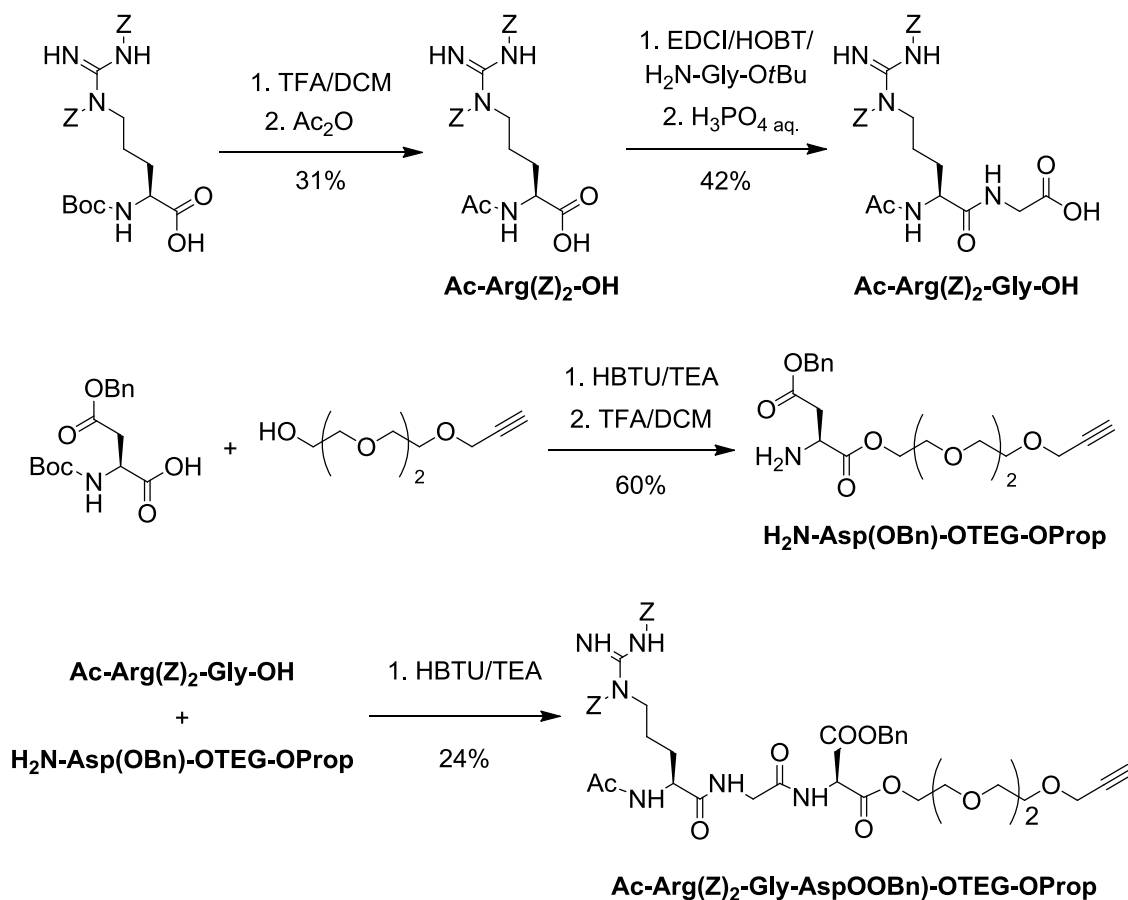
Once proven the feasibility of the synthetic pathway, a new more complete scheme, affording the RGD peptide decorated with the previously reported linker was optimized and the best experimental conditions are reported in Scheme 13.

In detail, the *N*-terminus of the arginine was protected as acetyl derivative in order to have a stable moiety mimicking a peptidic bond. All the new amidic bond have been formed by using HBTU as the coupling reagent and TEA as the organic base. The last reaction between the two fragments, one containing the arginine and the glycine and the other one containing the aspartate and the linker, showed to be particularly challenging; different coupling reagent, i.e. HBTU, DCC, EDCI used in combination with HOBT, and solvents, i.e. DCM and DMF and their



mixture, were used, but the best yield we could attain was the 24% wt, after careful purification by column chromatography.

The final product featured protecting groups labile in front of the heterogenous hydrogenation. In conclusion, we found a reliable synthetic pathway affording, with yields ranging from moderate to good, the protected tripeptide composed by arginine, glycine and aspartic acid, functionalised with a chain of triethylene glycol bearing a terminal triple bond as useful precursor to be linked to the HA scaffold via a classical click cycloaddition catalysed by Cu<sup>I</sup>.



**Scheme 13: Synthesis of the protected RGD sequence bearing a water soluble linker with a terminal alkyne functionality**

#### 2.4.4 CONCLUSION

Bioconjugation between HA and bioactive compounds is a key point in the development of hydrogels for tissue engineering. We explored the versatility of the 1,3-dipolar cycloaddition reaction catalysed by Cu<sup>I</sup> to “click” on the HA scaffold different terminal alkynes, both hydrophilic and hydrophobic, trying to develop a methodology applicable to a wide variety of compounds. We were interested as well in the modification of these active molecules directly on the conjugate derivative, in order to allow the design of a strategy contemplating the insertion of different peptides, fatty acid, growth factors... with a specific architecture.

A new strategy toward the functionalization of the HA with an azido group has been devised. Specifically, the primary hydroxyl group in the HA repeating unit was selected as the reacting centre with electrophilic species like anhydrides. The synthesis and the characterization of the HA bromoacetate derivative (HABA) had been previously reported.<sup>26</sup> We took advantage from this derivative to insert an azido group by reaction with sodium azide via an S<sub>N</sub>2 nucleophilic substitution. The progress of the reaction could be monitored by IR analysis through the growth of the typical azide band at 2150 cm<sup>-1</sup>.

The presence of this group in HA allowed us to perform a Sharpless cycloaddition reaction, initially tested with propargyl alcohol, which is the classical model reagent for this transformation. The substitution degree was initially estimated by examining the <sup>1</sup>H NMR spectra: the ratio between the integral of the aromatic proton of the triazole ring and the signal of the methyl group were indicative of a 4% substitution level.

In order to have an even more precise indication, a derivative bearing more aromatic signals was prepared by reaction of the azido derivative with the benzoate of the propargyl alcohol; in this case, however, we found that the adducts with hydrophobic molecules display a poor solubility in water.

Our attention has been focused on the introduction of the RGD (Arginine-Glycine-Aspartate) motif in order to promote cells adhesion on the hydrogel. Hence the precursor of this sequence bearing a terminal alkyne has been synthesised, but the click-reaction failed probably because in aqueous environment the peptide was not completely soluble.

Even using the tetrabutylammonium salt of the HA and a mixture of DMSO and water we were not able to isolate the pure desired product in a pure state.

To overcome this problem, a water soluble linker based on a triethylene glycol core bearing a terminal alkyne was synthesized.

HA was successfully conjugated with a unit of protected arginine through a  $\text{Cu}^I$  catalysed reaction; deprotection from the Z protecting groups was completed by heterogeneous hydrogenation. From the  $^1\text{H}$  NMR spectra it was possible to verify the success of the reaction by recognizing and estimating the two aromatic signals, one relative to the Z protecting groups and the other to the triazole unit.

Once proven the feasibility of the synthetic pathway, a new more complete scheme affording the RGD peptide decorated with the water-soluble linker was optimized.

## **2.5 PROLIFERATION AND DIFFERENTIATION OF MESOANGIOBLASTS ON HYALURONAN DERIVATIVES**

### **2.5.1 INTRODUCTION**

Regenerative medicine is the process of creating living, functional tissues to repair or replace tissue or organ functions lost due to age, disease, damage, or congenital defects. This field holds the promise of regenerating damaged tissues and organs in the body by stimulating previously irreparable organs to heal themselves. Regenerative medicine also empowers scientists to grow tissues and organs in the laboratory and safely implant them when the body cannot cure itself. Importantly, regenerative medicine has the potential to solve the problem of the shortage of organs available for donation compared to the number of patients that require life-saving organ transplantation. Regenerative medicine is essentially focused on human cells. These may be somatic, adult stem or embryo-derived cells.<sup>55</sup>

Related to regenerative medicine, the field of tissue engineering has developed to meet the tremendous need for organs and tissues. Numerous strategies currently used to engineer tissues depend on employing a specific, both organic and inorganic, material. These scaffolds serve as a synthetic extra cellular matrix (ECM) to organize cells into a three-dimensional architecture and to present stimuli, which direct the growth and the formation of a desired tissue. Depending on the tissue of interest and on the specific application, the required material used as the scaffold and its properties are quite different.<sup>32,56</sup>

Recent work has suggested application of mesoangioblasts for stem cell therapies for muscular dystrophy. Experiments in dystrophic mice have shown that mesoangioblasts transplantation can restore muscle function.<sup>57,58</sup> More recently, mesoangioblast transplantation was used to ameliorate the effects of muscular dystrophy in golden retrievers with a congenital muscular dystrophy.<sup>59</sup>

Mesoangioblasts are multipotent progenitors of mesodermal tissues, and are physically associated with the embryonic dorsal aorta in avian and mammalian species. They have in common the anatomical location, the expression of endothelial and/or pericyte markers, the ability to proliferate in culture and the ability to undergo differentiation into various types of mesoderm cells upon proper culture conditions. Their ability to extensively self-renew *in vitro*, while retaining multipotency, qualifies mesoangioblasts as a novel class of stem cells. When transplanted *in vivo*, they give rise to multiple differentiated mesodermal phenotypes.<sup>60</sup> Since the corresponding human cells, more precisely defined as “pericyte-derived cells”, have been recently isolated and characterised, a clinical trial with these cells is planned in the near future.<sup>61</sup>

Anyway, the possibility of using this novel strategy for the cell therapy in genetic diseases is strictly related to the capacity to expand mesoangioblasts in culture in a reproducible and efficient way. That is why our aim is to investigate the ability of the HA to act as a basement for cells culture; cells are in fact very sensitive to their environment and the contact with something mimicking the ECM could, in theory, assure a better proliferation and differentiation.

Hyaluronic acid (HA) which is the simplest glycosaminoglycan (GAG) is found in nearly every mammalian tissue and fluid. Its presence is especially prevalent during wound healing and in the synovial fluid of joints. HA is a linear polysaccharide characterized by a repeating unit constituted by the disaccharide of (1-3) and (1-4)-linked  $\beta$ -D-glucuronic acid and *N*-acetyl- $\beta$ -glucosamine units.<sup>6</sup>

A variety of chemical modifications of native hyaluronan have already been devised to provide new materials. The resulting hyaluronan derivatives have physicochemical properties that may significantly differ from the native polymer, but most derivatives retain the biocompatibility and biodegradability and, in some cases, the pharmacological properties of native

hyaluronan.<sup>11</sup>

We have taken advantage of this attractive building block for preparing new polymers; hence several different methods to provide modified HA have been performed in order to develop robust protocols to be used either to introduce drugs, ligands or other bioactive molecules retained to play an important role in cells proliferation and differentiation, or to cross-link the linear chains affording reticulated networks with defined mechanical properties and increased resistance to clearance (See 2.2, 2.3, 2.4).

Human pericyte-derived cells were cultured using HA and its derivatives as substrates to evaluate their biological influence on *in vitro* proliferation and differentiation.

## **2.5.2 EXPERIMENTAL PROCEDURES**

### **2.5.2.1 Materials**

Sodium Hyaluronate (HA) RESILEN-200 (average molecular weight 235 kDa) was gently supplied by Kyowa Italiana Farmaceutici s.r.l. (Milan, Italy). HA derivatives were synthesised as previously reported (See 2.2.2, 2.3.2, 2.4.2).

Megacell DMEM, fetal bovine serum, glutamine, non-essential amino acids, trypan blue, penicillin and streptomycin were purchased from Sigma (Milan, Italy). Human basic fibroblast growth was purchased from Peprotech (Milan, Italy).  $\beta$ -Mercaptoethanol was purchased from GIBCO (Milan, Italy). Reduced growth factors Matrigel was purchased from BD Biosciences (Milan, Italy) and prepared as previously reported.<sup>61</sup>

### **2.5.2.2 Proliferation and differentiation of pericyte-derived cells on HA derivatives**

#### **2.5.2.2.1 Isolation and culture of human adult pericyte-derived cells**

Cells were isolated from non-dystrophic patients undergoing diagnostic biopsy as previously reported.<sup>61</sup> Briefly, tissue fragments were cultured for 7-8 days. After the initial outgrowth of fibroblast-like cells, small round and refractile cells were observed. Because of their poor adhesion (many of these cells were floating), this cell population was easily collected by gently pipetting the original culture and was plated on petri dishes at a density of  $5 \cdot 10^4$  cells per 30-mm dish. The medium consisted of MegaCell DMEM supplemented with 5% fetal bovine serum,  $5 \text{ ng ml}^{-1}$  basic fibroblast growth factor, 2 mM glutamine, 0.1 mM  $\beta$ -mercaptoethanol, 1% non essential aminoacids,  $100 \text{ IU ml}^{-1}$  penicillin and  $100 \text{ mg ml}^{-1}$  streptomycin.

#### **2.5.2.2.2 Analysis of cell proliferation**

Cells were plated at a density of  $5 \cdot 10^3$  cells per  $\text{cm}^2$  on different substrates, and passed on average every three days. At each passage, the number of cells was counted in triplicate: cells

isolated from enzymatic digestion were stained with Trypan blue, and living cells were counted in a haemocytometer.

### **2.5.2.2.3 Differentiation assays**

Cells undergoes differentiation following previously reported protocols.<sup>61</sup> Specifically, differentiation into skeletal muscle cells was induced by coculturing human adult pericyte-derived cells with C<sub>2</sub>C<sub>12</sub> mouse myoblasts at 1:5 ratio on the proliferation substrates. Alternatively, spontaneous skeletal myogenic differentiation of human pericyte-derived cells was induced by plating cells onto matrigel-coated dishes in differentiation medium. After 7 days, cultures were fixed and stained with antibodies against striated myosin (MF<sub>20</sub>) and MyoD.

### **2.5.2.2.4 Immunofluorescence microscopy**

Cells were fixed with 4% paraformaldehyde for 10 minutes on the differentiation substrates. Cells were processed for immunofluorescence microscopy as previously described.<sup>62</sup>

### **2.5.2.2.5 Matrigel coating of tissue culture surfaces**

Matrigel coated petri dishes have to be freshly prepared and cannot be stored. Reduced Matrigel stock solution was diluted 1:80 in cold DMEM and then carefully applied on petri dishes covering the all surface. After 30 minutes incubation at 37 °C (5% CO<sub>2</sub> incubator), the Matrigel leaving the surface wet was gently removed. Finally the surface was rinsed with the appropriate culture medium before planting cells.

### **2.5.2.2.6 HA coating of tissue culture surfaces**

Natural hyaluronan and its derivatives were dissolved in pure water with a final concentration of 12.5 mg/mL and filtered over a sterile microfilter (pore size 2.0 µm). The solutions were then carefully applied on petri dishes covering the all surface and removing the excess of liquid. After 8 hours of incubation at 37 °C (5% CO<sub>2</sub> incubator under UV lamp) covered with their lead, cells



were planted with the appropriate culture medium.

### ***2.5.2.3 Images Analysis***

For each sample four different regions were acquired. The analysis was performed on an average number of 50 cells per sample using ImageJ software.

*Segmentation of phase contrast images:* in order to segment the phase contrast images, the contrast of the original image was increased. After this first step the image was thresholded and using the “find edges” ImageJ plugin the edges of the cell were identified. The last operation was done using the “Analyse Particle” plugin which quantitatively characterise the cell morphology providing values of parameters such as the area and the circularity of the cell which is equal to 1 for a perfect circle while approaching zero for very elongated shapes (circularity =  $4\pi \times \text{area}/\text{perimetre}^2$ ).

*Segmentation of fluorescence images:* fluorescence images were used to quantify the number of differentiated cells (sarcomeric myosin positive cells) and the red region representing the myotubes which characterise the differentiated cells. The blue and red channels (blue: nuclei stained with DAPI; red: myotubes stained with anti-sarcomeric myosin antibody) of the original image were separated, thresholded and converted into binary images. The difference between these two images (performed with the “Image Calculator” plugin) provided the image with all the nuclei outside the red region (undifferentiated cells). Using the “Analyse Particle” plugin the following values were measured: total number of cells, total number of undifferentiated cells (the difference between these two values represents the number of differentiated cells) and area of the red region.

### 2.5.3 RESULTS AND DISCUSSION

We based our study on different methodologies that can be used for the chemical modification of the HA, key building block for producing advanced biomaterials. The synthesised HA-based compounds must retain complete biocompatibility when used as substrates in cell cultures. Natural or modified HA has never been used in human pericyte derived cell cultures.

Considering that all the different strategies presented (See 2.2, 2.3, 2.4) afforded polymers that could be dissolved in water giving viscous solutions, the general method used to test their biocompatibility has been that to coat petri dishes with a solution of the desired compound, remove the excess of liquid and plant cells on it.

As first point, solutions at different concentration of sodium hyaluronate (**HA-Na**) with average molecular weight 235 kDa were tried as substrates during human pericyte derived cells proliferation in order to identify the more suitable one. As discriminating factor the population doubling was considered.

The best result was obtained by using 12.5 mg/mL of **HA-Na**, hence this concentration was maintained constant with all the HA-derivatives used because they have been synthesised using a polymer of average molecular weight 235 kDa as starting material.

A set of compounds was tested to investigate cells proliferation and differentiation (Figure 37). Specifically HA-coated petri dishes were used during the proliferation while differentiation was carried out using two different protocols; indeed mesoangioblast differentiation into skeletal muscle *in vitro* can be induced by coculturing human adult pericyte-derived cells with mouse myoblasts (hence on the same substrate present during the proliferation) or by plating cells onto matrigel-coated dishes in differentiation medium.

The aim of the investigation was that to provide data about the biological properties displayed by the hyaluronan, to see whether the cation could exhibit an effect, to check the

---

## Chemical Modification of the Hyaluronic Acid

biocompatibility of the new functional groups grafted on the HA, i.e. a triazole moiety, urethanic bridges and aliphatic chains. Furthermore we were interested as well in checking if differences occurred in the behaviour of the azide derivative respect to its click-product.

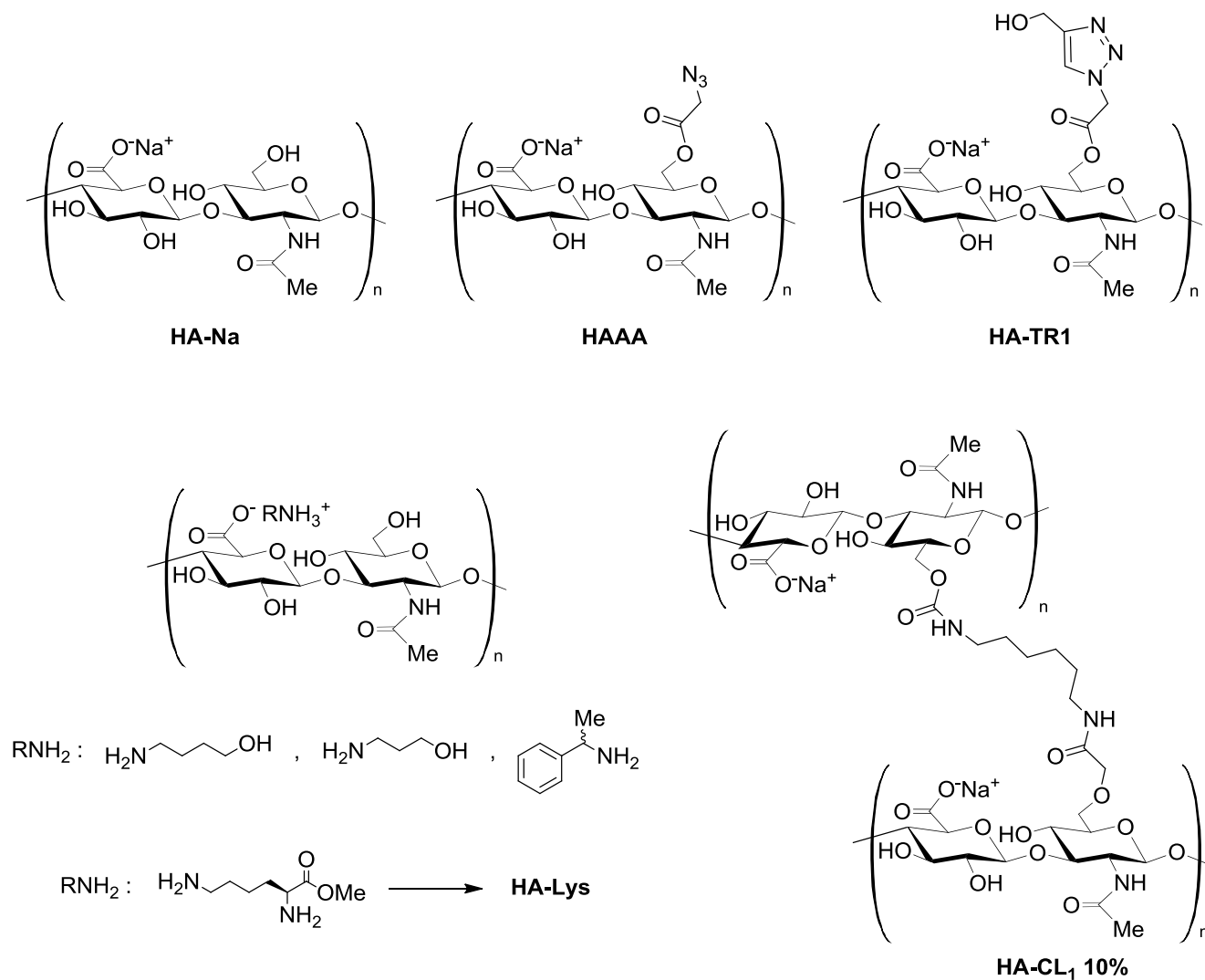


**Figure 37: HA-derivatives tested as substrates for stem cell cultures**

The structures of the compounds tested as substrates in pericyte-derived stem cells are reported. **HA-Na** (average molecular weight 235 kDa) is commercially available and has been used as starting material for the synthesis of all the other HA-derivatives depicted.

Since the very first trials, the azido derivative (**HAAA**) and all the ammonium salts, except the lysinium one (**HA-Lys**), displayed very high toxicity towards stem cells. These results could be easily rationalised for the ammonium salts, considering that the free amines found are toxic; on the contrary organic azides have no intrinsic toxicity unless they are unstable.<sup>63</sup>

Proliferation on the sodium and lysinium hyaluronate (**HA-Na** and **HA-Lys**), the triazole-derivative (**HA-TR1**) and the cross-linked polymers (**HA-CL<sub>1</sub> 10%**) of human pericyte derived cells occurred with good results. For some of the substrates the population doubling was measured (Figure 38). The data demonstrated that, after 6 days cells, have a proliferation rate of approximately 7 population doublings in the standard conditions while on the other samples the value ranges approximately between 5.5 and 6 hence just slightly lower.

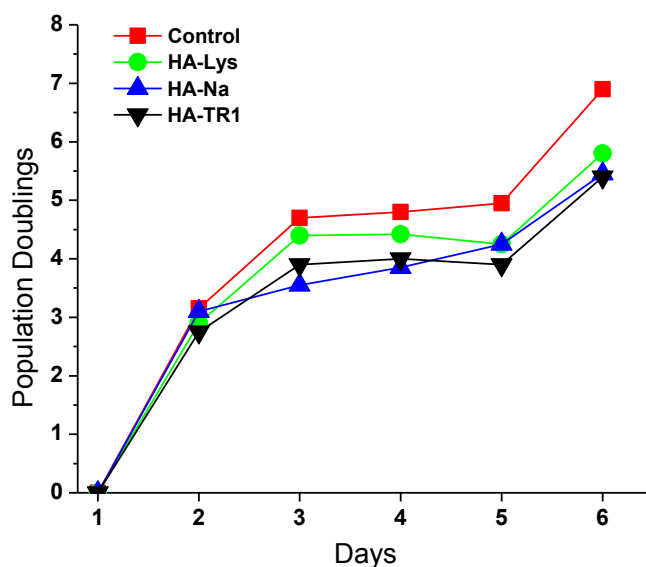


**Figure 38: Population doubling of human pericyte derived cells on HA coated petri dishes**

Proliferation was also checked monitoring cells via contrast phase microscopy. For a precise

---

evaluation of cell morphology an algorithm was developed in order to perform a segmentation of phase contrast images and measure cell area and circularity that have been chosen as distinguishing parameters (Figure 39).

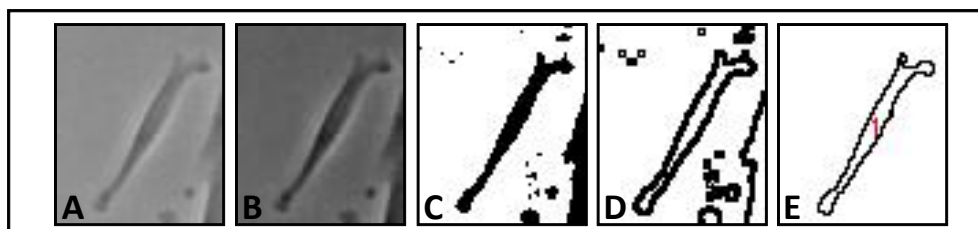


**Figure 39: Segmentation of phase contrast images**

Operation performed on the original image (A): enhancing the contrast (B), thresholding (C) and finding the edges of the cell (D) and identification and morphological characterisation of the cell (E).

The data obtained from the segmentation of phase contrast images highlighted that in most cases there are no significant differences between the standard conditions and the HA-based substrates. Anyway a general trend was noticed: the more the hydrophilicity of the functional group inserted is the lower the area mean value of the cells is, the same could be said for the circularity but in this case differences are less marked.

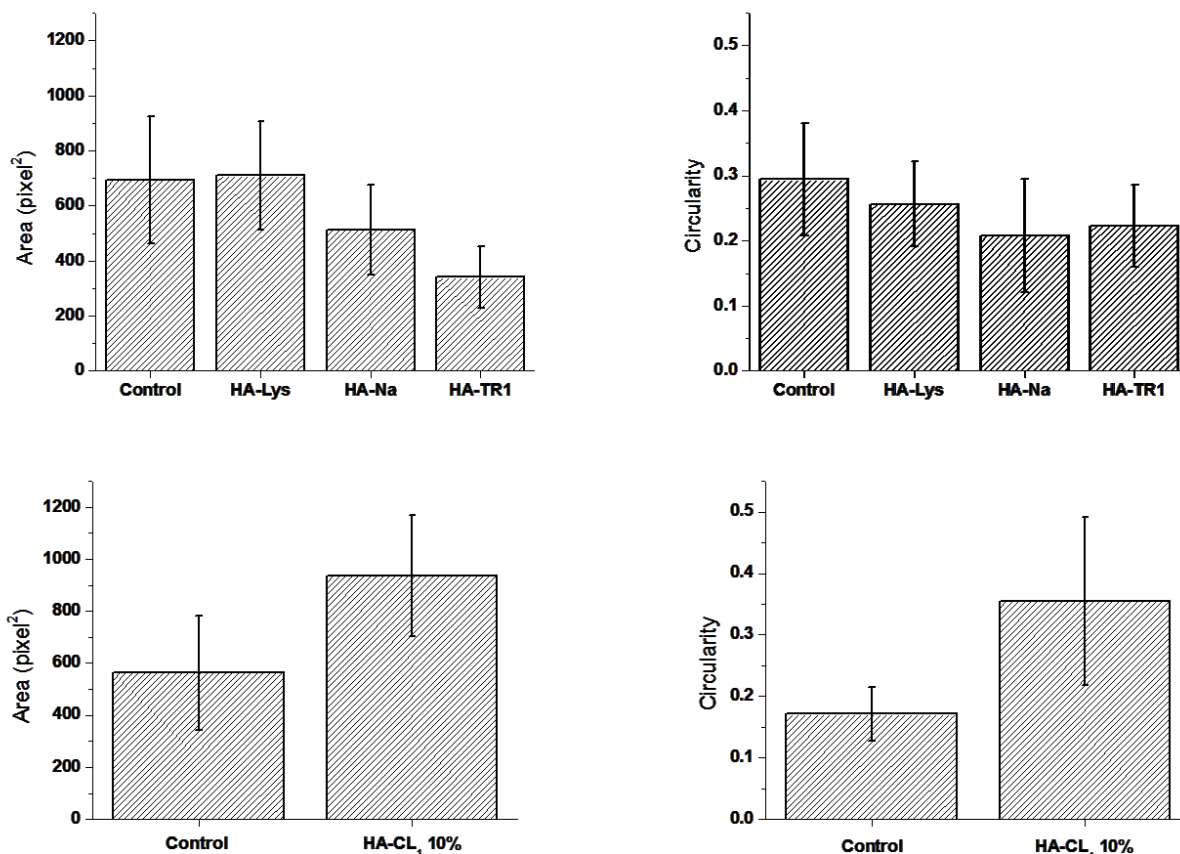


**Figure 40: Morphological analysis of human pericyte derived cells planted on HA-derivatives**

Area and Circularity of cells on different substrates. The area mean value of **HA-TR1** and **HA-CL<sub>1</sub> 10%** showed a significant difference with the area mean values of the Control. Moreover the circularity mean value of the Control is significant different from the circularity mean value of the **HA-CL<sub>1</sub> 10%**.

Our hypothesis is based on the assumption that, usually, on hydrophobic substrates such as tissue culture polystyrene, cell attachment is typically mediated through adsorbed matrix proteins, while on hydrophilic, non-ionic and non-protein adsorbing substrates, such as HA,<sup>64</sup> the negligible protein adsorption and the lack of strong polar adhesion forces frustrate cell adhesion. Thus the introduction of less hydrophilic groups, e.g. the alkyl chain of **HA-CL<sub>1</sub>**, could guarantee a minimum level of adsorption of matrix proteins to promote cells spreading.

The scale of hydrophobicity would then be: **HA-TR1 < HA-Na < HA-Lys < HA-CL<sub>1</sub> 10%**.

If at a first sight **HA-TR1** could hardly look less hydrophobic of **HA-Na**, looking at the simulated partition coefficient octanol/water (LogD) at physiological pH, i.e. 7.4, of the two corresponding residues it showed to be effectively more hydrophilic.

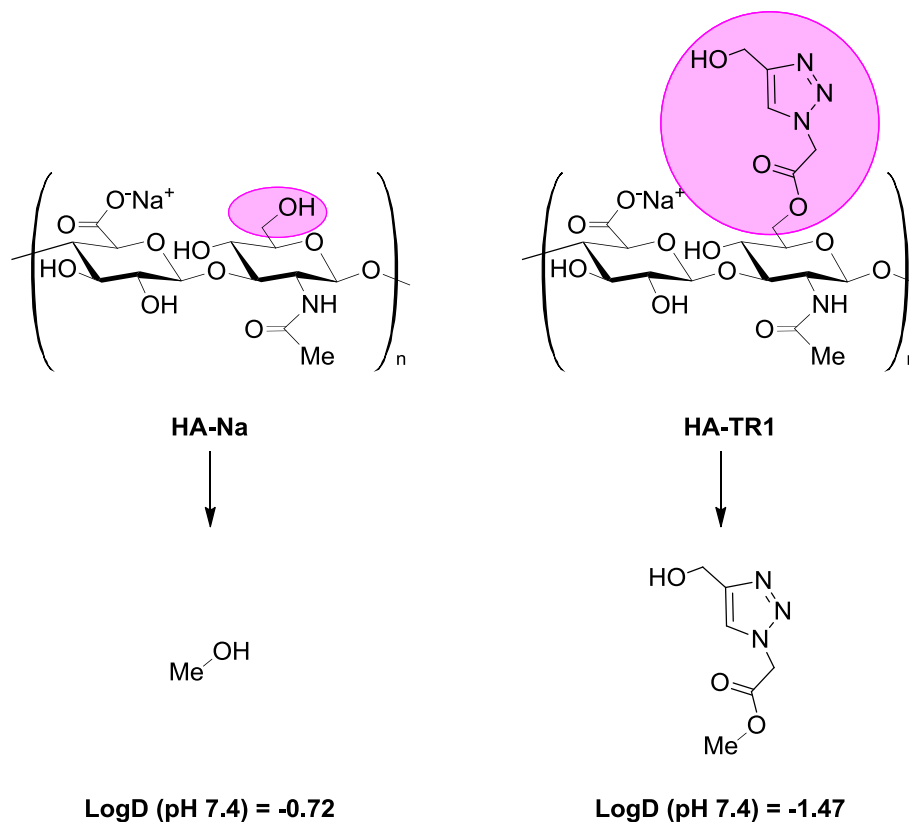


**Figure 41: Comparison of hydrophobicity between HA-Na and HA-TR1**

The partition coefficient of the two corresponding residues was simulated at physiological pH value (pH 7.4) with the simulator provided in ACD/Labs 6.00.

Cells differentiation into skeletal muscle was induced following two protocols as already mentioned. As first point it is important to highlight that cells can undergo differentiation only if

they are in good condition. Indeed myotubes formation could be regarded as a proof of the biocompatibility of the substrates.

Myogenic differentiation of human pericyte-derived cells could be appreciated by immunofluorescence microscopy (Figure 42-A).

To have a quantitative idea about the efficiency of the differentiation process, images were analysed calculating two different parameters: the ratio between the total number of cells and the differentiated ones (DAPI stained nuclei inside the red region characterised by the expression of sarcomeric myosin) and the area of the sarcomeric myosin region (red). The first parameter gives an indication about how many cells differentiate (no differentiation = 0, total differentiation = 1 respect to the control) while the second parameter indicates how good is the differentiation (higher values of the red region indicate more sarcomeric myosin produced by differentiated cells). The combination of these two parameters gives an indication of the efficiency of the overall differentiation process. (Figure 42)

All the cells cultured on the HA-derivatives retained the capacity to differentiate proving the biocompatibility of the substrates. As already explained the area of the myotubes will be regarded as the main parameter indicating the goodness of the substrate to promote skeletal muscle formation. The data analysed showed as matrigel significantly overcomes HA-based substrates. Moreover only little differences were observed for pericyte-derived cells cultured in the same conditions but with different substrates. In particular very promising results were obtained by using **HA-Lys**. **HA-TR1** behaved as the native HA demonstrating that the moiety inserted does not modify the biocompatibility of the polymer. The insertion of urethane groups and aliphatic bridges has been completely tolerated as well. (Figure 43)



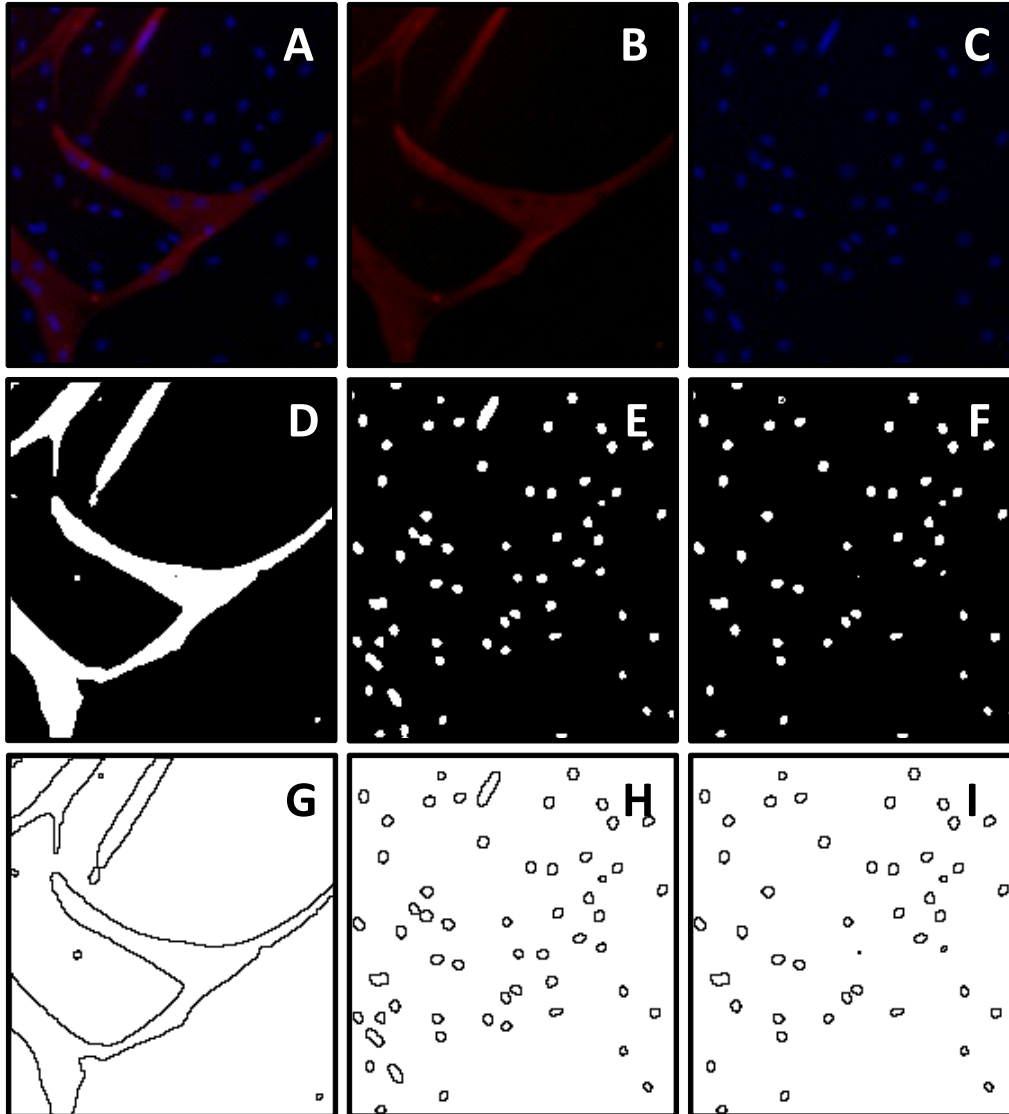


**Figure 42: Analysis of images recorded by immunofluorescence microscopy**

Immunofluorescence microscopy allows to recognize myotubes (stained red by anti-sarcomeric myosin antibody) and all nuclei (stained blue by DAPI). The original fluorescence image (A) was separated into the red and blue channels (B-C) and thresholded (D-E). The difference between image D and F provides the nuclei outside the red region (F). Through the “Analyse Particle” plugin applied on image D, E and F it is possible to calculate the area of the red region (G), the number of all cells (H) and the number of the undifferentiated cells and hence to back-calculate the number of differentiated cells.

## Chemical Modification of the Hyaluronic Acid

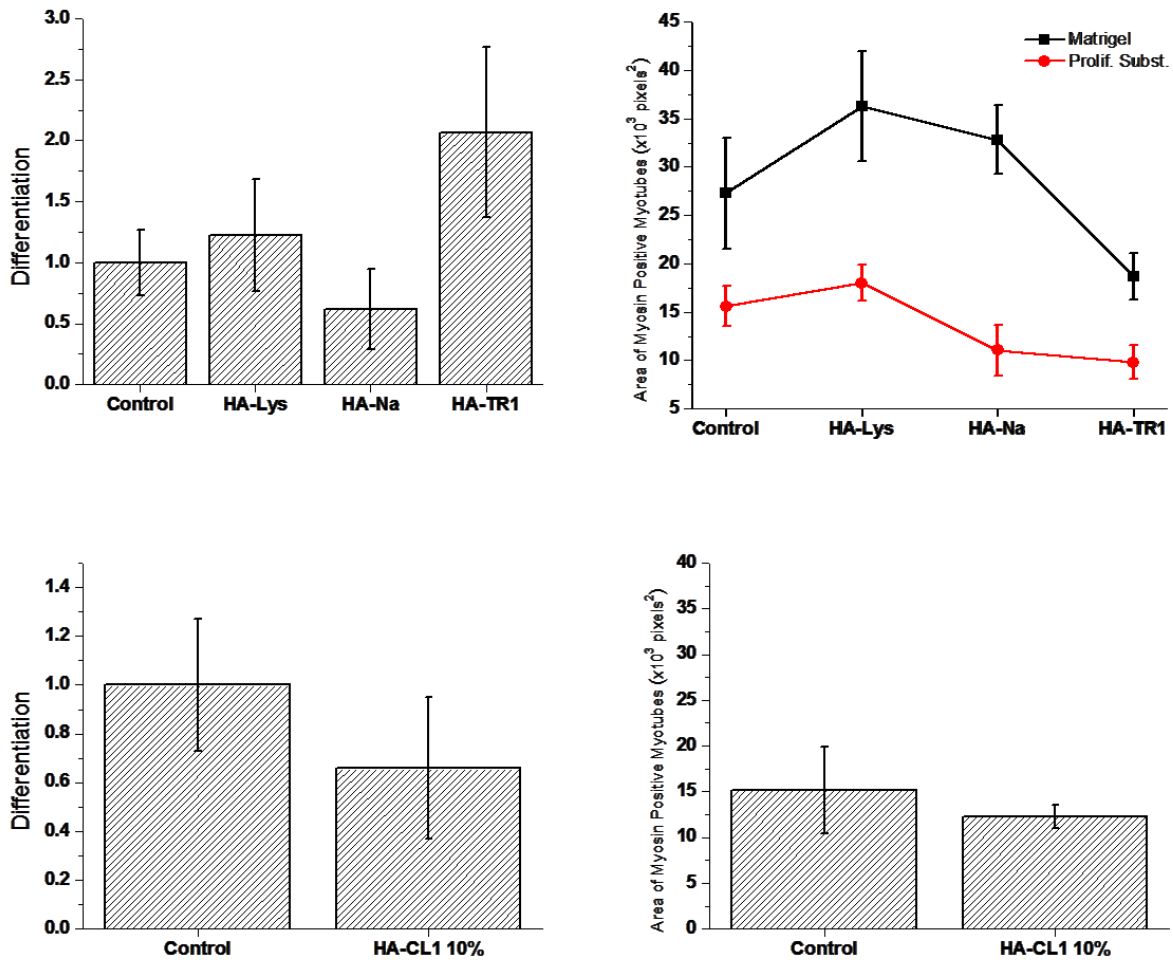


**Figure 43: Analysis on the differentiation of human pericyte derived cells planted on HA-derivatives**

The two parameters chosen as indicators of the ability of cells to differentiate are reported. Specifically *Differentiation* indicates the ratio between the number of nuclei inside the red region and the total number of nuclei; each value obtained has been normalised to the control. Only cells differentiated on the substrate of proliferation were analysed in this way. The red area indicates the area of myosin positive myotubes and has been measured for all the experiments performed.

#### 2.5.4 CONCLUSION

Mesoangioblasts are multipotent progenitors of mesodermal tissues, able to proliferate in culture and to undergo differentiation into various types of mesoderm cells upon proper culture conditions, hence they are qualified as a novel class of stem cells. The corresponding human cells, more precisely defined as “pericyte-derived cells”, have been recently isolated and characterised, a clinical trial with these cells is planned in the near future.<sup>61</sup> Indeed recently the application of mesoangioblasts for stem cell therapies has been looked as attractive issue to provide symptoms amelioration in the case of muscular dystrophy.<sup>65</sup>

The capacity to expand and differentiate mesoangioblasts *in vitro* is a key point for the possibility of using this novel strategy for the cell therapy in genetic diseases. Thus new HA has been chemically modified to explore different reactions that might be applied on this biopolymer both for its bioconjugation and cross-linking.

A variety of chemical modifications of native hyaluronan have already been devised to provide new materials. The resulting hyaluronan derivatives have physicochemical properties that may significantly differ from the native polymer. Hence to check whether the strategy investigated brought to the synthesis of derivatives retaining the biocompatibility and biodegradability and the pharmacological properties of native hyaluronan, they have been used as substrates for human pericyte derived cell proliferation and differentiation.

The results obtained highlighted that two of the strategies reported for the chemical modification of the HA, i.e. Sharpless cycloaddition and reaction with diisocyanates, add on the polymeric scaffold moieties completely atoxic and that ensure the biocompatibility of the native polymer. Moreover the biological effect of the counterion was investigated and different HA-ammonium salts have been tested showing that the biological effect expressed can be related to the one which is exhibited by the amine itself.

## 2.6 ACKNOWLEDGEMENTS

*I would like to thank Professor Francesco Sannicolò for the invaluable advice and support he had given me, and for guiding me through this exciting project.*

*I am deeply grateful as well to all the other people of his research group, in particular to Professor Tiziana Benincori, Doctor Simona Rizzo and Doctor Luca Vaghi for all the help they had never refused me to solve every little daily trouble in the laboratory.*

*The HA-amidation using DMTMM was carried out at the University of Manchester, hence Professor Nicola Tirelli is sincerely acknowledged for his support to this project; I would also like to express my special thank Doctor Erwin Hohn for his precious help during the synthesis of the HA-conjugate and Doctor Robert Evans for the DOSY experiment.*

*Professor Stefano Turri from the Dipartimento di Chimica, Materiali ed Ingegneria Chimica "G. Natta", Politecnico of Milan, is acknowledged for the rheological studies.*

*Thanks to Professor Giulio Cossu and his research group, especially to Doctor Stefania Antonini, from the Stem Cell Research Institute, San Raffaele Scientific Institute, Milan, for the stem cell cultures.*

*A very important acknowledgement is for Roberto Donno (University of Manchester) who has been so kind to teach me how to analyse cell images.*

## 2.7 REFERENCES

- 1 Crescenzi, V., Francescangeli, A., Renier, D. & Bellini, D. New cross-linked and sulfated derivatives of partially deacetylated hyaluronan: Synthesis and preliminary characterization. *Biopolymers* **64**, 86-94, doi:10.1002/bip.10131 (2002).
- 2 Campoccia, D. *et al.* Semisynthetic resorbable materials from hyaluronan esterification. *Biomaterials* **19**, 2101-2127, doi:10.1016/s0142-9612(98)00042-8 (1998).
- 3 Della, V. F. & Romeo, A. Hyaluronic acid esters and their medical and cosmetic uses and formulations. EP216453A2 (1987).
- 4 Cho, H.-J. *et al.* Self-assembled nanoparticles based on hyaluronic acid-ceramide (HA-CE) and Pluronic® for tumor-targeted delivery of docetaxel. *Biomaterials* **32**, 7181-7190, doi:10.1016/j.biomaterials.2011.06.028 (2011).
- 5 Huin-Amargier, C., Marchal, P., Payan, E., Netter, P. & Dellacherie, E. New physically and chemically crosslinked hyaluronate (HA)-based hydrogels for cartilage repair. *Journal of Biomedical Materials Research Part A* **76A**, 416-424, doi:10.1002/jbm.a.30536 (2006).
- 6 Jeanloz, R. W. & Forchielli, E. STUDIES ON HYALURONIC ACID AND RELATED SUBSTANCES: I. PREPARATION OF HYALURONIC ACID AND DERIVATIVES FROM HUMAN UMBILICAL CORD. *Journal of Biological Chemistry* **186**, 495-511 (1950).
- 7 Hirano, K. *et al.* Preparation of the methyl ester of hyaluronan and its enzymatic degradation. *Carbohydrate Research* **340**, 2297-2304, doi:10.1016/j.carres.2005.07.016 (2005).
- 8 Pasqui, D., Atrei, A. & Barbucci, R. A Novel Strategy To Obtain a Hyaluronan Monolayer on Solid Substrates. *Biomacromolecules* **8**, 3531-3539, doi:10.1021/bm700834d (2007).
- 9 Oh, E. J., Park, K., Choi, J.-S., Joo, C.-K. & Hahn, S. K. Synthesis, characterization, and preliminary assessment of anti-Flt1 peptide-hyaluronate conjugate for the treatment of corneal neovascularization. *Biomaterials* **30**, 6026-6034, doi:10.1016/j.biomaterials.2009.07.024 (2009).
- 10 Homma, A. *et al.* Novel hyaluronic acid-methotrexate conjugates for osteoarthritis treatment. *Bioorganic & medicinal chemistry* **17**, 4647-4656 (2009).
- 11 Schanté, C. E., Zuber, G., Herlin, C. & Vandamme, T. F. Chemical modifications of hyaluronic acid for the synthesis of derivatives for a broad range of biomedical

- applications. *Carbohydrate Polymers* **85**, 469-489, doi:10.1016/j.carbpol.2011.03.019 (2011).
- 12 Burdick, J. A. & Prestwich, G. D. Hyaluronic Acid Hydrogels for Biomedical Applications. *Advanced Materials* **23**, H41-H56, doi:10.1002/adma.201003963 (2011).
- 13 Nakajima, N. & Ikada, Y. Mechanism of Amide Formation by Carbodiimide for Bioconjugation in Aqueous Media. *Bioconjugate Chemistry* **6**, 123-130, doi:10.1021/bc00031a015 (1995).
- 14 Pouyani, T., Harbison, G. S. & Prestwich, G. D. Novel Hydrogels of Hyaluronic Acid: Synthesis, Surface Morphology, and Solid-State NMR. *Journal of the American Chemical Society* **116**, 7515-7522, doi:10.1021/ja00096a007 (1994).
- 15 Bulpitt, P. & Aeschlimann, D. New strategy for chemical modification of hyaluronic acid: Preparation of functionalized derivatives and their use in the formation of novel biocompatible hydrogels. *Journal of Biomedical Materials Research* **47**, 152-169, doi:10.1002/(sici)1097-4636(199911)47:2<152::aid-jbm5>3.0.co;2-i (1999).
- 16 Bergman, K., Elvingson, C., Hilborn, J., Svensk, G. & Bowden, T. Hyaluronic Acid Derivatives Prepared in Aqueous Media by Triazine-Activated Amidation. *Biomacromolecules* **8**, 2190-2195, doi:10.1021/bm0701604 (2007).
- 17 Farkaš, P. & Bystrický, S. Efficient activation of carboxyl polysaccharides for the preparation of conjugates. *Carbohydrate Polymers* **68**, 187-190, doi:10.1016/j.carbpol.2006.07.013 (2007).
- 18 Dömling, A. & Ugi, I. Multicomponent Reactions with Isocyanides. *Angewandte Chemie International Edition* **39**, 3168-3210, doi:10.1002/1521-3773(20000915)39:18<3168::aid-anie3168>3.0.co;2-u (2000).
- 19 Crescenzi, V. *et al.* Hyaluronan networking via Ugi's condensation using lysine as cross-linker diamine. *Carbohydrate Polymers* **53**, 311-316, doi:10.1016/s0144-8617(03)00079-1 (2003).
- 20 de Nooy, A. E. J., Capitani, D., Masci, G. & Crescenzi, V. Ionic Polysaccharide Hydrogels via the Passerini and Ugi Multicomponent Condensations: Synthesis, Behavior and Solid-State NMR Characterization. *Biomacromolecules* **1**, 259-267, doi:10.1021/bm005517h (2000).
- 21 De, B. A. N. & Maelson, T. Gel for preventing adhesion between body tissues. WO8600912A1 (1986).
-

- 22 Endre A. Balazs, A. L. Cross-linked gels of hyaluronic acid and products containing such gels. US4582865 (1968).
- 23 Ventura, C. *et al.* Butyric and Retinoic Mixed Ester of Hyaluronan: A NOVEL DIFFERENTIATING GLYCOCONJUGATE AFFORDING A HIGH THROUGHPUT OF CARDIOGENESIS IN EMBRYONIC STEM CELLS. *Journal of Biological Chemistry* **279**, 23574-23579, doi:10.1074/jbc.M401869200 (2004).
- 24 Pravata, L. *et al.* New Amphiphilic Lactic Acid Oligomer–Hyaluronan Conjugates: Synthesis and Physicochemical Characterization. *Biomacromolecules* **9**, 340-348, doi:10.1021/bm700843m (2007).
- 25 Burdick, J. A., Chung, C., Jia, X., Randolph, M. A. & Langer, R. Controlled Degradation and Mechanical Behavior of Photopolymerized Hyaluronic Acid Networks. *Biomacromolecules* **6**, 386-391, doi:10.1021/bm049508a (2004).
- 26 Serban, M. A. & Prestwich, G. D. Synthesis of Hyaluronan Haloacetates and Biology of Novel Cross-Linker-Free Synthetic Extracellular Matrix Hydrogels. *Biomacromolecules* **8**, 2821-2828, doi:10.1021/bm700595s (2007).
- 27 Garrett, C. E., Jiang, X., Prasad, K. & Repič, O. New observations on peptide bond formation using CDMT. *Tetrahedron Letters* **43**, 4161-4165, doi:10.1016/s0040-4039(02)00754-2 (2002).
- 28 Schanté, C. E., Zuber, G., Herlin, C. & Vandamme, T. F. Improvement of hyaluronic acid enzymatic stability by the grafting of amino-acids. *Carbohydrate Polymers* **87**, 2211-2216, doi:10.1016/j.carbpol.2011.10.050 (2012).
- 29 Ouasti, S., Kingham, P. J., Terenghi, G. & Tirelli, N. The CD44/integrins interplay and the significance of receptor binding and re-presentation in the uptake of RGD-functionalized hyaluronic acid. *Biomaterials* **33**, 1120-1134, doi:10.1016/j.biomaterials.2011.10.009 (2012).
- 30 Wang, X., Messman, J., Mays, J. W. & Baskaran, D. Polypeptide Grafted Hyaluronan: Synthesis and Characterization. *Biomacromolecules* **11**, 2313-2320, doi:10.1021/bm1004146 (2010).
- 31 Udenfriend, S. *et al.* Fluorescamine: A Reagent for Assay of Amino Acids, Peptides, Proteins, and Primary Amines in the Picomole Range. *Science* **178**, 871-872, doi:10.1126/science.178.4063.871 (1972).
- 32 Martina, M. & Hutmacher, D. W. Biodegradable polymers applied in tissue engineering

- research: a review. *Polymer International* **56**, 145-157, doi:10.1002/pi.2108 (2007).
- 33 Muthusamy, S., Gnanaprakasam, B. & Suresh, E. Desymmetrization of Cyclic Anhydrides Using Dihydroxy Compounds: Selective Synthesis of Macrocyclic Tetralactones. *Organic Letters* **8**, 1913-1916, doi:10.1021/ol060509k (2006).
- 34 Bock, V. D., Hiemstra, H. & van Maarseveen, J. H. CuI-Catalyzed Alkyne–Azide “Click” Cycloadditions from a Mechanistic and Synthetic Perspective. *European Journal of Organic Chemistry* **2006**, 51-68, doi:10.1002/ejoc.200500483 (2006).
- 35 Kolb, H. C., Finn, M. G. & Sharpless, K. B. Click Chemistry: Diverse Chemical Function from a Few Good Reactions. *Angewandte Chemie International Edition* **40**, 2004-2021, doi:10.1002/1521-3773(20010601)40:11<2004::aid-anie2004>3.0.co;2-5 (2001).
- 36 Nimmo, C. M. & Shoichet, M. S. Regenerative Biomaterials that “Click”: Simple, Aqueous-Based Protocols for Hydrogel Synthesis, Surface Immobilization, and 3D Patterning. *Bioconjugate Chemistry* **22**, 2199-2209, doi:10.1021/bc200281k (2011).
- 37 Huisgen, R. Cycloadditions — Definition, Classification, and Characterization. *Angewandte Chemie International Edition in English* **7**, 321-328, doi:10.1002/anie.196803211 (1968).
- 38 Rostovtsev, V. V., Green, L. G., Fokin, V. V. & Sharpless, K. B. A Stepwise Huisgen Cycloaddition Process: Copper(I)-Catalyzed Regioselective “Ligation” of Azides and Terminal Alkynes. *Angewandte Chemie International Edition* **41**, 2596-2599, doi:10.1002/1521-3773(20020715)41:14<2596::aid-anie2596>3.0.co;2-4 (2002).
- 39 Crescenzi, V., Cornelio, L., Di Meo, C., Nardecchia, S. & Lamanna, R. Novel Hydrogels via Click Chemistry: Synthesis and Potential Biomedical Applications. *Biomacromolecules* **8**, 1844-1850, doi:10.1021/bm0700800 (2007).
- 40 Testa, G. *et al.* Influence of dialkyne structure on the properties of new click-gels based on hyaluronic acid. *International Journal of Pharmaceutics* **378**, 86-92 (2009).
- 41 Piluso, S. *et al.* Hyaluronic acid-based hydrogels crosslinked by copper-catalyzed azide-alkyne cycloaddition with tailorable mechanical properties. *Int. J. Artif. Organs* **34**, 192-197, doi:10.5301/ijao.2011.6394 (2011).
- 42 Hu, X., Li, D., Zhou, F. & Gao, C. Biological hydrogel synthesized from hyaluronic acid, gelatin and chondroitin sulfate by click chemistry. *Acta Biomaterialia* **7**, 1618-1626, doi:10.1016/j.actbio.2010.12.005 (2011).
-



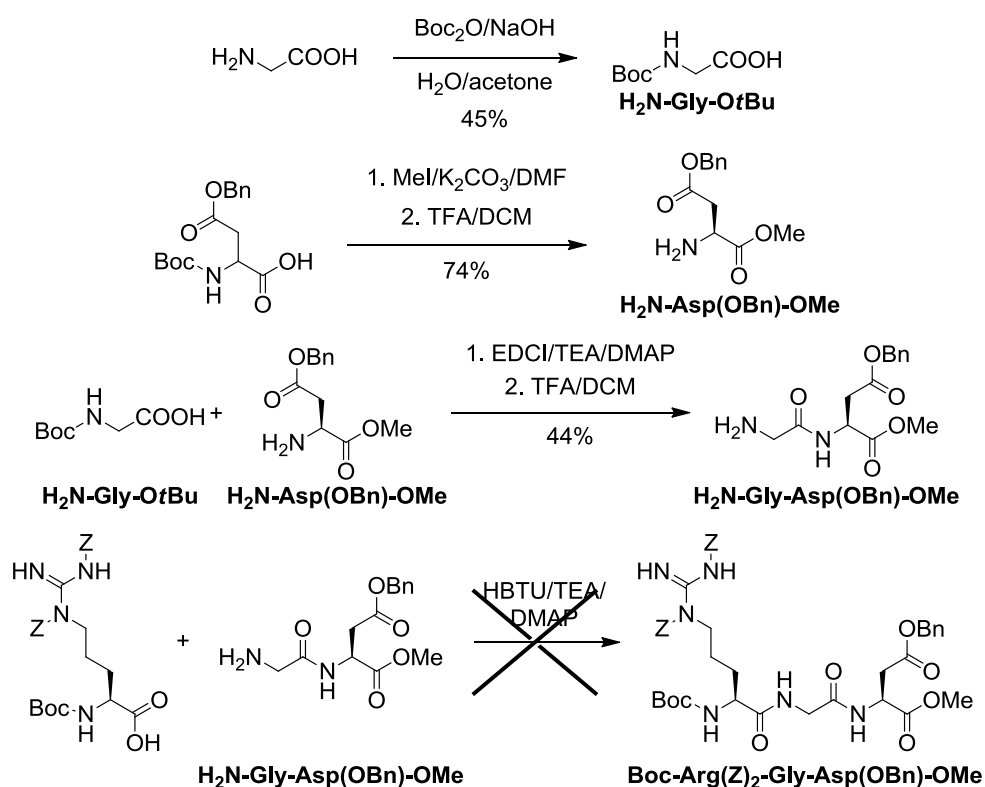
- 43 Ma, M., Paredes, A. & Bong, D. Intra- and Intermembrane Pairwise Molecular Recognition between Synthetic Hydrogen-Bonding Phospholipids. *Journal of the American Chemical Society* **130**, 14456-14458, doi:10.1021/ja806954u (2008).
- 44 Ott, I. *et al.* Antitumor-Active Cobalt-Alkyne Complexes Derived from Acetylsalicylic Acid: Studies on the Mode of Drug Action. *Journal of Medicinal Chemistry* **48**, 622-629, doi:10.1021/jm049326z (2004).
- 45 Vollmar, A. & Dunn, M. S. A Convenient Synthesis of t-Alkyl Esters of Amino Acids<sup>1a</sup>. *The Journal of Organic Chemistry* **25**, 387-390, doi:10.1021/jo01073a020 (1960).
- 46 Roche, S. P., Faure, S., El Blidi, L. & Aitken, D. J. Total Synthesis of Cyclotheonamide C by Use of an  $\alpha$ -Keto Cyanophosphorane Methodology for Peptide Assembly. *European Journal of Organic Chemistry* **2008**, 5067-5078, doi:10.1002/ejoc.200800591 (2008).
- 47 Ameijde, J. v. & Liskamp, R. M. J. Synthesis of novel trivalent amino acid glycoconjugates based on the cyclotrimeratrylene ('CTV') scaffold. *Organic & Biomolecular Chemistry* **1**, 2661-2669 (2003).
- 48 Baccaro, A., Weisbrod, S. H. & Marx, A. DNA Conjugation by the Staudinger Ligation: New Thymidine Analogues. *Synthesis* **2007**, 1949-1954, doi:10.1055/s-2007-983728 (2007).
- 49 Jukic, D. *et al.* Synthesis and biological activities of neurokinin pseudopeptide analogues containing a reduced peptide bond. *European Journal of Medicinal Chemistry* **26**, 921-928, doi:10.1016/0223-5234(91)90134-9 (1991).
- 50 Testa, G. *et al.* Influence of dialkyne structure on the properties of new click-gels based on hyaluronic acid. *International Journal of Pharmaceutics* **378**, 86-92, doi:10.1016/j.ijpharm.2009.05.051 (2009).
- 51 Anastas, P. & Warner, J. *Green Chemistry: Theory and Practice*. (Oxford Univ Press, 1998).
- 52 Barker, T. H. The role of ECM proteins and protein fragments in guiding cell behavior in regenerative medicine. *Biomaterials* **32**, 4211-4214, doi:10.1016/j.biomaterials.2011.02.027 (2011).
- 53 Collier, J. H. & Segura, T. Evolving the use of peptides as components of biomaterials. *Biomaterials* **32**, 4198-4204, doi:10.1016/j.biomaterials.2011.02.030 (2011).
- 54 Williams, D. F. The role of short synthetic adhesion peptides in regenerative medicine;
-

- The debate. *Biomaterials* **32**, 4195-4197, doi:10.1016/j.biomaterials.2011.02.025 (2011).
- 55 Mason, C. & Dunnill, P. A brief definition of regenerative medicine. *Regenerative Medicine* **3**, 1-5, doi:10.2217/17460751.3.1.1 (2007).
- 56 Drury, J. L. & Mooney, D. J. Hydrogels for tissue engineering: scaffold design variables and applications. *Biomaterials* **24**, 4337-4351, doi:10.1016/s0142-9612(03)00340-5 (2003).
- 57 Sampaolesi, M. *et al.* Cell Therapy of  $\alpha$ -Sarcoglycan Null Dystrophic Mice Through Intra-Arterial Delivery of Mesoangioblasts. *Science* **301**, 487-492, doi:10.1126/science.1082254 (2003).
- 58 Guttinger, M., Tafi, E., Battaglia, M., Coletta, M. & Cossu, G. Allogeneic mesoangioblasts give rise to alpha-sarcoglycan expressing fibers when transplanted into dystrophic mice. *Experimental Cell Research* **312**, 3872-3879, doi:10.1016/j.yexcr.2006.08.012 (2006).
- 59 Sampaolesi, M. *et al.* Mesoangioblast stem cells ameliorate muscle function in dystrophic dogs. *Nature (London, U. K.)* **444**, 574-579, doi:10.1038/nature05282 (2006).
- 60 Cossu, G. & Bianco, P. Mesoangioblasts — vascular progenitors for extravascular mesodermal tissues. *Current Opinion in Genetics & Development* **13**, 537-542, doi:10.1016/j.gde.2003.08.001 (2003).
- 61 Tonlorenzi, R., Dellavalle, A., Schnapp, E., Cossu, G. & Sampaolesi, M. Isolation and characterization of mesoangioblasts from mouse, dog, and human tissues. *Curr Protoc Stem Cell Biol* **Chapter 2**, Unit 2B.1 (2007).
- 62 Minasi, M. G. *et al.* The meso-angioblast: a multipotent, self-renewing cell that originates from the dorsal aorta and differentiates into most mesodermal tissues. *Development* **129**, 2773-2783 (2002).
- 63 Prescher, J. A. & Bertozzi, C. R. Chemistry in living systems. *Nat Chem Biol* **1**, 13-21, doi:nchembio0605-13 10.1038/nchembio0605-13 (2005).
- 64 Ouasti, S. *et al.* Network connectivity, mechanical properties and cell adhesion for hyaluronic acid/PEG hydrogels. *Biomaterials* **32**, 6456-6470, doi:10.1016/j.biomaterials.2011.05.044 S0142-9612(11)00576-X [pii] (2011).
- 65 Cossu, G. & Sampaolesi, M. New therapies for Duchenne muscular dystrophy: challenges, prospects and clinical trials. *Trends in Molecular Medicine* **13**, 520-526, doi:10.1016/j.molmed.2007.10.003 (2007).
-

## 2.8 SUPPORTING INFORMATION

### 2.8.1.1 Trial for the synthesis of RGD sequence with unprotected N-terminus

As cited in 2.4.3, the synthesis of a RGD sequence that could be selectively deprotected at the N-terminus of the arginine was attempted. The aim was that to functionalise this tripeptide in a different position, in order to be able to study the differences observed during the HA functionalisation and, eventually, the differences in the biological response. We started from the protection and coupling of glycine and aspartate as shown in Scheme S 1. Unfortunately we did not succeed in the synthesis of the tripeptide using HBTU as coupling reagent, but only the starting materials were recovered.



Scheme S 1: Pathway followed for the synthesis of Boc-Arg(Z)<sub>2</sub>-Gly-Asp(OBn)-OMe

### 2.8.1.1.1 Synthetic procedures

#### *Synthesis of Boc-Gly-OH:*

To a stirred solution of glycine (5.0 g, 67 mmol, 1 eq.) in 35 mL of water, 2.7 g of NaOH (67 mmol, 1 eq.) in 20 mL of water were added. The mixture was cooled at 0 °C, then a solution of Boc anhydride (14.5 g, 67 mmol, 1 eq.) in 25 mL of acetone was slowly added dropwise over 30 minutes. The reaction was allowed to warm at room temperature and stirred overnight. The acetone was removed under reduced pressure, the solution was acidified with a saturated solution of citric acid and extracted with DCM (3 x 15 mL). The organic layer was dried over MgSO<sub>4</sub>, filtered and the solvent removed affording the pure product. Yield: 45% wt. White solid. <sup>1</sup>H NMR (200 MHz, CDCl<sub>3</sub>) (δ = ppm): 5.05 (bs, 1H), 3.98 (d, *J* = 5.4 Hz, 2H), 1.46 (s, 9H).

#### *Synthesis of Boc-Asp(OBn)-OMe:*

To a stirred solution of Boc-Asp(OBn)-OH (2.4 g, 7.1 mmol, 1 eq.) in 17 mL of dry DMF 1.5 g of K<sub>2</sub>CO<sub>3</sub> (10.9 mmol, 1.5 eq.) was added and the suspension cooled at 0 °C; after 10 minutes, 1.0 g of MeI (7.1 mmol, 1 eq.) were added. The reaction mixture was allowed to warm at room temperature and stirred for 3 h. The mixture was then diluted with 25 mL of water and extracted with AcOEt (3 x 25 mL); the combined organic layers were washed with a saturated solution of NaHCO<sub>3</sub> (25 mL) and brine (3 x 25 mL). The organic phase was dried over Na<sub>2</sub>SO<sub>4</sub> and filtered over a plug of silica gel. Evaporation of the solvent afforded the pure product. Yield: 88% wt. White solid. <sup>1</sup>H NMR (300 MHz, CDCl<sub>3</sub>) (δ = ppm): 7.34 (m, 5H), 5.47 (d, *J* = 9.3 Hz, 1H), 5.12 (s, 2H), 4.58 (m, 1H), 3.70 (s, 3H), 3.04 (dd, *J* = 4.4, 16.9 Hz, 1H), 2.86 (dd, *J* = 4.8, 16.8 Hz, 1H), 1.44 (s, 9H).

#### *Synthesis of H<sub>2</sub>N-Asp(OBn)-OMe:*

4.36 g of Boc-Asp(OBn)-OMe (13.0 mmol, 1 eq.) were dissolved in 50 mL of a 1:3 v/v solution of TFA and DCM and the mixture was stirred for 5 h. 50 mL of DCM were added and the solution

---

was then extracted with 0.1 M HCl<sub>aq.</sub> (3 x 30 mL); the pH of the combined organic phases was adjusted to 9 with 1 M NaOH. The aqueous layer was then extracted with DCM (3 x 25 mL); evaporation of the solvent afforded the pure product. Yield: 84% wt. Yellow oil. <sup>1</sup>H NMR (200 MHz, CDCl<sub>3</sub>) (δ = ppm): 7.36 (m, 5H), 5.15 (s, 2H), 3.58 (dd, *J* = 2.1, 5.0 Hz, 1H), 3.70 (s, 3H), 2.82 (dd, *J* = 5.0, 6.7 Hz, 2H), 1.75 (bs, 2H); FT-IR (cm<sup>-1</sup>): 3311, 3064, 3034, 2954, 1738, 1686, 1660, 1536, 1520, 1453, 1406, 1317, 1277, 1247, 1216, 1166, 997, 852, 755, 699.

### *Synthesis of Boc-Gly-Asp(OBn)-OMe:*

To a stirred solution of Boc-Gly-OH (0.63 g, 3.6 mmol, 1 eq.), DMAP (90 mg, 0.7 mmol, 0.2 eq.) and TEA (1.2 g, 10.8 mmol, 3 eq.) in 7.5 mL of DCM cooled at 0 °C a solution of EDCI (820 mg, 4.3 mmol, 1.2 eq.) in 20 mL of DCM was added dropwise. The reaction temperature was allowed to progressively raise to room temperature in 30 minutes, then the reaction was stirred at room temperature overnight. The mixture was washed with a saturated solution of NaHCO<sub>3</sub> (50 mL), a saturated solution of citric acid (50 mL) and brine (50 mL), the organic phase was dried over Na<sub>2</sub>SO<sub>4</sub> and filtered. Evaporation of the solvent afforded the pure product. Yield: 50% wt. Yellow oil. [α]<sub>D</sub><sup>25</sup> (c = 0.1 w/v; CHCl<sub>3</sub>): + 26.741; <sup>1</sup>H NMR (300 MHz, CDCl<sub>3</sub>) (δ = ppm): 7.35 (m, 5H), 5.12 (s, 2H), 4.87 (m, 1H), 3.79 (d, *J* = 5.7 Hz, 2H), 3.70 (s, 3H), 3.08 (dd, *J* = 4.3, 17.1 Hz, 1H), 2.89 (dd, *J* = 4.5, 17.1 Hz, 1H), 1.46 (s, 9H); <sup>13</sup>C NMR (200 MHz; CDCl<sub>3</sub>) (δ = ppm): 170.97, 170.59, 169.56, 156.03, 135.38, 128.51, 128.32, 128.24, 79.81, 66.70, 52.61, 48.47, 43.97, 36.24, 28.22; FT-IR (cm<sup>-1</sup>): 3339, 3065, 3034, 2978, 1737, 1683, 1719, 1455, 1438, 1390, 1366, 1280, 1250, 1217, 1171, 1051, 1029, 995, 944, 864, 752, 699; FAB-MS 395 (M+H)<sup>+</sup>.

### *Synthesis of H<sub>2</sub>N-Gly-Asp(OBn)-OMe:*

1.3 g of Boc-Gly-Asp(OBn)-OMe (3.3 mmol, 1 eq.) were dissolved in 50 mL of a 1:3 v/v solution of TFA and DCM and the mixture was stirred for 3 h. Then, the same work-up described in 0 was applied affording the pure product. Yield: 87% wt. White solid (m.p. 207-209 °C). [α]<sub>D</sub><sup>25</sup> (c = 0.1 w/v; DMSO): + 12.723; <sup>1</sup>H NMR (200 MHz, CDCl<sub>3</sub>) (δ = ppm): 7.35 (m, 5H), 5.14 (s, 2H), 4.91

---

(m, 1H), 3.71 (s, 3H), 3.36 (s, 2H), 3.08 (dd,  $J = 4.70, 16.8$  Hz, 1H), 2.89 (dd,  $J = 4.5, 16.8$  Hz, 1H); FT-IR ( $\text{cm}^{-1}$ ): 3192, 1741, 1686, 1661, 1497, 1358, 1331, 1310, 1270, 1219, 1172, 1145, 1097, 988, 822.

*Synthesis of Boc-Arg(Z)<sub>2</sub>-Gly-Asp(OBn)-OMe:*

To a solution of 70 mg of Boc-Arg(Z)<sub>2</sub>-OH (0.13 mmol, 1 eq.), TEA (53 mg, 0.52 mmol, 4 eq.), DMAP (2 mg, 0.01 mmol, 0.1 eq.) in 2 mL of dry DCM, HBTU (60 mg, 0.16 mmol, 1.2 eq.) was added, under nitrogen atmosphere. After 30 minutes, a solution of H<sub>2</sub>N-Gly-Asp(OBn)-OMe (38 mg, 0.13 mmol, 1 eq.) in 3 mL of dry DMF was added. The reaction was monitored by TLC and <sup>1</sup>H NMR, but the no new products were detected.

# 3 EFFECTS OF ENVIRONMENTAL FACTORS AND REACTANT ARCHITECTURE ON THE OUTCOME OF THE MICHAEL-TYPE ADDITION USED FOR BIOCONJUGATION

## 3.1 INTRODUCTION

### 3.1.1 The Michael reaction

The Michael reaction refers to the addition of a nucleophile (Michael donor) to an activated  $\alpha,\beta$ -unsaturated carbonyl compound (Michael acceptor) and it is typically base-catalyzed (Figure 44).<sup>1</sup>

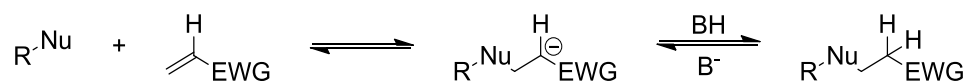
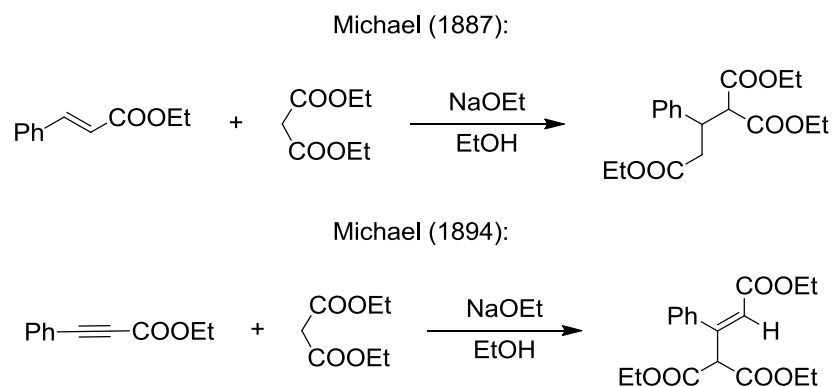


Figure 44: Schematic depiction of the Michael addition reaction.

T. Komnenos published in 1883 the first example of the addition of a carbon nucleophile to an electron-deficient double bond; in particular he reported the reaction between the anion of diethyl malonate and ethylidene malonate. After this first report, in 1887, A. Michael systematically investigated the reaction of stabilized anions with  $\alpha,\beta$ -unsaturated systems; during this study he synthesized a substituted pentanedioic acid diester through the addition of diethyl malonate to the double bond of ethyl cinnamate in the presence of sodium ethoxide.

In 1894, he enlarged the scope of the reaction to triple bonds, acting as electrophiles (Figure 45). This method of forming new carbon-carbon bonds became exceedingly popular by the early 1900s and today all the reactions involving the addition of stabilized carbon nucleophiles to activated  $\pi$ -systems are called Michael additions and the products are named Michael adducts.<sup>2</sup>



**Figure 45: Classical examples of Michael addition**

Nowadays, however, it is current use to refer to Michael-type addition to include a wide variety of molecules that show reactivity in 1,4-conjugate addition reactions: virtually, any electron-withdrawing group can be used. Furthermore, a broad range of acceptors and of non-carbon donors and both inter- and intramolecular versions have been reported, such as reactions involving non-enolate nucleophiles such as amines, thiols, and phosphanes.<sup>3</sup> In this thesis particular attention will be given to thiol-containing nucleophiles and examples of their use in Michael-type addition reactions will be discussed.

As a general feature, Michael donors derived from the deprotonation of CH-activated compounds such as aldehydes, ketones, nitriles,  $\beta$ -dicarbonyl compounds, etc. as well as from deprotonation of heteroatoms; the broad diversity of different donor-acting nucleophiles often

---



allows the use of relatively weak bases (e.g. triethylamine) in catalytic amounts, since the product of Michael addition is itself an anion that can further react with various electrophiles. The choice of the base catalyst has a tremendous effect on reaction kinetics and suitable bases are required to promote the deprotonation and so the activation of the donor depending on the  $pK_a$  of the nucleophile.

Another important feature characterising this reaction is that it is so versatile that it can be performed both in protic and aprotic solvents. This reaction, in fact, works even in aqueous media; the conjugated carbon centre, in  $\alpha,\beta$ -unsaturated carbonyl compounds, is considerably “softer” if compared to the non-conjugated site, while water is a “hard” solvent. Consequently, one of the implications deriving from this property of water, is that such reactions can tolerate water since the nucleophiles and the electrophiles are soft whereas water is hard; in other words water will not significantly compete with other nucleophiles in such reactions. Hence, various conjugate additions have been successfully carried out in aqueous media, most of all using soft heteroatom-based nucleophiles such as amines, thiols, phosphanes, and some halides.

Concerning the selectivity of the reaction, it can be highly diastereoselective when both the Michael donor and the acceptor display a defined stereochemistry; moreover, during the last decade, great efforts have been made to develop asymmetric versions providing an important tool for total synthesis of complex molecules.<sup>4</sup>

### 3.1.2 Reaction mechanism and kinetics

The generally accepted mechanism<sup>2,5</sup> is illustrated in Figure 46, where the addition of a malonate anion across the double bond of ethyl cinnamate is taken as the benchmark reaction. First of all, an enolate is generated via deprotonation by the base. The enolate anion then reacts in a 1,4-conjugate addition to the olefin of the acrylate system. Until proton transfer occurs, the resulting anion is stabilized by the carbonyl ester group and this intermediate is

---

itself a base indeed. The reaction is reversible in protic solvents and the thermodynamically most stable product usually predominates. The overall driving force for the conjugate addition is the enthalpic change that accompanies the replacement of a  $\pi$ -bond with a  $\sigma$ -bond. Thus, there is the preference for 1,4-addition over 1,2-addition.

In some cases, however, kinetically controlled reaction conditions can afford attack at the  $\alpha$ -carbon rather than at the  $\beta$ -carbon of the olefin, but the careful choice of the reaction medium and the use of additives can suppress these undesired reactions.

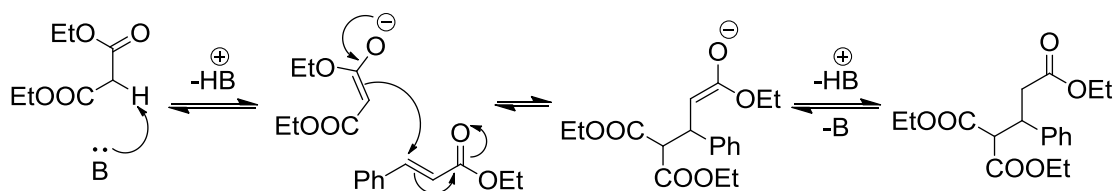


**Figure 46: Mechanism of Michael addition**

The kinetics of the addition obey a second order rate law (See Equation 1, where Nu = nucleophile and El = electrophile):

$$v = k_{\text{obs}}[\text{Nu}][\text{El}] \quad \text{Equation 7}$$

If the nucleophile derives from a deprotonation process, its concentration is a function of the base strength and of the equilibrium constant of the deprotonation process ( $K_a$ ).

In conclusion, the most important factors affecting the reaction rate are the reactants architecture and the reaction medium (solvent, buffer system, base strength).

---

### 3.1.2.1 Michael-type acceptor effect

Typical acceptors in the Michael-type addition are olefins activated for nucleophilic attack. Actually, for allowing the reaction to occur, the anion resulting from the nucleophilic attack by the donor must be stabilized as well. Thus, the electronic availability and the steric hindrance at the double bond play a key role. A class of compounds that meets these requirements is that of the  $\alpha,\beta$ -unsaturated carbonyl compounds.

The reactivity of the acceptor will decrease if electron rich substituents are present, such as in the case of alkyl, aryl or alkoxy substituted olefins such as styrene derivatives or vinyl ethers. Moreover, the larger the groups located in the  $\alpha$  and  $\beta$  positions, the slower the reaction rate, although this effect can be offset by stronger polar contributions. For example, alkyl methacrylates are relatively poor Michael acceptors compared to the corresponding acrylates. Surely, differences in reactivity between acceptors can be overtaken by tuning the nucleophilicity of the Michael donors. For instance, with poor Michael acceptors, stronger nucleophiles, such as carbanions, are necessary to successfully achieve the Michael addition. On the other hand, better acceptors readily accept weaker nucleophiles such as amines and thiols.

Aptula et al reported in 2007<sup>6</sup> an exhaustive study where the reactivity of a set of  $\alpha,\beta$ -unsaturated compounds was evaluated towards the sulfhydryl group of the cysteine residue of the tripeptide glutathione (GSH) as a thiol-containing model nucleophile. The comparison was focused on polarized  $\alpha,\beta$ -unsaturated compounds featuring double or triple bonds and included the ones containing an aldehyde, ketone, ester, sulfoxide, sulfone, sulfonate, nitro, or cyano moiety, as well as *ortho*- and *para*-pyridyl compounds and *ortho*- and *para*-quinones (Figure 47). Specifically, they calculated the  $RC_{50}$  value for each compound; the reactive end point ( $RC_{50}$ ) represents the required concentration of electrophile so that half the available free thiol would be bound at the fixed time of 2 h. It was observed that acetylenic derivatives are more

reactive than their corresponding olefinic analogues; methyl substitution on a vinyl carbon atom reduces the reactivity, but the methyl substitution on the  $\alpha$ -carbon atom produces a larger rate reduction; an additional unsaturated group increases the reactivity.

A further study developed by Schwöbel,<sup>7</sup> where a broader set of Michael-type acceptors was used in order to develop a model to predict the kinetic rate constants of such compounds towards glutathione (GSH), under the same experimental conditions (i.e. phosphate buffer at pH 7.4 and 25°C), gave evidence of the same trend observed before; in short, they fixed as a general reactivity scale the sequence propiolate > acrylate > crotonate >> methacrylate.

A direct comparison of the reactivity between acrylate and methacrylate<sup>8</sup> confirms that methyl substitution on the  $\alpha$ -carbon atom of the vinyl group reduces the reactivity. This decrease in reactivity is perceived to be due to a combination of steric and electronic aspects: first,  $\alpha$ -methylation sterically hinders the thiol attack and secondly and more importantly, the electron-donating  $\alpha$ -methyl moiety decreases the partial positive charge on the  $\beta$ -carbon atom, making it less electrophilic.

Moreover, the rather small variability in reaction rate within different methacrylates and acrylates, indicates that the electronic effect of the ester group is less important than the effect of the substitution pattern on the  $\alpha$  carbon.

Other studies<sup>9</sup> including the amide group as electron withdrawing moiety revealed that its ability to activate the double bond is comparable to that exhibited by the ciano group, that is the kinetic rate constant is one order of magnitude lower than the one measured for the corresponding ester.

Another well known Michael acceptor that showed to react very quickly in Michael-type addition is maleimide. Kinetic investigations<sup>10</sup> revealed that its derivatives react with thiols (2-mercaptoethanol, free cysteine and the cysteine residues present at the *N*-terminus of

---

## Effects of Environmental Factors and Reactant Architecture on the Outcome of the Michael-Type Addition Used for Bioconjugation

peptides) faster than with bromoacetyl derivatives in aqueous media, even at pH 6.5. The use of maleimide containing compounds involves, however, substantial drawbacks which cannot be neglected (See 3.1.3 for a detailed discussion).

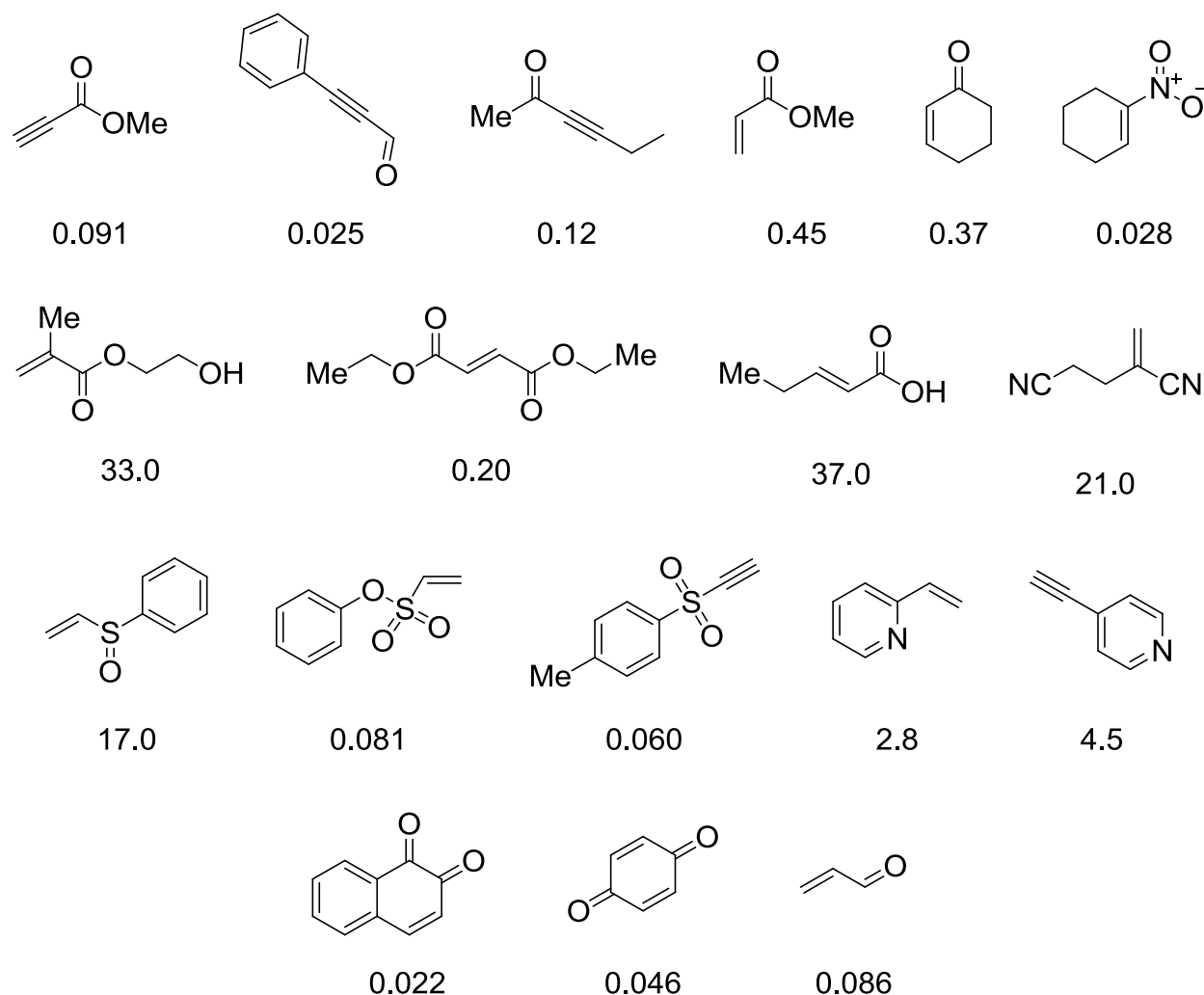


**Figure 47 : Reactivity towards GSH of selected Michael-type acceptors**

Michael acceptors considered by Aptula<sup>6</sup> for the determination of a scale of reactivity; specifically, the kinetics of the Michael-addition reaction between the reported electrophiles and GSH as thiol-containing model nucleophile were followed (phosphate buffer at pH 7.4, room temperature) with a spectrophotometric assay to determine the reactive end point ( $RC_{50}$ , expressed in mM), that indicates the concentration of electrophile required to react with half of the available free thiol in 2 h; the values obtained are reported below the relative compound.

### ***3.1.2.2 Michael-type donor effect***

As mentioned before, Michael reaction initially referred to the 1,4-addition between an activated-methylene function and a conjugated double bond, leading to the formation of a new carbon-carbon bond; the initial step of the carbon-Michael addition is the deprotonation of the donor. In order to increase the acidity of the hydrogen to be removed, the donors must be able to stabilize the resulting negative charge. Stabilized carbanions usually result from ketones, aldehydes, nitriles, amides, nitrones, sulfones, malonates and acetoacetates. To know in advance the  $pK_a$  of the Michael-type donor results particularly useful for the choice of the proper base; stronger bases than required, in fact, may promote side reactions, such as ester or amide hydrolysis.

Since when the scope of the reaction has been thoroughly investigated, the use of heteroatomic nucleophiles became very popular and donors featuring nitrogen, sulfur, oxygen and phosphorus as nucleophilic centres have been widely used.

Specifically, when a nitrogen-donor is involved in the Michael addition, the reaction is often called aza-Michael reaction. Since amines can act both as nucleophiles and bases, no additional bases are generally required in these reactions. The reaction tends to follow second-order kinetics based on the concentration of the olefin acceptor and the donor amine. As drawback, it must be taken into account that primary amines can react with two equivalents of acceptor to form tertiary amines. The aza-Michael version of the conjugated addition indeed represents one of the most attractive procedures for the asymmetric synthesis of  $\beta$ -amino carbonyl compounds and related derivatives. This class of compounds is extremely important because of their ubiquitous occurrence as constituents of a plethora of biologically important natural and synthetic products and, moreover, they have been shown to be very versatile intermediates to them. In conclusion, the aza-Michael reaction tremendously increased in importance in recent years as an excellent synthetic tool for forming new carbon-nitrogen bonds.

The first enantioselective conjugate amine additions reported in the literature<sup>11</sup> was carried out with the  $\text{TiCl}_2$ -BINOL complex as Lewis acid catalyst to promote the coordination with the *N*-acyloxazolidinone, creating a chiral environment in which the primary amine preferentially attacks one face of the complex, resulting in the formation of one prevailing diastereomer. The oxazolidinone ring can then be removed to afford  $\beta$ -amino acids (Figure 48). Although, the enantioselectivity was modest (maximum enantiomeric excess: 42%), this first attempt opened a new field in asymmetric synthesis using the aza-Michael addition to generate  $\beta$ -amino acids.

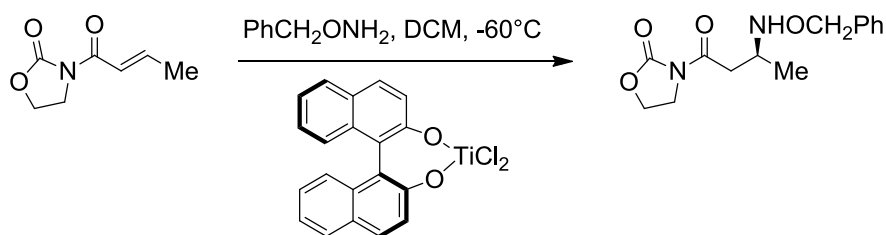


**Figure 48 : The first example of a stereoselective aza-Michael addition**

Another important class of heteroatomic donors used in combination with Michael-type acceptors are thiol-containing compounds. The importance of thiol-containing donors is due to the presence of cysteine residues in proteins and, by consequence, in biological systems.

Thiols have the advantage of being, in general, more nucleophilic than amines<sup>12</sup>, but, considering that thiolates are even more reactive, bases are often used to deprotonate them. The deprotonation of mercaptans needs mild bases because of their relatively high acidity. Kinetic studies proved that the thiolate anion is often the active species in Michael additions involving thiols. Hence, it is well known that the thiol Michael addition reaction rate increases with increasing the pH value, due to the higher concentration of the thiolate anion in solution.<sup>13</sup> A recent paper<sup>14</sup> presented a quantitative structure-reactivity relationship for the Michael-type

---

addition of thiols onto acrylates; specifically a homologous series of peptides with charged amino acids flanking a cysteine, was reacted with PEG-diacrylate in order to elaborate the dependence between the Michael-type reactivity and the structure of the reaction partners. Peptides featuring different primary structures showed different behaviors in the Michael-type addition: it was found that charged amino acids located close to the SH groups considerably altered the  $pK_a$  of the cysteine residue (single titrations were performed in order to determine each  $pK_a$ ). The conclusion was that a linear correlation between the thiolate concentration, hence its  $pK_a$ , and the second order reaction kinetics could be made, and is a key point in tailoring the reaction kinetics to the needs of an application.

A further issue to take into account is that thiols undergo oxidation leading to the formation of disulfides, and that this reaction becomes faster as more basic is the reaction medium.

### ***3.1.2.3 Reaction medium effect***

Based on the frontier orbital theory, a two-terms equation can be used to explain the differences in reactivity of a series of electrophiles toward a specific nucleophile. The two terms are a coulombic attraction/repulsion term and a term related to the overlap of the frontier orbitals: the highest occupied orbital [HOMO] of the nucleophile and the lowest unoccupied orbital [LUMO] of the electrophile. Surely both of them are influenced by the interaction with the solvent and the eventual additives. Looking at the increasing importance of Michael-type addition as a tool for bioconjugation, water as solvent must be considered with particular attention. The consequences of water “hardness” have already been discussed in 3.1.1. Usually, buffered systems with controlled pH are used, hence the actual behavior of the water as solvent can be tuned by carefully selecting salts featuring cation-anion bonds with different percentages of ionic/covalent character. In fact, the interaction between the ions in solution and the charged intermediates might amplify steric or electronic factors, thus influencing the outcome of the reaction.



Even if we were particularly interested in the use of Michael-type addition as a tool for effecting bioconjugation processes, we will, nevertheless, report some general considerations about the variables affecting the reaction (i.e. base catalyst and solvent system).

Considering that the Michael donors often derive from the deprotonation of a conjugate acid-precursor, the choice of the base catalyst has a tremendous effect on the reaction kinetics. As previously noted, the concentration of the Michael donor species is highly dependent upon the relative base strength. In the case of strong bases the concentration of the enolate anion approximately corresponds to the concentration of the base, even though the main drawback with using strong bases, such as hydroxide and methoxide anions, is that they may promote side reactions such as ester hydrolysis. In this light, non-nucleophilic bases are often desirable and the careful choice of the base remains a key point.

Other factors affecting the reaction kinetics are the stabilization of the charges assisted by the solvent. Basically, any kind of solvent, if capable to dissolve catalyst, donor and acceptor, can be used (e.g. methanol, ethanol, diethyl ether, tetrahydrofuran, benzene, xylene, dioxane and mixtures of these solvents). Initially, protic solvents were considered as highly desirable in the carbon-Michael reaction as particularly efficient to promote a rapid proton transfer and to stabilize charged intermediates.

The stabilisation of the charges effected by the solvent greatly affects the base strength as well; for example, *N*-methylimidazole was proven to act as basic catalyst in the Michael addition of malonodinitrile to chalcone (Figure 49) both in the common organic solvents and in ionic liquids (ILs)<sup>15</sup> {i.e. [emim]SO<sub>4</sub>Et (1-ethyl-3-methylimidazolium ethylsulfate), [bmim]PF<sub>6</sub> (1-butyl-3-methylimidazolium hexafluorophosphate) and [bmmim]PF<sub>6</sub> (1-butyl-2,3-dimethylimidazolium hexafluorophosphate)}, and its basicity is higher in ILs than in conventional solvents. For reactions studied in ILs, residual amounts of *N*-methylimidazole or the acidity of the IL itself can have strong effects on the outcome of the reaction.

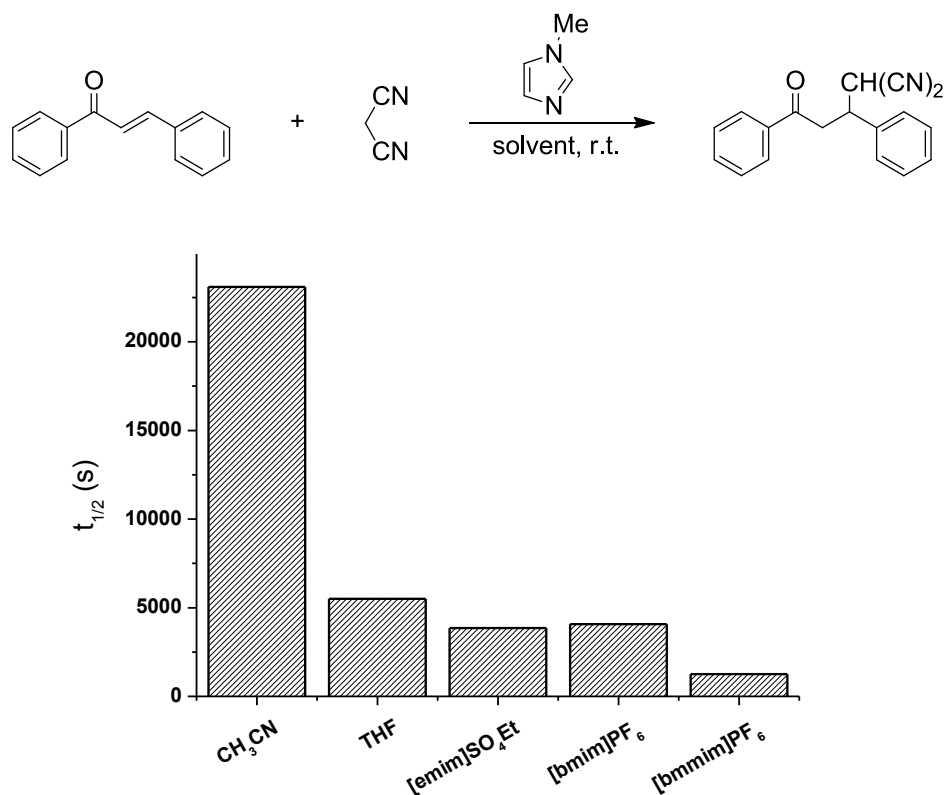


**Figure 49: Solvent effect on the reaction rate of the Michael addition of malonodinitrile to chalcone catalyzed by 5% mol of *N*-methylimidazole**

The Michael addition of malonodinitrile to chalcone in various ILs as well as in conventional organic solvents was studied in the following conditions: chalcone (1.0 mmol), malonodinitrile (10.0 mmol) and the catalyst (5% mol) were stirred for 4 h at room temperature. Samples of the reaction mixture were taken at different times in order to spectrophotometrically determine the values of the rate constants of the reaction ( $t_{1/2}$  is the half-life time of the Michael addition).

### 3.1.3 Reversibility of Michael-type reaction

As already mentioned in the description of the reaction mechanism (See 3.1.2), the Michael addition is a reversible reaction in protic solvents. The relative concentration of the reactants depends on the thermodynamic balance; this means that the thermodynamically most stable product usually predominates. A general consideration from the kinetic point of view is that the

---

higher the reaction rate of the Michael addition reaction, the higher is the kinetics of the retro-Michael reaction as well: this means that the factors affecting the rate constant are the same already discussed before.

Recently this reversibility was regarded with particular attention in the design of controlled drug delivery systems, an issue particularly important in the field of biomaterials. Controlling the rate and the extent of the retro-type reaction might indeed be a tool to reach this goal. Michael-type addition reactions have recently emerged as a widely employed strategy for the covalent conjugation of proteins, peptides, and drugs to various polymers and other molecules by the reaction of free cysteine or thiols with acrylamides, acrylates, vinyl sulfones, and maleimides.

The retro-Michael reaction in the case of thiol-adducts has been observed in reducing environments, indicating that, in the presence of other thiol-based nucleophiles, the Michael-adduct deriving from a given thiol can undergo the exchange of the thiol moiety. Sulfide exchange is regarded with particular interest for designing new strategies of drug delivery systems due to the weak reducing capacity of blood (ca. 2-20  $\mu\text{M}$  glutathione) compared to that of reductive cellular compartments, or highly reductive and hypoxic tumor tissues (ca. 0.5-10 mM glutathione).

Ploemen reported in 1994<sup>16</sup> a study about the reversibility of the conjugation reaction of the diuretic drug ethacrynic acid (Figure 50) with glutathione. Ethacrynic acid and its glutathione-adduct are known to be potent inhibitors of glutathione *S*-transferase family members, which are enzymes involved in xenobiotic metabolism. They observed a time-dependent transfer of ethacrynic acid to *N*-acetyl-L-cysteine or glutathione (GSH) *S*-transferase P1-1 (featuring a cysteine residue in position 47) when the glutathione conjugate was incubated with a 5-fold molar excess of one of two other thiol containing nucleophiles. With increasing pH values, the pseudo first order rate constant of transfer increased from 0.010  $\text{h}^{-1}$  (pH 6.4) to 0.040  $\text{h}^{-1}$  (pH

7.4) and  $0.076 \text{ h}^{-1}$  (pH 8.4).

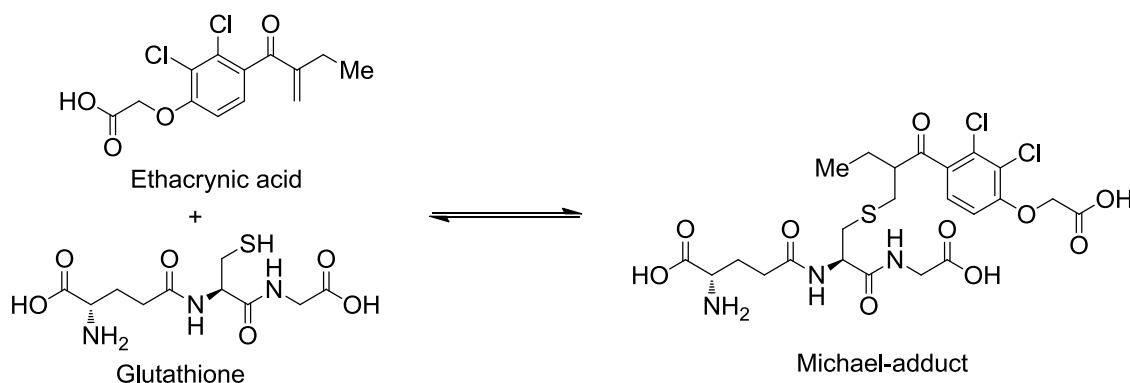


**Figure 50: Reversible Michael-type addition reaction between ethacrynic acid and glutathione**

Ethacrynic acid, trade name Edecrin, is a diuretic drug used to treat high blood pressure and the swelling caused by diseases like congestive heart failure, liver failure, and kidney failure. Glutathione (GSH) is a tripeptide cysteine with important function as antioxidant. The Michael-type adduct of these two compounds is an inhibitor of glutathione *S*-transferase family members, which are enzymes involved in xenobiotic metabolism.

The conclusion is that, under normal physiological conditions, the inhibition of glutathione *S*-transferase P1-1 by covalent binding of ethacrynic acid would be reversed by glutathione; moreover this inhibition mediated by the glutathione is reversible itself depending on the *in vivo* concentration of glutathione.

More recently the stability of Michael-type adducts between different thiols and maleimide was studied.<sup>17</sup> Maleimides have been commonly employed in disulfide-based drug conjugation and polymer network formation due to their specificity to thiols, fast aqueous reaction kinetics, lack of byproducts, and the stability of the thioether addition products. While the wide use of maleimide-thiol conjugation reactions have been motivated by the product stability, the study reports details on the reversibility of maleimide-thiol conjugation reactions and on the

hydrolytic stability of the conjugate itself. They have found that the rate and the extent of exchange, which is governed by the rate of the retro-addition, can be modulated by increasing or decreasing the Michael donor reactivity.

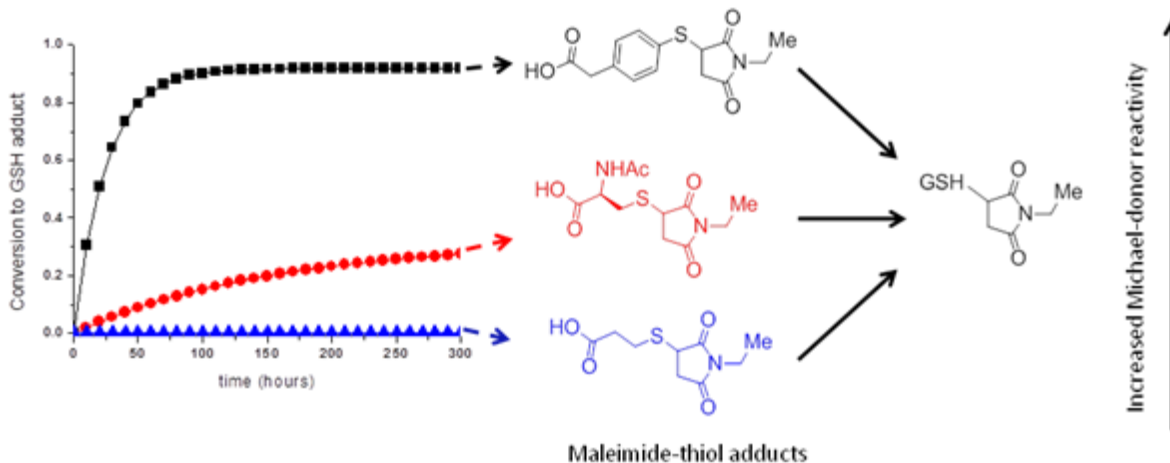


**Figure 51: Degradation of maleimide-thiol adducts in reducing environment**

Succinimide thioethers, formed by the Michael-type addition of thiols to *N*-ethylmaleimide, undergo retro and exchange reactions in the presence of other thiol compounds at physiological pH and temperature. Model studies ( $^1\text{H}$  NMR, HPLC) of the conjugated adduct with 3-mercaptopropionic acid, incubated with glutathione, showed half-lives of conversion from 20 to 80 h, while extents of conversion from 20% to 90% were found for 4-mercaptophenylacetic acid, *N*-acetylcysteine and *N*-acetylcysteine conjugates.

If the reversibility of the Michael addition is on the one hand a tool to tune the stability of the adducts, on the other hand it does not often allow to have conjugates as stable as required. For example, a recent study about the development of new ways to synthesise antibody-drugs conjugates demonstrated that, for maximal intratumoral drug delivery, the linkers are required to be highly stable in the systemic circulation, in order to allow an efficient drug release at the target site. In this respect, maleimide-based conjugates showed half-lives in circulation of 1-2 days, while amide linkers ensure much longer half-lives of about 7 days.<sup>18</sup> The mechanism of

---

the drug release from maleimide-adducts likely involves, even in this case, a retro-Michael reaction that takes place in plasma; specifically, some of the released drug-maleimide derivatives became covalently bound to the cysteine-34 of serum albumin.

These studies led to the development of strategies of controlled drug-release taking advantage from the tunable reactivity of the thiol function in cysteine coupled with maleimide linkers in the generation of antibody conjugates. An impressive recent investigation<sup>19</sup> reports on engineered antibodies featuring cysteines at three sites differing in solvent accessibility and local charge. This strategy allowed the control of the rate of the retro-Michael reaction, causing drug release and maleimide exchange with reactive thiols of the plasma (e.g. albumin, free cysteine and glutathione), or of hydrolysis of the succinimide ring in the linker, thereby preventing this exchange reaction (Figure 52). Thus, the chemical and structural dynamics of the conjugation site can influence antibody conjugate performances by modulating the stability of the antibody-linker interface.

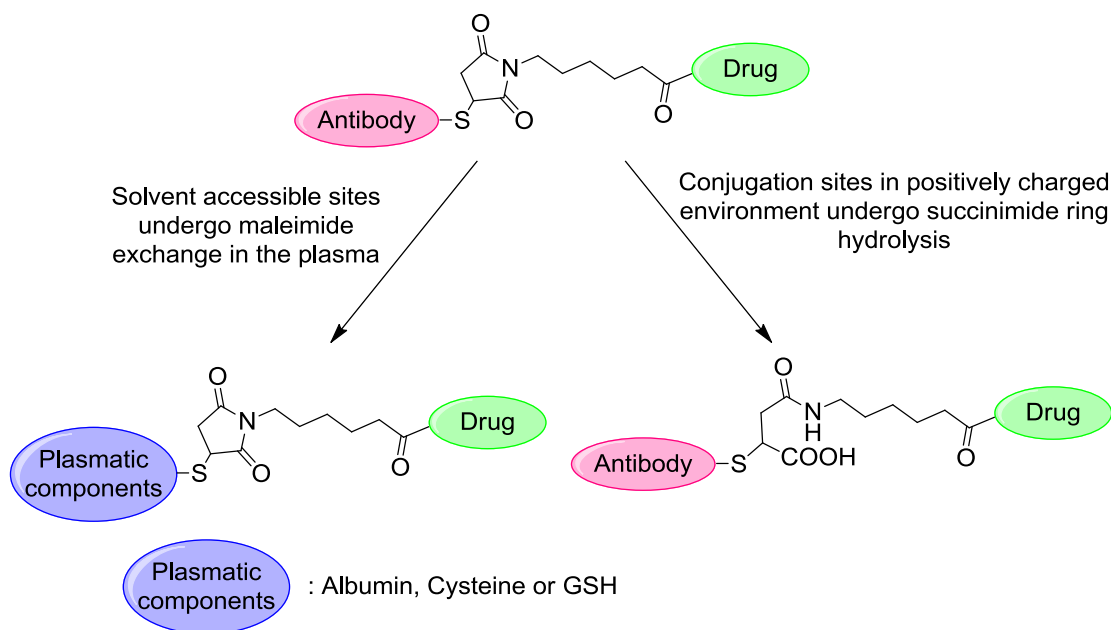


**Figure 52: Proposed mechanism for the influence of the conjugation site on linker stability and therapeutic activity of antibody conjugates.**

The maleimide exchange from the antibody conjugate and hydrolysis of succinimide ring in the linker are key steps that influence conjugate stability and therapeutic activity. Specifically, if the thiol belongs to a solvent accessible site, this brings to retro-Michael reaction with other plasmatic thiols and the reaction outcome depends on the relative concentration of the different nucleophiles; hence, reactive thiols cause low stability of the antibody conjugate decreasing the therapeutic activity. On the contrary, a partially accessible site with a positively charged environment promotes the hydrolysis of the succinimide ring in the linker, enhancing the linker stability and the conjugate therapeutic activity.

### 3.1.4 Bioconjugates via Michael addition

The technology of bioconjugation encompasses several disciplines in the life sciences fields. Bioconjugation recently increased in importance as a tool for providing materials useful for biomedical applications and fundamental studies. Bioconjugates consist in polymers covalently bound to biopolymers (proteins, polysaccharides, polynucleotides, antibodies) or bioactive species (pharmaceuticals). This goal can be reached by crosslinking and modifying the native state and functional groups of peptides and proteins, sugars and polysaccharides, nucleic acids

---

and oligonucleotides, lipids, and almost any other imaginable typology of molecules that can be chemically derivatised. This strategy is often used to improve the resistance to clearance from the bloodstream in terms of excretion from the liver or kidneys, thus increasing circulatory lifetimes of protein drugs. Furthermore, the linkage with particular peptidic fragments mediating the recognition process may be crucial to bind the bioactive fragment to proteins receptor. Recognition properties are important in artificial organs and implants as well as in biosensors. Moreover, through a careful modification or tailored conjugation strategies, the structure and the function of proteins can be investigated, the active site conformation elucidated, or the receptor-ligand interactions revealed. Polymer-protein and polymer-drug conjugates have been used also to improve the solubility of a suitable molecule within the body.

Michael addition chemistry has been recently regarded with particular attention for linking biomolecules to different substrates. This reaction, in fact, benefits from mild reaction conditions and high functional group tolerance as well as from high conversions and favourable reaction rates. In biological applications, such as protein derivatisation, the mild Michael addition reaction conditions represent a highly favourable situation, since high temperatures, oxidizing environments, radicals and organic solvents are not compatible.

In a recent application,<sup>20</sup> a Michael-type addition was successfully used as a convenient tool for surface functionalization. As reaction partners, thiols and acrylates were used and the comparison of two strategies has been reported. In particular, the aim was to generate a PEGylated surface decorated with peptidic groups.

A first attempt contemplated the generation of thiol functions on a poly(styrenic) surface, followed by reaction with an excess PEG-diacrylate (first Michael-type addition); the free acrylate functions would be employed for conjugation with a thiol-containing peptide (second Michael-type addition).

---



The second route involved the initial acryloylation of a PEGylated particle, followed by conjugation with a thiol-containing peptide (Figure 53).

The use of a Michael-type addition in heterogeneous conditions revealed that the localization of the reaction partners is crucial: the combination thiol on the surface/acrylate in solution showed that the thiol groups distributed on the surface lack in reactivity. Disulfide formation can be excluded, due to the reducing reaction environment; thus, the poor reactivity is likely to be ascribed to the hydrophobicity of the thiols and of the polymeric surface, which do not kinetically favor the reaction with products dissolved in water or in the very polar solvents employed. On the contrary, employing previously PEGylated materials functionalized with acrylates and soluble thiols the target was reached.

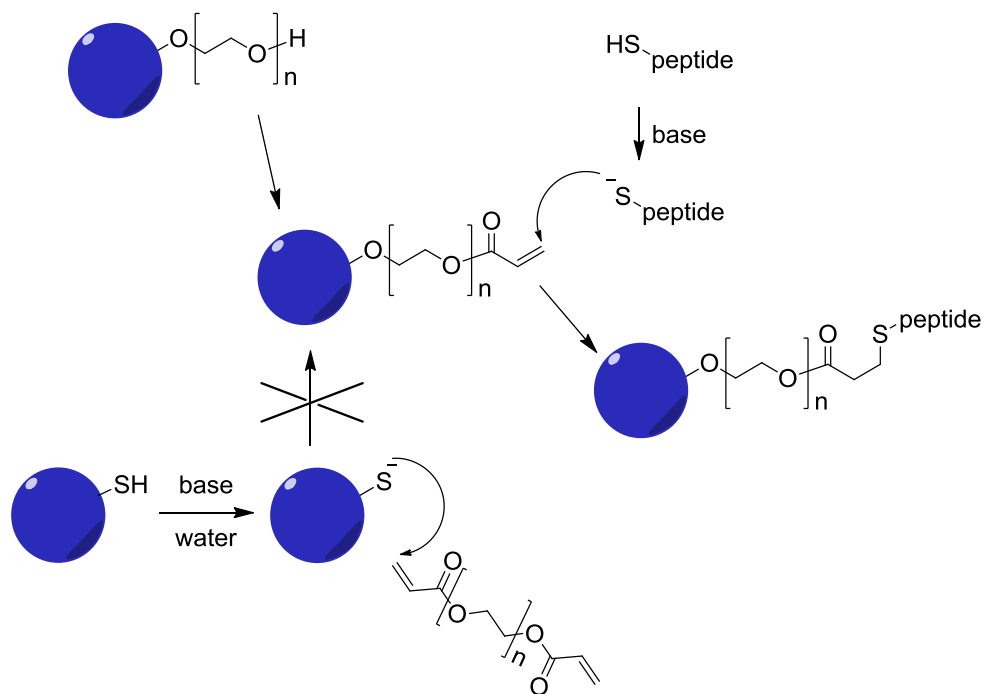


**Figure 53: Strategies for the Use of Michael-type for surfaces modification**

The two different strategies for the bioconjugation with peptides and macroparticles. As highlighted one the introduction of the Michael-type acceptor first, and then of soluble thiols successfully worked.

---

Another application of this method for attaching biological molecules to hydrogels is described, using a chemical scheme that can be performed in contact with proteins, cells, and tissues<sup>21</sup>. This was accomplished using a conjugate addition reaction on acrylamides which readily react with thiol groups; in particular peptides containing a single thiol group were coupled to the PEG-diacrylamide in aqueous solution at room temperature in about 2 h. Only a portion of the acrylamide groups were targeted for reaction with peptide, thus to leave a sufficient amount of PEG-diacrylamide to be polymerized by free-radical mechanisms via photoinitiation. The photopolymerization step can be performed in contact with cells, providing a means to produce bioactive scaffolds for tissue engineering. The presence of particular peptidic sequence is required so that cells will respond only to the incorporated ligand. PEG, in fact, is well known to possess low adhesion to proteins so the decoration of the substrates with ligands allowing cell-adhesion, such as RGD protein, is often a critical issue. Hence, currently, strong interest exists in functionalizing polymers with the RGD protein to promote cell adhesion for tissue scaffolds. The RGD protein selectively promotes cell adhesion, while avoiding non-specific adsorption of proteins. Furthermore, cell spreading, a change in the cellular morphology, occurs in the presence of the RGD coating, indicating cell signaling has occurred.

#### ***3.1.4.1 Bioconjugates via Michael addition on Hyaluronic acid***

Bioconjugation on HA is often required to improve its possibility to reach the biological target, and this property is extremely related to its efficacy as carriers. Several strategies for modifying and functionalising HA have already been reported (See 2.1), but, focusing on the use of Michael-type addition, an example is the paper by Ouasti *et al.*<sup>22</sup> who conjugated the cell adhesion peptide RGD onto the backbone of a HA-derivative to study the influence of the peptide on the cellular uptake of HA via the RGD-specific integrins and CD44 receptors present on cell surfaces. Specifically, they first synthesised methacrylated HA by conjugating *N*-(3-aminopropyl)-methacrylamide onto the HA carboxylic acid group via EDC-mediated amidation reaction. This was followed by a second conjugation reaction with a RGD-containing

---

peptide including a cysteine to feature a thiol nucleophile, via Michael-type addition (Figure 54).

Moreover the aza-version of the Michael-type addition was performed as well on the HA backbone<sup>23</sup>; the aim in this case was the synthesis of a poly(*L*-leucine) grafted HA that may have advantages for mimicking natural processes occurring in proteins and thus have potential use in biomedical applications. The combination of polysaccharide and polypeptide, in fact, should provide tailored biomaterials that can be used in tissue engineering as hydrogels and as drug carriers in delivery system. In particular, poly(*L*-leucine) was grafted on hyaluronan via a Michael addition reaction between primary amine terminated poly(*L*-leucine) and acrylate-functionalized HA. The precursor hyaluronan, as tetrabutyl ammonium salt, form was first functionalized with acrylate groups by reaction with acryloyl chloride in the presence of triethylamine in *N,N*-dimethylformamide. Michael addition at high a molar grafting ratio gave only 0.20 degree of conversion with respect to the repeat unit of HA, even with high excess of peptide, indicating grafting limitation due to insolubility of the final product; soluble graft copolymers were obtained only for low grafting ratios (<0.039).

In conclusion, due to its versatility even for the application on HA, Michael addition is a precious tool for bioconjugating specific bioactive molecule on it and hence a detailed study to investigate all the factors affecting the reaction outcome is really useful in order to be able to tune the reaction kinetics and the stability of the final adduct. Thus we deeply studied the effect of the reagents architecture (influence of the Michael donor and acceptor), their stability and that of the Michael adducts.

Effects of Environmental Factors and Reactant Architecture on the Outcome of the Michael-Type Addition Used for Bioconjugation

---

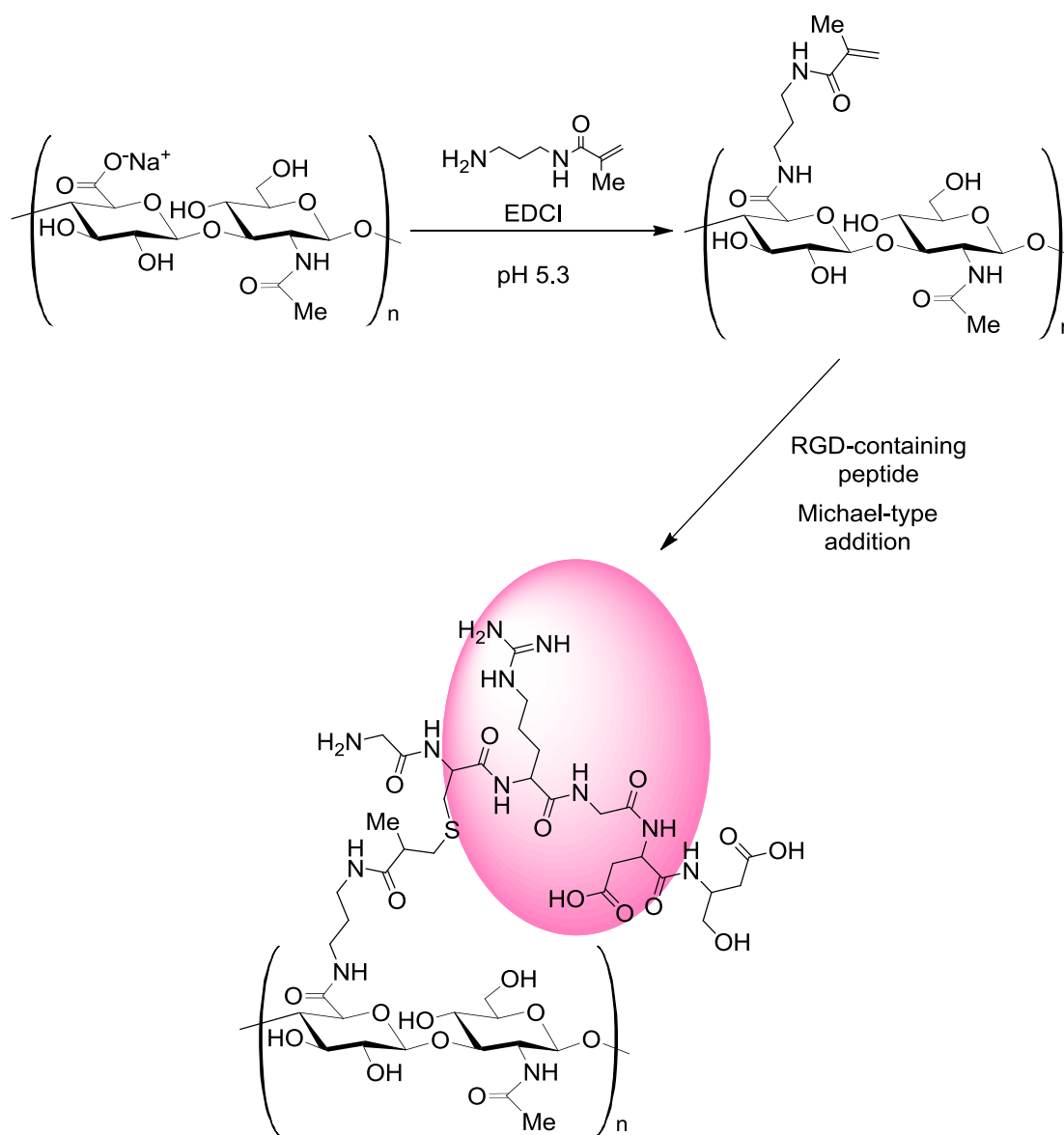


**Figure 54: Bioconjugation on HA with a RGD-containing peptide via Michael-type addition**

HA (of 64, 234, or 1100 kDa) was functionalized with RGD-containing peptides through the EDC-mediated reaction with 3-aminopropyl methacrylamide which was then reacted with the peptidic thiol in a Michael-type addition.

## 3.2 EXPERIMENTAL PROCEDURES

### 3.2.1 Materials

5,5'-Dithiobis-(2-nitrobenzoic acid) (DTNB; Ellman's reagent) was supplied by Invitrogen (Oregon, USA); all other reagents including 3-mercaptopropionic acid (3-MPA), 2-hydroxyethyl acrylate (**1**), 2-hydroxyethyl methacrylate (**2**), and Sephadex® G-10 were purchased from Sigma-Aldrich (Gillingham, Dorset, UK) and used without further purification. All the other reagents were of analytical grade and used without further purification.

### 3.2.2 General methods

#### 3.2.2.1 Molecular characterization

Absorbance readings were recorded on a Biotek® Synergy 2 multi-mode microplate reader (NorthStar Scientific Ltd., Leeds, UK). <sup>1</sup>H NMR spectra were recorded using Bruker AC-300 MHz or AC-400 MHz spectrometers. FT-IR spectra were recorded in ATR mode (Golden Gate) on a Tensor 27 Bruker spectrometer. Crude reactions were analyzed via reversed phase chromatography on a Agilent 1100 series HPLC equipped with analytical (5 µm particle size, 4.6 x 150 mm) Zorbax Eclipse XDB-C18 column and a Laserchrom S3210 UV/VIS detector set at 220 nm.

#### 3.2.2.2 Ellman's test

Monitoring the reaction kinetics of thiols and Michael-type acceptors was carried out by measuring the remnant thiol content of reaction samples (quenched at different time points) by Ellman's test. Briefly, an aliquot of 50 µL of each quenched reaction mixture was pipetted into a 96-wells plate, followed by addition of 250 µL of a freshly-prepared 300 µM DTNB aqueous solution in Tris buffer (1 M, pH 7.0). The content in each well was gently mixed by repeatedly pipetting the solution in and out with the help of a multichannel micropipette, and

then by shaking the 96-wells plate inside the microplate reader for 1.5 minutes at 30 °C. The absorbance was then recorded at 412 nm.

### **3.2.2.3 HPLC analysis**

An analytical linear gradient elution from 0% to 75% of solvent B and 100% to 25 % of solvent A, run over 20 min at 1 mL/min, was used, where solvent A is 0.1% trifluoroacetic acid (TFA) in water and solvent B is 0.1% TFA in acetonitrile.

### **3.2.2.4 Statistics**

Spectrophotometric experiments were carried out in triplicate, and the mean and standard deviations calculated for each reaction condition.

## **3.2.3 Synthetic procedures**

### **3.2.3.1 Synthesis of Michael-type acceptors**

#### **3.2.3.1.1 General procedure for the synthesis of compounds 3-6:**

A solution of 710 mg of TEA (7.0 mmol, 1.2 eq.) and 725 mg of *N*-acetyethanolamine (7.0 mmol, 1.2 eq., for compounds **3-4**), or 715 mg of *N*-acetyethyldiamine (7.0 mmol, 1.2 eq., for compounds **5-6**) in 10 mL of dry DCM was cooled down to 0 °C. Then, 525 mg of acryloyl chloride (5.8 mmol, 1.0 eq., for compounds **3-5**) or 610 mg of methacryloyl chloride (5.8 mmol, 1.0 eq., for compounds **4-6**) dissolved in 10 mL of dry DCM were added dropwise under an argon atmosphere. The reaction mixture was allowed to reach room temperature and stirred overnight. In order to prevent radical condensation of the alkene groups, BHT (ca. 10 mg) was added before removal of the solvent in a rotary evaporator. The crude products were purified by flash column chromatography on silica gel (70-230 mesh) eluted with AcOEt/EtOH mixtures, and BHT was added before solvent evaporation (ca. 1% wt. BHT in the concentrate).

*2-(Acetylamino)ethyl acrylate (3)*: Eluent: AcOEt/EtOH-98/2. Yield: 92% wt. Colourless oil. <sup>1</sup>H NMR (300 MHz, CDCl<sub>3</sub>) (δ = ppm): δ 6.43 (d, *J* = 17.3 Hz, 1H), 6.12 (dd, *J* = 17.3, 10.4 Hz, 1H), 5.95 (bs, 1H), 5.87 (d, *J* = 10.4 Hz, 1H), 4.24 (t, *J* = 5.3 Hz, 2H), 3.55 (m, 2H), 1.99 (s, 3H); FT-IR (cm<sup>-1</sup>): 3285, 3087, 1722, 1637, 1549, 1409, 1373, 1269, 1185, 1066, 1040, 984, 810, 669; HPLC retention time: 6.31 min (Supporting information Figure S 1).

*2-(Acetylamino)ethyl 2-methylacrylate (4)*: Eluent: AcOEt/EtOH-98/2. Yield: 57% wt. Colourless oil. <sup>1</sup>H NMR (400 MHz, CDCl<sub>3</sub>) (δ = ppm): 6.12 (s, 1H), 5.80 (bs, 1H), 5.60 (s, 1H), 4.25 (t, *J* = 5.5, 2H), 3.57 (m, 2H), 1.99 (s, 3H), 1.95 (s, 3H); FT-IR (cm<sup>-1</sup>): 3294, 3083, 2959, 1717, 1652, 1548, 1452, 1373, 1320, 1293, 1159, 1040, 943, 815, 654; HPLC retention time: 8.25 min (Supporting information Figure S 2).

*N-[2-(acetylamino)ethyl]acrylamide (5)*: Eluent: AcOEt/EtOH-80/20. Yield: 53% wt. White solid. <sup>1</sup>H NMR (300 MHz, CDCl<sub>3</sub>) (δ = ppm): 6.69 (bs, 1H), 6.47 (bs, 1H), 6.26 (d, *J* = 17.0 Hz, 1H), 6.11 (dd, *J* = 17.0, 10.1 Hz, 1H), 5.65 (d, *J* = 10.1 Hz, 1H), 3.43 (m, 4H), 1.98 (s, 3H); FT-IR (cm<sup>-1</sup>): 3278, 3087, 2945, 1648, 1626, 1551, 1446, 1408, 1369, 1327, 1291, 1244, 1104, 1061, 986, 953, 807, 715; HPLC retention time: 4.52 min (Supporting information Figure S 3).

*N-[2-(acetylamino)ethyl]-2-methylacrylamide (6)*: Eluent: AcOEt/EtOH gradient from 90:10 to 80:20. Yield: 86% wt. White solid. <sup>1</sup>H NMR (300 MHz, CDCl<sub>3</sub>) (δ = ppm): 6.70 (bs, 1H), 6.24 (bs, 1H), 5.75 (s, 1H), 5.35 (s, 1H), 3.44 (m, 4H), 1.99 (s, 3H), 1.96 (s, 3H); FT-IR (cm<sup>-1</sup>): 3300, 3090, 2934, 1650, 1616, 1543, 1445, 1369, 1333, 1287, 1237, 1224, 1099, 1045, 998, 146, 919, 851, 643; HPLC retention time: 5.63 min (Supporting information Figure S 4).

### 3.2.3.1.2 Synthesis of *N*-[2-(2,5-dioxo-2,5-dihydro-1*H*-pyrrol-1-yl)ethyl]acetamide (7):

686 mg of maleic anhydride (4.7 mmol, 1.0 eq.) were added to a stirred solution of 480 mg of *N*-acetylethyldiamine (450 μL, 4.7 mmol, 1.0 eq.) in dry DCM (10 mL). The reaction mixture was

---

stirred at room temperature overnight. Then, the solvent was evaporated, 10 mL of acetic acid were added, and the final solution was refluxed for 4 h. After removal of acetic acid under vacuum the obtained solid was purified by flash column chromatography on silica gel (70-230 mesh) using AcOEt/EtOH (95/5) as eluent. Yield: 50% wt. White solid.  $^1\text{H}$  NMR (400 MHz,  $\text{CDCl}_3$ ) ( $\delta$  = ppm): 6.73 (s, 2H), 5.78 (s, 1H), 3.70 (t,  $J$  = 5.2 Hz, 2H), 3.46 (m, 2H), 1.94 (s, 3H); FT-IR ( $\delta$  =  $\text{cm}^{-1}$ ): 3284, 3107, 1693, 1652, 1556, 1449, 1417, 1378, 1366, 1336, 1292, 1172, 1111, 981, 913, 839, 761, 697, 651, 632; HPLC retention time: 5.30 (Supporting information Figure S 5).

### 3.2.3.2 Synthesis of Michael-adducts

#### 3.2.3.2.1 General procedure for the synthesis of Michael-type adducts $\text{MA}_{1-4}/\text{NAC}$ :

Michael-type acceptor **1**, **2**, **3** or **4** (5.0 mmol, 1.0 eq., respectively 580, 650, 785 and 855 mg), 816 mg of *N*-acetyl cysteine (NAC) (5.0 mmol, 1.0 eq.), and 555 mg of TEA (5.5 mmol, 1.1 eq.) were dissolved in 5 mL of degassed anhydrous MeOH under an inert atmosphere. The reaction mixture was stirred for 24 h (the complete consumption of the Michael-type acceptor was monitored by TLC analysis with potassium permanganate staining). Afterwards, Dowex<sup>®</sup> 50WX8 hydrogen-form resin (2 g) was added in order to remove TEA. After the suspension was gently shaken for 30 min, the resin was removed, the filtrate concentrated in a rotary evaporator, and the product obtained finally purified by flash column chromatography on silica gel (230-400 mesh).

*N*-acetyl-*S*-[3-(2-hydroxyethoxy)-3-oxopropyl]cysteine (**MA1-NAC**): Eluent: gradient from pure AcOEt to AcOEt/EtOH-90/10. Yield: 50% wt. Colourless oil.  $^1\text{H}$  NMR (300 MHz, MeOD) ( $\delta$  = ppm): 4.57 (m, 1H), 4.16 (t,  $J$  = 4.8 Hz, 2H), 3.73 (t,  $J$  = 4.8 Hz, 2H), 3.06 (dd,  $J$  = 13.9, 4.6 Hz, 1H), 2.84 (m, 3H), 2.67 (t,  $J$  = 7.0 Hz, 2H), 2.01 (s, 3H); FT-IR ( $\text{cm}^{-1}$ ): 3331, 2933, 1719, 1648, 1541, 1416, 1376, 1345, 1185, 1078, 1039, 888, 836, 589; HPLC retention time: 6.25 (Supporting information Figure S 6).



*N*-acetyl-*S*-[3-(2-hydroxyethoxy)-2-methyl-3-oxopropyl]cysteine (**MA2-NAC**): Eluent: gradient from pure AcOEt to AcOEt/EtOH-90/10. Yield: 60% wt. Colourless oil. <sup>1</sup>H NMR (300 MHz, MeOD) ( $\delta$  = ppm): 4.65 – 4.52 (m, 1H), 4.16 (t,  $J$  = 4.8 Hz, 2H), 3.74 (t,  $J$  = 4.8 Hz, 2H), 3.05 (m, 1H), 2.88 (m, 2H), 2.73 (m, 2H), 2.01 (s, 3H), 1.24 (d,  $J$  = 6.5 Hz, 3H); FT-IR (cm<sup>-1</sup>): 3336, 2937, 1719, 1650, 1540, 1456, 1417, 1376, 1341, 1212, 1169, 1123, 1076, 943, 896, 847, 759; HPLC retention time: 7.35 (Supporting information Figure S 7).

*N*-acetyl-*S*-{3-[2-(acetylamino)ethoxy]-3-oxopropyl}cysteine (**MA3-NAC**): Eluent: gradient from pure AcOEt to AcOEt/EtOH-70/30. Yield: 45% wt. Colourless oil. <sup>1</sup>H NMR (300 MHz, MeOD) ( $\delta$  = ppm): 6.14 (m, 1H), 5.71 (t,  $J$  = 5.4 Hz, 2H), 4.99 (t,  $J$  = 5.3 Hz, 2H), 4.62 (dd,  $J$  = 13.9, 4.7 Hz, 1H), 4.41 (m, 3H), 4.21 (t,  $J$  = 7.0 Hz, 2H), 3.57 (s, 3H), 3.51 (s, 3H); FT-IR (cm<sup>-1</sup>): 3283, 3088, 2933, 1725, 1631, 1542, 1427, 1373, 1345, 1297, 1216, 1184, 1126, 1041, 832; HPLC retention time: 6.58 min (Supporting information Figure S 8).

*N*-acetyl-*S*-{3-[2-(acetylamino)ethoxy]-2-methyl-3-oxopropyl}cysteine (**MA4-NAC**): Eluent: gradient from pure AcOEt to AcOEt/EtOH-70/30. Yield: 48% wt. White solid. <sup>1</sup>H NMR (300 MHz, MeOD) ( $\delta$  = ppm): 4.53 (m, 1H), 4.15 (t,  $J$  = 5.1 Hz, 2H), 3.44 (t,  $J$  = 5.3 Hz, 2H), 3.05 (m, 1H), 2.85 (m, 2H), 2.72 (m, 2H), 2.01 (s, 3H), 1.95 (s, 3H), 1.22 (d,  $J$  = 6.4 Hz, 3H); FT-IR (cm<sup>-1</sup>): 3292, 3087, 2936, 1724, 1649, 1543, 1429, 1374, 1343, 1298, 1210, 1165, 1122, 1041; HPLC retention time: 7.56 min (Supporting information Figure S 9).

### 3.2.3.2.2 Synthesis of *N*-acetyl-*S*-(3-{[2-(acetylamino)ethyl]amino}-3-oxopropyl)cysteine (**MA5-NAC**):

82 mg of NAC (0.5 mmol, 1 eq.) and 78 mg of **5** (0.5 mmol, 1 eq.) were dissolved in 1 mL of degassed aqueous NH<sub>3</sub> and the resulting solution stirred overnight at room temperature. The mixture was acidified with 1M HCl (aq); the sample was freeze-dried and purified by column chromatography on Sephadex® G-10 (eluent: H<sub>2</sub>O/EtOH-50/50, flow 0.9 mL/min). Yield: 28% wt. White solid. <sup>1</sup>H NMR (300 MHz, D<sub>2</sub>O) ( $\delta$  = ppm): 4.44 (dd,  $J$  = 8.0, 4.5 Hz, 1H), 3.34-3.28 (m,

---

4H), 3.06 (dd,  $J = 13.9, 4.5$  Hz, 1H), 2.90 (dd,  $J = 13.9, 8.1$  Hz, 1H), 2.82 (t,  $J = 6.8$  Hz, 2H), 2.53 (t,  $J = 6.8$  Hz, 4H), 2.04 (s, 3H), 1.97 (s, 3H); FT-IR ( $\text{cm}^{-1}$ ): 3277, 3085, 1629, 1543, 1430, 1374, 1263, 1221, 1040, 974, 585; HPLC retention time: 5.26 min (Supporting information Figure S 10).

### 3.2.3.2.3 Synthesis of *N*-acetyl-*S*-(3-[[2-(acetylamino)ethyl]amino]-2-methyl-3-oxopropyl)cysteine (MA6-NAC):

82 mg of NAC (0.5 mmol, 1 eq.) and 85 mg of **6** (0.5 mmol, 1 eq.) were dissolved in 1 mL of degassed aqueous  $\text{NH}_3$  and the resulting solution stirred for 3 days at room temperature.  $\text{NaCNBH}_4$  (0.5 mmol) was added every 24 h to reduce the possibly formed disulfides. The reaction mixture was then acidified with HCl 1M (aq); the sample was freeze dried. The white solid obtained was washed with AcOEt and then purified by column chromatography on Sephadex® G-10 (eluent:  $\text{H}_2\text{O}/\text{EtOH}$ -50/50, flow 0.9 mL/min). Yield: 45% wt. White solid.  $^1\text{H}$  NMR (300 MHz,  $\text{D}_2\text{O}$ ) ( $\delta = \text{ppm}$ ): 4.43 (m, 1H), 3.32 (m, 4H), 3.02 (m, 1H), 2.92 (m, 2H), 2.68 (m, 3H), 2.04 (s, 3H), 1.97 (s, 3H), 1.15 (d,  $J = 6$  Hz, 3H); FT-IR ( $\text{cm}^{-1}$ ): 3124, 3036, 2810, 1718, 1633, 1556, 1387, 1302, 1239, 1119, 1043, 1008, 964; HPLC retention time: 5.72, 5.80 min (Supporting information Figure S 11).

### 3.2.3.2.4 Synthesis of compounds *N*-acetyl-*S*-(1-[2-(acetylamino)ethyl]-2,5-dioxopyrrolidin-3-yl)cysteine (MA7-NAC):

82 mg of NAC (0.5 mmol, 1 eq.) and 91 mg of **7** (0.5 mmol, 1 eq.) were dissolved in 2 mL of degassed anhydrous MeOH under argon atmosphere and stirred overnight at room temperature. The reaction product was purified by column chromatography on Sephadex® G-10 (eluent:  $\text{H}_2\text{O}/\text{EtOH}$ -50/50, flow 0.9 mL/min). Yield: 30% wt. White solid.  $^1\text{H}$  NMR (300 MHz,  $\text{D}_2\text{O}$ ) ( $\delta = \text{ppm}$ ): 4.53 – 4.41 (m, 1H), 4.10 – 3.99 (m, 1H), 3.71-3.60 (m, 2H), 3.49 – 3.41 (m, 1H), 3.39 – 3.19 (m, 3.5H), 3.02 (dd,  $J = 13.7, 8.4$  Hz, 0.5H), 2.72-2.61 (m, 1H), 2.05 (s, 3H), 1.91 (s, 3H); FT-IR ( $\text{cm}^{-1}$ ): 3288, 1775, 1695, 1639, 1543, 1433, 1397, 1328, 1291, 1183, 1108, 1040, 950, 686; HPLC retention time: 5.74 min (Supporting information Figure S 12).

---

### 3.2.4 Determination of thiol pK<sub>a</sub>

The pK<sub>a</sub> of the thiols used as nucleophiles in Michael-type addition (3-MPA and NAC) and in thiol exchange studies (NAC and glutathione (GSH)) have been determined spectrophotometrically by recording the thiolate UV absorbance at 233 nm as a function of pH (ranging from 3.3 to 12.8)<sup>14,24</sup> under the conditions used for the two sets of reactions. Specifically:

*pK<sub>a</sub> under the conditions for Michael-type addition;* pK<sub>a</sub> values of 3-MPA and NAC: 100 mM Tris buffer solutions were prepared, and the pH was adjusted to the desired value by addition of concentrated NaOH (aq) or HCl (aq). Thiol solutions at different pH values were prepared in a mixture of the aforementioned Tris buffer solutions and EtOH (80:20 v/v) to a final concentration of 0.33 mM (NOTE: samples were analyzed at this stage to ensure a precise and reproducible preparation of the solutions). These freshly prepared solutions were incubated at 30 °C for 30 min, and finally scanned in the UV absorbance region from 190 to 250 nm; 233 nm was the wavelength at which the thiolate showed an absorbance peak, while the contribution of the absorbance of the thiol was insignificant. The absorbance readings at 233 nm were plotted as a function of pH and the resultant titration curves were fitted using a sigmoid (Boltzmann) non-linear function, where the pH value at the inflection point corresponded to the pK<sub>a</sub> value of the thiol.

*pK<sub>a</sub> under the conditions for thiol exchange studies;* pK<sub>a</sub> values of NAC and GSH: 50 mM phosphate buffer solutions were prepared from monobasic and dibasic sodium phosphate, and the pH was adjusted to the desired value by addition of concentrated NaOH (aq) or HCl (aq). Thiol solutions at different pH values were prepared in the aforementioned phosphate buffers to a final concentration of 1 mM (NOTE: samples were analyzed at this stage to ensure a precise and reproducible preparation of the solutions). These freshly prepared solutions were incubated at 37 °C for 30 min, and finally scanned in the UV absorbance region from 190 to 250

nm; the  $pK_a$  values of the thiols were determined from the UV absorbance readings at 233 nm as described above.

### 3.2.5 Thiol oxidation study

To determine the extent of thiol oxidation (i.e. disulfide formation) over the course of the Michael-type addition reaction, the change in thiol concentration of different solutions of 3-MPA (with pH 7.9, 8.1, 8.6 and 9.0) and NAC (with pH 7.9, 8.1 and 8.6) was measured via Ellman's test at different time points. Briefly, different thiol solutions (with a final concentration of 1 mM) were prepared in a 80:20 v/v mixture of Tris buffer (100 mM, pH 7.9, 8.1, 8.6 or 9.0) and EtOH. 200  $\mu$ L of each solution was then pipetted into a 96-well plate and left to incubate at 30 °C for 30 min in the microplate reader. Subsequently, the first four reaction solutions of time point 0 (each with a different pH) were quenched by the addition of 100  $\mu$ L of 250 mM HCl (aq). This step was repeated every 40 minutes for 4 hours, after which the Ellman's test was carried out as described in 3.2.2.2.

### 3.2.6 Validation of Ellman's assay

The reactivity of 2-nitro-5-thiobenzoate (NTB<sup>-</sup>), which results from DTNB reduction during Ellman's assay, towards the different Michael-type acceptors used in this study (**1-7**) was determined in order to validate this assay for the determination of Michael-type addition reaction kinetics. Briefly, 25  $\mu$ L of 3-MPA 2 mM (Tris 1 M, pH 7.0) and 250  $\mu$ L DTNB 300  $\mu$ M (Tris 1 M, pH 7.0) were introduced and mixed for 1.5 min in a 96-well plate at 30 °C. The absorbance at 412 nm was recorded (as described in 3.2.2.2), then 25  $\mu$ L of the desired Michael-type acceptor (18 mM for **1** and **3**; 180 mM for **2**, **4**, **5** and **6**; 2 mM for **7** in Tris 1 M, pH 7.0) were added, and the decay in absorbance at this wavelength was monitored at different time points for 20 minutes and compared to the one registered after the addition of 25  $\mu$ L of buffer (Tris 1 M, pH 7.0).

### 3.2.7 Determination of the observed Michael-type addition rate constants

All Michael-type addition reactions between 3-MPA and NAC and various Michael-type acceptors were carried out at 30 °C in a 96-well plate at different pH values, including 7.9, 8.1, 8.6, 9.0 (Tris buffer, 100 mM) and at three different thiol : Michael-type acceptor molar ratios (1:3, 1:6, 1:9 for compounds **1**, **3** and **7**, and 1:30, 1:60, 1:90 for compounds **2**, **4**, **5** and **6**). The reaction kinetics were followed by measuring the unreacted thiol concentration via Ellman's test at different time points. The observed Michael-type addition rate constants,  $k_{obs}$ , were then calculated from Equation 8 and Equation 9 (taking into account the degree of thiol oxidation occurring during the course of the reaction; this was done by separately monitoring the change in thiol concentration under the same reaction conditions as the Michael-type additions and then subtracting the slope of a plot of  $\ln([thiol]/[thiol_0])$  vs  $t$  from the slope of the Michael-type reaction plots found from Equation 8 (see 3.2.5 for a detailed description of the thiol oxidation study).

$$\ln \left( \frac{[thiol][alkene_0]}{[thiol_0][alkene]} \right) = k_{eff}t \quad \text{Equation 8}$$

$$k_{eff} = k_{obs}([thiol_0] - [alkene_0]) \quad \text{Equation 9}$$

As an example for the kinetic assay with 3-MPA acid and 2-hydroxyethyl acrylate at pH 7.9, the following steps were taken: three different acrylate solutions (with a final acrylate concentration of 6, 12 and 18 mM in a 40:60 v/v mixture of ethanol and Tris buffer, 100 mM, pH 7.9) and one thiol solution (2 mM in Tris buffer 100 mM, pH 7.9) were prepared. 100  $\mu$ L of

---

each acrylate solution was then pipetted into 10 individual wells of a 96-well plate. On the same plate, around 300  $\mu\text{L}$  of the thiol solution were pipetted into 15 further wells, and the whole plate was left to incubate at 30  $^{\circ}\text{C}$  for 30 min in the microplate reader. Thereafter, the Michael-type addition reactions were carried out: 100  $\mu\text{L}$  of the thiol solution were added to the first three wells containing 100  $\mu\text{L}$  of a 6, 12 or 18 mM acrylate solution (resulting in a final thiol:acrylate molar ratio of 1:3 in the first well, 1:6 in the second well, and 1:9 in the third well) and the reactants were mixed thoroughly by pipetting. This step was repeated every 5 minutes until all 30 wells contained the thiol/acrylate mixture. Subsequently, the reaction solutions were quenched by adding 100  $\mu\text{L}$  of 250 mM HCl (aq), after which the Ellman's test was carried out using 50  $\mu\text{L}$  of each quenched reaction mixture.

### 3.2.8 Stability of Michael-type acceptors

#### 3.2.8.1 $^1\text{H}$ NMR studies

Compounds **1** and **7** (10 mM) were incubated at 30  $^{\circ}\text{C}$  in Tris buffer 100 mM (in  $\text{D}_2\text{O}$ , the pH was adjusted at pH 7.4 and 7.9 with DCl in  $\text{D}_2\text{O}$ )<sup>25</sup> recording spectra at different time points.

#### 3.2.8.2 Absorbance studies

The hydrolysis of compound **7** was studied spectrophotometrically by monitoring its concentration at different pH values (7.9, 8.1, 8.6 and 9.0; Tris 100 mM/EtOH 80:20 v/v) and initial concentrations (2, 3 and 5 mM). The absorbance readings at 300 nm of the different solutions (150  $\mu\text{L}$  in each well of a 96-well plate) were recorded at 30  $^{\circ}\text{C}$ .

### 3.2.9 Stability of Michael-type adducts

In order to evaluate the stability of the synthesised conjugates in reducing environment and determine if retro Michael reaction, leading to thiol exchange, occurs at physiological pH and temperature, Michael-type adducts **MA<sub>1-5</sub>/NAC** and **MA7-NAC** were dissolved at a

## Effects of Environmental Factors and Reactant Architecture on the Outcome of the Michael-Type Addition Used for Bioconjugation

---

concentration of 1 mM in 50 mM phosphate buffers (pH 7.4 and 7.9, prepared from monobasic and dibasic sodium phosphate) containing 10 mM GSH. All samples were incubated at 37 °C. 400 µL samples were collected periodically and added to 100 µL of 1.0 M hydrochloric acid solution to reduce the pH and quench the retro Michael reactions. Samples were stored at -20 °C until analyzed using RP-HPLC; injections were carried out under the above-defined conditions (See 3.2.2.3) and areas of peaks were integrated to calculate conversion curves.

### 3.3 RESULTS AND DISCUSSION

#### 3.3.1 Thiol titration

It is well known that the  $pK_a$  value of a given compound is strongly dependent upon temperature, solvent and buffer system; hence we determined spectrophotometrically<sup>14,24</sup> the  $pK_a$  value of the thiol/thiolate equilibrium (Figure 55) for 3-MPA and NAC using the same experimental conditions of the studies in which they are involved. The titration curves were obtained by plotting the absorbance values at 233 nm as pH function (Figure 57); at this wavelength the absorbance of the thiolate showed a peak, while the absorbance of the thiol was negligible (Figure 56). Thus, it was possible to assume the thiolate concentration directly proportional to the absorbance values and calculating the  $pK_a$  from the inflection point of the titration curve. The  $pK_a$  found for the GSH agrees with the commonly accepted value,<sup>26</sup> validating the method. The results are summarised in Table 1 where it is possible to notice the great influence of temperature and medium on the  $pK_a$ .

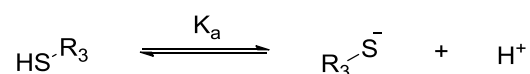


Figure 55: Thiol/thiolate equilibrium

Table 1: Measured  $pK_a$  of the different sulphur containing nucleophiles

| Compound | Temperature | Solvent                           | $pK_a$ |
|----------|-------------|-----------------------------------|--------|
| 3-MPA    | 30 °C       | Tris buffer 100 mM/EtOH 80:20 v/v | 11.3   |
| NAC      | 30 °C       | Tris buffer 100 mM/EtOH 80:20 v/v | 10.7   |
| NAC      | 37 °C       | Phosphate buffer 50 mM            | 9.8    |
| GSH      | 37 °C       | Phosphate buffer 50 mM            | 8.7    |



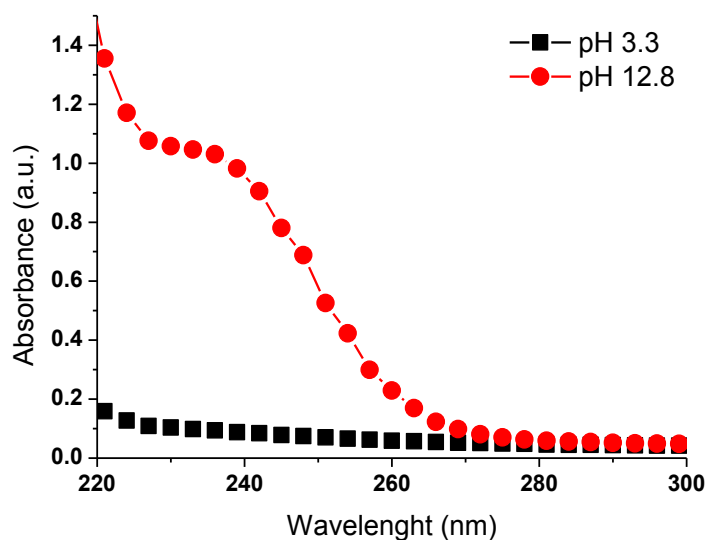


Figure 56: Recorded UV absorbance spectra of thiol (at low pH) and thiolate (at high pH) for 3-MPA in TRIS buffer 100 mM/EtOH 80:20 v/v, at 30°C

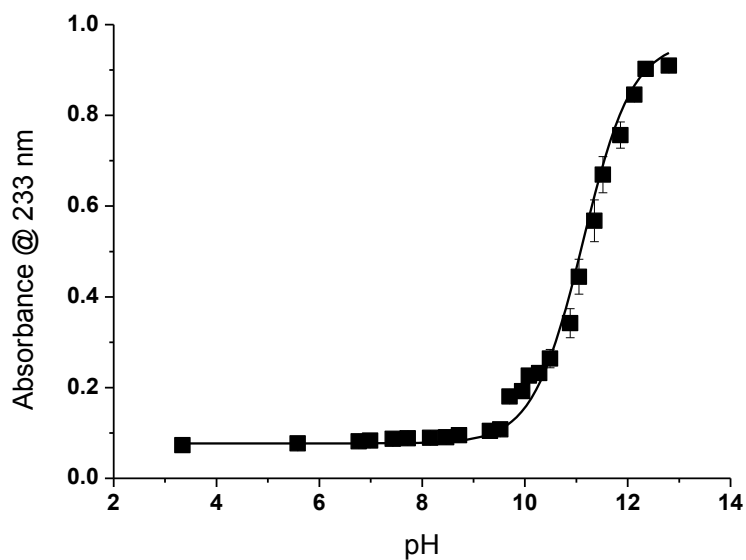


Figure 57: Titration curve for 3-MPA in TRIS 100 mM/EtOH 80:20 v/v, at 30°C

---

### 3.3.2 Kinetic studies

Michael-type addition reaction is a favourable tool for the conjugation of bioactive peptides onto polymeric carriers. The rate constants of Michael-type addition of two different sulphur containing nucleophiles (3-MPA and NAC) having different  $pK_a$  values (See 3.3.1), onto the double bond of various  $\alpha,\beta$ -unsaturated Michael acceptor compounds (the structures of the different Michael acceptors chosen for this study are depicted in Scheme 14), were determined. Various Michael-type acceptors featuring acrylate, methacrylate, acrylamide, methacrylamide and maleimide groups have been selected for this study. Considering that amino-terminated Michael-type acceptors might be required for their conjugation to macromolecules via amide bond formation, some compounds feature a terminal *N*-acetyl group, mimicking the structures (and therefore the kinetics and the hydrolysis properties) of the final Michael-type acceptor conjugates.

The reaction kinetics of thiols towards Michael-type acceptors follow a second order rate law,<sup>7,14,27</sup> meaning that the reaction rate is second order overall and first order with respect to both reactants (See Equation , where Nu = nucleophile and El = electrophile):

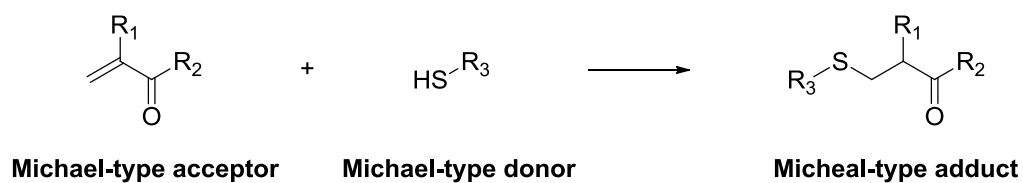
$$v = k_{\text{obs}}[\text{Nu}][\text{El}] \quad \text{Equation 7}$$

The integrated rate law has been previously described in Equation 8 and Equation 9.

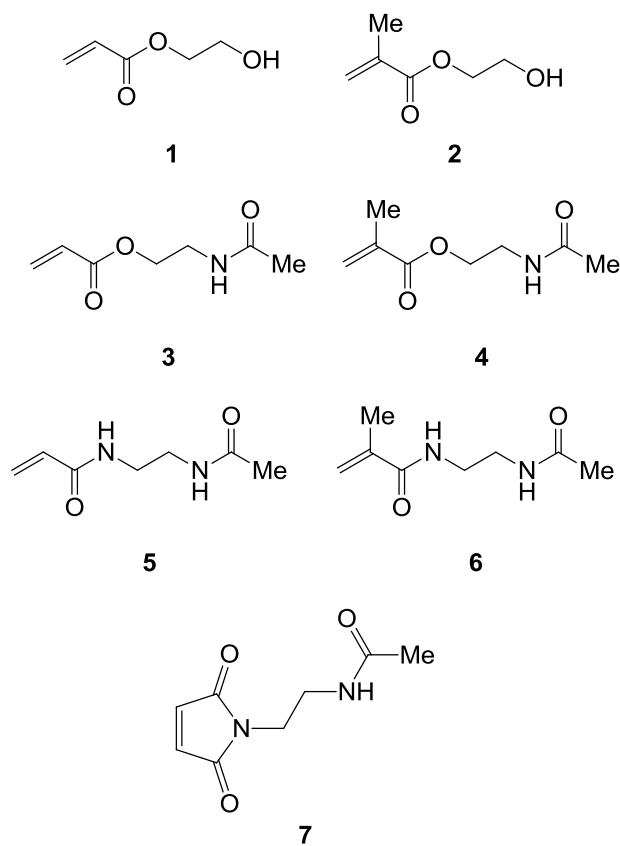
In our experiments, monitoring of the Michael-type reaction at different pH values and thiol : alkene molar ratios was performed by measuring the concentration of the unreacted thiol via Ellman's test at different time points. From the absorbance values measured during the Ellman's test the amount of unreacted thiol (and then of the acceptor as well) in the reaction solutions could be calculated by using the calibration curves previously obtained (Supporting Information Figure S 13 and Figure S 14).

Effects of Environmental Factors and Reactant Architecture on the Outcome of the Michael-Type Addition Used for Bioconjugation

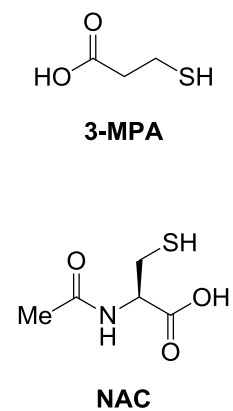
---



**Michael-type acceptors**



**Michael-type donors**



**Scheme 14: General scheme of Michael-type addition and reactants employed for this study**

### 3.3.2.1 Thiol oxidation study

Thiols spontaneously undergo oxidation producing disulfur bonds, thus losing their nucleophilicity; this oxidation is pH and temperature dependant. In our case an overestimation of the reaction rate might occur by not taking into account this side reaction; hence, in order to determine the extent of thiol oxidation occurring over the course of the Michael-type reaction, the change in thiol concentration over time of different thiol solutions (with pH 7.9, 8.1, 8.6 and 9.0) was measured via Ellman's test. The thiol oxidation kinetics is expected to follow a first order rate law. Indeed, a representation of  $\ln([\text{thiol}]/[\text{thiol}]_0)$  vs  $t$  (Figure 58) results in a straight line. From this plot the amount of thiol oxidation occurring in the same time interval as the Michael-type addition reaction can be calculated: for pH 7.9, 8.1, 8.6 and 9.0 the amount of thiol oxidation after 1 h was 5%, 7%, 11% and 21%, respectively for 3-MPA; for pH 7.9, 8.1 and 8.6 the amount of thiol oxidation after 1 h was 9%, 12%, and 14% for NAC. Thiolate oxidation is expectedly more rapid than thiol oxidation; in fact the rate constant is higher at more basic conditions (Table 2); moreover the lower  $pK_a$  of NAC, with respect to 3-MPA, reflects a higher concentration of thiolate at the same pH, this is the reason why it more easily undergoes disulfide bond formation. In order to take into account this side reaction over the course of the Michael-type addition we subtracted the slope of the plot  $\ln([\text{thiol}]/[\text{thiol}]_0)$  vs  $t$  from the slope of the Michael-type addition reactions plots.

Effects of Environmental Factors and Reactant Architecture on the Outcome of the Michael-Type Addition Used for Bioconjugation

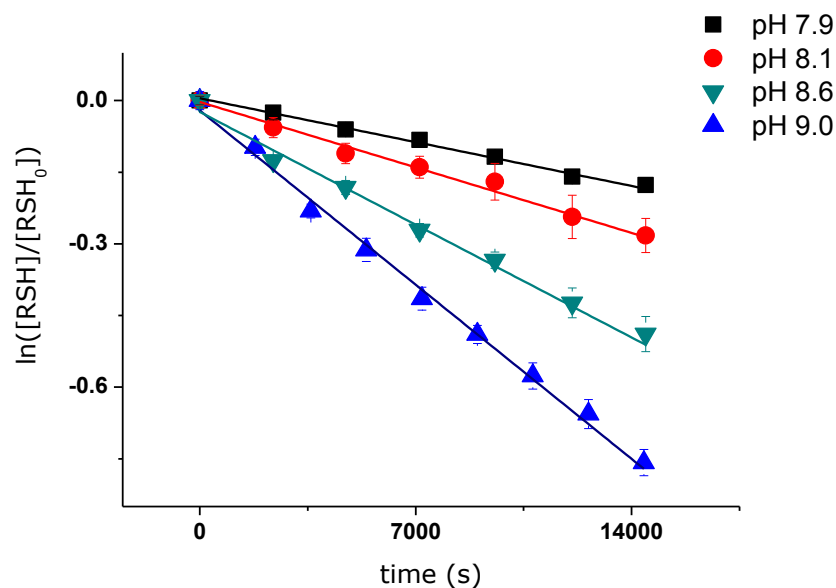


**Figure 58: Oxidation of 3-MPA at different pH values**

Time-dependent oxidation of 3-MPA at different pH values was monitored by measuring the thiol concentration via Ellman's test at different time points (in Tris buffer 100 mM/EtOH 80:20 v/v at 30 °C). The slopes of the fitted lines represent the first order rate constant. Error bars represent standard deviations (n = 3). R<sup>2</sup> values higher than 0.97 were obtained in all cases.

**Table 2: Calculated thiol oxidation rate constants**

| Compound | pH  | Rate constant (10 <sup>-5</sup> *s <sup>-1</sup> ) |
|----------|-----|--|
| 3-MPA    | 7.9 | -1.3 ± 0.1   |
| 3-MPA    | 8.1 | -2.0 ± 0.0   |
| 3-MPA    | 8.6 | -3.4 ± 0.2   |
| 3-MPA    | 9.0 | -5.2 ± 0.2   |
| NAC      | 7.9 | -2.7 ± 0.0   |
| NAC      | 8.1 | -3.4 ± 0.0   |
| NAC      | 8.6 | -3.8 ± 0.0   |

Thiol solutions (with a final concentration of 1 mM) were prepared in a 80:20 v/v mixture of Tris buffer (100 mM) and EtOH and left to incubate at 30 °C.

### 3.3.2.2 Validation of Ellman's assay

In order to check the feasibility of the Ellman's test, used to determine the thiol concentration and then the rate constant of Michael-type reactions, the reactivity of 2-nitro-5-thiobenzoate ( $\text{NTB}^-$ ), which results from DTNB reduction during Ellman's assay, towards the different Michael-type acceptors used in this study (**1-7**) was determined. For this purpose 3-MPA was reacted with DTNB and the absorbance readings at 412 nm were recorded as already reported in 3.2.2.2, subsequently the different Michael-type acceptors **1-7** were added and the decrease in absorbance monitored at different time points (Figure 59: Evaluation of the stability of Michael-type acceptors towards  $\text{NTB}^-$ ) Among the different Michael-type acceptors only **7**, featuring a maleimide moiety, showed reactivity towards  $\text{NTB}^-$ . So the kinetic evaluation of the Michael-type reaction can easily be performed using the Ellman's test for compounds **1-6** but not for compound **7**.

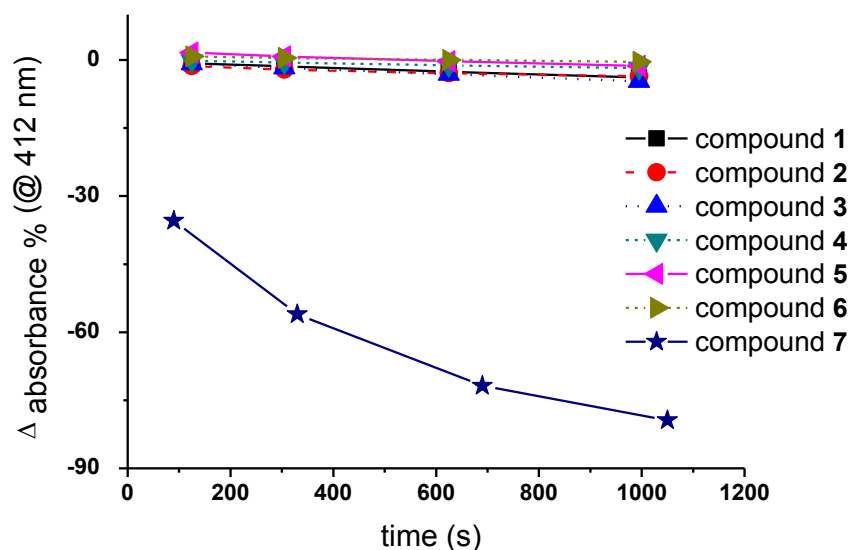


Figure 59: Evaluation of the stability of Michael-type acceptors towards  $\text{NTB}^-$

---

### 3.3.2.3 Determination of the observed Michael-type addition rate constant

We monitored the kinetics of the Michael-type reaction between 3-MPA or NAC and various Michael-type acceptors (1-7) at different pH values and thiol : alkene molar ratios by measuring the concentration of unreacted thiol via Ellman's test at different time points. From the data of unreacted thiol we backcalculated the amount of unreacted alkene, and then plotted  $\ln([\text{thiol}][\text{alkene}]_0/[\text{thiol}]_0[\text{alkene}])$  vs  $t$  (an example of the graph obtained is reported in Figure 60). As expected, the data obtained perfectly fitted the lines demonstrating the second order kinetics. Furthermore the pH dependence underlines that the most reactive nucleophile is the thiolate, hence increasing its concentration (with higher pH values), the addition appeared to be faster.<sup>12</sup>

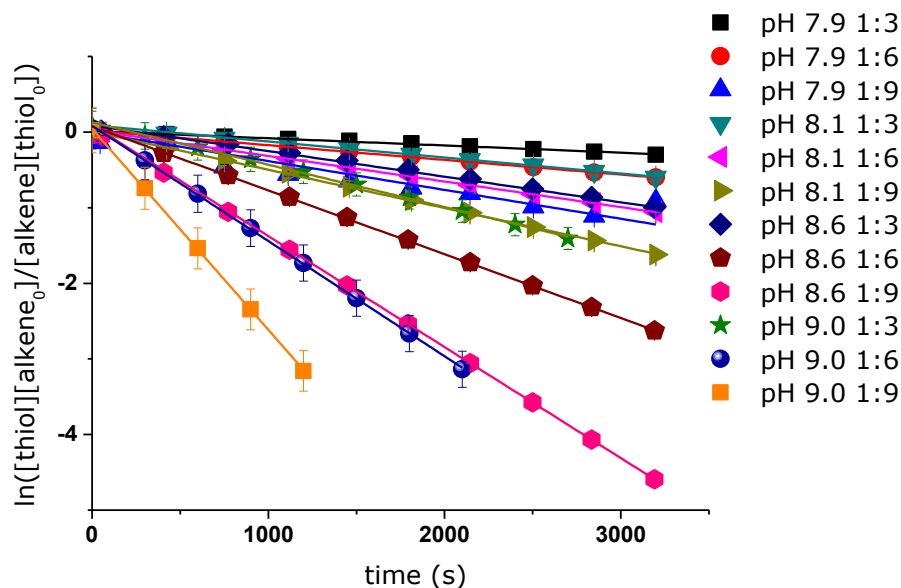


Figure 60 : Reaction between 3-MPA acid and 2-hydroxyethyl acrylate (1)

The reaction was carried out at 30 °C at different pH values and thiol : alkene molar ratios. By measuring the thiol concentration in the reaction wells via Ellman's test at different time points (taking into account the degree of thiol oxidation occurring during the course of the reaction), it was possible to obtain  $k_{\text{eff}}$ . Error bars represent standard deviations ( $n = 3$ ).  $R^2$  values higher than 0.95 were obtained in all cases.

Equation 8 and Equation 9 describe the integrated rate law for a second order kinetics:

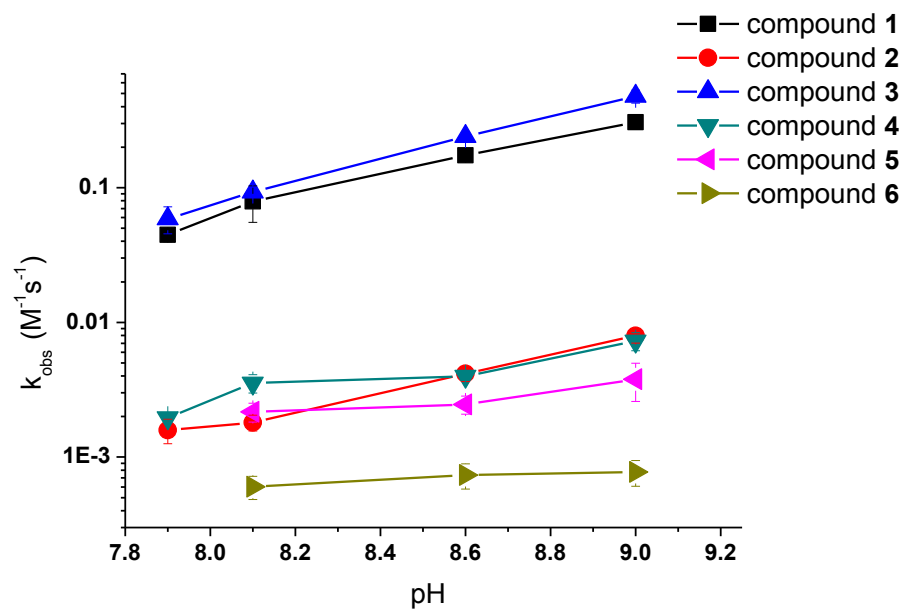
$$\ln \left( \frac{[\text{thiol}][\text{alkene}_0]}{[\text{thiol}_0][\text{alkene}]} \right) = k_{\text{eff}}t \quad \text{Equation 8}$$

$$k_{\text{eff}} = k_{\text{obs}}([\text{thiol}_0] - [\text{alkene}_0]) \quad \text{Equation 9}$$

The slopes obtained from the plot in Figure 60 are  $k_{\text{eff}}$  (expressed in  $\text{s}^{-1}$  - Equation 8) from which is possible to calculate  $k_{\text{obs}}$  (expressed in  $\text{M}^{-1}\text{s}^{-1}$  - Equation 9) that is the real rate constant observed, independent from initial concentration. Figure 61 shows the relationship between  $k_{\text{obs}}$  and pH for compounds **1-6** in the reactions with 3-MPA (with our experimental settings was not possible to measure the rate constant for compound **7**, since the reaction reached quantitative conversion even at the first time point<sup>10</sup>). As expected,<sup>8,12</sup> the reactivity of compounds featuring the same functional groups (acrylates **1** and **3** or methacrylates **2** and **4**) was almost the same. Not surprisingly both steric hindrance and electronic availability of the double bond play an important role in determining the reactivity scale and the combination of both factors in methacrylamide **6** is responsible for its very slow kinetic behaviour in Michael-type reaction. From these results, it is possible to establish a trend of reactivity: acrylates  $\gg$  methacrylates  $>$  acrylamides  $\gg$  methacrylamides. Table 3 summarises the calculated  $k_{\text{obs}}$  of all Michael-type acceptors studied at different pH values, with both 3-MPA and NAC as donors; NAC, in particular, showed to be a better nucleophile. This can be explained by considering that, at the same pH, there is a higher amount of NAC in its deprotonated form respect to the 3-MPA (refer to the  $\text{pK}_a$  reported in Table 1) and thiolates are better nucleophiles than thiols.



## Effects of Environmental Factors and Reactant Architecture on the Outcome of the Michael-Type Addition Used for Bioconjugation

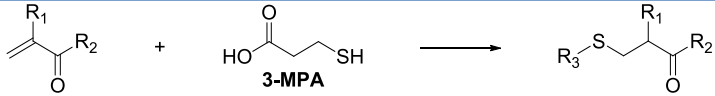


**Figure 61 :  $k_{\text{obs}}$  as a function of pH for Michael-type addition reaction between compounds 1-6 and 3-MPA**

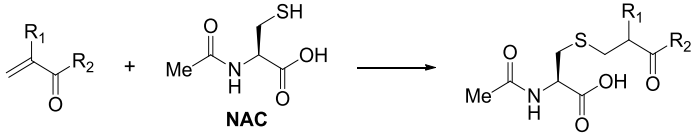
The plot illustrates the pH-dependence of  $k_{\text{obs}}$  of the Michael-type addition between 3-MPA and different Michael acceptors. Each point is the average value obtained from the three different thiol : alkene molar ratio and error bars represent standard deviations.

Effects of Environmental Factors and Reactant Architecture on the Outcome of the Michael-Type Addition Used for Bioconjugation

**Table 3: Experimental rate constants ( $k_{\text{obs}}$ ) for Michael-type addition reaction**

|  |        |   |      |        |   |      |        |   |     |        |   |      |
|--|--------|---|------|--------|---|------|--------|---|-----|--------|---|------|
| k <sub>obs</sub> (10 <sup>3</sup> /M <sup>-1</sup> s <sup>-1</sup> )               |        |   |      |        |   |      |        |   |     |        |   |      |
| Acceptor   | pH 7.9 |   |      | pH 8.1 |   |      | pH 8.6 |   |     | pH 9.0 |   |      |
| 1  | 44.7   | ± | 5.1  | 79.1   | ± | 23.8 | 173.9  | ± | 8.5 | 305.5  | ± | 26.2 |
| 2  | 1.6    | ± | 0.3  | 1.8    | ± | 0.2  | 4.2    | ± | 0.5 | 8.0    | ± | 1.0  |
| 3  | 58.8   | ± | 13.3 | 92.7   | ± | 8.1  | 239.9  | ± | 7.4 | 477.0  | ± | 52.5 |
| 4  | 2.0    | ± | 0.1  | -      | ± | -    | 4.0    | ± | 0.2 | 7.3    | ± | 1.1  |
| 5  | -      |   |      | 2.2    | ± | 0.3  | 2.5    | ± | 0.4 | 3.8    | ± | 1.2  |
| 6  | -      |   |      | 0.6    | ± | 0.1  | 0.7    | ± | 0.2 | 0.8    | ± | 0.2  |
| 7 <sup>a</sup>   | -      |   |      | -      |   |      | -      |   |     | -      |   |      |

|  |        |   |     |        |   |     |        |   |     |  |  |  |
|--|--------|---|-----|--------|---|-----|--------|---|-----|--|--|--|
| k <sub>obs</sub> (10 <sup>3</sup> /M <sup>-1</sup> s <sup>-1</sup> )                 |        |   |     |        |   |     |        |   |     |  |  |  |
| Acceptor   | pH 7.9 |   |     | pH 8.1 |   |     | pH 8.6 |   |     |  |  |  |
| 1  | 263.1  | ± | 0.0 | 357.4  | ± | 0.0 | 1235.0 | ± | 0.0 |  |  |  |
| 2  | 1.7    | ± | 0.0 | 2.1    | ± | 0.1 | 7.5    | ± | 0.0 |  |  |  |
| 3  | 262.6  | ± | 0.0 | 430.3  | ± | 0.0 | 750.0  | ± | 0.0 |  |  |  |
| 4  | 0.9    | ± | 0.0 | 1.8    | ± | 0.0 | 9.6    | ± | 0.0 |  |  |  |
| 5  | 1.7    | ± | 0.0 | 2.2    | ± | 0.0 | 4.2    | ± | 0.0 |  |  |  |
| 6  | 0.4    | ± | 0.0 | 0.8    | ± | 0.0 | 1.0    | ± | 0.0 |  |  |  |

<sup>a</sup> The Michael-type addition between compound **7** and 3-MPA was conducted in a 96-well plate as described in **3.2.7** and then analysed by HPLC; the conversion showed to be quantitative even at the first time point (40 s). Hence we decided not to repeat the experiment with NAC.

Taking into account that thiols, in solution, are in equilibrium between the protonated and deprotonated form (i.e. the thiol and thiolate), the contribution of both these reactive species towards the rate constant of the Michael-type addition reaction should be evaluated finding an absolute rate constant. The rate of this type of reaction is pH dependent and the value of  $k_{obs}$  is given by Equation 10, that was used to determine the individual Michael-type addition rate constants (i.e. the rate constants of the thiol and thiolate,  $k_{thiol}$  and  $k_{thiolate}$ , respectively):

$$k_{obs} = \alpha k_{thiolate} + (1 - \alpha) k_{thiol} = (k_{thiolate} - k_{thiol}) \alpha + k_{thiol} \quad \text{Equation 10}$$

$$\alpha = [\text{thiolate}]/([\text{thiol}] + [\text{thiolate}]) = K_a/([H^+] + K_a) \quad \text{Equation 11}$$

Where  $\alpha$  is the fraction of nucleophile in the ionized form, as defined by Equation 11;  $k$  is the reaction rate constant of thiol and thiolate respectively and  $K_a$  is the dissociation constants for the equilibrium thiol/thiolate of 3-MPA or NAC. This clearly explains and demonstrates that, since,  $pK_a^{3\text{-MPA}} = 11.3$  and  $pK_a^{NAC} = 10.7$  (See 3.3.1), at the same pH:  $k_{obs}^{3\text{-MPA}} < k_{obs}^{NAC}$ . Figure 62 shows the plot of  $k_{obs}$  vs  $\alpha$  for the reaction between **1** and 3-MPA, which is characterised by a linear trend and can be fitted with a line to obtain the reaction rate constant of the protonated 3-MPA or NAC ( $k_{thiol}$ ), from the intercept of the plotted lines; instead, the values of  $k_{thiolate}$  can be calculated from the slope.

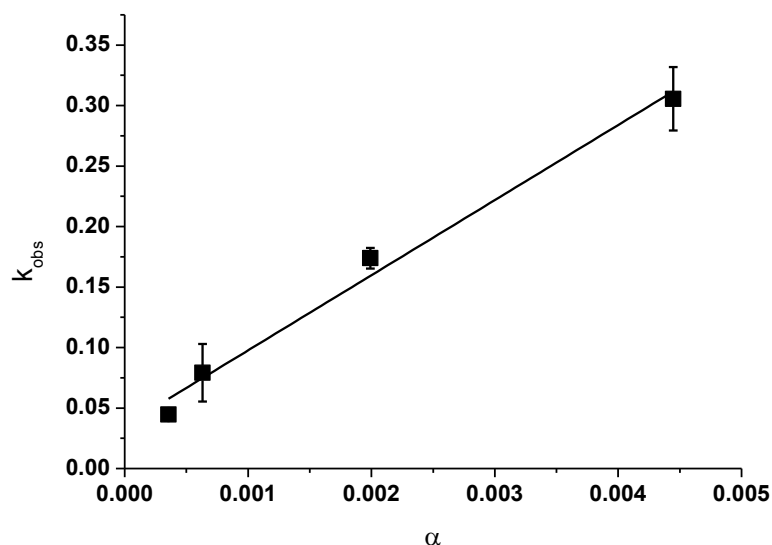


**Figure 62:  $k_{obs}$  vs  $\alpha$  obtained from the results of the Michael-type addition of 3-MPA and 2-hydroxyethyl acrylate 1**

The four points are relative to the different pH. The error bars refer to the error in the calculated  $k_{obs}$ .  $R^2 = 0.98$ .

The use of Equation 10 and Equation 11 in combination with the calculated  $pK_a$  of 3-MPA and NAC (See 3.3.1), allowed us to determine  $k_{thiol}$  and  $k_{thiolate}$ . Table 4 summarises the results of the rate constants determined for the Michael-type acceptors 1-6.

As expected, it was calculated that  $k_{thiolate} \gg k_{thiol}$ , since the thiolate is a much more powerful nucleophile than the thiol. However, these results demonstrate that the contribution of the thiol as a nucleophile cannot be neglected, especially when the  $pH < pK_a$  (that is, when the concentration of thiol in solution is higher than that of the thiolate).

**Table 4: Individual rate constants of thiol and thiolate of the Michael-type addition between 3-MPA or NAC and Michael-type acceptors 1-6**

| Acceptor | Reaction with 3-MPA                          |   | Reaction with NAC                            |   |
|----------|--|---|--|---|
|          | $k_{\text{thiol}} (10^3/\text{M}^*\text{s})$ | $k_{\text{thiolate}} (10^3/\text{M}^*\text{s})$ | $k_{\text{thiol}} (10^3/\text{M}^*\text{s})$ | $k_{\text{thiolate}} (10^3/\text{M}^*\text{s})$ |
| 1        | 35.6 ± 11.3                                  | 62125.1 ± 4572.8                                | 11.4 ± 52.9                                  | 154404.5 ± 10927.3                              |
| 2        | 0.9 ± 0.1                                    | 1587.7 ± 36.7                                   | 0.1 ± 0.4                                    | 927.1 ± 88.9                                    |
| 3        | 28.4 ± 6.1                                   | 101670.3 ± 2462.5                               | 204.7 ± 64.3                                 | 70466.8 ± 13269.0                               |
| 4        | 1.5 ± 0.1                                    | 1297.5 ± 25.3                                   | 0.0 ± 0.4                                    | 1377.6 ± 87.4                                   |
| 5        | 1.8 ± 0.2                                    | 434.3 ± 81.3                                    | 1.2 ± 0.1                                    | 387.3 ± 16.9                                    |
| 6        | 0.6 ± 0.1                                    | 40.7 ± 20.9                                     | 0.5 ± 0.2                                    | 72.6 ± 49.9                                     |

### 3.3.3 Stability of Michael-type acceptors

Maleimide containing compounds (e.g. **7**) might seem the best choice for bioconjugation because of their rapid Michael-type reaction with sulfhydryl group of proteins.

Despite the fast reaction rate, the use of this functionality involves relevant disadvantages; it has already been reported in literature<sup>17</sup> that the resulting succinimide thioether formed during the Michael-type addition of thiols to maleimide, previously accepted as stable, undergoes retro and exchange reactions in the presence of other thiol compounds at physiological pH and temperature. If on the one hand this can be used to design a strategy of controlled release of

bioactive molecules,<sup>18,28</sup> on the other hand it does not allow to have stable adducts. Moreover, the adduct can be easily hydrolysed bringing to the formation of the ring-opened product and, after ring-opening, the resultant thioether is stable, hence the planning of a controlled release becomes even more difficult.

Another issue that needs taking into account is that the reaction with thiol compounds is generally carried out in aqueous media, so the thiol will have to compete with the hydrolytic reaction of the maleimide ring that can lead to a maleamic acid (Figure 63) and to an undesirable heterogeneity.<sup>19,29-32</sup>

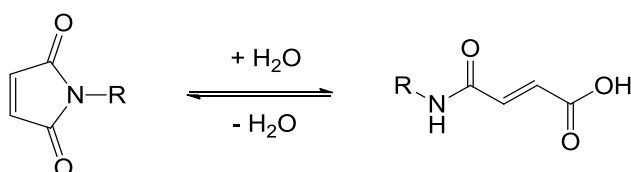


**Figure 63: Hydrolysis of maleimide based compounds**

In order to clearly established the liability of the maleimide-ring, we investigated the stability of compound **7** in front of hydrolysis by using different techniques; after incubation at different pH values, the ring opening was monitored either by <sup>1</sup>H NMR or by measuring the UV absorbance of the maleimide at 300 nm (See 3.2.8.1 and 3.2.8.2). We chose to study the hydrolytic behaviour of this compound in the same environment present in the kinetic studies concerning the Michael-type addition (i.e. Tris buffer 100 mM/EtOH 80:20 v/v at 30 °C).

The spectrum of **7** displays an absorbance peak at 300 nm,<sup>30</sup> wavelength at which the hydrolysed product (obtained after incubation of **7** at pH 12 for 24 h) does not show a relevant absorbance (Figure 64). Recording the absorbance readings at 300 nm of the different

---

solutions, it was possible to measure the amount of hydrolysed product (Figure 65) referring to a previously obtained calibration curve (Supporting information Figure S 15).

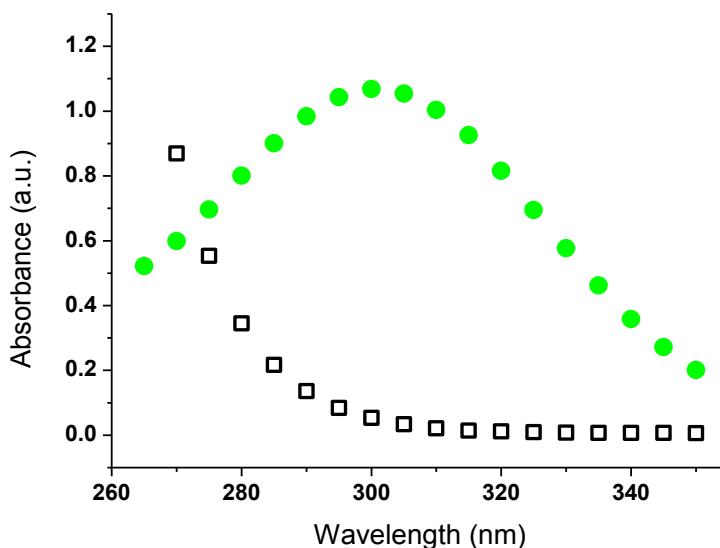


**Figure 64: Spectra of maleimide 7 and hydrolysed form**

The spectrum of compound **7** (1 mM) was recorded in water at 30°C (●), while the squares (□) are relative to the ring opened product obtained after incubation of **7** (1mM) at pH 12 for 24 hours.

To double check the results, we incubated compound **7** (10 mM) in Tris buffer 100 mM (in D<sub>2</sub>O, see 3.2.8.1) recording spectra at different time points. Almost the same results were obtained from the ratio of the integrated peaks of the initial and the hydrolysed compounds (Figure 66).

As expected, we found that the maleimide moiety is highly unstable even at the lowest pH used during our kinetic study. This means that, despite its high reactivity towards nucleophiles in Micheal-type addition reaction, the control of the reaction outcome using maleimide-containing compounds is scarcely predictable and particular care has to be taken to minimize the undesired side-reactions and to preserve the integrity of the Michael-type acceptor structure until the bioconjugation occurs.

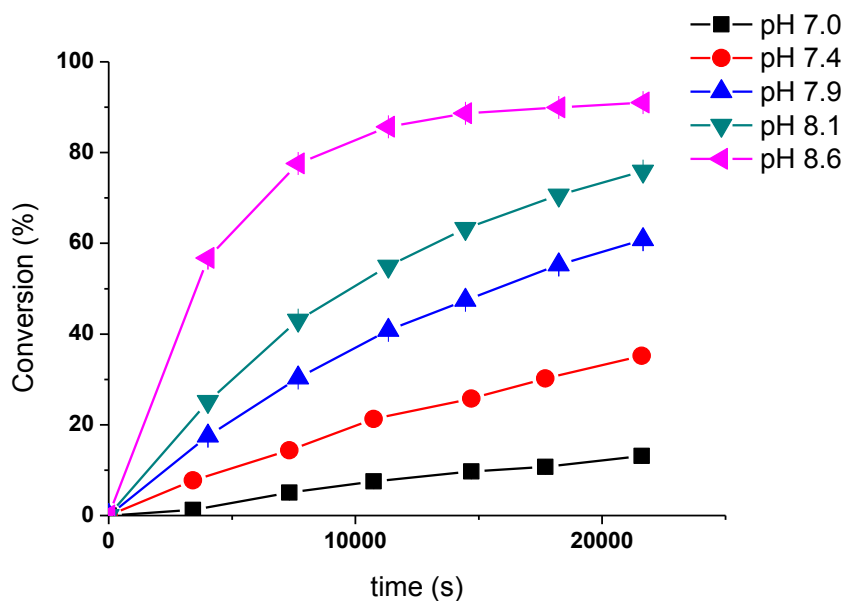


**Figure 65: Spectrophotometrical study of the hydrolysis of compound 7**

The ring opening of compound **7** was monitored by recording the absorbance values at 300 nm at different times after incubation of a 2 mM solution in Tris buffer (100 mM)/EtOH 80:20 v/v at 30 °C.

The hydrolysis rate of different acrylates and methacrylates was already studied<sup>8</sup> demonstrating that the neutral hydrolysis rate is negligible compared to the basic one. Moreover it was established that the hydrolysis does not interfere with the reactivity towards thiols. We confirmed these data by repeating the <sup>1</sup>H NMR experiment to follow the hydrolysis of acrylate **1**; by incubating the Michael acceptor (10 mM) in Tris buffer 100 mM (in D<sub>2</sub>O, see 3.2.8.1) the amount of hydrolysed product was under the detection limit even after 12 hours.



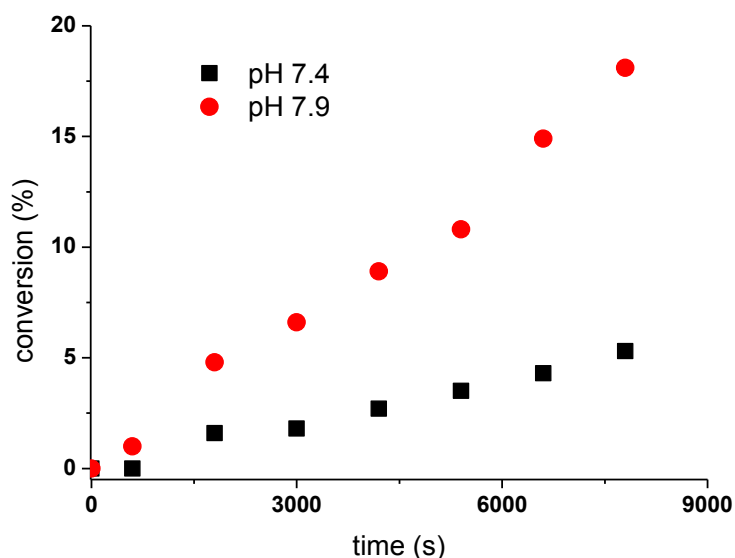


**Figure 66:**  $^1\text{H}$  NMR study of the hydrolysis of compound **7**

Maleimide derivative **7** (10 mM) was incubated at 30°C in Tris buffer 100 mM (in  $\text{D}_2\text{O}$ ) at pH 7.4 and 7.9<sup>25</sup> recording spectra at different time points.

### 3.3.4 Stability of Michael-type adducts

Michael-type adducts with acceptors **1-7** and NAC were synthesised as reported in Scheme 15. We focused our attention on the cysteine containing compounds because they better mimic the structure, and hence the chemical behaviour, of peptide-polymer bioconjugates.

A preliminary screening devoted to select the most suitable experimental conditions (See Supporting information 3.7.1), performed with the acrylate **1** and 3-MPA, highlighted that polar protic solvent, i.e. methanol, and triethyl amine as organic base represent the best combination to reach high level of conversion in short times. These experimental conditions were maintained for the synthesis of the adducts with compounds **1-4** and NAC.

We found that the use of TEA with compound **7** promoted the formation of several by-products, but, fortunately, the reaction did not require any catalyst: hence the reagents were simply mixed in methanol as solvent.

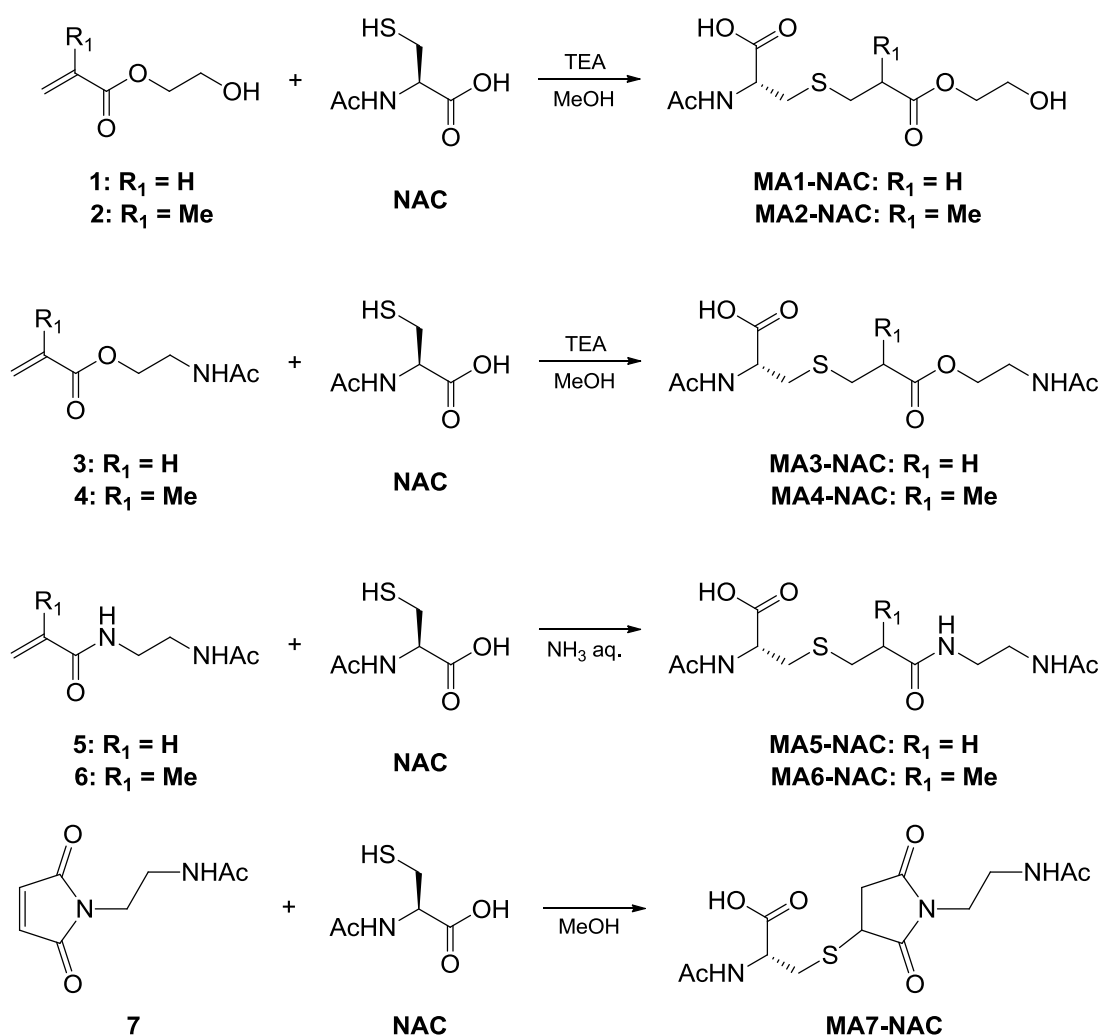
To force the conversion to completeness in a shorter time period, harsher conditions were used with compound **5**. In fact, after 12 h, using the aforementioned method, the Michael-acceptor **5** was still present in the reaction mixture while, with the experimental setting already reported by Adediran,<sup>33</sup> the conversion was quantitative after 12 h and no by-products were revealed by HPLC analysis.

To the best of our knowledge, the stability of Michael-type adducts with acrylates, methacrylates, acrylamides and methacrylamides, in front of hydrolysis or retro Michael reaction has never been studied in detail. Recently maleimide-conjugates, commonly employed due to maleimide specificity to thiols, fast aqueous reaction kinetics, lack of byproducts and the supposed stability of the thioether addition products, were shown to undergo thiol exchange in reducing environment at physiological pH and temperature.<sup>17</sup> Reports about this kind of investigation with all the different Michael-type acceptors used for this study are very limited, despite their large use as homobifunctional cross-linkers, heterobifunctional cross-linkers, as well as in PEGylation reactions and for the conjugation of peptides or other bioactive molecules.<sup>21</sup>

So we focused our attention on the stability of the synthesised thioethers (Scheme 15) at physiological temperature and pH value, i.e. 37 °C and pH 7.4, in a reducing environment using a solution containing GSH 10 mM; an higher pH value was used as well, i.e. 7.9, to have a clearer idea about the reaction mechanism and the factors influencing the adduct-stability. To determine the selectivity of these retro and thiol-exchange or hydrolysis reactions, and to obtain a quantitative measure of the time scales of these reactions, we designed an experimental procedure to follow the evolution of the system using HPLC analysis (See 3.2.9).

Effects of Environmental Factors and Reactant Architecture on the Outcome of the Michael-Type Addition Used for Bioconjugation

Michael-adduct **MA<sub>1-7</sub>/NAC** 1 mM were incubated at 37 °C in a solution of phosphate buffer, at pH 7.4 or 7.9, containing GSH 10 mM. Periodically, small aliquots of the mixture were quenched by adding hydrochloric acid and rates of consumption of the thioethers, under these various conditions, determined by monitoring the changes in peak areas by HPLC experiments. In order to determine the identities of the compounds present in the final fractions HPLC-MS analysis was performed.



Scheme 15 : Synthesis of Michael-type adducts with NAC

The kinetic analysis revealed a pseudo-first order kinetics for the consumption of the Michael adduct, hence the rate constant ( $k$ ) can be measured by plotting the natural logarithm of the thioethers concentration vs time and considering the slopes of the fitted line. The data obtained (Figure 67 and Table 5) perfectly follow the trend observed for the rate constants ( $k_{\text{obs}}$ ) relative to the addition reaction (Figure 61) which means the higher the pH value is the higher the rate constant is, and the reactivity scale observed for the Michael acceptor is the same for the relative Michael adducts. Moreover both the reaction products deriving from the two acrylates (**1** and **3**) and the two methacrylates (**2** and **4**) exhibit basically the same rate constant indicating a negligible influence of the amide moiety at the  $\gamma$ -position to the carbonyl group.

To identify the chemical species present in each solution HPLC-MS analysis was performed; for compound **MA<sub>1,4</sub>-NAC** the peaks relative to the hydrolysed Michael acceptor were found, furthermore no traces of the adducts with GSH indicating a retro-Michael pathway were found. For compound **MA5-NAC** nothing else apart from the starting compound was observed, thus indicates a very high stability of amidic bonds to hydrolysis. While the decomposition of compound **MA7-NAC** is much more complicate and both the reaction of hydrolysis or thiol exchange could be observed, but a detailed study about the different mechanism involved and their kinetics has already been reported,<sup>17</sup> so there was no need to singularly calculate each single rate constant.

## Effects of Environmental Factors and Reactant Architecture on the Outcome of the Michael-Type Addition Used for Bioconjugation

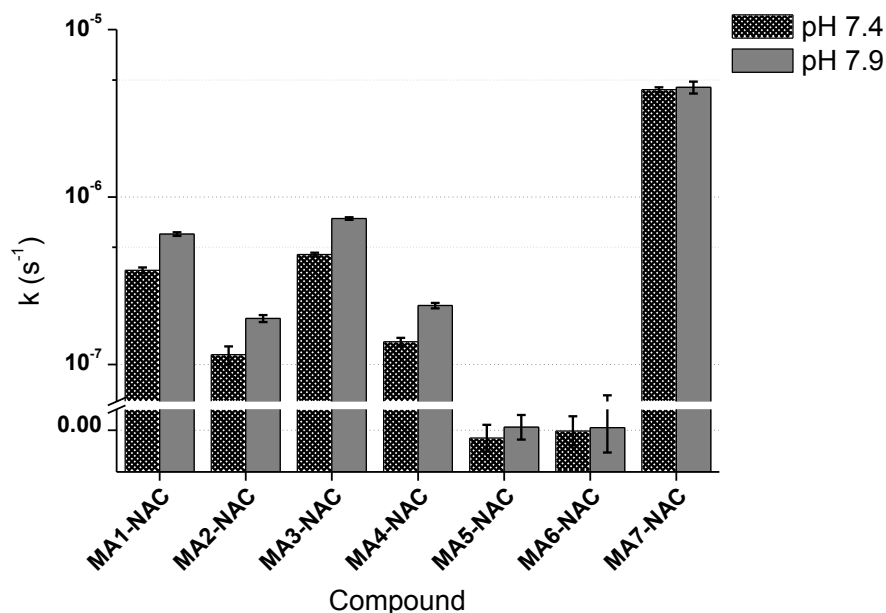


**Figure 67: Measured rate constants for the disappearance of Michael-type adducts in 50 mM phosphate buffer at pH 37°C with 10 times molar excess of GSH**

Michael-type adducts were dissolved at a concentration of 1 mM in 50 mM phosphate buffers (pH 7.4 and 7.9, prepared from sodium phosphate monobasic and sodium phosphate dibasic) containing 10 mM GSH. All samples were incubated at 37 °C for 15 days. Samples were collected periodically and quenched with 1.0 M hydrochloric acid solution. Samples were stored at -20 °C until analyzed; areas of peaks were integrated to calculate conversion curves. The pseudo-first order kinetic rate constant is reported. Error bars refer to the standard error on the slope of the fitted lines.

So we demonstrated that, among the Michael adduct synthesised with the NAC, only the one containing a succinimide moiety is susceptible to undergo retro-Michael reaction, on the contrary the other adduct does not show thiol exchange even after 15 days of incubation and high amount of GSH. Hence what we calculated for compounds **MA<sub>1-6</sub>/NAC** is the kinetics of the hydrolysis of the Michael adducts. The acrylate-deriving compounds showed to be three times faster hydrolysed than the ones deriving from methacrylates, while compounds containing amides are hydrolysed with a rate constant lower than the detection limit of our experimental setting.

Effects of Environmental Factors and Reactant Architecture on the Outcome of the Michael-Type Addition Used for Bioconjugation

This scale of reactivity can be used to rationally choose the best Michael acceptor in terms of reactivity and stability required for each particular application, furthermore the possibility to tune the release of bioactive molecules can be achieved by varying the  $\alpha,\beta$ -unsaturated system.

**Table 5: Pseudo-first order rate constants measured for the disappearance of Michael-type adducts with NAC incubated in reducing environment**

| Compound | pH 7.4                                 |   |     | pH 7.9                                 |   |     |
|----------|--|---|-----|--|---|-----|
|          | $k \cdot 10^7 \text{ (s}^{-1}\text{)}$ |   |     | $k \cdot 10^7 \text{ (s}^{-1}\text{)}$ |   |     |
| MA1-NAC  | 3.6                                    | ± | 0.2 | 6.0                                    | ± | 0.1 |
| MA2-NAC  | 1.1                                    | ± | 0.1 | 1.9                                    | ± | 0.1 |
| MA3-NAC  | 4.5                                    | ± | 0.1 | 7.4                                    | ± | 0.1 |
| MA4-NAC  | 1.4                                    | ± | 0.1 | 2.2                                    | ± | 0.1 |
| MA5-NAC  | -0.2                                   | ± | 0.3 | 0.1                                    | ± | 0.3 |
| MA6-NAC  | -0.2                                   | ± | 0.4 | 0.6                                    | ± | 0.6 |
| MA7-NAC  | 43.7                                   | ± | 1.5 | 45.2                                   | ± | 3.7 |

### 3.4 CONCLUSION

We performed a complete quantitative study in order to investigate all the environmental factors, including the reactants architecture, having an effect on the reaction outcome of Michael-type addition on unsaturated double bonds. This has been possible by using high-throughput experimental settings taking advantages of tools such as 96-well plates, in which spectroscopic experiments were carried out, automated HPLC analysis and parallel reactors.

In particular we focused our attention on thiol containing nucleophiles, in fact Michael-type addition is a helpful tool for bioconjugating polymers with cysteine-containing peptides. For this study we considered seven different Michael acceptors featuring acrylic, methacrylic, acrylamidic, methacrylamidic or maleimidic moieties and thiol compounds with different  $pK_a$  values, i.e. 3-mercaptopropionic acid, *N*-acetyl cysteine and glutathione.

We observed that the addition follow a second order kinetics. Hence we were able to calculate the individual rate constants for both thiol and thiolate, the one relative to the thiol revealed to be at least two orders of magnitude smaller than the one of the deprotonated nucleophile. Thus the reaction rate is strongly influenced by the difference between the pH and  $pK_a$  values, which is to say to the relative concentration of thiolate in the reaction mixture. We also established a trend of reactivity for the different Michael acceptors that is maleimide >> acrylates >> methacrylates > acrylamides >> methacrylamides.

The investigation regarding the stability of the Michael acceptors revealed that maleimide is highly susceptible to hydrolysis also at physiological pH, so even if it immediately reacts with thiolated nucleophiles, precautions are necessary to prevent ring opening before Michael addition occurs. The other reagents showed to be stable enough to be handled without any particular care; moreover the hydrolysis rate is completely negligible in the time frame of the Michael-type addition.

Michael adducts between the seven acceptors and NAC as benchmark peptido-mimetic were synthesised. A long term study (15 days) was carried out on these adducts to determine whether retro-Michael reaction might occur in physiological environment (pH 7.4 and 37 °C) in the presence of an excess of GSH, an antioxidant widely present extra- and intra-cellularly. The latter demonstrated that only succinimide-containing undergo thiol exchange, while for the other compounds only hydrolysis was observed and the kinetics of this reaction was measured allowing a perfect knowledge of the stability of the adducts and allowing indeed the planning of a defined strategy for controlled released of bioactive molecules or to ensure the bioconjugate stability.



### 3.5 ACKNOWLEDGEMENTS

*This project has been carried out in the laboratory of Professor Nicola Tirelli (University of Manchester) and I would really like to express my deepest gratitude to him.*

*I also want to thank all the people I had the pleasure of working with in Manchester, specially Doctor Enrique Lallana-Ozores and Jennifer Wedgwood for assisting me in this project, and Roberto Donno who designed the reactor used in the study about the stability of Michael adducts.*

*But first of all my appreciation is for Professor Francesco Sannicolò who gave me the opportunity of carrying out part of my PhD abroad, having a great scientific and personal experience.*

### 3.6 REFERENCES

- 1 Bergmann, E. D., Ginsburg, D. & Pappo, R. The Michael reaction. *Org. React. (N. Y.)* **10**, 179-563 (1959).
- 2 Kurti, L., Czako, B. & Editors. Strategic Applications of Named Reactions in Organic Synthesis. (Academic Press, 2005).
- 3 Brian, D. M., Kalpana, V., Kevin, M. M. & Timothy, E. L. Michael addition reactions in macromolecular design for emerging technologies. *Prog Polym Sci* **31**, 487-531, doi:10.1016/j.progpolymsci.2006.03.001 (2006).
- 4 Angelo, J. d., Cave, C., Desmaele, D. & Dumas, F. The asymmetric Michael addition reactions using chiral imines: Application to the synthesis of compounds of biological interest. *Trends Org. Chem.* **4**, 555-616 (1993).
- 5 Hoz, S. Is the transition state indeed intermediate between reactants and products? The Michael addition reaction as a case study. *Accounts of Chemical Research* **26**, 69-74, doi:10.1021/ar00026a006 (1993).
- 6 Schultz, T. W., Yarbrough, J. W., Hunter, R. S. & Aptula, A. O. Verification of the Structural Alerts for Michael Acceptors. *Chemical Research in Toxicology* **20**, 1359-1363, doi:10.1021/tx700212u (2007).
- 7 Schwöbel, J. A. H. *et al.* Prediction of Michael-Type Acceptor Reactivity toward Glutathione. *Chemical Research in Toxicology* **23**, 1576-1585, doi:10.1021/tx100172x (2010).
- 8 Freidig, A. P., Verhaar, H. J. M. & Hermens, J. L. M. Quantitative structure-property relationships for the chemical reactivity of acrylates and methacrylates. *Environmental Toxicology and Chemistry* **18**, 1133-1139, doi:10.1002/etc.5620180609 (1999).
- 9 Liu, S. & Hanzlik, R. P. Structure-activity relationships for inhibition of papain by peptide Michael acceptors. *Journal of Medicinal Chemistry* **35**, 1067-1075, doi:10.1021/jm00084a012 (1992).
- 10 Schelté, P., Boeckler, C., Frisch, B. & Schuber, F. Differential Reactivity of Maleimide and Bromoacetyl Functions with Thiols: Application to the Preparation of Liposomal Diepitope Constructs. *Bioconjugate Chemistry* **11**, 118-123, doi:10.1021/bc990122k (2000).

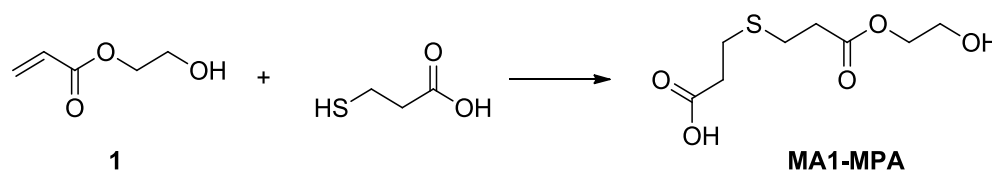
- 11 Falborg, L. & Jorgensen, K. A. Asymmetric titanium-catalysed Michael addition of O-benzylhydroxylamine to  $\alpha,\beta$ -unsaturated carbonyl compounds: synthesis of  $\beta$ -amino acid precursors. *Journal of the Chemical Society, Perkin Transactions 1*, 2823-2826 (1996).
- 12 Friedman, M., Cavins, J. F. & Wall, J. S. Relative Nucleophilic Reactivities of Amino Groups and Mercaptide Ions in Addition Reactions with  $\alpha,\beta$ -Unsaturated Compounds<sup>1,2</sup>. *Journal of the American Chemical Society* **87**, 3672-3682, doi:10.1021/ja01094a025 (1965).
- 13 Rizzi, S. C. & Hubbell, J. A. Recombinant protein-co-PEG networks as cell-adhesive and proteolytically degradable hydrogel matrixes. Part I: Development and physicochemical characteristics. *Biomacromolecules* **6**, 1226-1238, doi:10.1021/bm049614c (2005).
- 14 Lutolf, M. P., Tirelli, N., Cerritelli, S., Cavalli, L. & Hubbell, J. A. Systematic Modulation of Michael-Type Reactivity of Thiols through the Use of Charged Amino Acids. *Bioconjugate Chemistry* **12**, 1051-1056, doi:10.1021/bc015519e (2001).
- 15 Mečiarová, M., Cigáň, M., Toma, Š. & Gáplovský, A. Kinetic Study of Michael Addition Catalyzed by N-Methylimidazole in Ionic Liquids: Residual N-Methylimidazole in Ionic Liquids as a Strong Base. *European Journal of Organic Chemistry* **2008**, 4408-4411, doi:10.1002/ejoc.200800621 (2008).
- 16 Ploemen, J. H., Van Schanke, A., Van Ommen, B. & Van Bladeren, P. J. Reversible conjugation of ethacrynic acid with glutathione and human glutathione S-transferase P1-1. *Cancer Res* **54**, 915-919 (1994).
- 17 Baldwin, A. D. & Kiick, K. L. Tunable degradation of maleimide-thiol adducts in reducing environments. *Bioconjug Chem* **22**, 1946-1953, doi:10.1021/bc200148v (2011).
- 18 Alley, S. C. *et al.* Contribution of linker stability to the activities of anticancer immunoconjugates. *Bioconjug Chem* **19**, 759-765, doi:10.1021/bc7004329 (2008).
- 19 Shen, B. Q. *et al.* Conjugation site modulates the in vivo stability and therapeutic activity of antibody-drug conjugates. *Nat Biotechnol* **30**, 184-189, doi:10.1038/nbt.2108
- 20 Heggli, M., Tirelli, N., Zisch, A. & Hubbell, J. A. Michael-Type Addition as a Tool for Surface Functionalization. *Bioconjugate Chemistry* **14**, 967-973, doi:10.1021/bc0340621 (2003).
- 21 Elbert, D. L., Pratt, A. B., Lutolf, M. P., Halstenberg, S. & Hubbell, J. A. Protein delivery from materials formed by self-selective conjugate addition reactions. *J. Controlled*

- Release* **76**, 11-25, doi:10.1016/s0168-3659(01)00398-4 (2001).
- 22 Ouasti, S., Kingham, P. J., Terenghi, G. & Tirelli, N. The CD44/integrins interplay and the significance of receptor binding and re-presentation in the uptake of RGD-functionalized hyaluronic acid. *Biomaterials* **33**, 1120-1134, doi:10.1016/j.biomaterials.2011.10.009 (2012).
- 23 Wang, X., Messman, J., Mays, J. W. & Baskaran, D. Polypeptide Grafted Hyaluronan: Synthesis and Characterization. *Biomacromolecules* **11**, 2313-2320, doi:10.1021/bm1004146 (2010).
- 24 De, D. R. H., Broekhuysen, J., Bechet, J. & Mortier, A. Etude spectrophotometrique de la dissociation de la fonction sulfhydryle et structure moleculaire de la cysteine. *Biochim Biophys Acta* **19**, 45-52 (1956).
- 25 Covington, A. K., Paabo, M., Robinson, R. A. & Bates, R. G. Use of the glass electrode in deuterium oxide and the relation between the standardized pD (paD) scale and the operational pH in heavy water. *Anal. Chem.* **40**, 700-706, doi:10.1021/ac60260a013 (1968).
- 26 DeCollo, T. V. & Lees, W. J. Effects of Aromatic Thiols on Thiol-Disulfide Interchange Reactions That Occur during Protein Folding. *J. Org. Chem.* **66**, 4244-4249, doi:10.1021/jo015600a (2001).
- 27 Mather, B. D., Viswanathan, K., Miller, K. M. & Long, T. E. Michael addition reactions in macromolecular design for emerging technologies. *Progress in Polymer Science* **31**, 487-531, doi:10.1016/j.progpolymsci.2006.03.001 (2006).
- 28 Lin, D., Saleh, S. & Liebler, D. C. Reversibility of Covalent Electrophile-Protein Adducts and Chemical Toxicity. *Chem. Res. Toxicol.* **21**, 2361-2369, doi:10.1021/tx800248x (2008).
- 29 Machida, M., Machida, M. I. & Kanaoka, Y. Fluorescent thiol reagents. Part XIV. Hydrolysis of N-substituted maleimides: stability of fluorescence thiol reagents in aqueous media. *Chem. Pharm. Bull.* **25**, 2739-2743, doi:10.1248/cpb.25.2739 (1977).
- 30 Matsui, S. & Aida, H. Hydrolysis of some N-alkylmaleimides. *J. Chem. Soc., Perkin Trans. 2*, 1277-1280 (1978).
- 31 Kalia, J. & Raines, R. T. Catalysis of imido group hydrolysis in a maleimide conjugate. *Bioorganic & Medicinal Chemistry Letters* **17**, 6286-6289, doi:10.1016/j.bmcl.2007.09.002 (2007).
-

- 32 Kawamura, M. & Higashi, M. Induced Circular Dichroism and Magnetic Circular Dichroism Spectra of Maleimide and Related Molecules. *Helvetica Chimica Acta* **86**, 2342-2348, doi:10.1002/hlca.200390188 (2003).
- 33 Adediran, S. A., Kumar, I., Nagarajan, R., Sauvage, E. & Pratt, R. F. Kinetics of Reactions of the Actinomadura R39 dd-Peptidase with Specific Substrates. *Biochemistry* **50**, 376-387, doi:10.1021/bi101760p (2010).

## 3.7 SUPPORTING INFORMATION

### 3.7.1 SCREENING DIFFERENT CONDITIONS FOR MICHAEL-TYPE REACTION BETWEEN 3-MERCAPTOPROPIONIC (3-MPA) ACID AND 2-HYDROXYETHYL ACRYLATE (1)



**Scheme S 2: Michael-type reaction between 3-MPA and compound 1**

The reaction between 3-MPA acid and 2-hydroxyethyl acrylate (**1**) (Scheme S 2) was performed under different experimental conditions in order to determine which one was leading to the highest conversion in the shortest time. Table S 1 summarises the results.

Effects of Environmental Factors and Reactant Architecture on the Outcome of the Michael-Type Addition Used for Bioconjugation

**Table S 1: Different experimental condition tested for the Michael-type reaction between 3-MPA and compound 1**

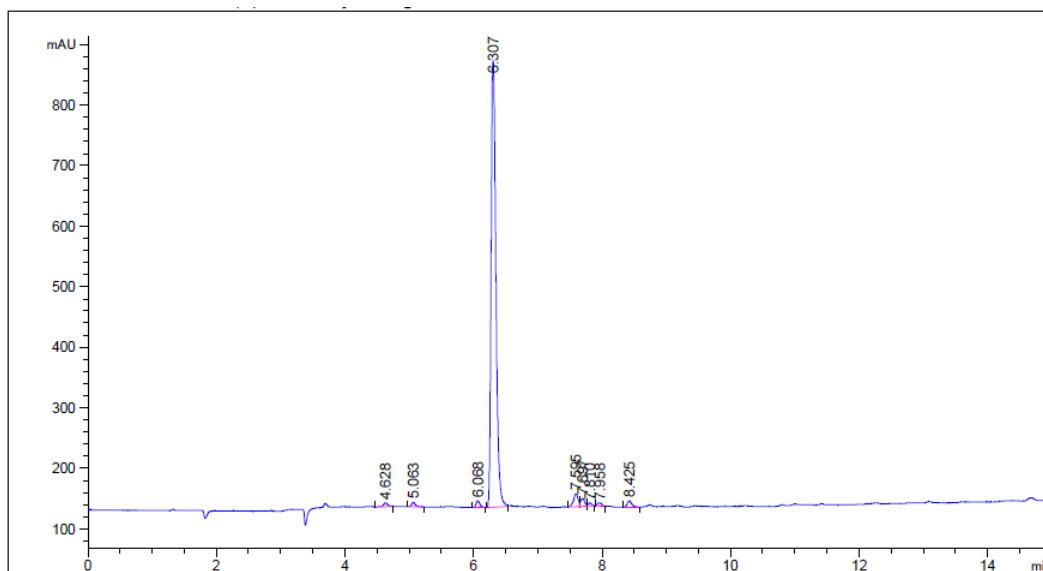
| Entry | Substrate | Solvent               | Base/Catalyst                  | Base or catalyst (mol/mol) | Time | Conversion        |
|-------|-----------|-----------------------|--------------------------------|----------------------------|------|-------------------|
| 1     | 1         | MeOH                  | K <sub>2</sub> CO <sub>3</sub> | 60%                        | 12 h | <50% <sup>a</sup> |
| 2     | 1         | MeOH                  | K <sub>2</sub> CO <sub>3</sub> | 60%                        | 48 h | 87% <sup>b</sup>  |
| 3     | 1         | MeOH                  | phosphine resin                | 5%                         | 12 h | <50% <sup>a</sup> |
| 4     | 1         | MeOH                  | phosphine resin                | 5%                         | 48 h | 76% <sup>b</sup>  |
| 5     | 1         | DCM                   | phosphine resin                | 5%                         | 12 h | <50% <sup>a</sup> |
| 6     | 1         | DCM                   | phosphine resin                | 5%                         | 48 h | 3% <sup>b</sup>   |
| 7     | 1         | MeOH                  | TEA                            | 110%                       | 12 h | 89% <sup>b</sup>  |
| 8     | 1         | MeOH                  | TEA                            | 110%                       | 48 h | 89% <sup>b</sup>  |
| 9     | 1         | DCM                   | TEA                            | 110%                       | 12 h | <50% <sup>a</sup> |
| 10    | 1         | DCM                   | TEA                            | 110%                       | 48 h | 94% <sup>b</sup>  |
| 11    | 1         | H <sub>2</sub> O/EtOH | Tris (pH 8.1)                  | -                          | 12 h | 85% <sup>b</sup>  |

a evaluated by TLC

b evaluated by <sup>1</sup>H NMR

### 3.7.2 HPLC ANALYSIS OF THE SYNTHESISED COMPOUNDS

Figure S 1: HPLC analysis of 2-(acetylamino)ethyl acrylate (3)



=====  
Area Percent Report  
=====

Sorted By : Signal  
Multiplier : 1.0000  
Dilution : 1.0000  
Use Multiplier & Dilution Factor with ISTDs

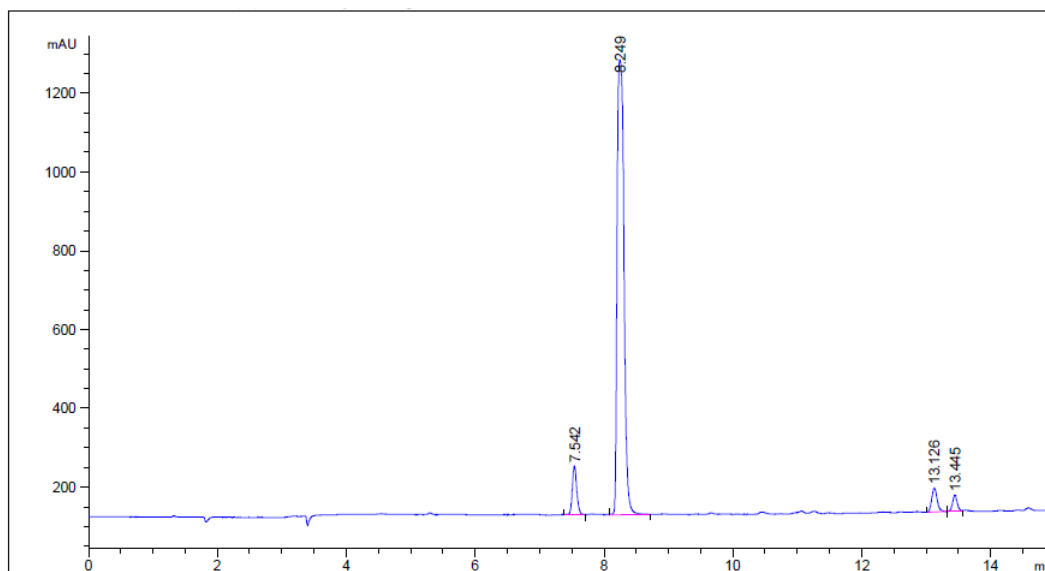
Signal 1: ADC1 A, ADC1 CHANNEL A

| Peak # | RetTime [min] | Type | Width [min] | Area [mAU*s] | Height [mAU] | Area %  |
|--------|---------------|------|-------------|--------------|--------------|---------|
| 1      | 4.628         | BV   | 0.0598      | 29.99839     | 6.26947      | 0.7167  |
| 2      | 5.063         | BB   | 0.0551      | 31.97249     | 7.29974      | 0.7639  |
| 3      | 6.068         | VB   | 0.0520      | 45.66802     | 10.98252     | 1.0911  |
| 4      | 6.307         | BV   | 0.0818      | 3818.68701   | 738.73877    | 91.2363 |
| 5      | 7.595         | BV   | 0.0645      | 105.23103    | 21.33791     | 2.5142  |
| 6      | 7.697         | VV   | 0.0535      | 57.74872     | 12.96364     | 1.3797  |



# Effects of Environmental Factors and Reactant Architecture on the Outcome of the Michael-Type Addition Used for Bioconjugation

Figure S 2: HPLC analysis of 2-(acetylamino)ethyl 2-methylacrylate (4)



=====  
Area Percent Report  
=====

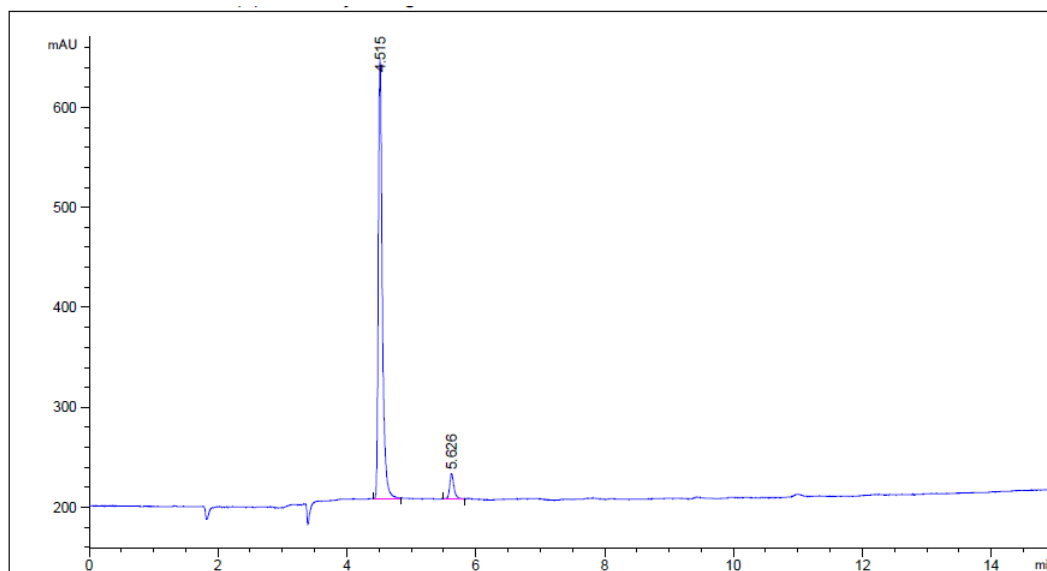
Sorted By : Signal  
Multiplier : 1.0000  
Dilution : 1.0000  
Use Multiplier & Dilution Factor with ISTDs

Signal 1: ADC1 A, ADC1 CHANNEL A

| Peak # | RetTime [min] | Type | Width [min] | Area [mAU*s] | Height [mAU] | Area %  |
|--------|---------------|------|-------------|--------------|--------------|---------|
| 1      | 7.542         | BB   | 0.0734      | 592.67169    | 123.70874    | 6.1470  |
| 2      | 8.249         | VV   | 0.1186      | 8471.98633   | 1154.65320   | 87.8686 |
| 3      | 13.126        | BB   | 0.0868      | 358.98834    | 60.86364     | 3.7233  |
| 4      | 13.445        | BV   | 0.0762      | 218.00792    | 42.22522     | 2.2611  |

# Effects of Environmental Factors and Reactant Architecture on the Outcome of the Michael-Type Addition Used for Bioconjugation

Figure S 3: HPLC analysis of *N*-[2-(acetylamino)ethyl]acrylamide (5)



=====  
Area Percent Report  
=====

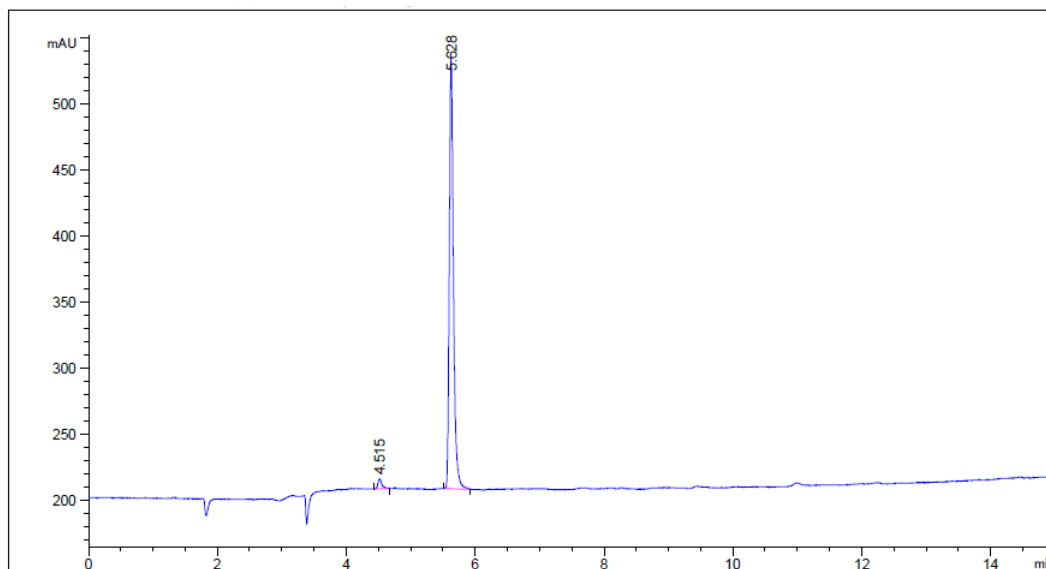
Sorted By : Signal  
Multiplier : 1.0000  
Dilution : 1.0000  
Use Multiplier & Dilution Factor with ISTDs

Signal 1: ADC1 A, ADC1 CHANNEL A

| Peak # | RetTime [min] | Type | Width [min] | Area [mAU*s] | Height [mAU] | Area %  |
|--------|---------------|------|-------------|--------------|--------------|---------|
| 1      | 4.515         | BV   | 0.0645      | 1903.10229   | 439.70447    | 94.2517 |
| 2      | 5.626         | BV   | 0.0603      | 116.06797    | 25.40605     | 5.7483  |

# Effects of Environmental Factors and Reactant Architecture on the Outcome of the Michael-Type Addition Used for Bioconjugation

Figure S 4: HPLC analysis of *N*-[2-(acetylamino)ethyl]-2-methylacrylamide (6)



=====  
Area Percent Report  
=====

Sorted By : Signal  
Multiplier : 1.0000  
Dilution : 1.0000  
Use Multiplier & Dilution Factor with ISTDs

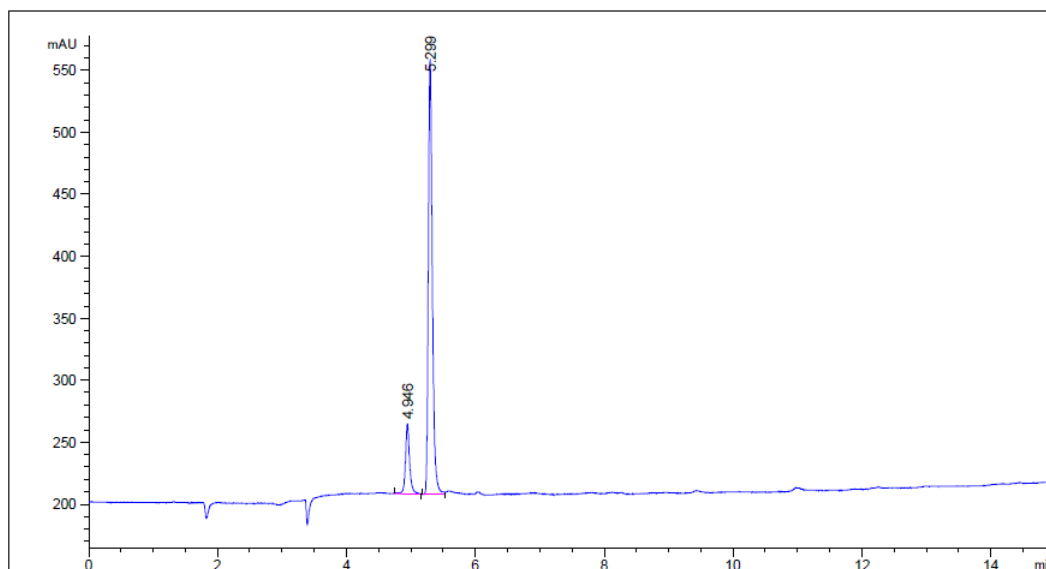
Signal 1: ADC1 A, ADC1 CHANNEL A

| Peak # | RetTime [min] | Type | Width [min] | Area [mAU*s] | Height [mAU] | Area %  |
|--------|---------------|------|-------------|--------------|--------------|---------|
| 1      | 4.515         | BB   | 0.0521      | 32.92281     | 7.59292      | 2.2197  |
| 2      | 5.628         | BB   | 0.0674      | 1450.29382   | 325.88782    | 97.7803 |

Effects of Environmental Factors and Reactant Architecture on the Outcome of the Michael-Type Addition Used for Bioconjugation

---

Figure S 5: HPLC analysis of *N*-[2-(2,5-dioxo-2,5-dihydro-1H-pyrrol-1-yl)ethyl]acetamide (7)



=====  
Area Percent Report  
=====

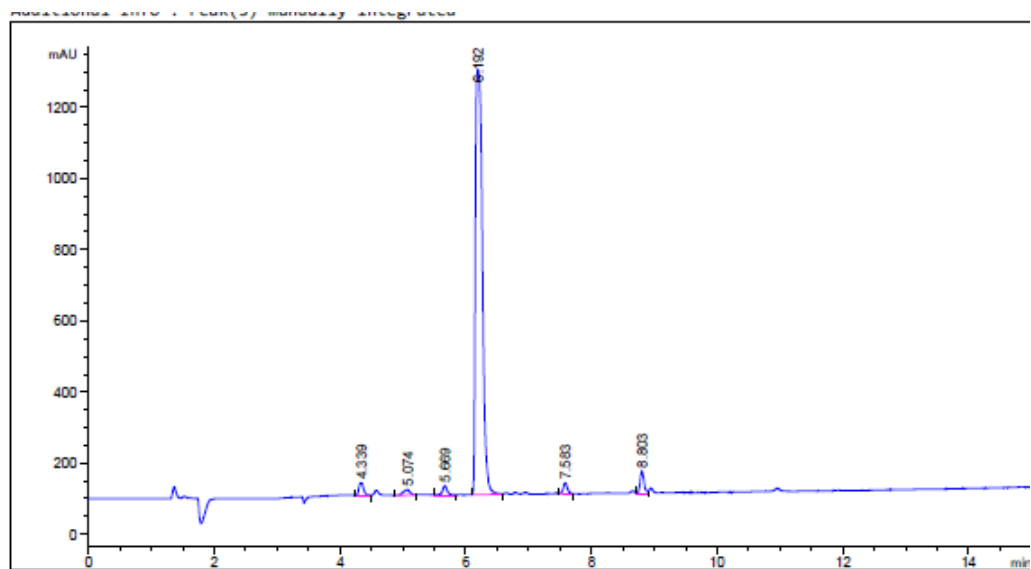
Sorted By : Signal  
Multiplier : 1.0000  
Dilution : 1.0000  
Use Multiplier & Dilution Factor with ISTDs

Signal 1: ADC1 A, ADC1 CHANNEL A

| Peak # | RetTime [min] | Type | Width [min] | Area [mAU*s] | Height [mAU] | Area %  |
|--------|---------------|------|-------------|--------------|--------------|---------|
| 1      | 4.946         | W    | 0.0664      | 255.93987    | 56.98703     | 14.4808 |
| 2      | 5.299         | BV   | 0.0657      | 1511.50391   | 351.11429    | 85.5192 |

# Effects of Environmental Factors and Reactant Architecture on the Outcome of the Michael-Type Addition Used for Bioconjugation

Figure S 6: HPLC analysis of *N*-acetyl-S-[3-(2-hydroxyethoxy)-3-oxopropyl]cysteine (MA1-NAC)



=====  
Area Percent Report  
=====

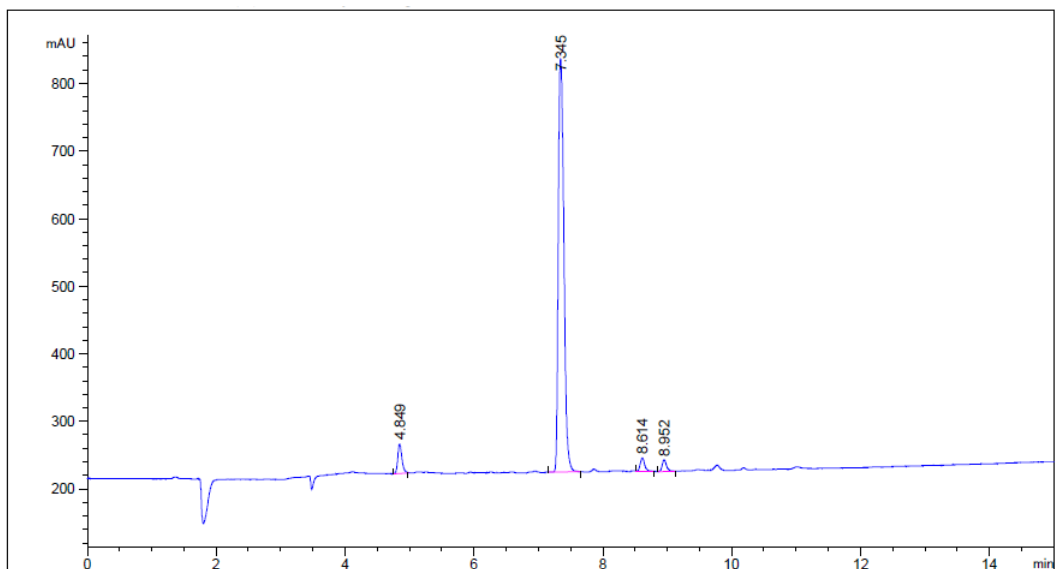
Sorted By : Signal  
Multiplier : 1.0000  
Dilution : 1.0000  
Use Multiplier & Dilution Factor with ISTDs

Signal 1: ADC1 A, ADC1 CHANNEL A

| Peak # | RetTime [min] | Type | Width [min] | Area [mAU*s] | Height [mAU] | Area %  |
|--------|---------------|------|-------------|--------------|--------------|---------|
| 1      | 4.339         | BB   | 0.0780      | 182.65822    | 34.36213     | 1.8165  |
| 2      | 5.074         | BV   | 0.0875      | 110.85276    | 16.27111     | 1.1024  |
| 3      | 5.669         | VB   | 0.0666      | 125.16327    | 25.57277     | 1.2448  |
| 4      | 6.192         | BV   | 0.1046      | 9226.77930   | 1194.89514   | 91.7609 |
| 5      | 7.583         | VV   | 0.0649      | 146.16988    | 31.06505     | 1.4537  |
| 6      | 8.803         | VV   | 0.0630      | 263.61261    | 62.14681     | 2.6216  |

Effects of Environmental Factors and Reactant Architecture on the Outcome of the Michael-Type Addition Used for Bioconjugation

Figure S 7: HPLC analysis of *N*-acetyl-S-[3-(2-hydroxyethoxy)-2-methyl-3-oxopropyl]cysteine (MA2-NAC)



=====  
Area Percent Report  
=====

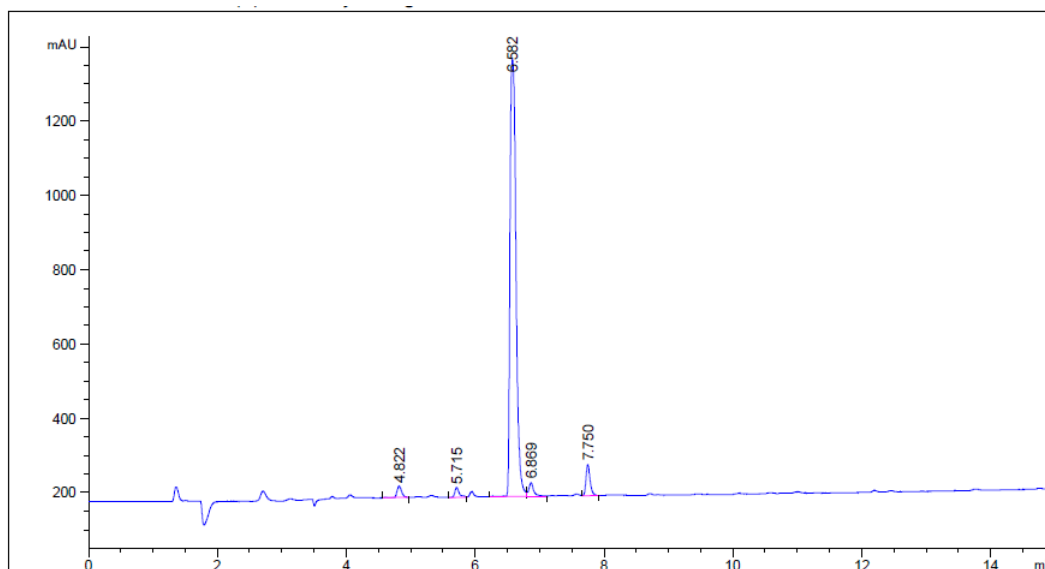
Sorted By : Signal  
Multiplier : 1.0000  
Dilution : 1.0000  
Use Multiplier & Dilution Factor with ISTDs

Signal 1: ADC1 A, ADC1 CHANNEL A

| Peak # | RetTime [min] | Type | Width [min] | Area [mAU*s] | Height [mAU] | Area %  |
|--------|---------------|------|-------------|--------------|--------------|---------|
| 1      | 4.849         | BV   | 0.0602      | 196.98683    | 44.00850     | 4.8505  |
| 2      | 7.345         | BV   | 0.0970      | 3677.44629   | 612.61707    | 90.5524 |
| 3      | 8.614         | VV   | 0.0644      | 103.32182    | 20.28370     | 2.5442  |
| 4      | 8.952         | BB   | 0.0658      | 83.37028     | 17.43672     | 2.0529  |

# Effects of Environmental Factors and Reactant Architecture on the Outcome of the Michael-Type Addition Used for Bioconjugation

Figure S 8: HPLC analysis of *N*-acetyl-S-{3-[2-(acetamino)ethoxy]-3-oxopropyl}cysteine (MA3-NAC)



=====  
Area Percent Report  
=====

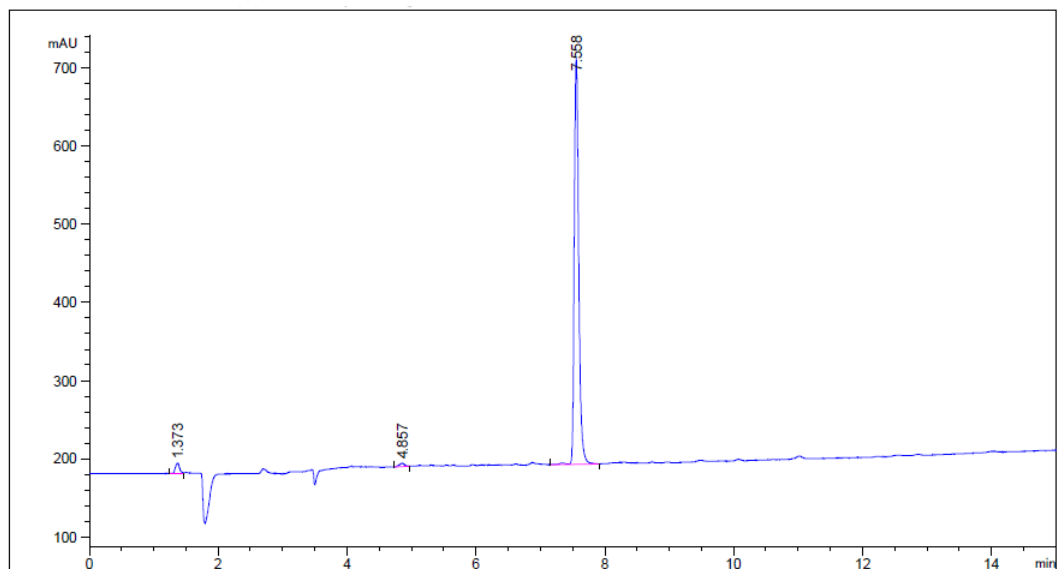
Sorted By : Signal  
Multiplier : 1.0000  
Dilution : 1.0000  
Use Multiplier & Dilution Factor with ISTDs

Signal 1: ADC1 A, ADC1 CHANNEL A

| Peak # | RetTime [min] | Type | Width [min] | Area [mAU*s] | Height [mAU] | Area %  |
|--------|---------------|------|-------------|--------------|--------------|---------|
| 1      | 4.822         | BB   | 0.0820      | 152.65163    | 29.66220     | 1.8068  |
| 2      | 5.715         | BV   | 0.0719      | 126.49437    | 26.40858     | 1.4972  |
| 3      | 6.582         | BV   | 0.1034      | 7601.11572   | 1175.50549   | 89.9677 |
| 4      | 6.869         | VB   | 0.0810      | 196.36192    | 36.33780     | 2.3242  |
| 5      | 7.750         | VB   | 0.0697      | 372.09363    | 83.92081     | 4.4041  |

Effects of Environmental Factors and Reactant Architecture on the Outcome of the Michael-Type Addition Used for Bioconjugation

Figure S 9: HPLC analysis of *N*-acetyl-S-{3-[2-(acetylamino)ethoxy]-2-methyl-3-oxopropyl}cysteine (MA4-NAC)



=====  
Area Percent Report  
=====

Sorted By : Signal  
Multiplier : 1.0000  
Dilution : 1.0000  
Use Multiplier & Dilution Factor with ISTDs

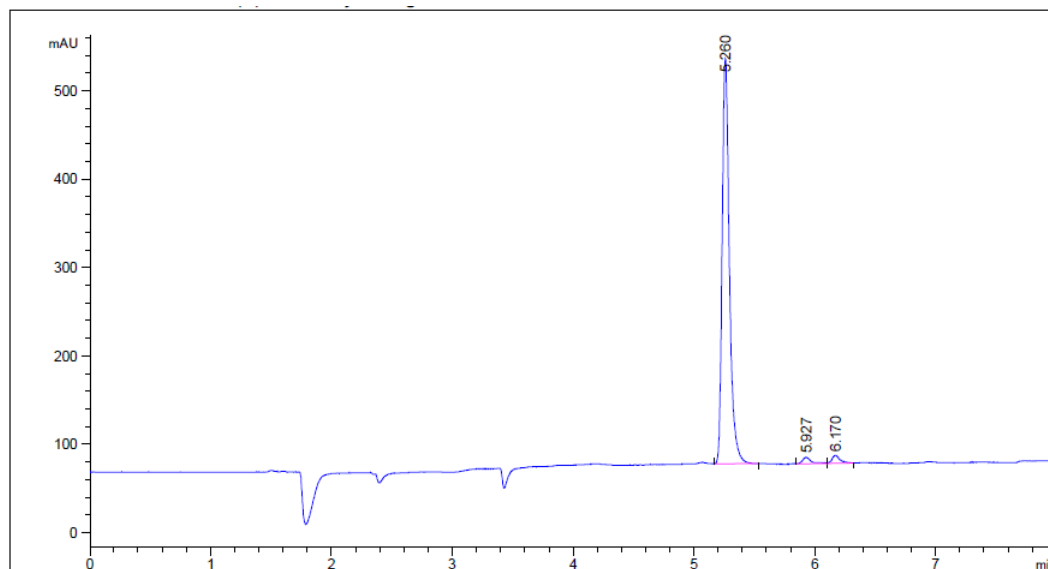
Signal 1: ADC1 A, ADC1 CHANNEL A

| Peak # | RetTime [min] | Type | Width [min] | Area [mAU*s] | Height [mAU] | Area %  |
|--------|---------------|------|-------------|--------------|--------------|---------|
| 1      | 1.373         | BV   | 0.0765      | 63.55561     | 13.59404     | 2.4658  |
| 2      | 4.857         | BB   | 0.0856      | 26.95005     | 4.64999      | 1.0456  |
| 3      | 7.558         | BB   | 0.0740      | 2486.95850   | 518.55713    | 96.4886 |



Effects of Environmental Factors and Reactant Architecture on the Outcome of the Michael-Type Addition Used for Bioconjugation

Figure S 10: HPLC analysis of *N*-acetyl-S-(3-[[2-(acetylamino)ethyl]amino]-3-oxopropyl)cysteine (MA5-NAC)



=====  
Area Percent Report  
=====

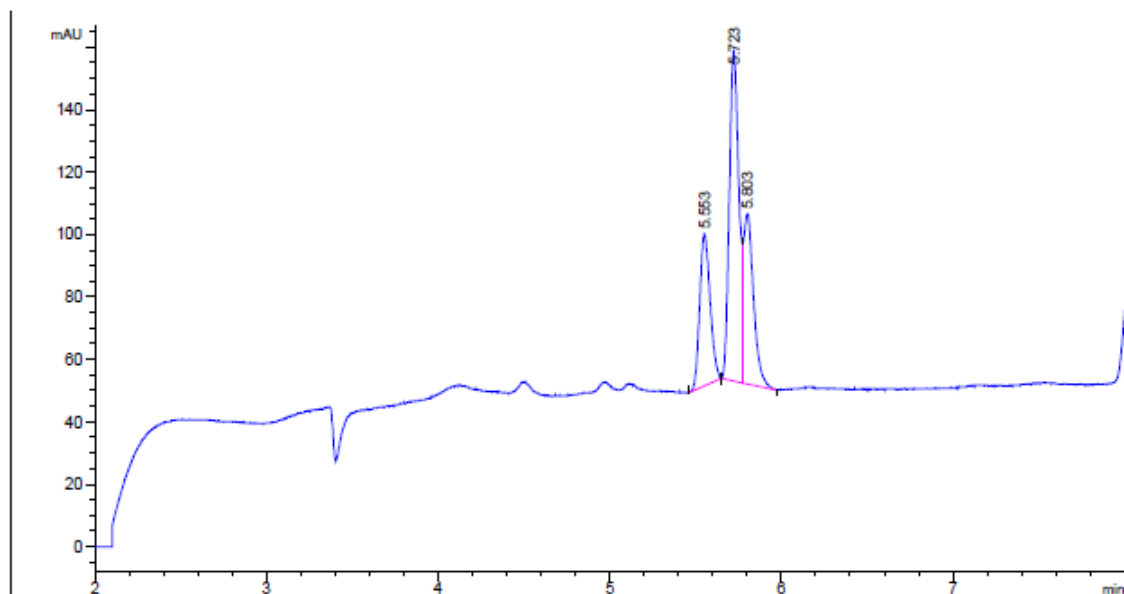
Sorted By : Signal  
Multiplier : 1.0000  
Dilution : 1.0000  
Use Multiplier & Dilution Factor with ISTDs

Signal 1: ADC1 A, ADC1 CHANNEL A

| Peak # | RetTime [min] | Type | Width [min] | Area [mAU*s] | Height [mAU] | Area %  |
|--------|---------------|------|-------------|--------------|--------------|---------|
| 1      | 5.260         | VB   | 0.0636      | 1907.58325   | 457.87448    | 96.2382 |
| 2      | 5.927         | BV   | 0.0709      | 34.24109     | 7.15200      | 1.7275  |
| 3      | 6.170         | VB   | 0.0648      | 40.32398     | 8.90645      | 2.0344  |

Effects of Environmental Factors and Reactant Architecture on the Outcome of the Michael-Type Addition Used for Bioconjugation

Figure S 11: : HPLC analysis of *N*-acetyl-S-{1-[2-(acetylamino)ethyl]-2,5-dioxopyrrolidin-3-yl}cysteine (MA6-NAC)



=====  
Area Percent Report  
=====

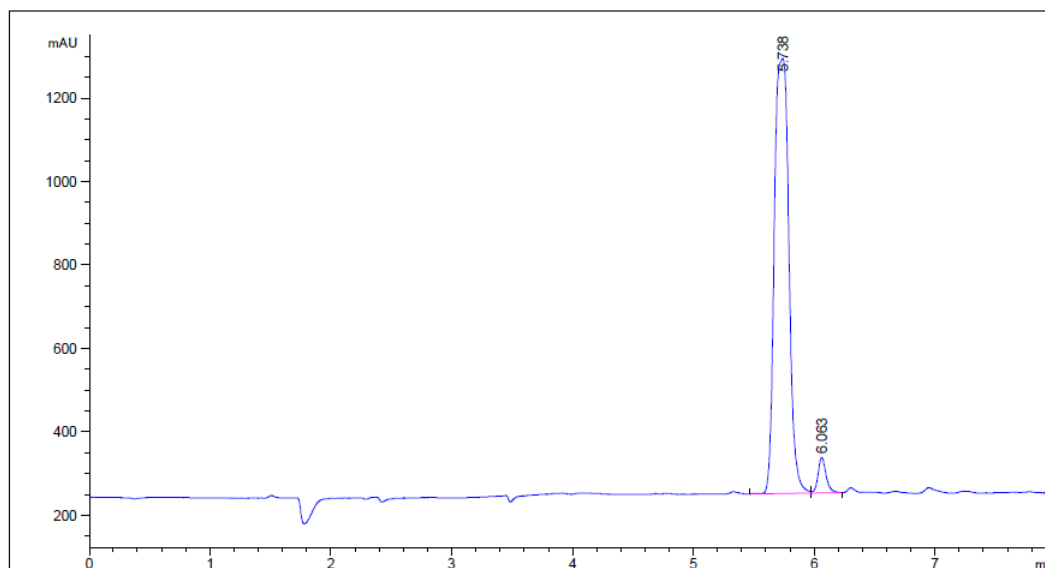
Sorted By : Signal  
Multiplier : 1.0000  
Dilution : 1.0000  
Use Multiplier & Dilution Factor with ISTDs

Signal 1: ADC1 A, ADC1 CHANNEL A

| Peak # | RetTime [min] | Type | Width [min] | Area [mAU*s] | Height [mAU] | Area %  |
|--------|---------------|------|-------------|--------------|--------------|---------|
| 1      | 5.553         | BB   | 0.0644      | 204.95045    | 48.86002     | 24.4548 |
| 2      | 5.723         | BV   | 0.0591      | 408.99725    | 105.75055    | 48.8018 |
| 3      | 5.803         | VB   | 0.0599      | 224.13112    | 54.57595     | 26.7434 |

Effects of Environmental Factors and Reactant Architecture on the Outcome of the Michael-Type Addition Used for Bioconjugation

Figure S 12: HPLC analysis of *N*-acetyl-S-{1-[2-(acetylamino)ethyl]-2,5-dioxopyrrolidin-3-yl}cysteine (MA7-NAC)



=====  
Area Percent Report  
=====

Sorted By : Signal  
Multiplier : 1.0000  
Dilution : 1.0000  
Use Multiplier & Dilution Factor with ISTDs

Signal 1: ADC1 A, ADC1 CHANNEL A

| Peak # | RetTime [min] | Type | Width [min] | Area [mAU*s] | Height [mAU] | Area %  |
|--------|---------------|------|-------------|--------------|--------------|---------|
| 1      | 5.738         | BV   | 0.1153      | 8695.22070   | 1042.69104   | 95.6433 |
| 2      | 6.063         | VB   | 0.0700      | 396.07968    | 85.50590     | 4.3567  |

### 3.7.3 Calibration curves of 3-MPA and NAC via Ellman's assay

The evaluation of the thiol concentration necessary to evaluate the kinetic of Michael-type addition reactions with different electrophiles was performed via Ellman's test. So, first of all, a calibration curve relating absorbance (at 412 nm) and concentration was plotted. Hence, several solutions with different concentration of thiol (3-MPA or NAC with concentrations ranging from 4.8 mM to  $1.2 \cdot 10^{-4}$  mM) were reacted with excess of DTNB.

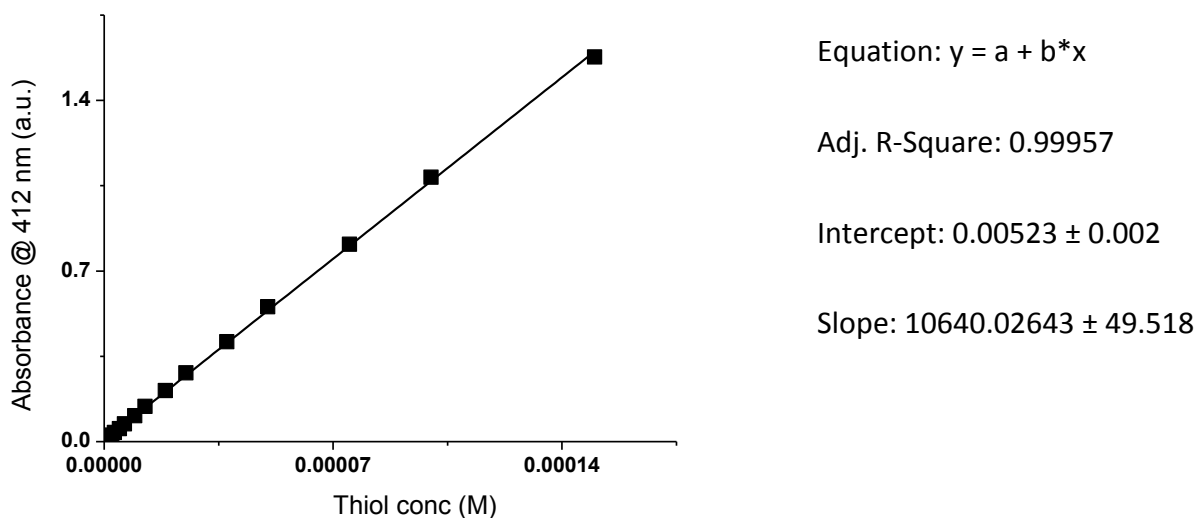


Figure S 13: Calibration curve of 3-MPA

Effects of Environmental Factors and Reactant Architecture on the Outcome of the Michael-Type Addition Used for Bioconjugation

---

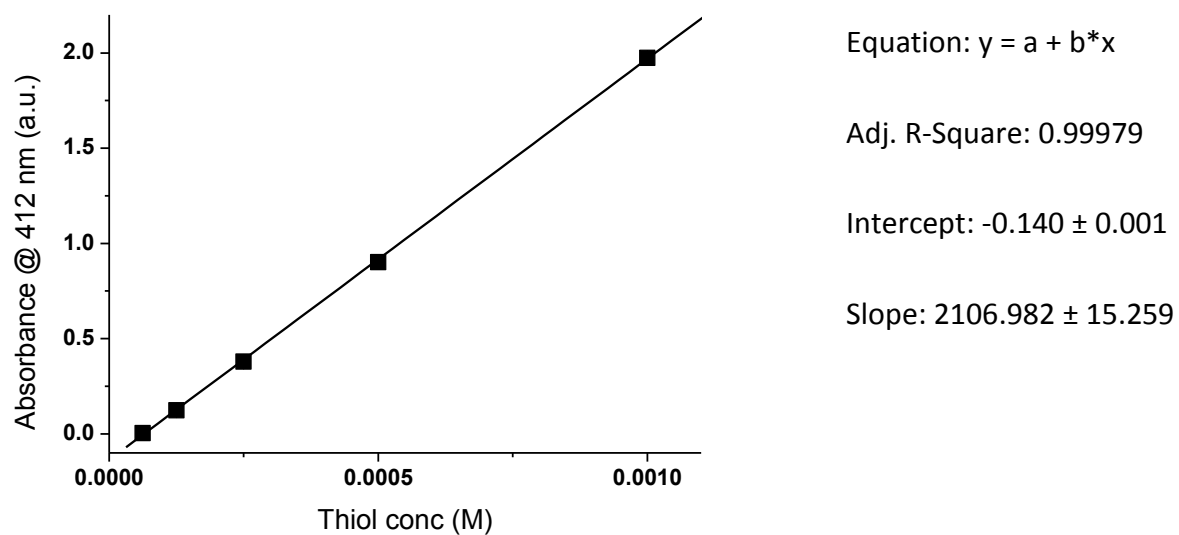


Figure S 14: Calibration curve of NAC

### 3.7.4 Calibration curve of maleimide **7**

The stability of the maleimide moiety contained in compound **7** was checked recording absorbance at 300 nm and calculating the concentration of the starting compound referring to this calibration curve recorded in Tris buffer 100 mM/EtOH 80:20 v/v at 30 °C.

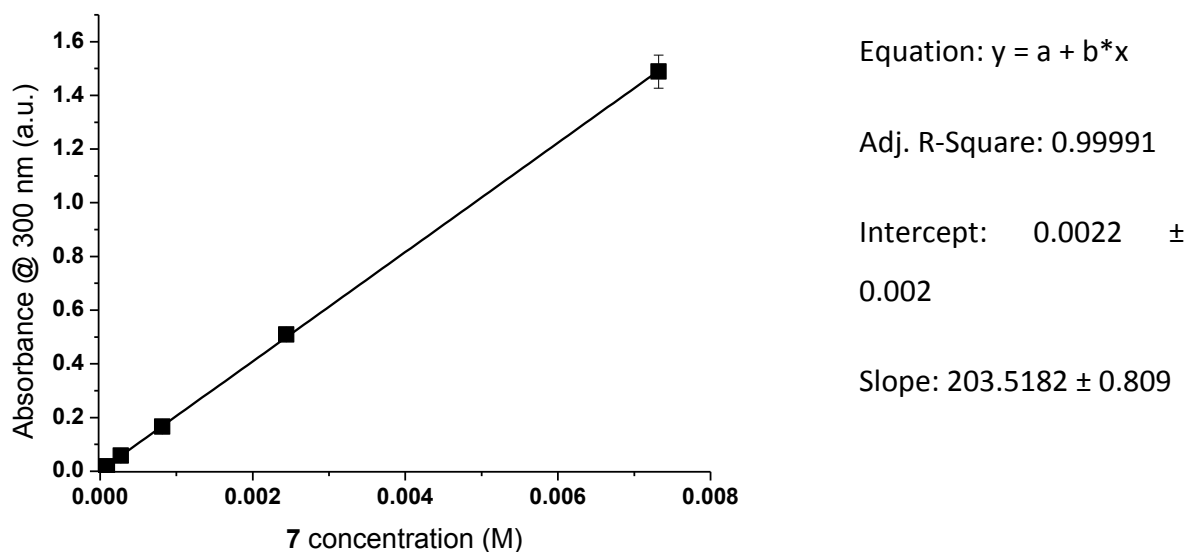


Figure S 15: Calibration curve of **7**